

STACKED

The building design, systems engineering and performance analysis of plant factories for urban food production

Graamans, L.J.A.

DOI

[10.7480/abe.2021.05](https://doi.org/10.7480/abe.2021.05)

Publication date

2021

Document Version

Final published version

Citation (APA)

Graamans, L. J. A. (2021). *STACKED: The building design, systems engineering and performance analysis of plant factories for urban food production*. [Dissertation (TU Delft), Delft University of Technology]. A+BE | Architecture and the Built Environment. <https://doi.org/10.7480/abe.2021.05>

Important note

To cite this publication, please use the final published version (if applicable).
Please check the document version above.

Copyright

Other than for strictly personal use, it is not permitted to download, forward or distribute the text or part of it, without the consent of the author(s) and/or copyright holder(s), unless the work is under an open content license such as Creative Commons.

Takedown policy

Please contact us and provide details if you believe this document breaches copyrights.
We will remove access to the work immediately and investigate your claim.



STACKED

The building design, systems
engineering and performance
analysis of plant factories for
urban food production

Luuk Graamans

STACKED

The building design, systems engineering and performance analysis of plant factories for urban food production

Luuk Graamans



21#05

Design | Sirene Ontwerpers, Véro Crickx

Cover photo | Luuk Graamans

Keywords | climate system; energy system; food resilience; resource use efficiency; urban agriculture; vertical farming

ISBN 978-94-6366-408-0

ISSN 2212-3202

© 2021 Luuk Graamans

This dissertation is open access at <https://doi.org/10.7480/abe.2021.05>

Attribution 4.0 International (CC BY 4.0)

This is a human-readable summary of (and not a substitute for) the license that you'll find at: <https://creativecommons.org/licenses/by/4.0/>

You are free to:

Share — copy and redistribute the material in any medium or format

Adapt — remix, transform, and build upon the material

for any purpose, even commercially.

This license is acceptable for Free Cultural Works.

The licensor cannot revoke these freedoms as long as you follow the license terms.

Under the following terms:

Attribution — You must give appropriate credit, provide a link to the license, and indicate if changes were made. You may do so in any reasonable manner, but not in any way that suggests the licensor endorses you or your use.

Unless otherwise specified, all the photographs in this thesis were taken by the author. For the use of illustrations effort has been made to ask permission for the legal owners as far as possible. We apologize for those cases in which we did not succeed. These legal owners are kindly requested to contact the author.

STACKED

The building design, systems engineering
and performance analysis of plant factories
for urban food production

Dissertation

for the purpose of obtaining the degree of doctor
at Delft University of Technology
by the authority of the Rector Magnificus, prof.dr.ir. T.H.J.J. van der Hagen
chair of the Board for Doctorates
to be defended publicly on
Thursday, 11th of March 2021 at 12:30 o'clock

by

Luuk Jan Adriaan GRAAMANS
Master of Science in Architecture, Urbanism and Building Sciences,
Delft University of Technology, the Netherlands
born in Utrecht, the Netherlands

This dissertation has been approved by the promotor.

Composition of the doctoral committee:

Rector Magnificus, Prof.dr.ir. A.A.J.F. van den Dobbelsteen	Chairperson Delft University of Technology, promotor
Dr.ir. M.J. Tenpierik	Delft University of Technology, promotor
Dr. C. Stanghellini	Wageningen University & Research, copromotor

Independent members:

Prof.dr.ir. A. van Timmeren	Delft University of Technology
Prof. G. Keeffe	Queen's University Belfast, the United Kingdom
Dr. R. Choudhary	University of Cambridge, the United Kingdom
Prof.dr.ir. L.F.M. Marcelis	Wageningen University & Research. the Netherlands
Prof.dr.ir.arch. I.S. Sariyildiz	Delft University of Technology, reserve member

This research was partially funded by the EU European Regional Development Fund “Kansen voor West” with the programme “Fieldlab FreshTeq”, and partially supported by Staaif Food Group and Westland Infra.

Aan mijn moeder

Contents

List of Tables	9
List of Figures	10
List of abbreviations and symbols	13

1 General introduction 21

1.1	Background	21
1.2	Research framework	31
1.3	Structure of the thesis	34

2 System configuration 47

2.1	Introduction	49
2.2	Theoretical background	50
2.3	Materials: Model overview	56
2.4	Methods: Model validation	59
2.5	Model results & discussion	62
2.6	Outlook	66
2.7	Conclusion	71

3 System evaluation 79

3.1	Introduction	81
3.2	Methodology	82
3.3	Results	95
3.4	Discussion	96
3.5	Outlook	103
3.6	Concluding remarks	104

4 System optimisation 113

- 4.1 Introduction 115
- 4.2 Materials and methods 117
- 4.3 Results 129
- 4.4 Discussion 130
- 4.5 Conclusions 142
- 4.6 Outlook 143

5 System integration 165

- 5.1 Introduction 167
- 5.2 Theoretical background 170
- 5.3 Materials and methods 176
- 5.4 Results and discussion: Energy production and demand 185
- 5.5 Results and discussion: Urban energy balance 190
- 5.6 Conclusions 201

6 Conclusions and outlook 227

- 6.1 Conclusions 227
- 6.2 Method evaluation 234
- 6.3 Broader implications 237
- 6.4 Recommendations for future research 240
- 6.5 Outlook 244

- Summary 247
- Samenvatting 251
- Dankwoord 255
- Curriculum vitae 259
- List of publications 261

List of Tables

- 2.1 The location, crop production data and interior climate conditions for the experiments conducted at Wageningen UR and the Kennedy Space Center. The different sets of VCD are represented by numbers (0-4) and the different balances are represented by letters (A-F). 61
- 2.2 The specific sets of crop production data and interior climate conditions used in determining the distribution of energy fluxes from the crop (and lighting system) to the surrounding air via simulation. The results are presented in Figure 2.6. 67
- 3.1 Key model parameters for the design of plant factories and greenhouses in Sweden (SWE), the Netherlands (NLD) and the United Arab Emirates (UAE). 93
- 3.2 The energy potential of resources as used to determine system loads from KASPRO output. 94
- 3.3 Coefficients of performance for the conversion of system loads in electric systems. These coefficients were determined using the Carnot efficiency of a heat pump, following the method presented by Meggers et al. [38] and using temperatures weighted for corresponding load. 95
- 4.1 Geometry of simulation models. 127
- 4.2 Parameters for annual energy demand simulations. Middle values are typically aligned with the current accepted building practice. Variables not considered in a specific simulation set (#) are marked by X. The variables are expanded upon in Section 4.2.3. 128
- 4.3 Constant model input for annual energy demand simulations. 129
- 4.4 Range of effects of façade properties on the annual energy demand of plant factories. Colour intensity illustrates the relative effect in comparison with the baseline per location. The characteristics of these baselines are given by listing their U-value (U), albedo or solar heat gain coefficient (A or SHGC), and wall-to-floor ratios (W/F). In addition, the transparency (T) is listed and indicated by transparent (T) or opaque (O). The effect of orientation is relative to the north-facing orientation for each W/F ratio (Δ). 138
- 5.1 Building characteristics per building function from PLUTO 2019 v1 [76]. The calculated averages are weighted for the floor area of each building. 177
- 5.2 Electricity use and residual heat production of plant factories in Sweden (SWE), the Netherlands (NLD) and the United Arab Emirates (UAE). Values are given per m^2 of production area (in W m^{-2}) and for the total production area of $7.01 \cdot 10^7 \text{ m}^2$ (in MW). 189

List of Figures

- 1.1 Schematic study design. 35
- 2.1 Green house energy balance, adapted from Sabeh [11]. 53
- 2.2 Plant factory energy balance. 53
- 2.3 The simulated transpiration compared to measurements for various PPFD. Measurements are represented by diamonds (photoperiod) and squares (dark period), simulations by circles (photoperiod) and triangles (dark period). 63
- 2.4 The simulated crop transpiration compared to measurements for various cultivation area cover percentages. Measurements are represented by diamonds, simulations by circles. 63
- 2.5 The simulated transpiration compared to measurements for various vapour concentration deficits. Results under light are represented by solid markers and results in dark are represented by outlines. Diamonds represent the (control) VCD Set 0 ($4.4/2.7 \text{ g m}^{-3}$), squares represent VCD set 1 ($3.7/2.3 \text{ g m}^{-3}$), triangles represent VCD set 2 ($2.3/0.5 \text{ g m}^{-3}$), circles represent VCD set 3 ($5.2/3.5 \text{ g m}^{-3}$) and stars represent VCD set 4 ($3.3/3.3 \text{ g m}^{-3}$). 65
- 2.6 The distribution of energy fluxes from the crop (and lighting system) to the surrounding air, following four different climate sets. The diagrams illustrate the results at a PPFD of $600 \mu\text{mol m}^{-2} \text{ s}^{-1}$ or $140 \mu\text{mol m}^{-2} \text{ s}^{-1}$ and a temperature regime of $21/19^\circ\text{C}$ or $25/23^\circ\text{C}$. Positive fluxes are represented in solid red, negative fluxes in blue. 68
- 3.1 The calculated total dry weight production (A), photosynthesis (B) and respiration (C) of lettuce at different leaf temperatures and combinations of CO_2 concentration (ppm) and PPFD ($\mu\text{mol m}^{-2} \text{ s}^{-1}$). Calculations include a complete production cycle of 60 days, a photoperiod of 16 h d^{-1} , and a constant temperature during photo-/dark periods. The maximum value on each curve is indicated by X. 85
- 3.2 Average daily radiation per month ($\text{MJ m}^{-2} \text{ d}^{-1}$) and monthly average, minimum and maximum temperatures ($^\circ\text{C}$) for Kiruna (SWE, stars), Amsterdam (NLD, triangles) and Abu Dhabi (UAE, circles). January is the lower left data point in each cycle. 87
- 3.3 Moving average of daily dry matter production ($\text{g m}^{-2} \text{ d}^{-1}$) (A) and total annual dry weight production ($\text{kg m}^{-2} \text{ y}^{-1}$) per cultivation area (B). Squares represent the plant factories, triangles represent greenhouses in NLD, circles represent greenhouses in the UAE, and crosses and stars represent greenhouses in SWE without and with artificial illumination, respectively. 97
- 3.4 Energy load of plant factories and greenhouses in UAE, NLD and SWE, normalised for cultivation area (MJ m^{-2}) (A) and for dry matter production ($\text{MJ kg}_{\text{dw}}^{-1}$) (B). 97
- 3.5 Electricity use per kg lettuce dry matter production ($\text{kWh}_e \text{ kg}_{\text{dw}}^{-1}$) by end use. Electricity use has been calculated according to the methods described in Section 3.2.4.2. 99

- 3.6 Average daily water use ($\text{kg m}^{-2} \text{d}^{-1}$) (A) and total annual water use per cultivation area ($\text{kg m}^{-2} \text{y}^{-1}$) in plant factories and greenhouses (B). The negative values of UAE in summertime can be explained by the fact that the calculations include the influence of infiltration of water vapour. During the summer months the absolute vapour content of air is higher outside the greenhouse. This results in water vapour infiltrating the facility and consequently being condensed and retrieved. 99
- 3.7 Average annual water use per kg of fresh weight (kg kg^{-1}), divided for biomass and sources of water vapour. A dry matter content of 7% has been assumed throughout this study. The plant factory displays a theoretical water use efficiency of 1 to 1 [9]. 101
- 3.8 Average daily CO_2 use ($\text{kg m}^{-2} \text{d}^{-1}$) (A) and total annual CO_2 use ($\text{kg m}^{-2} \text{y}^{-1}$) per cultivation area in plant factories and greenhouses (B). 101
- 3.9 Resource use for electricity (A), CO_2 (B) and water (C) of the plant factory (PF) and greenhouses (SWE, SWE(+), NLD and UAE), normalised for total dry matter production (kg_{dw}). 102
- 3.10 Estimation of the advantages of plant factories versus greenhouses based on relative electricity use efficiency (red) and water scarcity (blue). Water scarcity is subdivided into (approaching) physical and economic scarcity [48]. 103
- 4.1 Average daily radiation per month ($\text{MJ m}^{-2} \text{d}^{-1}$) and monthly average, minimum and maximum temperatures ($^{\circ}\text{C}$) for Kiruna (SWE, stars), Amsterdam (NLD, triangles) and Abu Dhabi (UAE, circles). January is the lower left data point in each cycle. Adapted from Graamans et al. [8]. 121
- 4.2 Schematic representation of the cooling system design. A continuous line represents the flow of air and a dashed line the flow of the refrigerant. 125
- 4.3 Annual energy demand ($\text{kWh m}^{-2} \text{y}^{-1}$) of plant factories featuring opaque façades in UAE, SWE and NLD, as a result of variation in insulation (U-value in $\text{W m}^{-2} \text{K}^{-1}$) and reflection of solar radiation (albedo). Values are indicated by L (low: $A=0.10$, $U=0.05$), M (medium: $A=0.50$, $U=0.20$) and H (high: $A=0.90$, $U=5.75$) and refer to values listed in Table 4.2. Presented simulations feature a W/F ratio of 0.39 and face north. 133
- 4.4 Annual energy demand ($\text{kWh m}^{-2} \text{y}^{-1}$) of plant factories featuring transparent façades in UAE, SWE and NLD, as a result of variation in insulation (U-value in $\text{W m}^{-2} \text{K}^{-1}$) and solar heat gain coefficient (SHGC). Values are indicated by L (low: $\text{SHGC}=0.30$, $U=0.50$), M (medium: $\text{SHGC}=0.55$, $U=1.25$) and H (high: $\text{SHGC}=0.80$, $U=5.75$) and refer to the values listed in Table 4.2. Presented simulations feature a W/F ratio of 0.39 and face north. 133
- 4.5 Annual energy demand ($\text{kWh m}^{-2} \text{y}^{-1}$) of plant factories in UAE, NLD and SWE featuring opaque façades, as a result of variation in insulation (U-value in $\text{W m}^{-2} \text{K}^{-1}$) and reflection of solar radiation (albedo) in combination with W/F ratio. Values are indicated by L (low: $A=0.10$, $U=0.05$), M (medium: $A=0.50$, $U=0.20$) and H (high: $A=0.90$, $U=5.75$) and refer to values listed in Table 4.2. The long façade faces north in presented simulations. 135
- 4.6 Annual energy demand ($\text{kWh m}^{-2} \text{y}^{-1}$) of plant factories in UAE, NLD and SWE featuring transparent façades, as a result of variation in insulation (U-value in $\text{W m}^{-2} \text{K}^{-1}$) and solar heat gain coefficient (SHGC) in combination with W/F ratio. Values are indicated by L (low: $\text{SHGC}=0.30$, $U=0.50$), M (medium: $\text{SHGC}=0.55$, $U=1.25$) and H (high: $\text{SHGC}=0.80$, $U=5.75$) and refer to the values listed in Table 4.2. The long façade faces north in presented simulations. 135

- 4.7 Energy demand (A) in kWh m⁻² y⁻¹ and final electricity use (B) in kWh m⁻² y⁻¹ for the most efficient opaque and transparent constructions in each location. The relative delta (%) illustrates the difference with the industry-standard plant factory in the specific location (opaque, U=0.05 W m⁻² K⁻¹, A=0.55, W/F=0.39). The y-axis lists location, W/F ratio (-), U-value (W m⁻² K⁻¹), SGHC (-) or albedo (-) (dependent on transparency), and transparency (O for opaque and T for transparent) from left to right. The long façade faces north in presented simulations. 137
- 4.8 Sensitivity analysis illustrating the relative change in total energy demand (y-axis) as a result of relative change in LED efficiency, U-value, and albedo or SHGC, respectively (x-axis) in UAE, NLD and SWE. The base values for these parameters are 52% LED efficiency (red:blue=80:20, 2.70 μmol J⁻¹) for opaque - LED efficiency, 2.90 W m⁻² K⁻¹ for opaque - Uvalue, 0.50 for opaque - albedo, 3.215 W m⁻² K⁻¹ for transparent - U-value, and 0.55 for transparent - SHGC. 141
- 5.1 Comparison between reported (R) and calculated (C) values for annual energy use per building function (A in kWh m⁻²) and total annual energy use (B in TWh) for New York City. The calculated total energy use after improvement of the building stock is also listed (F). Residential (S) and (M) and (L) denote buildings housing 1-2, 3-6 or more than 6 families, respectively (Table 5.1). 186
- 5.2 Calculated annual energy consumption in SynCity. Energy consumption is presented per building function (A and B in kWh m⁻²) and total annual energy use (C in TWh) for Sweden (SWE), the Netherlands (NLD) and the United Arab Emirates (UAE). Please note the different yaxes for each graph. 187
- 5.3 Annual energy distribution (A) and load duration curve (B) for wind, solar and wave energy for subarctic Sweden (SWE), the Netherlands (NLD) and the United Arab Emirates (UAE). The annual energy distribution illustrates the share of total capacity realised per hour and is ordered chronologically. The load duration curve illustrates the capacity utilisation for each increment of the total energy generation and is shown in descending order of magnitude. 189
- 5.4 Primary energy use for all scenarios in Sweden (SWE), the Netherlands (NLD) and the United Arab Emirates (UAE) in TWh. 191
- 5.5 Hourly distribution profile of the energy imbalance (in MW) in Sweden (SWE), the Netherlands (NLD) and the United Arab Emirates (UAE). Scenarios B1-B2 and F1-F3 exclusively use intermittent RES (A) and scenarios B3-B4 and F4-F5 feature a more diverse energy production distribution (B). Positive values (orange) represent import and negative values (blue) represent export. 194
- 5.6 Sensitivity analysis illustrating the relative change in energy imbalance (y-axis) as a result of relative change in LED efficiency, plant factory area, share of wind in RES production and thermal storage capacity. The base values for these parameters match Scenario F2 (Table 5C.1). The locations are Sweden (SWE), the Netherlands (NLD) and the United Arab Emirates (UAE). 197
- 5.7 Hourly distribution profile of the energy imbalance (in MW) following the integration of central heat pumps and thermal storage in Sweden (SWE), the Netherlands (NLD) and the United Arab Emirates (UAE), as described in Section 5.5.6. The positive values (orange) represent import and negative values (blue) represent export. 199
- 6.1 Simplified overview of the method and modules. 233

List of abbreviations and symbols

Abbreviations			
Abbreviation	In model	Description	Unit
BWh	-	Köppen-Geiger: Hot desert climate	-
CAC	CAC	cultivation area cover	%
Cfb	-	Köppen-Geiger: Temperate oceanic climate	-
CHP	CHP	combined heat and power	-
COP	COP	coefficient of performance	-
CPPS	-	closed plant production system	-
Dfc	-	Köppen-Geiger: Subarctic climate	-
DH	DH	district heating	-
DHW	DHW	domestic hot water	-
HVAC	-	heating, ventilation and air conditioning	-
LAI	LAI	leaf area index	$m_{\text{leaf}}^2 m_{\text{soil}}^{-2}$
LTDH	-	low-temperature district heating	-
NLD	NLD	the Netherlands	-
PAR	-	photosynthetically active radiation	W m^{-2}
PPFD	PPFD	photosynthetic photon flux density	$\mu\text{mol m}^{-2} \text{s}^{-1}$
RES	RES	renewable energy sources	-
RH	RH	relative humidity	%
RMSE	-	root mean-squared error	-
SHGC	SHGC	solar heat gain coefficient	-
SLA	-	specific leaf area	$\text{g}_{\text{dw}}^{-1}$
SWE	SWE	Sweden	-
U-value	U	heat transfer coefficient	$\text{W m}^{-2} \text{K}^{-1}$
UAE	UAE	the United Arab Emirates	-
VCD	-	vapour concentration deficit	g m^{-3}
W/F ratio	-	wall-to-floor ratio	-

Symbols			
Symbol	In model	Description	Unit
a	a	thermal diffusivity of air	$\text{m}^2 \text{s}^{-1}$
A	A	area	m^2
c_{fan}	c_fan	fan efficiency	%
c_g	c_g	energy conversion efficiency of natural gas	MJ m^{-3}
c_p	cp	specific heat capacity	$\text{J kg}^{-1} \text{K}^{-1}$
c_{pv}	c_pv	efficiency of photovoltaic arrays	-
c_{pw}	c_pw	power coefficient	-
c_r	c_r	reflection coefficient of the crop	%
c_{roof}	c_roof	roof space availability coefficient	-
c_{safe}	c_safe	safety factor	-
c_{st}	c_st	thermal energy storage coefficient	-
c_w	c_w	heat capacity of water	J g^{-1}
COP	COP	coefficient of performance	-
CAC	-	cultivation area cover percentage	%
d	d	wall thickness	m
e	e	saturated vapour pressure	kPa
EB	E_b	energy balance	-
E	E	electricity use	Whe
h	h	enthalpy (of refrigerant unless specified otherwise)	kJ kg^{-1}
H	H	sensible heat flux	W m^{-2}
I	I	radiation	W m^{-2}
l	-	mean leaf diameter	m
LAI	LAI	active leaf area index	$\text{m}^2_{\text{leaf}} \text{m}^{-2}_{\text{sol}}$
\dot{m}	m	refrigerant mass flow rate	kg s^{-1}
n	n	number of	-
n_{air}	n_air	number of air exchanges	h^{-1}
Nu	Nu	Nusselt number	-
p	p	pressure	bar
P	P	power	W
Pr	Pr	Prandtl number	-
$PPFD$	PPFD	photosynthetic photon flux density	$\mu\text{mol m}^{-2} \text{s}^{-1}$
q	q	generated power	W
Q	Q	energetic flux	W
r	R	resistance	s m^{-1}
R	rad	radius	m
Re	Re	Reynolds number	-
RH	RH	relative humidity	%
s	s	entropy (of refrigerant unless specified otherwise)	$\text{kJ kg}^{-1} \text{K}^{-1}$
$SHGC$	SHGC	solar heat gain coefficient	-

>>>

Symbols			
Symbol	In model	Description	Unit
T	T	temperature	°C
OT	OT	operation time	h
t	t	time	h
u	u	flow velocity	m s ⁻¹
U	U	heat transfer coefficient	W m ⁻² K ⁻¹
V	V	volumetric flow	m ³ s ⁻¹
w	w	water use	kg
W_c	W_c	compressor work input	W
x	Ratio	humidity ratio of moist air	kg kg ⁻¹
α	alpha	heat transfer coefficient	W m ⁻² K ⁻¹
A	Albedo	albedo (diffuse reflection out of total solar radiation)	-
β	beta	shearing exponent	-
γ	gamma	psychometric constant of 66.5	Pa K ⁻¹
δ	delta	relationship between saturation vapour pressure and air temperature	kPa K ⁻¹
ϵ	epsilon	vapour concentration (slope of the saturation function curve)	-
η_c	eta_c	isentropic compressor efficiency	-
κ	kappa	thermal conductivity	W m ⁻¹ K ⁻¹
λ	lambda	latent heat of the evaporation of water	J g ⁻¹
λE	La_E	latent heat flux	W m ⁻²
μ	mu	dynamic viscosity	N s m ⁻²
ν	nu	kinematic viscosity	m ² s ⁻¹
ρ	rho	density	kg m ⁻³
Φ'	phi_p	heat transfer in tube	W m ⁻¹
χ	X	vapour concentration	g m ⁻³
χ_{air}	X_t_a	vapour concentration of the air	g m ⁻³
χ_{air}^*	X_sat_a	saturated vapour concentration of the air	g m ⁻³
χ_s	X_sat_s	vapour concentration at the canopy level	g m ⁻³
X	chi	quality of fluid-vapour mixture	-

Superscripts		
Superscript	In model	Description
*	_sat	saturated

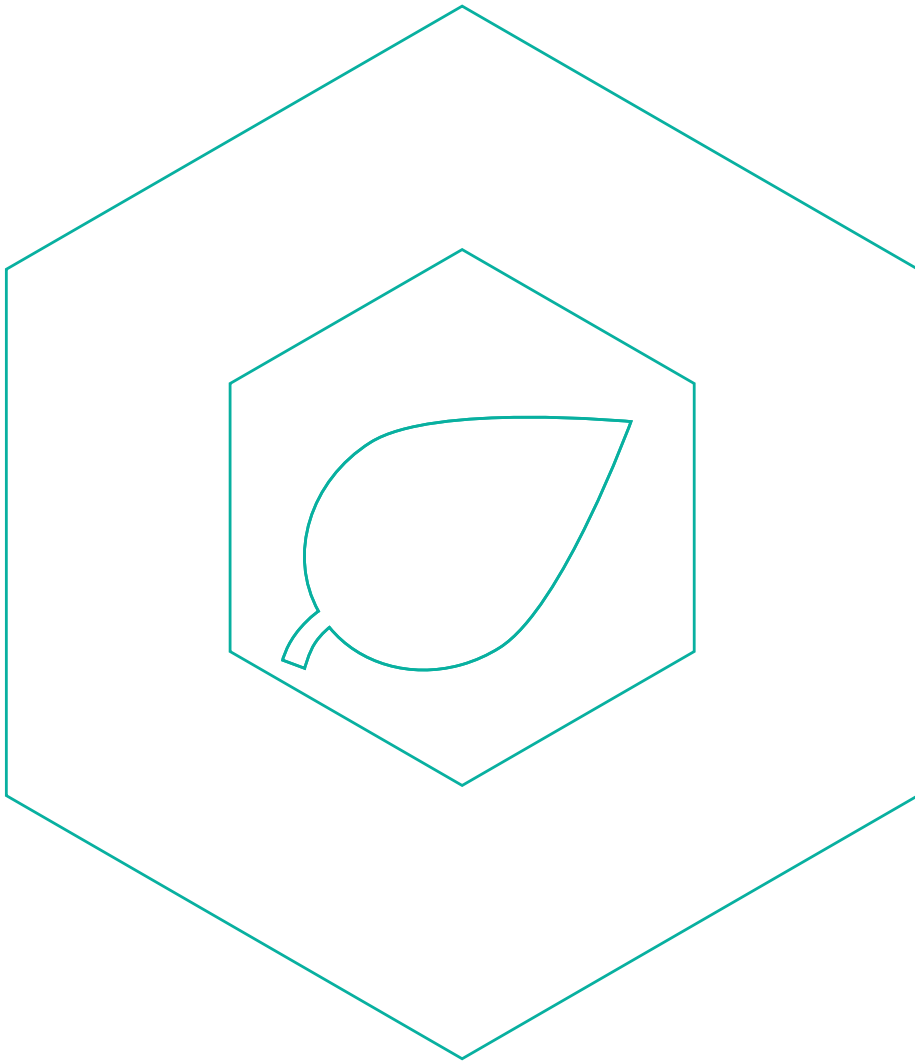
Subscripts		
Subscript	In model	Description
∞	-	uninhibited flow
0	_0	air entering the heat exchanger
10m	_10m	at a height of 10 meters
100m	_100m	at a height of 100 meters
1	_1	saturated vapour leaving the evaporator (including superheating)
1s	_1s	saturated vapour inside the evaporator
2	_2	superheated vapour leaving compressor (non-isentropic)
2s	_2s	superheated vapour leaving compressor (isentropic)
3	_3	saturated liquid leaving the condenser (including subcooling)
3s	_3s	saturation at condenser
4	_4	liquid-vapour mixture exiting throttling process and entering evaporator
a	_a	aerodynamic boundary layer
air	_air	air
c	_c	compressor
comp	-	various greenhouse components, including structural components
cool	_cool	cooling
con	_con	condensed
cond	_cond	at the condenser
DHW	_DHW	domestic hot water
dw	_DW	dry weight
elec	_elec	electricity
equip	-	equipment
evap	_evap	at the evaporator
ex	_ex	exterior
f4	_f4	liquid refrigerant at T_4
fac	-	façade
fan	_fan	single fan
fans,x	_fans_x	array of fans for function x
fans_hex,x	_fans_hex_x	array of fans in the heat exchanger for function x
fl	_fl	due to friction loss
fog	_fog	fogging system
full	_full	operation at full capacity
fw-dw	-	water content of biomass
g4	_g4	gas refrigerant at T_4
GH	_GH	greenhouse
g	_g	natural gas
gas	_gas	natural gas use
heat	_heat	heating
hex	_hex	heat exchanger

>>>

Subscripts		
Subscript	In model	Description
<i>HVAC</i>	_HVAC	heating, ventilation, air-conditioning system
<i>in</i>	_in	interior
<i>l</i>	_L	at tube length <i>l</i>
<i>lat</i>	_lat	latent heat transfer
<i>LED</i>	_LED	LED lighting system
<i>light</i>	_light	lighting system
<i>max</i>	_max	maximum
<i>net</i>	_net	net
<i>NIR</i>	_NIR	near-infrared radiation
<i>ns</i>	_NS	nutrient solution
<i>nTrans</i>	_ntrans	non-transmitted radiation
<i>out</i>	-	extracted to the exterior
<i>PAR</i>	_PAR	photosynthetically active radiation
<i>plant</i>	-	plant processes
<i>PF</i>	_PF	plant factory
<i>pv</i>	_pv	photovoltaic array
<i>pw</i>	_pv	power coefficient
<i>r</i>	_r	reflection
<i>rad</i>	-	radiation
<i>rc</i>	_rc	refrigeration capacity
<i>ref</i>	_ref	reference
<i>req</i>	_req	required
<i>roof</i>	_roof	roof
<i>s</i>	_sts	at the crop canopy level
<i>safe</i>	_safe	safety factor
<i>sen</i>	_sens	sensible
<i>set</i>	_set	setpoint
<i>soil</i>	-	between ground and air
<i>sol</i>	_solar	solar
<i>ss</i>	_ss	surface (stomatal)
<i>st</i>	_st	storage
<i>sub</i>	_sub	degree of subcooling
<i>sup</i>	_sup	degree of superheat
<i>th</i>	_th	thermal energy
<i>tot</i>	_tot	total
<i>tube</i>	_tube	tube
<i>tur</i>	_turbine	turbine
<i>vent</i>	-	natural and mechanical ventilation
<i>we</i>	_we	evaporation of water

>>>

Subscripts		
Subscript	In model	Description
<i>wind</i>	_wind	wind
<i>x</i>	_x	technology x



1 General introduction

1.1 Background

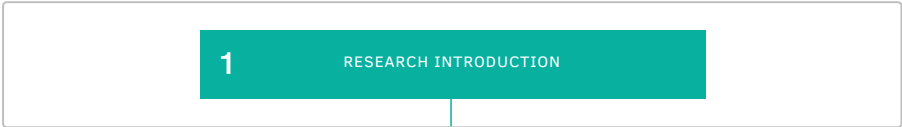
1.1.1 Vertical farms and plant factories

Vertical farms or plant factories are often heralded in mainstream media as a transformative technology that will shape the future [1]. These systems produce crops in vertically stacked layers inside a closed environment with full climate control. LED systems are used for illumination and hydroponic systems are generally used for the delivery of water and nutrients to the crop.

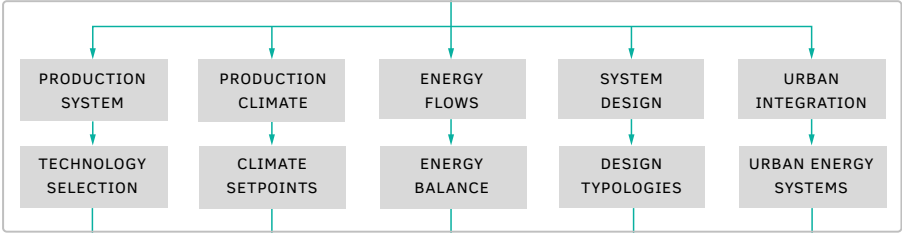
The technology has actually been around for several decades. Hydroponic systems were originally introduced in the 1930s and were developed to test nutrient combinations and growing conditions [2]. The use of three-dimensional space for the cultivation of plants, independently of seasons and climatic conditions, was technically described for the first time in a patent by Ruthner in 1966 [3]. At that time, the combination of hydroponics and high-density, three-dimensional cultivation was already expected to revolutionise global food production.

Since then, plant factories had mainly been proposed to enhance food production in metropolitan areas, in response to an expanding urban population and strong dependence on the global food network. In reality, however, the application has remained scarce. Only recently has the technology been promoted to ensure global food security, improve food quality and increase the sustainability of food production and supply. The extensive climate control that the plant factory offers is seen as the solution to all three challenges. The question remains whether this level of control is necessary, effective and/or efficient.

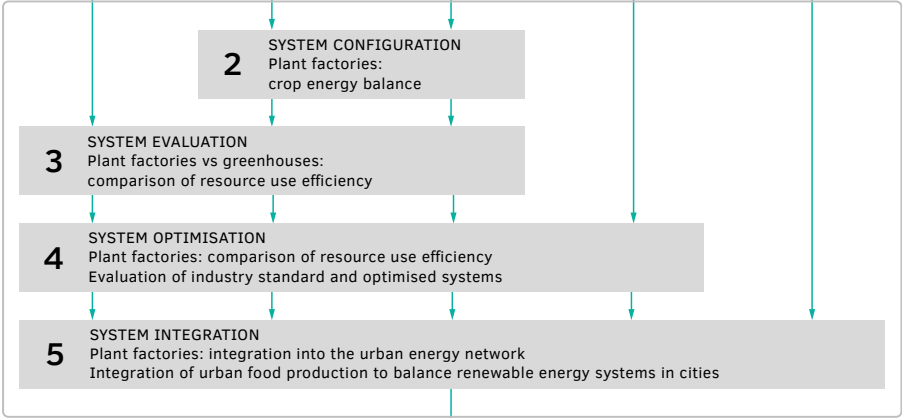
I. INTRODUCTION & METHODOLOGICAL FRAMEWORK



II. THEORETICAL FRAMEWORK



III. DESIGN & EXPERIMENTAL VALIDATION



IV. INTEGRATED DISCUSSION



1.1.2 Food security

Our present condition is one of quantifiable climate change, steady population growth and extensive urbanisation. Plant factories have been promoted as the preferred crop production system to increase global food security. Food security has four key dimensions – availability, accessibility, utilisation and stability – and is closely linked to climate change [4]. All actors within the food system – in production as well as in the supply networks – may be affected by climate change [5].

1.1.2.1 Population growth and urbanisation

The total global population is set to reach 9.7 billion by 2050 [6]. As a result, global food demand is expected to continue to rise at the steep pace that began in the 1950s [7], growing by 50% by 2050 compared to 2013 [8]. However, the capacity to appropriate new land, new water sources, or new fisheries to meet these demands is increasingly constrained [7]. Meanwhile, human activity is rapidly changing the environmental conditions within which global food production operates [9].

Research exploring the links between food security, climate change and urban dwellers is sparse. Since more than half the world's population is already living (and eating) in urban areas, investigating this connection should be made a priority. The global urban population is expected to increase further, from 4.2 billion today to 6.7 billion by 2050 [10]. Cities around the world are already facing challenges in managing the flows of food, as well as energy, data, water and supplies. At present, food is typically supplied to large cities via the continental and global food network. While this network is projected to increase in predominance and complexity [11], questions have been raised about its sustainability and resilience [12].

A resilient system can process changes in state variables, persist after disturbance [13] and maintain productivity [14]. In the current system, however, food production and the food supply network are sensitive to various disturbances, which may limit the availability, accessibility and stability of the food supply. The consequences may be exacerbated for cities, with high population densities and high risks of exposure to natural disasters [15]. Moreover, one of the great questions of this century is how to satisfy the increasing nutritional needs in the context of natural resource constraints and rapid climate change.

1.1.2.2 Vulnerability of crop production

Over the past decades, the global food security discourse has focused on improving food availability by increasing average yields. It has emphasised the role of highly productive, large-scale agricultural systems without much regard for their vulnerability to external shocks [16]. In the next decades, it is likely that such shocks will become more frequent, as global temperatures keep rising [17], air quality deteriorates [18], sea levels rise [19], extreme weather events occur more frequently [20] and new viruses spread globally [21].

Weather extremes directly influence the production climate and therefore disrupt food production [22, 23]. These extremes may include low [24] and high [25] temperatures, rainfall variability [26], droughts [27] and floods [5, 28]. Crop production may also be disrupted by pests and pathogens [29, 30], agroterrorism [31] and epidemics [32].

Structural climate change is also a credible threat. Research has started to project the impacts of climate change on the global production of products such as wheat [33], maize [34], soy [35], rice [36] and hop for beer [37]. Even in the most pessimistic scenarios, it is unlikely that climate change would result in a net decline in global yields. Aggregate crop productivity will likely continue to increase to 2050, driven by technological and agronomic improvements [23]. Instead, the question at the global scale is how much of a headwind climate change could present in the race to keep productivity up with demand.

Neither short-term climate variability nor structural climate change are new phenomena in agriculture. However, more areas are likely to undergo stronger effects of climate change and short-term weather variability will likely become more severe across all regions. These changes may exceed our historical experiences [20]. Adaptation strategies for current climate variability or long-term climate change should therefore focus on ensuring resilience for a broad range of future climate conditions [38]. Traditional agriculture is directly impacted by climate variability; its resilience may be improved by exercising greater control over the production climate, such as in plant factories.

1.1.2.3 Vulnerability of supply networks

The food supply network is responsible for food stability and accessibility and its resilience is paramount for global food security [39]. The present network can be described as “robust yet fragile”—robust to random failures but fragile under targeted, cascading disturbances [40]. Its just-in-time supply system increases risk in times of large disturbances [41]. The low diversity of producers allows these disturbances to become further amplified, both economically and ecologically [42]. Shocks early in the supply chain can become amplified as they move through the global system [43]. While there are financial benefits to participating in these trade networks, the drawback is a reduction in localised capacity to adapt [42].

Weather extremes highlight the fragility of the supply network. They have resulted in disruption of critical infrastructures, power shortages, et cetera [44]. Urban centres are amongst the most vulnerable locations, whether through rising sea levels, changes in temperature, or more extreme and uncertain weather conditions [45]. The risk of serious flooding in particular is expected to increase [26]. One recent example is the flooding of Queensland, Australia in 2010/2011, where large areas of agricultural land were inundated, affecting both long and short food supply chains in rural and urban areas [46]. This resulted in reduced access to food, deterioration in food quality and disruption of sourcing, transportation and distribution [5].

Several studies have predicted an immediate breakdown of the food network, following a disease pandemic (e.g. [47]). Yet the supply chains have been reasonably responsive in the short term during the COVID-19 pandemic, albeit with some lag [48]. In the longer term, pandemics are likely to influence the workforce by disrupting production and future import/export [49, 50].

Local production cannot replicate the full functionality of the global trade network. However, a degree of regional autonomy may increase the resilience of food systems. Alternative systems focusing on local production have been studied, but it remains uncertain whether these systems have the capacity to scale up [51] or respond effectively during times of crisis [5]. Localising agricultural production in plant factories may supplement the existing networks, thereby making the system as a whole more resilient. Fruits and vegetables are most suited for production close to urban centres, as they present less environmental and public health risks than for instance livestock [52, 53].

1.1.3 Food quality and diet

Plant factories have been promoted to contribute to a healthy diet by improving the commercial quality and nutritional value of crops while ensuring consistent production. Quality standards include freshness, cleanliness, freedom from disease, firmness, lack of damage, appearance, texture, aroma, consistency, origin and use-by-date [54]. These aspects will be elaborated below.

1.1.3.1 Nutritional content

An extensive control of the production climate can improve the nutritional content of crops such as leafy greens, tomatoes and strawberries. Studies have shown that the light spectrum, temperature, humidity and nutrient delivery can influence the formation of particular chemical compounds in leaves and fruits [55]. A wide range of compounds could be manipulated to improve nutritional value, including amino-acids, proteins, vitamins (A, C, E), carotenoids, flavonoids, minerals, glycosides and anthocyanins [56-63]. While links have been found between production climate and the formation of specific chemical components, the evidence is far from fully understood. More research on the overarching field of genetics, environment and management is needed to optimise the genetics and growing conditions of different crops for both quality and yield in controlled environments [63, 64].

Shorter supply chains can ensure that crops reach the consumer faster with a higher freshness and nutritional quality. Food may be transported over several thousand kilometres from producer to consumer, which can reduce nutritional quality due to storage and transport time [65-67]. For example, much of the fresh produce consumed on the east coast of the USA and Canada is produced in California, requiring transport over 3000 km [68]. Plant factories can effectively shorten these supply chains by enabling local production. The extensive control of temperature, humidity and light allow for production in any location and season.

1.1.3.2 Diet

The availability of fresh fruits and vegetables may play a role in the general health of the population. The exact make-up of a diverse, balanced and healthy diet will vary depending on individual needs (e.g. age, gender, lifestyle, degree of physical activity), but daily consumption of a variety of fruits (~200 g) and vegetables (~250 g) is

considered fundamental [69, 70]. However, the scientific support for such a diet remains inconclusive in an evidence-based review. The nutrients in fruits and vegetables provide support for the biological plausibility of health benefits [71]. However, prospective cohort studies find only weak support for the protectiveness of fruits and vegetables against chronic diseases [67]. Epidemiological studies have suggested an inverse relationship between a regular consumption of fruits and vegetables and the risk of various cancers, cardiovascular disease, and mortality [71]. There is currently a lack of convincing data that any specific fruit or vegetable is of particular importance [72].

A (moderate) shift from the current food consumption pattern from animal-based to plant-based products could reduce food GHG emissions (e.g. in Portugal emissions would decrease by up to 22% and agricultural land use by up to 24% [73]). In general, animal-based foods tend to have a higher footprint per kg of product than plant-based: on average¹, producing a kilogram of beef emits anywhere from 21 to 60 kg of carbon dioxide equivalent (CO₂eq), while the production of most fruits and vegetables emits around 1 kg CO₂eq kg⁻¹. Poultry and fish have medium footprints at approximately 6 and 5 kg CO₂eq kg⁻¹, respectively [74]. When taking into account nutritional value, the difference generally narrows: for example, 100 grams of protein² from legumes emits 0.7 kg CO₂eq, from poultry and fish around 4 kg CO₂eq and from beef 25 kg CO₂eq, on average [74]. It is important to note that this comparison does not account for the lower quality³ of plant-based relative to meat-based protein [82, 83]. It is currently impossible to define the optimal healthy and sustainable diet, but a shift to increase the share of fruits and vegetables can reduce global food emissions. The local production of fresh fruits and vegetables in plant factories could play a role in promoting this shift.

¹ The ecological footprint of products can differ greatly between locations.

² The importance and recommended intake of protein is widely debated, but is likely underestimated in most (inter)national dietary recommendations [75-80].

³ As determined by the Digestible Indispensable Amino Acid Score [81].

1.1.4 Sustainable production of food

Feeding 7.6 billion people using standard production methods is degrading terrestrial and aquatic ecosystems, depleting water resources, and driving climate change [74]. Plant factories have been promoted to contribute to a sustainable food system and minimise its environmental impact by reducing the resources required for crop production and transport.

1.1.4.1 Current situation

The development of a sustainable food system lies at the heart of the United Nations' Sustainable Development Goals. A sustainable food system is a food system that delivers food security and nutrition for all, without compromising the economic, social and environmental bases to generate food security and nutrition for future generations [84].

Modern agriculture requires more water (~66% of annual withdrawal [85]), human labour (~27% of global population [86]) and land (~40% of the world's ice-free land surface [87]) than any other industry. The global food supply chain creates ~13.7 billion metric tons of CO₂eq, 26% of all anthropogenic GHG emissions [74]. Non-food agriculture causes another ~2.8 billion metric tons (5%) of CO₂eq [74]. Finally, the supply chain is responsible for ~32% of global terrestrial acidification and ~78% of eutrophication [74].

The challenges related to transport and crop production will be discussed below.

1.1.4.2 Transport

The idea of reducing the travel distance of food (i.e., through local food production or low food miles) is popular with consumers wanting to reduce greenhouse gas (GHG) emissions [88]. However, transport contributes a small proportion of total emissions for most individual products (<10%; [74]) and for most diets (~6%; [89]). The exception is air transport, which emits 50 times more CO₂eq per ton kilometre than transport over water. Even so, it accounts for just 0.16% of annual food miles [74] and only affects the footprint at locations with a high dependency on air transport (e.g. Hong Kong [90]). The benefits from efficient resource use during production may be greater than from reduced food miles [91].

Shortening the supply chain may eliminate losses and waste on the path from cultivation to retail. These losses are mainly due to improper storage conditions, breaking the cold chain and stock management inefficiencies. Their share in total GHG emissions is larger than transport (~24% versus <10%, respectively [74]). Preliminary investigations found that reducing losses and waste can lower GHG emissions for food by 8.2–13.4% while reducing transport distances only lowers emissions by 2.6–3.5%, varying per diet [73]. Shorter chains are most effective in reducing GHG emissions for fresh (plant-based) products, for example fruit and vegetables: this category represents a relatively large share of total food losses and wastage (e.g. ~42% in Portugal [73]).

1.1.4.3 Crop production

The largest shares of GHG emissions from food are attributed to land use and the production phase: on average, land use accounts for 24% and the production phase for 58% (livestock & fisheries generate 31%, crop production for human consumption generates 21% and animal feed generates 6%) [74]. The selection and sustainable production of crops can therefore be more effective than limiting food miles. For example, importing Spanish lettuce to the UK during winter months results in three to eight times lower GHG emissions than producing it locally [92]; producing tomatoes in greenhouses in Sweden requires 10 times as much energy as importing in-season tomatoes from Southern Europe [93].

The sustainability of the crop production itself depends on numerous factors, ranging from local resource availability, to production climate, to selected production systems (open field, greenhouses with various levels of technology or plant factories). The production climate directly influences crop production and its resource use efficiency. System performance can be compared using crop yield and the corresponding use of water, energy and CO₂. The effects of the production climate on system performance has been a focal point of agricultural research, in particular the effects of air temperature [94], root-zone temperature [95], ventilation [96], humidity [97], nutrient delivery [98], light intensity [99], light spectrum [100] and light duration [101].

Control of a production climate does not necessarily increase resource use efficiency, but rather shifts it. As a general rule, an increase in control over the production climate results in a decrease in energy use and an increase in water use. For example, the production of lettuce requires approximately 3.2 MJ kg⁻¹ of energy and 9.3 l kg⁻¹ of water in a glass greenhouse with moderate climate control but 2.9 MJ kg⁻¹ and 24.0 l kg⁻¹ in the open field in Italy [102]. A LDPE-covered greenhouse

with low climate control uses approximately 0.94 MJ kg^{-1} and 24.2 l kg^{-1} , whereas open field production requires 1.19 MJ kg^{-1} and 42.8 l kg^{-1} to produce one kg of tomatoes in Barcelona, Spain [103]. Each location and situation demands a different production system with different levels of climate control. Plant factories can offer full control over the production climate, but the system performance and the resource use have yet to be determined.

1.1.5 Summary

Plant factories have been promoted to ensure food security, improve food quality and increase the sustainability of food production. These challenges are most prominent in metropolitan areas as a result of their dependence on the global food network and the expanding urban population. With respect to food security, plant factories have been promoted to ensure the availability, accessibility and stability of the food supply for an expanding (urban) population by playing a role in crop production, as well as in food supply networks. The impact of plant factories on urban and global food security has not been documented. However, extensive control over the production climate can increase the resilience of crop production against climate variability and other external factors. Furthermore, local production may provide resilience against extreme weather events. With respect to food quality, plant factories have been promoted to produce high-quality, nutritious crops through extensive control of the production climate. While more research is required to accurately control quality during production [63, 64], local production and shorter supply chains can already increase the quality and freshness of crops. With respect to sustainable food production, plant factories have been promoted to minimise the transport distance and resource use for crop production. The global food system is currently responsible for approximately 26% of global anthropogenic GHG emissions [74] and has great potential for climate change mitigation [87, 104-106]. Crop production and land use change make up the largest share of the total food system emissions, whereas transport makes up a relatively small share. The effectiveness of plant factories will primarily depend on the resource use for crop production. It is therefore important to investigate whether the level of climate control that plant factories offer is necessary, effective and/or efficient.

1.2 Research framework

1.2.1 Problem statement

Currently, there is no format available to provide a detailed insight into the technical potential of plant factories, particularly for the urban context. The agricultural and building engineering disciplines are independently extensive, but there is no comprehensive research that covers the system design, design implications and performance assessment of a plant factory. The present work was conceived to be the first of its kind in this respect. To this end, this study connects the agricultural engineering expertise from Wageningen University & Research with the building and systems engineering expertise from Delft University of Technology.

1.2.2 Research objectives

This research analyses the requirements of plant factories for the production of fresh vegetables in order to elucidate their potential. The results can serve to formulate design strategies for the (urban) food system of the future.

Main objective

The objective of this research is to quantify the resource use efficiency of plant factories and explore their potential as a method for urban food production.

The main objective is pursued as a combination of four sub-objectives:

- 1 To formulate the crop energy balance in plant factories;
- 2 To quantify and compare the resource use efficiency of plant factories and greenhouses for crop production;
- 3 To improve the resource use efficiency of plant factories through systems design;
- 4 To integrate the plant factory in the urban energy network.

1.2.3 Research questions

These aims are encompassed in the main research question:

How can closed agricultural production systems be designed for the urban context, in order to increase the resource use efficiency of crop production?

The following sub-questions cover the sub-objectives listed above:

- 1 *How can the crop energy balance be calculated using the production climate, in order to determine the vapour production and energy exchange by the crop canopy?*
- 2 *What is the resource use efficiency of water, energy, CO₂ and land area for crop production in plant factories in comparison to greenhouses?*
- 3 *How can façade and climate system design reduce the resource requirement for crop production in plant factories?*
- 4 *How can plant factories be integrated in the urban energy network to exchange resource streams with surrounding urban functions and reduce the resource requirement of the joint system?*

1.2.4 Boundary conditions

Several limitations are inherent in this type of research, given the imponderable and unpredictable factors underlying it. Variability in location, urban functions, culture, available technology and climate may be expected to result in a wide variety of outcomes. The principal boundary conditions for this study are listed below.

Main boundary conditions

- **Typology:** Plant factories are modelled as fully closed systems that are artificially illuminated.
- **Production:** This research focuses on abiotic factors. Production is influenced by biotic (genetics, growth, and disease) and abiotic (temperature, light, CO₂, water potential, nutrient availability) factors.
- **Resources:** The resources taken into account will be energy (e.g. electricity and natural gas), water, CO₂ and land area. The impact of nutrient balance and quantity as well as pesticides are excluded.

- **Location:** Three sites will be selected to represent diverse latitudes and climates, namely Kiruna in Sweden (subarctic climate), Amsterdam in the Netherlands (oceanic climate) and Abu Dhabi in the United Arab Emirates (hot desert climate).
- **Crop:** This study will focus on the production of lettuce. Lettuce was selected for its space/time efficiency, harvest index and energy use efficiency [107]. The selection of various species and types of crop and their impact on production are excluded.

Main outcome measures

- **Energy use efficiency:** Energy usage for dry weight production, expressed in $Wh\ g_{dw}^{-1}$
- **Electricity use efficiency:** Electricity usage for dry weight production, expressed in $Wh_e\ g_{dw}^{-1}$
- **Water use efficiency:** Water usage for dry weight production, expressed in $g_{H_2O}\ g_{dw}^{-1}$
- **CO₂ use efficiency:** CO₂ usage for dry weight production, expressed in $g_{CO_2}\ g_{dw}^{-1}$
- **Production capacity:** Total dry weight production per production area, expressed in $g_{dw}\ m^{-2}$
- **Land use efficiency:** Total dry weight production per land area, expressed in $g_{dw}\ m^{-2}$
(taking into account multiple production layers)

1.2.5 Approach and methodology

The main objective of this research is to quantify the resource use efficiency of food production in plant factories in an urban context. In order to determine the technical feasibility of plant factories this research has to connect multiple scales: from the crop, to the individual plant factory, to the city as a whole. These scales are captured in the various sub-objectives (Section 1.2.2). Their integration is illustrated in the schematic study design (Figure 1.1).

Each sub-objective relates to a strand of the literature study (II). The five main strands are the production system, production climate, energy flows, system design and urban integration. On the smallest scale, a model is formulated to determine the crop energy balance in plant factories (2). This energy balance is closely connected to the crop production climate, which in turn affects the resource requirement for climatisation. On the medium scale, the crop energy model is then combined with existing building and greenhouse energy models, as well as crop models, to calculate

the resource use efficiencies of individual greenhouses and plant factories (3). Further analysis of this data identifies the key factors for improving the performance of plant factories. Building and system design strategies to improve the resource use efficiency of plant factories are then formulated, calculated and analysed using the aforementioned models (4). The analysis provides insight in the performance of an optimised, individual plant factory. Finally, on the largest scale, the plant factory is integrated into the urban energy network using the aforementioned models in combination with energy systems analysis models (5). The analysis investigates potential exchanges between plant factories and surrounding functions and illustrates the potential for total urban energy use. The findings are standardised across the scales using the selected outcome measures. The methodology of each sub-objective is described in greater detail in Section 1.7 and the individual chapters.

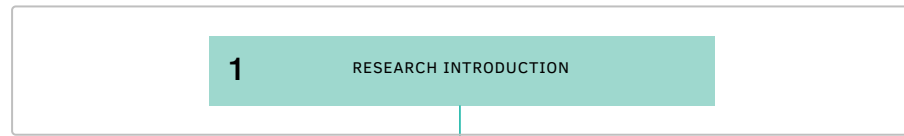
1.3 Structure of the thesis

This study consists of six chapters. Between the introduction (Ch 1) and general discussion (Ch 6), each of four chapters addresses one of the sub-objectives. These chapters have been published in or submitted to scientific journals as individual articles.

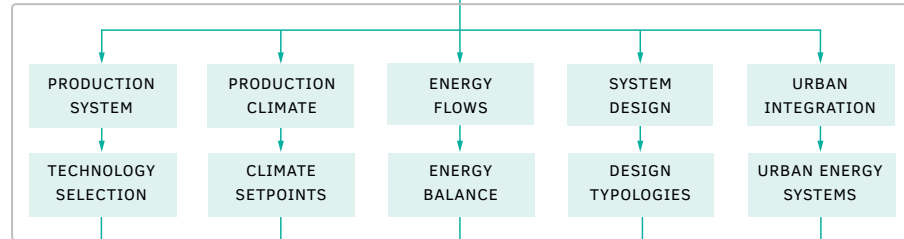
Chapter 2 – System configuration. Chapter 2 gives a detailed description of the crop energy balance model (Objective 1). That model is able to determine the relation between sensible and latent heat exchange from the crop canopy. It is validated for the effect of photosynthetic photon flux density, cultivation area cover and air humidity. This chapter illustrates the importance of transpiration as a design parameter for climatisation.

Chapter 3 – System evaluation. Chapter 3 investigates and compares the resource use efficiency of plant factories and greenhouses (Objective 2). To this end, the crop energy balance model is combined with a building energy model and greenhouse energy model to determine the use of energy, water and CO₂ for crop production. Crop production is estimated for the production climate, using an existing crop model. The estimate is applied to determine the resource use efficiency. The chapter provides insight into the effect of external climate on the resource use efficiency of different production systems.

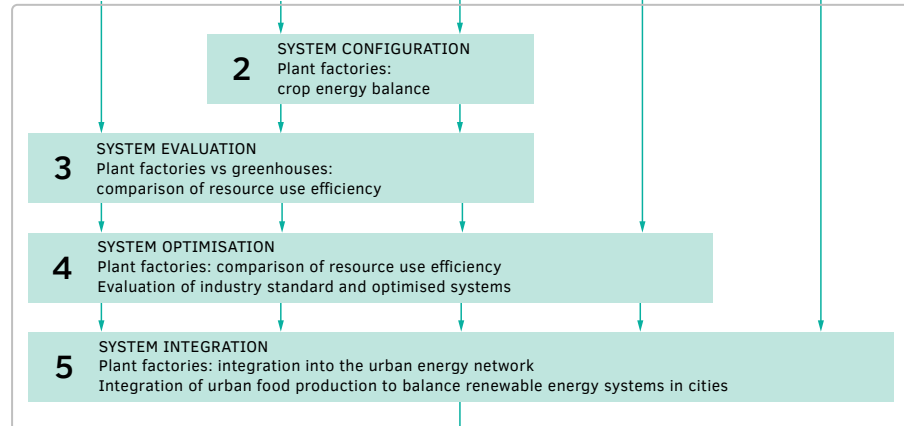
I. INTRODUCTION & METHODOLOGICAL FRAMEWORK



II. THEORETICAL FRAMEWORK



III. DESIGN & EXPERIMENTAL VALIDATION



IV. INTEGRATED DISCUSSION

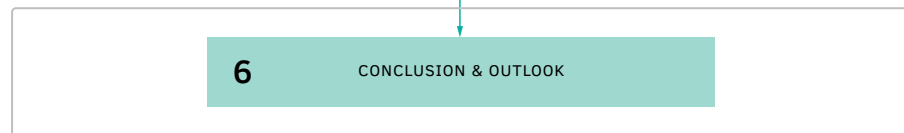


FIG. 1.1 Schematic study design.

Chapter 4 – System optimisation. Chapter 4 reduces the energy use of plant factories through system optimisation (Objective 3). It investigates the cooling system and façade of the plant factory in greater detail. To this end, the crop energy balance model is combined with a building energy model and a vapour compression refrigeration model. The sensitivity of the model to LED efficiency, as well as façade insulation, albedo and transparency are assessed. The chapter provides a foundation for the energy efficient design of plant factories, tailored to local climate.

Chapter 5 – System integration. Chapter 5 integrates the plant factory in the broader urban energy system (Objective 4). It investigates the imbalance in the production and consumption of renewable energy over time for synthetic cities. Then it explores the potential of plant factories as a flexible heat production technology to balance the energy systems. This is followed by an assessment of the sensitivity of the integrated model to LED efficiency, as well as to thermal storage capacity, renewable energy distribution, and heating capacity. The chapter presents strategies for an integrated energy system design, utilising the food-energy interface.

Chapter 6 – Conclusions and outlook. Chapter 6 synthesises the results obtained in this study. It gives the main conclusions and makes recommendations for future development and potential applications.

Reference list

- [1] Scott, M. (2019). These are the technologies that will transform the 2020s - From 5G to vertical farming. *Forbes*. <https://www.forbes.com/sites/mikescott/2019/12/09/these-are-the-technologies-that-will-transform-the-2020s-from-5g-to-vertical-farming/#45c230524a05>
- [2] Gericke, W. (1937). Hydroponics - Crop production in liquid culture media. *Science*, 85(2198), 177.
- [3] Ruthner, O. (1966). Apparatus for the artificial cultivation of plants, bacteria, and similar organism. In United States Patent Office (Ed.). USA.
- [4] FAO. (2008). *Climate change and food security: A framework document*.
- [5] MacMahon, A., Smith, K., & Lawrence, G. (2015). Connecting resilience, food security and climate change: lessons from flooding in Queensland, Australia. *Journal of Environmental Studies and Sciences*, 5(3), 378-391. doi:10.1007/s13412-015-0278-0
- [6] United Nations. (2019). *World Population Prospects 2019: Highlights (ST/ESA/SER.A/423)*. New York: United Nations, Department of Economic and Social Affairs, Population Division.
- [7] Myers, S.S., Smith, M.R., Guth, S., Golden, C.D., Vaitla, B., Mueller, N.D., Dangour, A.D., & Huybers, P. (2017). Climate change and global food systems: potential impacts on food security and undernutrition. *Annual review of public health*, 38, 259-277. doi:10.1146/annurev-publhealth-031816-044356
- [8] FAO. (2017). *The future of food and agriculture - trends and challenges*. Rome.
- [9] Whitmee, S., Haines, A., Beyrer, C., Boltz, F., Capon, A.G., de Souza Dias, B.F., Ezeh, A., Frumkin, H., Gong, P., & Head, P. (2015). Safeguarding human health in the Anthropocene epoch: report of The Rockefeller Foundation-Lancet Commission on planetary health. *The Lancet*, 386(10007), 1973-2028. doi:10.1016/S0140-6736(15)60901-1
- [10] United Nations. (2019). *World Urbanization Prospects 2018: Highlights (ST/ESA/SER.A/421)*. New York: United Nations, Department of Economic and Social Affairs, Population Division.
- [11] Newcombe, K. & Nichols, E.H. (1979). An integrated ecological approach to agricultural policy-making with reference to the urban fringe: The case of Hong Kong. *Agricultural Systems*, 4(1), 1-27. doi:10.1016/0308-521x(79)90011-8
- [12] Kennedy, C., Cuddihy, J., & Engel-Yan, J. (2007). The changing metabolism of cities. *Journal of industrial ecology*, 11(2), 43-59. doi:10.1162/jiec.0.1107
- [13] Holling, C.S. (1973). Resilience and stability of ecological systems. *Annual review of ecology and systematics*, 4(1), 1-23. doi:10.1146/annurev.es.04.110173.000245
- [14] Folke, C., Carpenter, S.R., Walker, B., Scheffer, M., Chapin, T., & Rockström, J. (2010). Resilience thinking: integrating resilience, adaptability and transformability. *Ecology and society*, 15(4). doi:10.5751/es-03610-150420
- [15] United Nations. (2018). *The World's Cities in 2018 - Data booklet (ST/ESA/SER.A/417)*. New York: United Nations, Department of Economic and Social Affairs, Population Division.
- [16] McKenzie, F.C. & Williams, J. (2015). Sustainable food production: constraints, challenges and choices by 2050. *Food Security*, 7(2), 221-233. doi:10.1007/s12571-015-0441-1
- [17] Rogelj, J., D. Shindell, K. Jiang, S. Fifita, P. Forster, V. Ginzburg, C. Handa, H. Khesghi, S. Kobayashi, E. Kriegler, L. Mundaca, & R. Séférian, and M.V. Vilarinho, 2018. (2018). Mitigation pathways compatible with 1.5°C in the context of sustainable development. In Masson-Delmotte, V. , Zhai, P., Pörtner, H.-O., Roberts, D., Skea, J., Shukla, P.R., Pirani, A., Moufouma-Okia, W., Péan, C., Pidcock, R., Connors, S., Matthews, J.B.R., Chen, Y., Zhou, X., Gomis, M.I., Lonnoy, E., Maycock, T., Tignor, M. &Waterfield, T. (Eds.), *Global Warming of 1.5°C. An IPCC Special Report on the impacts of global warming of 1.5°C above pre-industrial levels and related global greenhouse gas emission pathways, in the context of strengthening the global response to the threat of climate change, sustainable development, and efforts to eradicate poverty*: IPCC.
- [18] Jacob, D.J. & Winner, D.A. (2009). Effect of climate change on air quality. *Atmospheric environment*, 43(1), 51-63. doi:10.1016/j.atmosenv.2008.09.051
- [19] Oppenheimer, M., Glavovic, B.C. , Hinkel, J. , van de Wal, R., Magnan, A.K., Abd-Elgawad, A. , Cai, R., Cifuentes-Jara, M., DeConto, R.M., Ghosh, T., Hay, J., Isla, F., Marzeion, B., Meyssignac, B., & Sebesvari, Z. (2019). Sea level rise and implications for low-lying islands, coasts and communities. In Pörtner, H.-O., Roberts, D.C., Masson-Delmotte, V., Zhai, P., Tignor, M., Poloczanska, E., Mintenbeck, K., Alegría, A., Nicolai, M., Okem, A., Petzold, J., Rama, B. &Weyer, N.M. (Eds.), *IPCC Special Report on the Ocean and Cryosphere in a Changing Climate*: IPCC.

- [20] IPCC. (2007). *Climate change 2007: Impacts, Adaptation and Vulnerability. Contribution of Working Group II to the Fourth Assessment report of the Intergovernmental Panel on Climate Change*. Cambridge, UK: Cambridge University Press.
- [21] Heymann, D.L., Chen, L., Takemi, K., Fidler, D.P., Tappero, J.W., Thomas, M.J., Kenyon, T.A., Frieden, T.R., Yach, D., & Nishtar, S. (2015). Global health security: the wider lessons from the west African Ebola virus disease epidemic. *The Lancet*, 385(9980), 1884-1901. doi:10.1016/S0140-6736(15)60858-3
- [22] Gornall, J., Betts, R., Burke, E., Clark, R., Camp, J., Willett, K., & Wiltshire, A. (2010). Implications of climate change for agricultural productivity in the early twenty-first century. *Philosophical Transactions of the Royal Society B: Biological Sciences*, 365(1554), 2973-2989. doi:10.1098/rstb.2010.0158
- [23] Lobell, D.B. & Gourdji, S.M. (2012). The influence of climate change on global crop productivity. *Plant Physiology*, 160(4), 1686-1697. doi:10.1104/pp.112.208298
- [24] Engvild, K.C. (2003). A review of the risks of sudden global cooling and its effects on agriculture. *Agricultural and forest Meteorology*, 115(3-4), 127-137. doi:10.1016/S0168-1923(02)00253-8
- [25] Battisti, D.S. & Naylor, R.L. (2009). Historical warnings of future food insecurity with unprecedented seasonal heat. *Science*, 323(5911), 240-244. doi:10.1126/science.1164363
- [26] Cai, W., Wang, G.J., Santoso, A., McPhaden, M.J., Wu, L.X., Jin, F.F., Timmermann, A., Collins, M., Vecchi, G., & Lengaigne, M. (2015). Increased frequency of extreme La Niña events under greenhouse warming. *Nature Climate Change*, 5(2), 132-137. doi:10.1038/nclimate2492
- [27] Li, Y.P., Ye, W., Wang, M., & Yan, X.D. (2009). Climate change and drought: a risk assessment of crop-yield impacts. *Climate research*, 39(1), 31-46. doi:10.3354/cr00797
- [28] Rosenzweig, C., Tubiello, F.N., Goldberg, R., Mills, E., & Bloomfield, J. (2002). Increased crop damage in the US from excess precipitation under climate change. *Global Environmental Change*, 12(3), 197-202. doi:10.1016/S0959-3780(02)00008-0
- [29] Rosenzweig, C., Iglesias, A., Yang, X.B., Epstein, P.R., & Chivian, E. (2001). Climate change and extreme weather events-Implications for food production, plant diseases, and pests.
- [30] Bebb, D.P. & Gurr, S.J. (2015). Crop-destroying fungal and oomycete pathogens challenge food security. *Fungal Genetics and Biology*, 74, 62-64. doi:10.1016/j.fgb.2014.10.012
- [31] Cupp, O.S., Walker, D.E., & Hillison, J. (2004). Agroterrorism in the US: key security challenge for the 21st century. *Biosecurity and bioterrorism: biodefense strategy, practice, and science*, 2(2), 97-105. doi:10.1089/153871304323146397
- [32] McCloskey, B., Dar, O., Zumla, A., & Heymann, D.L. (2014). Emerging infectious diseases and pandemic potential: status quo and reducing risk of global spread. *The Lancet infectious diseases*, 14(10), 1001-1010. doi:10.1016/S1473-3099(14)70846-1
- [33] Asseng, S., Ewert, F., Martre, P., Rötter, R.P., Lobell, D.B., Cammarano, D., Kimball, B.A., Ottman, M.J., Wall, G.W., & White, J.W. (2015). Rising temperatures reduce global wheat production. *Nature Climate Change*, 5(2), 143. doi:10.1038/nclimate2470
- [34] Bassu, S., Brisson, N., Durand, J.L., Boote, K., Lizaso, J., Jones, J.W., Rosenzweig, C., Ruane, A.C., Adam, M., & Baron, C. (2014). How do various maize crop models vary in their responses to climate change factors? *Global change biology*, 20(7), 2301-2320. doi:10.1111/gcb.12520
- [35] Sakurai, G., Iizumi, T., & Yokozawa, M. (2011). Varying temporal and spatial effects of climate on maize and soybean affect yield prediction. *Climate research*, 49(2), 143-154. doi:10.3354/cr01027
- [36] Krishnan, P., Swain, D.K., Bhaskar, B.C., Nayak, S.K., & Dash, R.N. (2007). Impact of elevated CO₂ and temperature on rice yield and methods of adaptation as evaluated by crop simulation studies. *Agriculture, Ecosystems & Environment*, 122(2), 233-242. doi:10.1016/j.agee.2007.01.019
- [37] Xie, W., Xiong, W., Pan, J., Ali, T., Cui, Q., Guan, D., Meng, J., Mueller, N.D., Lin, E., & Davis, S.J. (2018). Decreases in global beer supply due to extreme drought and heat. *Nature plants*, 4(11), 964. doi:10.1038/s41477-018-0263-1
- [38] Ziervogel, G. & Ericksen, P.J. (2010). Adapting to climate change to sustain food security. *Wiley Interdisciplinary Reviews: Climate Change*, 1(4), 525-540. doi:10.1002/wcc.56
- [39] Barrett, C.B. (2010). Measuring food insecurity. *Science*, 327(5967), 825-828. doi:10.1126/science.1182768
- [40] Foti, N.J., Pauls, S., & Rockmore, D.N. (2013). Stability of the world trade web over time—an extinction analysis. *Journal of Economic Dynamics and Control*, 37(9), 1889-1910. doi:10.1016/j.jedc.2013.04.009
- [41] PMSEIC. (2010). *Australia and Food Security in a Changing World*. Canberra, Australia: The Prime Minister's Science, Engineering and Innovation Council.

- [42] Rotz, S. & Fraser, E.D.G. (2015). Resilience and the industrial food system: Analyzing the impacts of agricultural industrialization on food system vulnerability. *Journal of Environmental Studies and Sciences*, 5(3), 459-473. doi:10.1007/s13412-015-0277-1
- [43] Puma, M.J., Bose, S., Chon, S.Y., & Cook, B.I. (2015). Assessing the evolving fragility of the global food system. *Environmental Research Letters*, 10(2), 024007. doi:10.1088/1748-9326/10/2/024007
- [44] Smith, K., Lawrence, G., MacMahon, A., Muller, J., & Brady, M. (2016). The resilience of long and short food chains: a case study of flooding in Queensland, Australia. *Agriculture and Human Values*, 33(1), 45-60. doi:10.1007/s10460-015-9603-1
- [45] Nicholls, R.J., Wong, P.P., Burkett, V., Woodroffe, C.D., & Hay, J. (2008). Climate change and coastal vulnerability assessment: scenarios for integrated assessment. *Sustainability Science*, 3(1), 89-102. doi:10.1007/s11625-008-0050-4
- [46] Singh-Peterson, L. & Lawrence, G. (2015). Insights into community vulnerability and resilience following natural disasters: perspectives with food retailers in Northern NSW, Australia. *Local Environment*, 20(7), 782-795. doi:10.1080/13549839.2013.873396
- [47] Huff, A.G., Beyeler, W.E., Kelley, N.S., & McNitt, J.A. (2015). How resilient is the United States' food system to pandemics? *Journal of Environmental Studies and Sciences*, 5(3), 337-347. doi:10.1007/s13412-015-0275-3
- [48] Deaton, B.J. & Deaton, B.J. (2020). Food security and Canada's agricultural system challenged by COVID-19. *Canadian Journal of Agricultural Economics/Revue canadienne d'agroeconomie*. doi:10.1111/cjag.12227
- [49] Hobbs, J.E. (2020). Food supply chains during the COVID-19 pandemic. *Canadian Journal of Agricultural Economics/Revue canadienne d'agroeconomie*. doi:10.1111/cjag.12237
- [50] Laborde, D., Martin, W., Swinnen, J., & Vos, R. (2020). COVID-19 risks to global food security. *Science*, 369(6503), 500-502. doi:10.1126/science.abc4765
- [51] Mount, P. (2012). Growing local food: scale and local food systems governance. *Agriculture and Human Values*, 29(1), 107-121. doi:10.1016/j.appet.2010.11.237
- [52] Brown, K.H. & Jameton, A.L. (2000). Public health implications of urban agriculture. *Journal of public health policy*, 21(1), 20-39. doi:10.2307/3343472
- [53] Heederik, D., Sigsgaard, T., Thorne, P.S., Kline, J.N., Avery, R., Bønløkke, J.H., Chrischilles, E.A., Dosman, J.A., Duchaine, C., & Kirkhorn, S.R. (2007). Health effects of airborne exposures from concentrated animal feeding operations. *Environmental Health Perspectives*, 115(2), 298-302. doi:10.1289/ehp.8835
- [54] Edwards-Jones, G., Milà i Canals, L., Hounsborne, N., Truninger, M., Koerber, G., Hounsborne, B., Cross, P., York, E.I., Hospido, A., & Plassmann, K. (2008). Testing the assertion that 'local food is best': the challenges of an evidence-based approach. *Trends in Food Science & Technology*, 19(5), 265-274.
- [55] Bian, Z.H., Yang, Q.C., & Liu, W.K. (2015). Effects of light quality on the accumulation of phytochemicals in vegetables produced in controlled environments: a review. *Journal of the Science of Food and Agriculture*, 95(5), 869-877. doi:10.1002/jsfa.6789
- [56] Darko, E., Heydarizadeh, P., Schoefs, B., & Sabzalian, M.R. (2014). Photosynthesis under artificial light: the shift in primary and secondary metabolism. *Philosophical Transactions of the Royal Society B: Biological Sciences*, 369(1640), 20130243. doi:10.1098/rstb.2013.0243
- [57] Samuolienė, G., Brazaitytė, A., Sirtautas, R., Viršilė, A., Sakalauskaitė, J., Sakalauskienė, S., & Duchovskis, P. (2013). LED illumination affects bioactive compounds in romaine baby leaf lettuce. *Journal of the Science of Food and Agriculture*, 93(13), 3286-3291. doi:10.1002/jsfa.6173
- [58] Brazaitytė, A., Sakalauskienė, S., Samuolienė, G., Jankauskienė, J., Viršilė, A., Novičkovas, A., Sirtautas, R., Miliauskienė, J., Vaštakaitė, V., & Dabašinskas, L. (2015). The effects of LED illumination spectra and intensity on carotenoid content in Brassicaceae microgreens. *Food chemistry*, 173, 600-606. doi:10.1016/j.foodchem.2014.10.077
- [59] Cocetta, G., Casciani, D., Bulgari, R., Musante, F., Kolton, A., Rossi, M., & Ferrante, A. (2017). Light use efficiency for vegetables production in protected and indoor environments. *The European Physical Journal Plus*, 132(1), 1-15. doi:10.1140/epjp/i2017-11298-x
- [60] Choi, H.G., Moon, B.Y., & Kang, N.J. (2015). Effects of LED light on the production of strawberry during cultivation in a plastic greenhouse and in a growth chamber. *Scientia Horticulturae*, 189, 22-31. doi:10.1016/j.scienta.2015.03.022
- [61] Chen, X.L., Yang, Q.C., Song, W.P., Wang, L.C., Guo, W.Z., & Xue, X.Z. (2017). Growth and nutritional properties of lettuce affected by different alternating intervals of red and blue LED irradiation. *Scientia Horticulturae*, 223, 44-52. doi:10.1016/j.scienta.2017.04.037

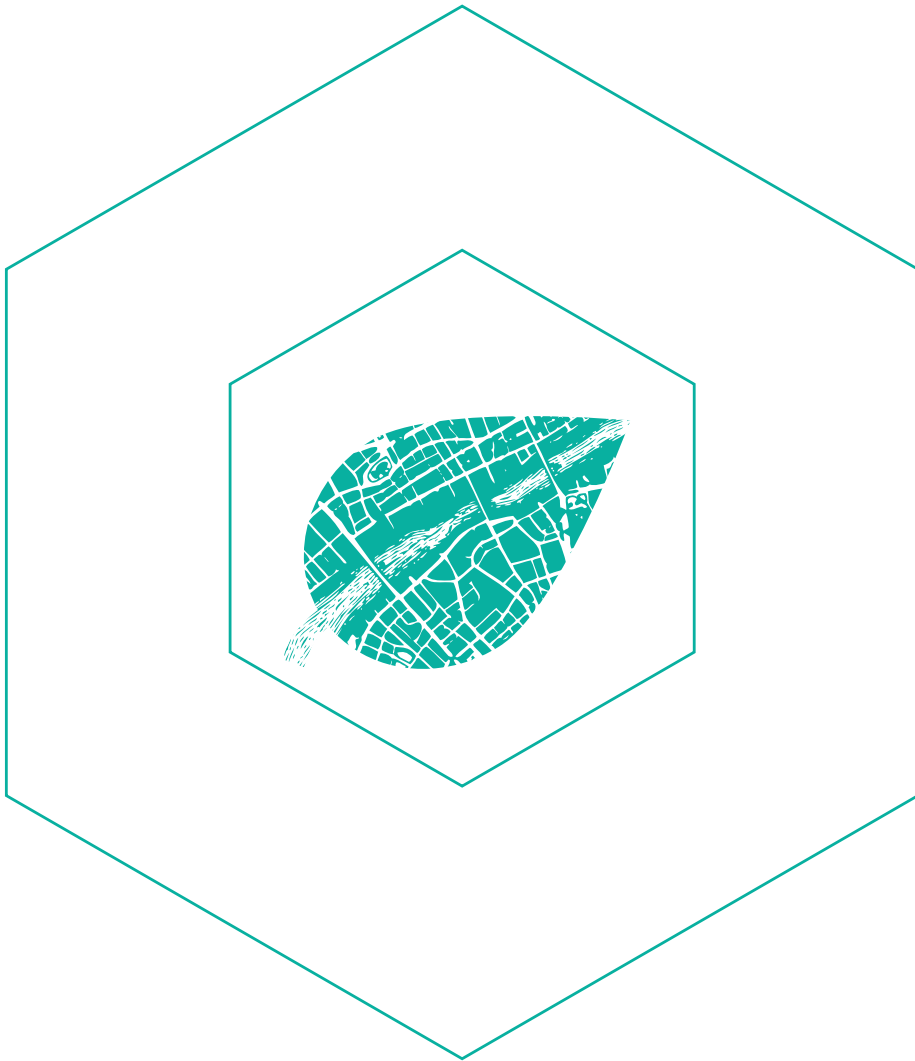
- [62] Lee, J.H., Oh, M.M., & Son, K.H. (2019). Short-term Ultraviolet (UV)-A Light-Emitting Diode (LED) radiation improves biomass and bioactive compounds of kale. *Frontiers in plant science*, 10(1042). doi:10.3389/fpls.2019.01042
- [63] Poiroux-Gonord, F., Bidel, L.P.R., Fanciullino, A.L., Gautier, H., Lauri-Lopez, F., & Urban, L. (2010). Health benefits of vitamins and secondary metabolites of fruits and vegetables and prospects to increase their concentrations by agronomic approaches. *Journal of Agricultural and Food Chemistry*, 58(23), 12065-12082. doi:10.1021/jf1037745
- [64] O'Sullivan, C.A., Bonnett, G.D., McIntyre, C.L., Hochman, Z., & Wasson, A.P. (2019). Strategies to improve the productivity, product diversity and profitability of urban agriculture. *Agricultural Systems*, 174, 133-144. doi:10.1016/j.agsy.2019.05.007
- [65] Rickman, J.C., Barrett, D.M., & Bruhn, C.M. (2007). Nutritional comparison of fresh, frozen and canned fruits and vegetables. Part 1. Vitamins C and B and phenolic compounds. *Journal of the Science of Food and Agriculture*, 87(6), 930-944. doi:10.1002/jsfa.2825
- [66] Rickman, J.C., Bruhn, C.M., & Barrett, D.M. (2007). Nutritional comparison of fresh, frozen, and canned fruits and vegetables II. Vitamin A and carotenoids, vitamin E, minerals and fiber. *Journal of the Science of Food and Agriculture*, 87(7), 1185-1196. doi:10.1002/jsfa.2824
- [67] Slavin, J.L. & Lloyd, B. (2012). Health benefits of fruits and vegetables. *Advances in nutrition*, 3(4), 506-516. doi:10.3945/an.112.002154
- [68] Dyer, J.A., Desjardins, R.L., Karimi-Zindashty, Y., & McConkey, B.G. (2011). Comparing fossil CO₂ emissions from vegetable greenhouses in Canada with CO₂ emissions from importing vegetables from the southern USA. *Energy for Sustainable Development*, 15(4), 451-459. doi:10.1016/j.esd.2011.08.004
- [69] WHO (Producer). (2020, 27 MAY 2020). World Health Organisation - Healthy diet fact sheet n° 394. Retrieved from <https://www.who.int/en/news-room/fact-sheets/detail/healthy-diet>
- [70] Willett, W., Rockström, J., Loken, B., Springmann, M., Lang, T., Vermeulen, S., Garnett, T., Tilman, D., DeClerck, F., & Wood, A. (2019). Food in the Anthropocene: the EAT–Lancet Commission on healthy diets from sustainable food systems. *The Lancet*, 393(10170), 447-492. doi:10.1016/S0140-6736(18)31788-4
- [71] Rodriguez-Casado, A. (2016). The health potential of fruits and vegetables phytochemicals: notable examples. *Critical reviews in food science and nutrition*, 56(7), 1097-1107. doi:10.1080/10408398.2012.755149
- [72] Chong, M.F.F., Macdonald, R., & Lovegrove, J.A. (2010). Fruit polyphenols and CVD risk: a review of human intervention studies. *British Journal of Nutrition*, 104(S3), S28-S39. doi:10.1017/S0007114510003922
- [73] Benis, K. & Ferrão, P. (2017). Potential mitigation of the environmental impacts of food systems through urban and peri-urban agriculture (UPA)—a life cycle assessment approach. *Journal of cleaner production*, 140, 784-795. doi:10.1016/j.jclepro.2016.05.176
- [74] Poore, J. & Nemecek, T. (2018). Reducing food's environmental impacts through producers and consumers. *Science*, 360(6392), 987-992. doi:10.1126/science.aag0216
- [75] Elango, R., Humayun, M.A., Ball, R.O., & Pencharz, P.B. (2011). Protein requirement of healthy school-age children determined by the indicator amino acid oxidation method. *The American journal of clinical nutrition*, 94(6), 1545-1552. doi:10.3945/ajcn.111.012815
- [76] Humayun, M.A., Elango, R., Ball, R.O., & Pencharz, P.B. (2007). Reevaluation of the protein requirement in young men with the indicator amino acid oxidation technique. *The American journal of clinical nutrition*, 86(4), 995-1002. doi:10.1093/ajcn/86.4.995
- [77] Marini, J.C. (2015). Protein requirements: are we ready for new recommendations? *The Journal of nutrition*, 145(1), 5-6. doi:10.3945/jn.114.203935
- [78] Rafii, M., Chapman, K., Elango, R., Campbell, W.W., Ball, R.O., Pencharz, P.B., & Courtney-Martin, G. (2015). Dietary protein requirement of men > 65 years old determined by the indicator amino acid oxidation technique is higher than the current estimated average requirement. *The Journal of nutrition*, 146(4), 681-687. doi:10.3945/jn.115.225631
- [79] Rafii, M., Chapman, K., Owens, J., Elango, R., Campbell, W.W., Ball, R.O., Pencharz, P.B., & Courtney-Martin, G. (2015). Dietary protein requirement of female adults > 65 years determined by the indicator amino acid oxidation technique is higher than current recommendations. *The Journal of nutrition*, 145(1), 18-24. doi:10.3945/jn.114.197517
- [80] Tang, M.H., McCabe, G.P., Elango, R., Pencharz, P.B., Ball, R.O., & Campbell, W.W. (2014). Assessment of protein requirement in octogenarian women with use of the indicator amino acid oxidation technique. *The American journal of clinical nutrition*, 99(4), 891-898. doi:10.3945/ajcn.112.042325

- [81] Wolfe, R.R., Rutherford, S.M., Kim, I.Y., & Moughan, P.J. (2016). Protein quality as determined by the digestible indispensable amino acid score: evaluation of factors underlying the calculation. *Nutrition reviews*, 74(9), 584-599. doi:10.1093/nutrit/nuw022
- [82] Marinangeli, C.P.F. & House, J.D. (2017). Potential impact of the digestible indispensable amino acid score as a measure of protein quality on dietary regulations and health. *Nutrition reviews*, 75(8), 658-667. doi:10.1093/nutrit/nux025
- [83] Huang, S.Q., Wang, L.M., Sivendiran, T., & Bohrer, B.M. (2018). Amino acid concentration of high protein food products and an overview of the current methods used to determine protein quality. *Critical reviews in food science and nutrition*, 58(15), 2673-2678. doi:10.1080/10408398.2017.1396202
- [84] FAO. (2018). *Sustainable food systems - Concept and framework*. Rome, Italy. doi:10.4060/CA1796EN
- [85] Brauman, K.A., Richter, B.D., Postel, S., Malsy, M., & Flörke, M. (2016). Water depletion: An improved metric for incorporating seasonal and dry-year water scarcity into water risk assessments. *Elem Sci Anth*, 4. doi:10.12952/journal.elementa.000083
- [86] FAO. (2018). *World food and agriculture - Statistical pocketbook 2018*. Rome, Italy. doi:10.4060/CA1796EN
- [87] Foley, J.A., Ramankutty, N., Brauman, K.A., Cassidy, E.S., Gerber, J.S., Johnston, M., Mueller, N.D., O'Connell, C., Ray, D.K., & West, P.C. (2011). Solutions for a cultivated planet. *Nature*, 478(7369), 337-342. doi:10.1038/nature10452
- [88] Lake, I.R., Hooper, L., Abdelhamid, A., Bentham, G., Boxall, A.B.A., Draper, A., Fairweather-Tait, S., Hulme, M., Hunter, P.R., & Nichols, G. (2012). Climate change and food security: health impacts in developed countries. *Environmental Health Perspectives*, 120(11), 1520-1526. doi:10.1289/ehp.1104424
- [89] Sandström, V., Valin, H., Krisztin, T., Havlík, P., Herrero, M., & Kastner, T. (2018). The role of trade in the greenhouse gas footprints of EU diets. *Global Food Security*, 19, 48-55. doi:10.1016/j.gfs.2018.08.007
- [90] Goldstein, B., Birkved, M., Quitzau, M.B., & Hauschild, M. (2013). Quantification of urban metabolism through coupling with the life cycle assessment framework: concept development and case study. *Environmental Research Letters*, 8(3), 035024. doi:10.1088/1748-9326/8/3/035024
- [91] Payen, S., Basset-Mens, C., & Perret, S. (2015). LCA of local and imported tomato: an energy and water trade-off. *Journal of cleaner production*, 87, 139-148. doi:10.1016/j.jclepro.2014.10.007
- [92] Hospido, A., i Canals, L.M., McLaren, S., Truninger, M., Edwards-Jones, G., & Clift, R. (2009). The role of seasonality in lettuce consumption: a case study of environmental and social aspects. *The International Journal of Life Cycle Assessment*, 14(5), 381-391. doi:10.1007/s11367-009-0091-7
- [93] Carlsson-Kanyama, A., Ekström, M.P., & Shanahan, H. (2003). Food and life cycle energy inputs: consequences of diet and ways to increase efficiency. *Ecological Economics*, 44(2-3), 293-307. doi:10.1016/S0921-8009(02)00261-6
- [94] Körner, O. & Challa, H. (2003). Design for an improved temperature integration concept in greenhouse cultivation. *Computers and electronics in agriculture*, 39(1), 39-59. doi:10.1016/S0168-1699(03)00006-1
- [95] Frantz, J.M., Ritchie, G., Cometti, N.N., Robinson, J., & Bugbee, B. (2004). Exploring the limits of crop productivity: beyond the limits of tipburn in lettuce. *Journal of the American Society for Horticultural Science*, 129(3), 331-338.
- [96] Campen, J.B. & Bot, G.P.A. (2003). Determination of greenhouse-specific aspects of ventilation using three-dimensional computational fluid dynamics. *Biosystems Engineering*, 84(1), 69-77. doi:10.1016/S1537-5110(02)00221-0
- [97] Körner, O. & Challa, H. (2003). Process-based humidity control regime for greenhouse crops. *Computers and electronics in agriculture*, 39(3), 173-192. doi:10.1016/S0168-1699(03)00079-6
- [98] Nienhuis, J.K. & de Vreede, P.J.A. (1996). *Utility of the environmental life cycle assessment method in horticulture*. Paper presented at the XIII International Symposium on Horticultural Economics 429.
- [99] Elings, A., Kempkes, F.L.K., Kaarsemaker, R.C., Ruijs, M.N.A., Van de Braak, N.J., & Dueck, T.A. (2004). *The energy balance and energy-saving measures in greenhouse tomato cultivation*. Paper presented at the International Conference on Sustainable Greenhouse Systems: Greensys2004.
- [100] Massa, G.D., Kim, H.H., Wheeler, R.M., & Mitchell, C.A. (2008). Plant productivity in response to LED lighting. *HortScience*, 43(7), 1951-1956. doi:10.21273/HORTSCI.43.7.1951
- [101] Watson, R.T., Boudreau, M.C., & van Iersel, M.W. (2018). Simulation of greenhouse energy use: An application of energy informatics. *Energy Informatics*, 1(1), 1. doi:10.1007/s42162-018-0005-7
- [102] Bartzas, G., Zaharaki, D., & Komnitsas, K. (2015). Life cycle assessment of open field and greenhouse cultivation of lettuce and barley. *Information Processing in Agriculture*, 2(3-4), 191-207. doi:10.1016/j.inpa.2015.10.001

- [103] Muñoz, P., Antón, A., Nuñez, M., Paranjpe, A., Ariño, J., Castells, X., Montero, J.I., & Rieradevall, J. (2007). *Comparing the environmental impacts of greenhouse versus open-field tomato production in the Mediterranean region*. Paper presented at the International Symposium on High Technology for Greenhouse System Management: Greensys2007, Naples. Italy.
- [104] Smith, P., Haberl, H., Popp, A., Erb, K.H., Lauk, C., Harper, R., Tubiello, F.N., de Siqueira Pinto, A., Jafari, M., & Sohi, S. (2013). How much land-based greenhouse gas mitigation can be achieved without compromising food security and environmental goals? *Global change biology*, 19(8), 2285-2302. doi:10.1111/gcb.12160
- [105] Davis, K.F., Gephart, J.A., Emery, K.A., Leach, A.M., Galloway, J.N., & D'Odorico, P. (2016). Meeting future food demand with current agricultural resources. *Global Environmental Change*, 39, 125-132. doi:10.1016/j.gloenvcha.2016.05.004
- [106] Bryngelsson, D., Wirsenius, S., Hedenus, F., & Sonesson, U. (2016). How can the EU climate targets be met? A combined analysis of technological and demand-side changes in food and agriculture. *Food Policy*, 59, 152-164. doi:10.1016/j.foodpol.2015.12.012
- [107] Dueck, T.A., Kempkes, F.L.K., Meinen, E., & Stanghellini, C. (2016). *Choosing crops for cultivation in space*. Paper presented at the 46th International Conference on Environmental Systems, Vienna, Austria.

INTERMEZZO 1

The main objective of this study is to quantify the resource use efficiency of crop production in plant factories and explore their potential as a method for urban food production. Insight into the role of plant processes in the total energy balance is required to adequately calculate resource use. The crop energy balance depends on the production climate and was described as a crop energy balance model. The model was used to estimate the vapour flux as well as the relation between sensible and latent heat. It provided valuable input for determining the climatisation and performance of plant factories.

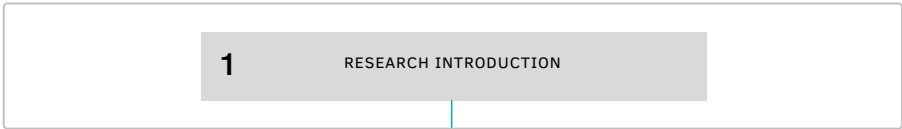


2 System configuration

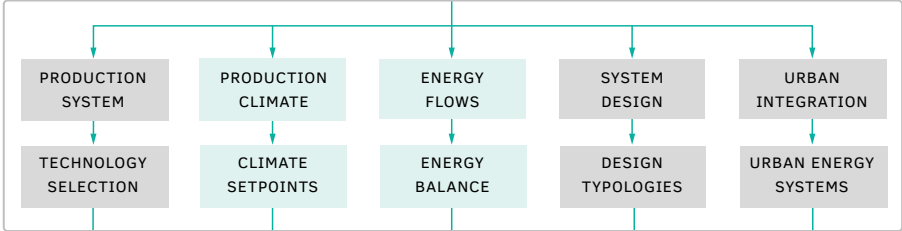
Plant factories; crop transpiration and energy balance
Graamans, L., van den Dobbelsteen, A., Meinen, E., Stanghellini, C.
Agricultural Systems. 2017; 153: 138-147.
[doi:10.1016/j.agsy.2017.01.003](https://doi.org/10.1016/j.agsy.2017.01.003)

ABSTRACT Population growth and rapid urbanisation may result in a shortage of food supplies for cities in the foreseeable future. Research on closed plant production systems, such as plant factories, has attempted to offer perspectives for robust (urban) agricultural systems. Insight into the explicit role of plant processes in the total energy balance of these production systems is required to determine their potential. We describe a crop transpiration model that is able to determine the relation between sensible and latent heat exchange, as well as the corresponding vapour flux for the production of lettuce in closed systems. Subsequently, this model is validated for the effect of photosynthetic photon flux, cultivation area cover and air humidity on lettuce transpiration, using literature research and experiments. Results demonstrate that the transpiration rate was accurately simulated for the aforementioned effects. Thereafter we quantify and discuss the energy productivity of a standardised plant factory and illustrate the importance of transpiration as a design parameter for climatisation. Our model can provide a greater insight into the energetic expenditure and performance of closed systems. Consequently, it can provide a starting point for determining the viability and optimisation of plant factories.

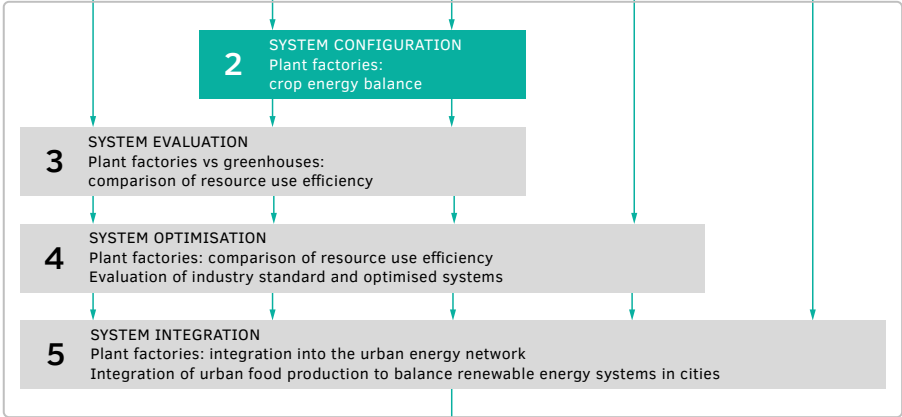
I. INTRODUCTION & METHODOLOGICAL FRAMEWORK



II. THEORETICAL FRAMEWORK



III. DESIGN & EXPERIMENTAL VALIDATION



IV. INTEGRATED DISCUSSION



2.1 Introduction

Expanding cities no longer derive their food supply from their hinterlands, but rely on the global food trade. Given the limited availability of land, water and nutrients, however, the sustainability of these networks is questionable [1-4]. Research on urban agriculture, plant factories and vertical farming has attempted to offer new perspectives for robust food production systems for cities. These systems generally focus on the development of local high-density production in closed plant production systems [5-8]. These systems can also be integrated into (structurally vacant) high-rise buildings for vertical farming.

Agriculture always has relied on sunlight to power photosynthesis. Greenhouse horticulture uses solar energy both for photosynthesis and heating, by creating a (semi-)closed environment. This is one of the reasons for its productivity. Greenhouses create a controlled environment for plant production where excess (solar) energy is discharged by ventilation and deficits can be compensated by heating. As management of microclimate is fundamental to greenhouse agriculture, it relies on a broad body of knowledge, in particular with regard to the related energetic fluxes and requirements.

Commercial vegetable production in closed systems, however, is a relatively new issue. It focuses on the development of new typologies, such as plant factories and vertical farms [9]. As a working definition, a vertical farm can be regarded as a multi-storey plant factory. In spite of the possible benefits, an obvious disadvantage of plant factories is the need for artificial lighting for photosynthesis and energy for air conditioning (cooling and vapour removal, both relying on forced air circulation). In particular, the combination of high-density crop production, limited dimensions and lack of natural ventilation is likely to result in a high demand for dehumidification.

The interior climate and the related energetic fluxes of plant factories have to be investigated in order to quantify these additional energy requirements. Closed systems limit the exchange of energy with the exterior climate. As a result, all energy entering the system has to leave the system through forced air circulation and conditioning. As cooling and vapour removal are quite different processes, however, the distribution between sensible and latent heat is a key factor. Therefore, the energy balance must be based on an accurate estimate of the crop transpiration coefficient, i.e. the fraction of the radiation load dissipated by the crop as latent heat.

To this end, it is essential to simulate the energetic behaviour of the crop – how it transpires, reflects light and exchanges heat and radiation. The results of research on the energy profile offer the starting point for the discussion on the possible benefits of plant factories compared with traditional greenhouses.

Objective

The main objective of this study was to explicate the energetic fluxes associated with the production of lettuce in plant factories. In particular, an approach for the estimation of transpiration was formulated and validated in order to illustrate the effect of the crop on the energetic distribution of sensible and latent heat.

Outline

We propose a model that is able to determine the relation between sensible heat and latent heat exchange and the corresponding vapour flux for the production of lettuce in closed systems. This model is validated by literature research as well as by experiments on the effect of photosynthetic photon flux density, cultivation area cover and vapour concentration deficit on lettuce transpiration. Subsequently the energy productivity of such a plant factory is quantified and discussed.

2.2 Theoretical background

This section addresses the energy balance and individual energetic fluxes resulting from closed plant production in a building structure. In particular, we specify our adaptation of the Penman-Monteith crop transpiration method, the ‘big leaf’ model.

2.2.1 Energy balance

Numerous models exist to analyse the energy balance in various greenhouse typologies, crops and production methods. It is necessary, however, to determine the impact of the plant factory typology on the various energy fluxes and the resulting interior climate. The plant processes play a key role in the total energy balance. In particular the crop transpiration is of paramount importance.

The following literature survey is intended to provide insight into the interdependency of various climatic variables. These data were used to formulate a model calculating the relative share of radiation load that is dissipated as sensible and latent heat.

2.2.1.1 Standard greenhouse energy balance

Using the greenhouse air as the control volume of interest, the control surface is composed of the glazing, the ground, components within the greenhouse and any open points of entry, including vents and gaps. The transfer of energy across these surfaces involves both sensible and latent heat exchanges [10]. The energy balance equation for greenhouses is adapted from Sabeh [11] and is illustrated in Figure 2.1 and represented by the following equation:

$$Q_{rad} + Q_{fac} + Q_{comp} + Q_{soil} + Q_{plant} + Q_{lat} + Q_{vent} + Q_{heat} = 0 \quad [2.1]$$

Q_{rad} represents heat transfer by radiation. Q_{fac} is the heat transfer across the glazing via conduction and convection. Q_{comp} represents the heat transfer by the various greenhouse components, including structural components and production systems. Q_{soil} is the heat transfer between the ground and greenhouse air. Q_{plant} represents the heat transfer by the evapotranspiration of plants, which transfers latent and sensible heat energy to the greenhouse air. Q_{lat} is the latent heat transfer of sensible energy in the air to water in the form of fog droplets. Q_{vent} represents the heat transfer by natural and mechanical ventilation, which removes energy from the greenhouse via air exchange. Finally, Q_{heat} is the energy added to the greenhouse using a heating system. This greenhouse energy balance represents a simplified, illustrative model and does not include elements of thermal inertia.

2.2.1.2 Plant factory energy balance

The energy balance as stated in Equation 2.1 applies to archetypical light-transmitting and naturally ventilated greenhouses, with solar energy as the exclusive source of photosynthetically active radiation (PAR). This equation has to be adapted in order to determine the energy balance for plant factories. The plant factory features a highly insulated construction, which limits thermal exchange with its surroundings. Therefore, the building structure can be considered as adiabatic; Q_{soil} can also be omitted.

Other differences with the standard greenhouse energy balance include the exclusive use of mechanical air circulation and conditioning for heating and cooling; Q_{vent} and Q_{heat} become Q_{HVAC} . The influence of structural elements is integrated within Q_{fac} . Finally, the energetic flux resulting from the inefficiency of production components/ systems (e.g. artificial lighting) is redefined as Q_{equip} . The energy balance for the plant factory is illustrated in Figure 2.2 and represented by the following equation:

$$Q_{rad} + Q_{fac} + Q_{plant} + Q_{lat} + Q_{equip} + Q_{HVAC} = 0 \quad [2.2]$$

The share of Q_{rad} and Q_{fac} in the total energy balance is likely to be reduced compared to standard greenhouses. This is the result of insulation properties and the relatively small surface area in plant factories, which usually consist of multiple layers. In the case of fully artificial production with an opaque façade the Q_{rad} can be omitted, resulting in the following equation:

$$Q_{fac} + Q_{plant} + Q_{lat} + Q_{equip} + Q_{HVAC} = 0 \quad [2.3]$$

Closed production systems allow for a highly steady interior climate. Consequently, the influence of thermal inertia in the energy balance of the facility is very small and is not included in this simplified energy balance equation. Additionally, the transpiration model below is formulated as a steady state model, as opposed to dynamic.

2.2.2 Plant processes

The crop has a tremendous impact on its environment; it absorbs and emits radiation, exchanges heat with air and transpires. The crop transpiration coefficient, that is the fraction of the radiation load dissipated as latent heat, is key in quantifying the energy requirement of the system. In this study the Penman-Monteith approach, the 'big leaf' model, is used to estimate the transpiration and consequent energetic fluxes of the production of lettuce in the fully controlled conditions of a plant factory. This approach permits certain simplifying assumptions.

Since the first data on crop transpiration became available around 1920, it has been demonstrated that the data is far from constant [12]. Penman demonstrated that crop transpiration primarily is a physical process. The components of this process are the energy available at the transpiring surface and the ability of air to extract vapour from this surface; it is partially influenced by the crop itself [13-15]. Monteith

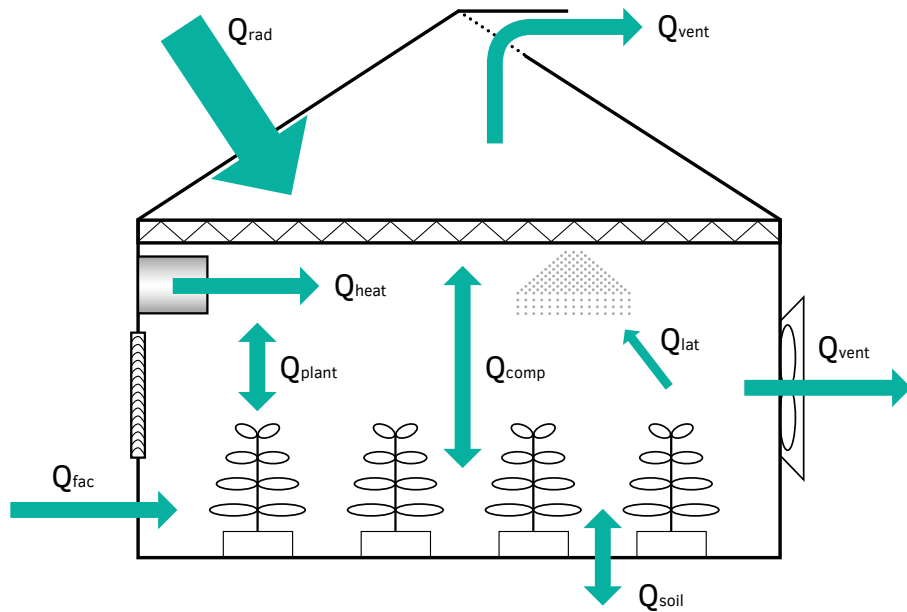


FIG. 2.1 Green house energy balance, adapted from Sabeh [11].

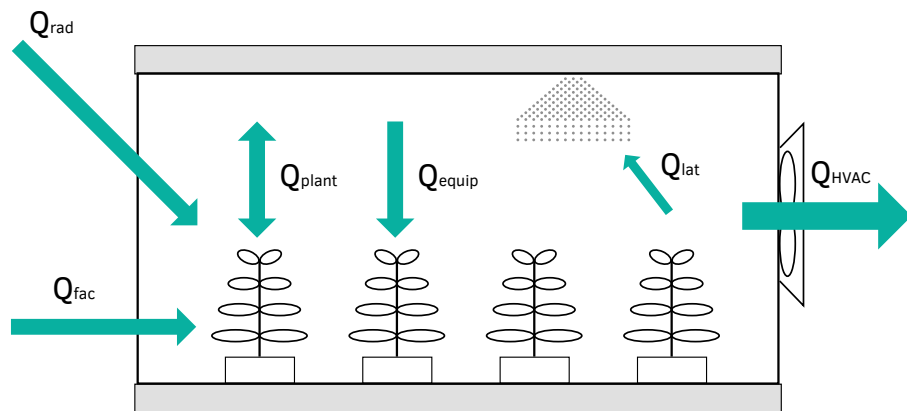


FIG. 2.2 Plant factory energy balance.

[16] re-wrote Penman's equation, explicitly identifying the parameters that are affected by the crop.

The Penman-Monteith (PM) equation [16] is based on the assumption that the three-dimensional crop canopy can be reduced to a one-dimensional 'big leaf' where net radiation is absorbed, heat is exchanged and water vapour escapes. This equation requires the crop to be homogeneous, level, continuous and extensive.

In a natural environment (open air) the sun is the only source of energy and the wind determines the removal rate of vapour from the transpiring surfaces. The PM equation describes this phenomenon and has been the basis of most crop transpiration models that were developed afterwards. A greenhouse, however, constitutes a peculiar environment. Therefore, there have been considerable research efforts to predict the (evapo)transpiration of greenhouse crops [10, 17, 18].

2.2.2.1 Crop energy balance

At equilibrium, the amount of energy arriving at the 'big leaf' surface must equal the amount leaving it. All fluxes of energy should be considered when deriving an energy balance equation. Energy directly related to photomorphogenesis, however, is limited [19] and can be considered negligible [20]. The energy balance equation for a transpiring plant surface is then comprised of net radiation (I_{net}), sensible heat exchange (H) and latent heat exchange (λE):

$$I_{net} - H - \lambda E = 0 \quad [2.4]$$

R_{net} , the amount of radiation intercepted and absorbed by the crop depends on the amount of leaves present and how they are distributed. Lettuce crops consist of multiple, irregular, overlapping leaves. This results in an increased transpiring surface, with respect to the projected surface of the 'big leaf'. Therefore, leaf area index (LAI) plays an essential role in determining the energy balance. In this study LAI is defined as the ratio of leaf area divided by cultivation panel area. See Section 2.3.1.4 and below for how the LAI of the lettuce crop is incorporated into the equations for sensible and latent heat exchange. The equation for the transfer of sensible heat from the leaf canopy to the surrounding climate is:

$$H = LAI \cdot \rho_{air} \cdot c_{p,air} \cdot \frac{T_s - T_{air}}{r_a} \quad [2.5]$$

This equation demonstrates that the sensible heat flux is commanded by a single resistance, namely the aerodynamic resistance to heat (r_a). The sensible heat flux depends on the difference between the temperature at the transpiring surface (T_s) and in the surrounding air (T_{air}). In order to calculate the latent heat exchange it is necessary to determine the transfer of vapour. This transfer is represented by the following equation:

$$\lambda E = LAI \cdot \lambda \cdot \frac{(\chi_s - \chi_{air})}{r_{ss} + r_a} \quad [2.6]$$

This equation accounts for the fact that the vapour flux from the substomatal cavities to the surrounding ‘free’ air encounters two consecutive resistances: the surface (or stomatal) resistance (r_{ss}) and the aerodynamic resistance (r_a) to vapour transfer. The latent heat flux depends on the difference between the vapour concentration at the transpiring surface (χ_s) and in the surrounding air (χ_{air}).

Penman [15] added the imperative fourth equation by postulating that the transpiring surface is saturated at its temperature and Monteith [16] applied only the first (linear) term of the Taylor’s expansion of the saturation hypothesis, leading to the following equation:

$$\chi_s \cong \chi_{air}^* + \frac{\rho_{air} \cdot c_{p,air}}{\lambda} \cdot \epsilon \cdot (T_s - T_{air}) \quad [2.7]$$

This allowed for the derivation of an analytical (PM) equation for crop transpiration that could be solved in a world still devoid of computer power. The limit to the applicability of the PM equation is the knowledge of the variables that have been introduced to describe the energy exchange of the ‘big leaf’.

2.2.2.2 Add-ons to the ‘big leaf’ model

The transfer of heat and water vapour between the ‘big leaf’ and the surrounding air is governed by various functions relating to air movement, temperature, vapour pressure deficit and radiation. Applying this model to greenhouse crops, several studies have combined the PM equation with the thermal balance equation of the canopy and consequently the entire greenhouse energy balance [10, 21]. Models for greenhouse crop transpiration have been described by Stanghellini [18], Chalabi et al. [22], Aikman et al. [23] and Jolliet [24]. The main differences between these models pertain to the radiation absorption coefficient and the (stomatal and boundary layer) resistances. In order to use the Penman-Monteith equation in a predictive setting, methods for determining the aerodynamic resistance and the

surface resistance (r_{ss}) should be available [25, 26]. The submodels for I_{net} , r_a and r_{ss} are explained below.

2.3 Materials: Model overview

This section addresses the submodels used in this study for net radiation, surface resistance and aerodynamic resistance. Consequently, we elucidate the MATLAB model that formulates the distribution of the sensible and latent component of the lettuce canopy.

2.3.1 Submodels

2.3.1.1 Submodel for net radiation

The net radiation (I_{net}) is the radiation (I_{light}) effectively absorbed by the crop, i.e. light that is intercepted (the ratio of projected leaf area to cultivation area, or cultivation area cover CAC) and not reflected (reflection coefficient c_r). This fraction generally depends on the amount of leaves, their distribution and orientation. The equation for the net radiation is:

$$I_{net} = (1 - c_r) \cdot I_{light} \cdot CAC \quad [2.8]$$

The reflection coefficient of lettuce for PAR, is reported to be 5-8% [27]. The present leaf area is either known or estimated as a function of degree-days. However, the correlation between leaf area and cultivation area cover is rather poor for closed crops such as lettuce. Pollet et al. [17] confirm this by concluding that cultivation area cover (soil cover in traditional agriculture) was best estimated through imaging of the vertical projected leaf area. In lettuce, the cultivation area cover remains relatively constant throughout its development. The coverage expands rapidly in the early stages of growth, certainly under the relatively high temperatures of plant factories. This expansion is followed by densification of the crop within these boundaries, an increase in LAI. This results in a high and consistent percentage

of cultivation area coverage [28]. We recommend a value of 90% cultivation area coverage for predictive, static calculations.

2.3.1.2 Submodel for surface (stomatal) resistance

The surface resistance (r_{ss}) represents the resistance of vapour flow through the transpiring crop, as well as from uncovered, evaporating soil surface [29]. What is generally known is that stomata open under increasing photosynthetic photon flux densities (PPFD), resulting in a decrease of resistance. Therefore, applying a single value for r_{ss} will reduce accuracy, and is not to be preferred, in spite of the standardisation, comparability, consistency and simplicity of calculations and simulations.

Several models for r_{ss} in lettuce have been designed, based on experimental data (i.e. [17, 25, 26]). These empirical equations generally represent the influence of air temperature, vapour pressure deficit and PPFD on surface resistance, following the multiplicative method first proposed by Jarvis [30]. The relevance of additional factors beyond light has since been debated [17], also in view of the limited validity of the multiplicative method outside the particular range for which parameters have been determined in each case [31].

Recently it has been shown that the spectral distribution may play a role in determining stomatal resistance. Wang et al. [32] found that different red/blue ratios in particular influence the r_s of lettuce and illustrate the response of stomatal conductance to irradiance. After extrapolating their data, we formulated a general equation for r_{ss} by fitting a rectangular hyperbola and approximating the parameters. This equation for r_{ss} uses the light-dependent term $PPFD$ in $\mu\text{mol m}^{-2} \text{s}^{-1}$:

$$r_{ss} = 60 \cdot \frac{1500 + PPFD}{200 + PPFD} \quad [2.9]$$

Faute de mieux, we adopted the hypothesis that r_{ss} can be approximated by the photosynthetic photon flux density and is less dependent on any synergistic interaction of all variables. This will allow us to approximate r_{ss} regardless of spectrum, lighting strategy and climate settings.

2.3.1.3 Submodel for aerodynamic boundary layer resistance

The aerodynamic boundary layer resistance influences the transfer of sensible heat and water vapour from the leaf surface into the surrounding air. To determine r_a , an analogy generally is made with the resistance to momentum transfer [26, 29, 33]. Aerodynamic resistance usually is described by an expression, derived from turbulent transfer and the assumption of a logarithmic wind profile [25, 34, 35]. This approach is evidently unsuitable for closed environments.

In the controlled environment of a plant factory, the relatively high air circulation rate is what determines vapour and heat removal from the crop. The air is subsequently conditioned without the need for fresh air in the plant factory. Fuchs [36] proposes a method that integrates the mean leaf diameter (l), the uninhibited air speed ($u_{air,\infty}$) and LAI:

$$r_a = 350 \cdot \frac{l^{0.5}}{u_{air,\infty}} \cdot LAI^{-1} \quad [2.10]$$

It has frequently been shown (e.g., [18]) that crop transpiration is only slightly dependent on the aerodynamic boundary layer resistance (as a consequence of the thermal feed-back). It is practical, however, to formulate standardised values for preliminary calculations, in order to improve their standardisation and simplicity. We recommend a LAI of 3 [28, 37] and a mean leaf diameter of 0.11 [38] for predictive, static calculations. In this research we used two static values for r_a : 100 s m⁻¹ with forced air circulation on and 200 s m⁻¹ with forced air circulation off.

2.3.1.4 Transpiring leaf area

The LAI of the lettuce crop is incorporated into the equations for sensible and latent heat exchange (Equations 2.5-2.6). As mentioned above the development and configuration of the leaves result in an increased transpiring surface. The LAI that is required in Equations 2.5-2.6 represents the 'effective' leaf area for latent and sensible heat transfer, as opposed to total leaf area. We estimated leaf area multiplying the accumulated dry weight by the specific leaf area (m² g⁻¹) estimated as a function of days after emergence, determined by Tei et al. [28].

2.3.2 Model overview

The MATLAB [39] model executes an iterative process to simultaneously solve Equations 2.4-2.7, processing the net PAR flux density, the surface and aerodynamic resistances as outlined above (Equations 2.8-2.10). The flows are denoted by a capital letter, followed by a subscript. The model parameters are listed in the list of symbols.

The iterative process is based on the aforementioned equations and is performed in a continuous loop. For each set interval of T_{air} , the model calculates the corresponding T_s at which the energy balance ($I_{net} - H - \lambda E$) is closest to zero. The model utilises a continuous loop to approach this value at the set discretisation and consequently indexes the value closest to zero. Finally, the model lists the different variables congruent with this zero energy balance, in particular the quantity of the sensible (H) and latent (λE) heat exchange.

2.4 Methods: Model validation

Our model was validated for three different interior climate regimes by separate experiments conducted in closed systems with artificial lighting. The first experiment [40] was conducted in NASA's Biomass Production Chamber at Kennedy Space Center. The second and third were conducted at Wageningen University & Research in the Netherlands as part of the Ground Demonstration of Plant Cultivation Technologies and Operation in Space (H2020 EDEN-ISS). A summary of the conditions of the experiments is in Table 2.1 and an extended description is given below.

2.4.1 Model validation for various photosynthetic photon flux densities

Our model was validated with the measured amount of transpired vapour at various PPFDs. Data were obtained in two LED-lighted climate chambers (2.88 x 2.20 x 3.06 m; 19.4 m³ each) with lettuce in a hydroponic deep flow system. Nutrient solution volumes remained covered and were replenished every three days. Air temperature

averaged 21°C in light and 19°C in dark conditions. Cooling and dehumidification were achieved by HVAC. Relative humidities averaged 73% in light and 82% in dark conditions. Air was continuously circulated in order to provide a mixed atmosphere. This required approximately 4000 m³ h⁻¹ or approximately 200 volume exchanges per hour. The individual climate chambers featured either high (400-600 µmol m⁻² s⁻¹) or low (100-300 µmol m⁻² s⁻¹) PPFD and the illumination on each balance was carefully adjusted to have three PPF densities within each range (Table 2.1).

A set-up of six independent digital balances (60 kg, 2g accuracy) was used to determine transpiration. The total weight of the crops, production system and nutrient solution was measured and documented by each balance every 30 seconds. The transpiration rates were determined by calculating the slope of the (decreasing) weight in time. Two distinct and precise slopes (photo- and dark period) could be determined, due to the steady climate in the cells and the large number of measurements.

The experiments used transplanted Batavia lettuce, 60 days after sowing, with a cultivation area cover of 100%. LAI was not measured but estimated based on literature. Tei et al. [28] reported a LAI of 4.4 for Saladin lettuce at 60 days after sowing. Batavia lettuce, however, has less overlapping, non-effective leaves. Consequently, we presumed a LAI of 3, following Tuzet et al. [37].

From this experiment we used two data sets; the transpired vapour and fresh weight⁴.

2.4.2 Model validation for a range in cultivation area cover

Our model was validated with evapotranspiration rates throughout the development of the crop and the corresponding cultivation area cover as reported by Wheeler et al. [40]. They produced lettuce in a closed chamber using a hydroponic nutrient film technique. The objective of that study was to track gas, water and nutrient balances in relation to the productivity of lettuce from seeding to harvest. Evapotranspiration rates were daily assessed by recording the replenishment of the nutrient solution reservoirs.

⁴ Fresh weight was tracked to differentiate between water uptake by the crop for assimilation and for transpiration.

TABLE 2.1 The location, crop production data and interior climate conditions for the experiments conducted at Wageningen UR and the Kennedy Space Center. The different sets of VCD are represented by numbers (0-4) and the different balances are represented by letters (A-F).

	EXP-1 – PPFD Wageningen UR		EXP-2* – CROP COVER Kennedy Space Center	EXP-3 – VCD (control) Wageningen UR	EXP-3 – VCD Wageningen UR	
Latitude	51.9865374° N		28.590181° N	51.9865374° N	51.9865374° N	
Longitude	5.6634339° E		-80.659198° E	5.6634339° E	5.6634339° E	
Typology	CPPS with DFT		CPPS with NFT	CPPS with DFT	CPPS with DFT	
Dimensions	1.44 m ² in 19.4 m ³		20 m ² in 113 m ³	0.72 m ² in 19.4 m ³	0.72 m ² in 19.4 m ³	
Cultivar	Batavia		Waldmann's Green	Batavia	Batavia	
Cycle duration	3 days		28 days	8 days	8 days	
Cultivation area cover (%)	100		0 – 95	91	82 – 95	
LAI	3.0		0 – 4.3	(A) 3.0 (B) 3.0 (C) 2.9	(D) 3.2 (E) 3.2 (F) 3.4	
Mean air temperature photo-/dark period (°C)	21/19		22.6/22.4	(0) 21/19	(1) 17/15 (3) 25/23	(2) 17/15 (4) 25/23
Relative Humidity (%)	73/83		71/75	(0) 76/86	(1) 75/82 (3) 79/86	(2) 78/96 (4) 89/93
VCD photo-/dark period (g m ⁻³)	5.0/2.8		5.9/5.0	(0) 4.4/2.7	(1) 3.7/2.3 (3) 5.2/3.5	(2) 2.3/0.5 (4) 3.3/3.3
CO ₂ levels (μmol mol ⁻¹)	700-800		1000	700-800	700-800	
Lighting system	LED		HPS	LED	LED	
PPFD (μmol m ⁻² s ⁻¹)	(A) 140 (114-166) (B) 200 (170-254) (C) 300 (262-338)	(D) 400 (300-477) (E) 450 (396-594) (F) 600 (506-691)	293	(A) 140 (126-148) (B) 300 (283-324) (C) 600 (550-651)	(D) 140 (123-147) (E) 300 (278-321) (F) 600 (555-645)	
PAR flux density (W m ⁻²)	(A) 28.2 (B) 41.0 (C) 58.6	(D) 79.6 (E) 90.8 (F) 118.8	58.89	(A) 28.2 (B) 59.2 (C) 119.6	(D) 27.8 (E) 59.6 (F) 119.8	
Photo-/Dark period (h)	16h/8		16h/8	16h/8	16h/8	
r _{ss} photo-/dark period (s m ⁻¹)	(A) 289/450 (B) 253/450 (C) 218/450	(D) 190/450 (E) 179/450 (F) 158/450	218/450	(A) 289/450 (B) 217/450 (C) 158/450	(D) 290/450 (E) 217/450 (F) 157/450	
r _a photo-/dark period (s m ⁻¹)	100/100		100/200	100/100	100/100	

* As reported by Wheeler et al. [40]

The air temperature averaged $22.6 \pm 0.4^\circ\text{C}$ in light and $22.4 \pm 0.2^\circ\text{C}$ in dark conditions. The relative humidity averaged $71 \pm 3\%$ in light and $75 \pm 2\%$ in dark conditions. Air was continuously circulated in order to provide a mixed atmosphere. From this experiment we used three data sets; the canopy cover, evapotranspiration rate and dry mass accumulation. The LAI was considered to be variable in accordance with Wheeler et al. [40].

2.4.3 Model validation for various vapour concentration deficits

The model was validated with a second experiment in the climate cells, following the same set-up described in Section 2.4.1. Nutrient solution volumes remained covered and were replenished every three days and aerated daily. The experiments used transplanted Batavia lettuce, 45 days after sowing. The specific leaf area (SLA) relationship [28] was applied to estimate the LAI from weight at harvest. The LAI varied between 2.9 and 3.4 (Table 2.1). The other specifications correspond to the boundary conditions mentioned in Section 2.4.1.

The objective of this experiment was to have two sets of pre-fixed levels of vapour concentration deficit (VCD). The first chamber (control) was continuously maintained at $21/19^\circ\text{C}$ and 75% relative humidity (VCD $4.4/2.7 \text{ g m}^{-3}$). The climate settings of the second chamber were changed stepwise every two days in order to attain a range of vapour concentration deficits. However, we discovered that our control of the humidity was very limited at each temperature set-point, which resulted in four separate levels of VCD (Table 2.2). Within each chamber we had three different PPFD on the three scales.

2.5 Model results & discussion

Sections 2.5.1-2.5.3 present the validation results and discuss them with respect to model performance for the transpiration rate. In Section 2.5.4 the energy balance and distribution in closed plant production systems has been illustrated and discussed for a standard production climate.

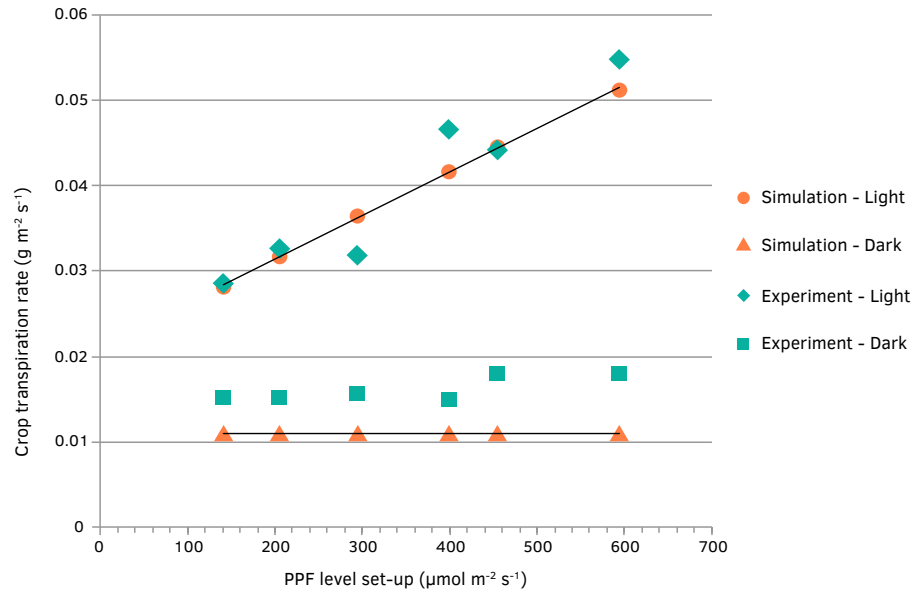


FIG. 2.3 The simulated transpiration compared to measurements for various PPFD. Measurements are represented by diamonds (photoperiod) and squares (dark period), simulations by circles (photoperiod) and triangles (dark period).

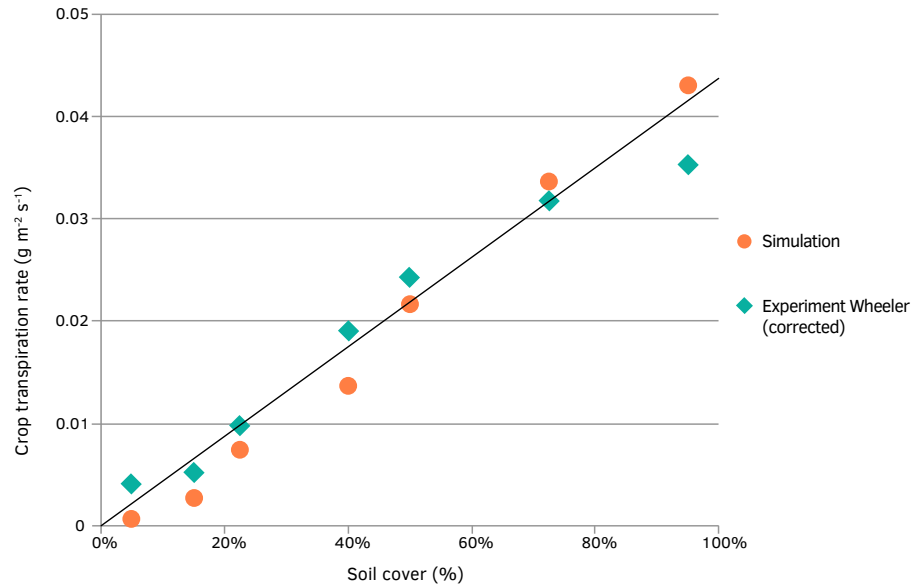


FIG. 2.4 The simulated crop transpiration compared to measurements for various cultivation area cover percentages. Measurements are represented by diamonds, simulations by circles.

2.5.1 Model validation for photosynthetic photon flux densities

In this experiment transpiration rates were continuously registered throughout the day for a full canopy cover illuminated under various PPFD. The average slope of the decline in weight of each set-up was used to determine transpiration rates at light and dark.

Our experiment resulted in a 24h average transpiration rate of $0.032 \text{ g m}^{-2} \text{ s}^{-1}$ ($115 \text{ g m}^{-2} \text{ h}^{-1}$). The model calculated a 24h average transpiration rate of $0.030 \text{ g m}^{-2} \text{ s}^{-1}$ ($108 \text{ g m}^{-2} \text{ h}^{-1}$). The corresponding root mean square error (RMSE) is $0.004 \text{ g m}^{-2} \text{ s}^{-1}$ ($15.87 \text{ g m}^{-2} \text{ h}^{-1}$). The simulated transpiration rate in our model has a considerable correlation with the experimental data as far as figures during light are concerned (Figure 2.3). In contrast, the simulated transpiration rate at dark was less consonant with the experiment: $0.011 \text{ g m}^{-2} \text{ s}^{-1}$ ($40 \text{ g m}^{-2} \text{ h}^{-1}$) versus $0.016 \text{ g m}^{-2} \text{ s}^{-1}$ ($58 \text{ g m}^{-2} \text{ h}^{-1}$), respectively.

As most transpiration occurs under light, this error will only have a limited bearing on the dimensioning of HVAC systems for plant factories. The discrepancy is likely caused by the stomatal resistance; at dark it is set at 450 s m^{-1} (Equation 2.9). Adaptation of the equation on the specific or cultivar level might improve correlation.

2.5.2 Model validation for crop cover

In the study of Wheeler et al. [40] ET rates were daily registered and the development of canopy cover and the accumulation of dry mass were periodically assessed. Their data were transcribed to determine the dry mass development in relation to canopy cover. The SLA relationship [28] was applied to estimate the development of LAI as a function of canopy cover.

The experiment resulted in an average ET rate of $3991 \text{ g m}^{-2} \text{ d}^{-1}$, of which Wheeler et al. [40] estimated that $1000 \text{ g m}^{-2} \text{ d}^{-1}$ was free evaporation from exposed water surface. They obtained this estimate by extrapolating measured ET rates to zero crop cover. In order to compare transpiration rates, we show our calculated values and the experimental data thus corrected (Figure 2.4). The RMSE is $361 \text{ g m}^{-2} \text{ d}^{-1}$ ($15.04 \text{ g m}^{-2} \text{ h}^{-1}$).

2.5.3 Model validation for vapour pressure deficit

In this experiment transpiration rates were continuously registered throughout the day for a full canopy cover illuminated under various PPFD. Scheduled changes to air temperature and RH offered insight into the effect of vapour concentration deficit on ET. Transpiration rates were determined as described in Section 2.5.1.

The experiment resulted in a wide range of transpiration rates. The simulated transpiration rates in our model have a fair correlation with the experimental data. Similar to Section 2.5.1, the correlation is greater under light than at dark (Figure 2.5). The RMSE under light is $15.96 \text{ g m}^{-2} \text{ h}^{-1}$, whereas at dark it is $18.06 \text{ g m}^{-2} \text{ h}^{-1}$.

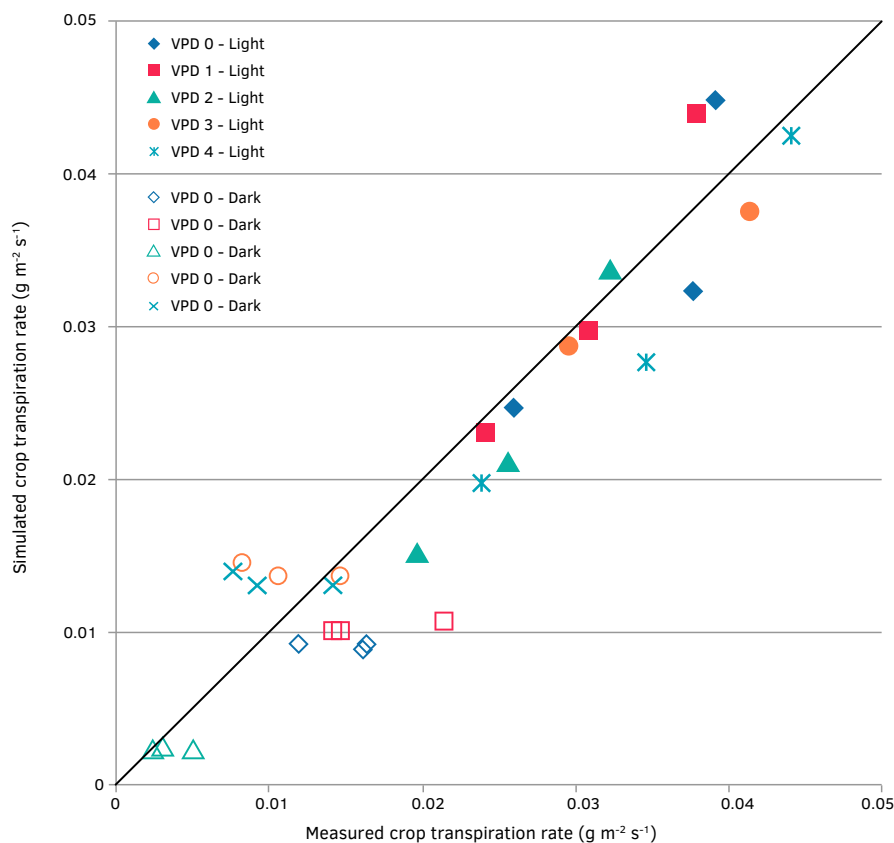


FIG. 2.5 The simulated transpiration compared to measurements for various vapour concentration deficits. Results under light are represented by solid markers and results in dark are represented by outlines. Diamonds represent the (control) VCD Set 0 ($4.4/2.7 \text{ g m}^{-3}$), squares represent VCD set 1 ($3.7/2.3 \text{ g m}^{-3}$), triangles represent VCD set 2 ($2.3/0.5 \text{ g m}^{-3}$), circles represent VCD set 3 ($5.2/3.5 \text{ g m}^{-3}$) and stars represent VCD set 4 ($3.3/3.3 \text{ g m}^{-3}$).

2.5.4 Distribution of energetic fluxes

We have simulated four sets of climate conditions in order to illustrate the variable distribution of energetic fluxes in a plant factory, as determined by plant processes. The differences between the sets of conditions are limited to temperature and PPFD (Table 2.2). The efficiency of the LED-lighting system (the conversion of electric power to I_{light}) of each experiment was set at 52% [41]. These simulations provide insight into the influence of temperature and PPFD on transpiration and the distribution of latent and sensible heat.

The Sankey diagram (Figure 2.6) illustrates the simulated fluxes and consequently the importance of transpiration as a design parameter for climatisation. Firstly, the latent heat flux constitutes the largest single flow of energy in each simulation and even exceeds the input energy at lower PPFD ($140 \mu\text{mol m}^{-2} \text{s}^{-1}$). Secondly, we can see that the relative share of the latent heat flux increases with higher air temperatures.

Plant factories are closed systems that generally rely on relatively high PPFD and temperatures to shorten production cycles. Following our simulations, the cooling demand of these plant factories is presumably relatively high, as a result of the increased sensible heat exchange with the lighting system and the decreased sensible heat exchange with the (cooling) plant canopy. The most important finding, however, is that the latent heat flux can even exceed the input energy in certain situations. This impact is greater than expected and necessitates an a priori assessment of the energetic fluxes for the design of plant factories. Our model can be used for such an assessment.

2.6 Outlook

2.6.1 General considerations

The aim of this study was to explicate the energetic fluxes associated with the production of lettuce in plant factories. Validation results showed that our model predicted the transpiration of the lettuce crop with great accuracy for different

lighting intensities, air humidities and stages of development (cultivation area cover and LAI). No additional calibration was deemed useful. The presented model offers two key advantages for the design of plant factories and vertical farms.

Firstly, our model offers a prospective and rather accurate insight into the role of plant processes in the total energy balance. The (evapo)transpiration is an important design parameter that has been frequently neglected in research on closed climate production.

Secondly, our model is versatile enough to be applied to different crops, types of growing environment and interior climates. We have demonstrated the accuracy of the model under a broad range of climate conditions (PPFD, temperature, RH) and crop development stages.

We envisaged designing this model as a simple and useful tool for the energetic optimisation of plant factories. In this process oversimplification might have played a role and relevant aspects may have been neglected. For example, the performance of the transpiration model can still be improved by implementing dynamic LAI and cultivation area cover models. This allows for a more accurate simulation throughout the different stages of crop development and for an optimisation of crop respacing.

TABLE 2.2 The specific sets of crop production data and interior climate conditions used in determining the distribution of energy fluxes from the crop (and lighting system) to the surrounding air via simulation. The results are presented in Figure 2.6.

	SET A – High PPFD & low temperature	SET B – High PPFD & high temperature	SET C – low PPFD & low temperature	SET D – Low PPFD & high temperature
Cultivation area cover (%)	95	95	95	95
LAI	3.0	3.0	3.0	3.0
Mean air temperature light/dark (°C)	21/19	25/23	21/19	25/23
Relative Humidity (%)	73/83	73/83	73/83	73/83
VCD light/dark (g m ⁻³)	5.0/2.8	6.3/3.5	5.0/2.8	6.3/3.5
Photosynthetic photon flux density (μmol m ⁻² s ⁻¹)	600	600	140	140
PAR flux density (W m ⁻²)	120	120	28	28
I_{net} (W m ⁻²)	108.3	108.3	25.3	25.3
r_{ss} photo-/dark period (s m ⁻¹)	158/450	158/450	289/450	289/450
r_a photo-/dark period (s m ⁻¹)	100/100	100/100	100/100	100/100

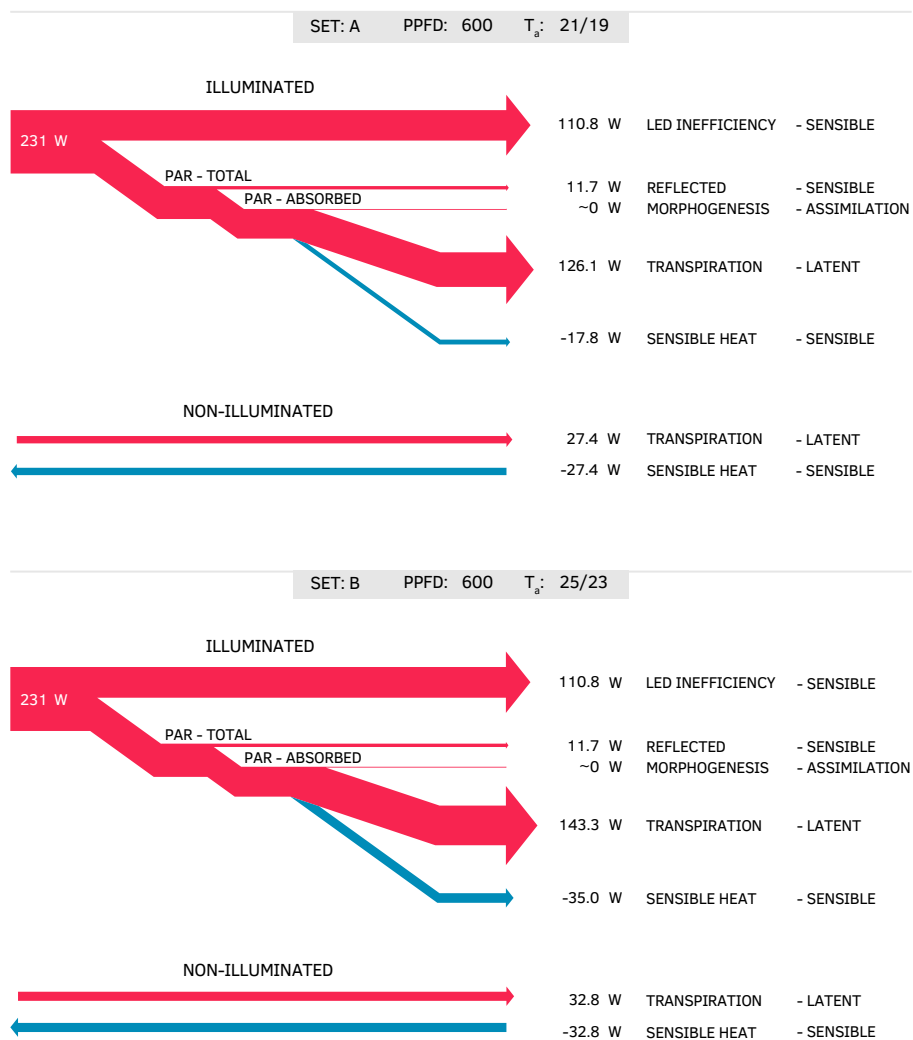
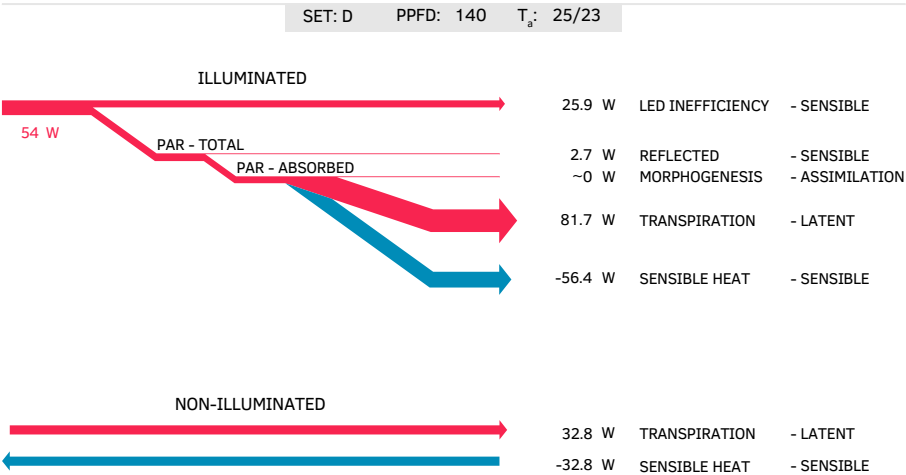
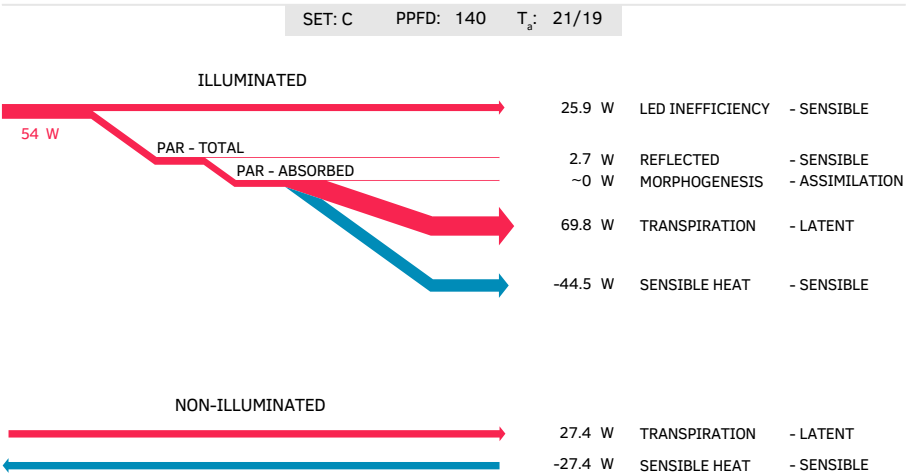


FIG. 2.6 The distribution of energy fluxes from the crop (and lighting system) to the surrounding air, following four different climate sets. The diagrams illustrate the results at a PPFD of 600 $\mu\text{mol m}^{-2} \text{s}^{-1}$ or 140 $\mu\text{mol m}^{-2} \text{s}^{-1}$ and a temperature regime of 21/19 °C or 25/23 °C. Positive fluxes are represented in solid red, negative fluxes in blue.



Predicting the transpiration of a fully developed crop may suffice for the design of plant factories, however, as HVAC systems are generally dimensioned according to the highest load. In this respect, other simplifications may prove to be non-critical as well, such as the obvious weakness of having empirical, crop specific parameters in the estimate of the surface (stomatal) resistance.

Given these results, the model is considered to be appropriate for a realistic simulation of the vapour flux associated with the production of lettuce in plant factories.

2.6.2 Total energy requirement for plant factories

The vapour flux and consequent dehumidification relatively require a large amount of energy. The other influential processes are artificial illumination and climatisation. Light for photosynthesis has to be artificially supplied in plant factories. Additionally, the need for forced air circulation and conditioning results in higher energy costs. Finally, the design and efficacy of plant factories will depend on economic consequences as well. The benefits of plant factories compared to traditional greenhouses have to compensate for these additional costs.

2.6.3 Comparison with greenhouses

We simulated the energy requirement of the production presented by Wheeler et al. [40] and compared this to the requirement of standard greenhouse production in the Netherlands [42]. Global solar radiation in the Netherlands is $3.54 \text{ GJ m}^{-2} \text{ y}^{-1}$ [43] and we assume a greenhouse transmissivity of 65%. No whitewash is applied. In addition to solar radiation, the greenhouse production of lettuce requires gas for heating ($94 \text{ kWhe m}^{-2} \text{ y}^{-1}$), storage and steaming ($52 \text{ kWhe m}^{-2} \text{ y}^{-1}$), as well as electricity for various other uses ($5 \text{ kWhe m}^{-2} \text{ y}^{-1}$) [42]. Without solar energy, greenhouses approximately require 1.55 kWhe to produce a single crop of lettuce (average fresh weight 289 g). When we integrate solar energy, however, one crop of lettuce requires approximately 8.08 kWhe . In the aforementioned plant factory a single crop with the same fresh weight would approximately require 7.57 kWhe .

Apart from lighting, greenhouses rely more on natural ventilation for dehumidification, whereas plant factories rely solely on mechanical air conditioning.

As a result, the vapour flux and the consequent latent cooling load are a significant factor in the total energy consumption of plant factories.

However, the plant factory could also present several benefits in other fields. The main differences in the total energy consumption between greenhouses and plant factories are the result of envelope design and plant processes. The exterior climate has a significant impact on the heating load in greenhouses due to heat transfer across the building envelope. In plant factories, however, the exterior climate has a much smaller effect than the internal loads imposed by lights and plants [44]. Katsoulas et al. [45] show that the highest attainable water use efficiency decreases with the coupling of greenhouse environment to the outside air (an indicator of ventilation requirements). They found that water use efficiency increased significantly in closed systems as the result of two processes: (1) the increased productivity due to a more adequate microclimate with a higher CO₂ concentration and (2) the ability to collect and reuse transpired water condensing at the cooling element. The high water use efficiency, CO₂ efficiency and production density of closed production systems offer perspectives for locations where resources such as land or water are scarce.

2.7 Conclusion

In this study a crop transpiration model was developed and validated. It describes the energetic fluxes associated with the production of lettuce in closed plant production systems. The model illustrates the energetic distribution of sensible heat and latent heat and the corresponding vapour production. This offers insight into the role of plant processes in the total energy balance of production in plant factories and vertical farming facilities.

The presented model can be used to analyse and optimise the design of plant factories. The model does not require extensive empirical data and can therefore readily provide an accurate estimate for a range of closed production climates. Models may be developed for high-density production in isolated systems, systems integrated into (structurally vacant) buildings or even as an integral part of the city. Transpiration can be integrated effectively as a design parameter and the total energy profile of plant factories can be assessed in detail. Future research can adapt

our model as input for more extensive analyses and calculations with regard to production output, production climate and energetic performance.

Acknowledgements

This work was partly supported by the EU-H2020 project “Ground Demonstration of Plant Cultivation Technologies and Operation in Space for Safe Food Production on-board ISS and Future Human Space Exploration Vehicles and Planetary Outposts” (EDEN-ISS, grant 636501). However, no endorsement from the European Commission of the results and conclusions is hereby implied.

The authors would like to express their gratitude to Olaf van Campenhout, for his skilful examination of the MATLAB model.

Model overview

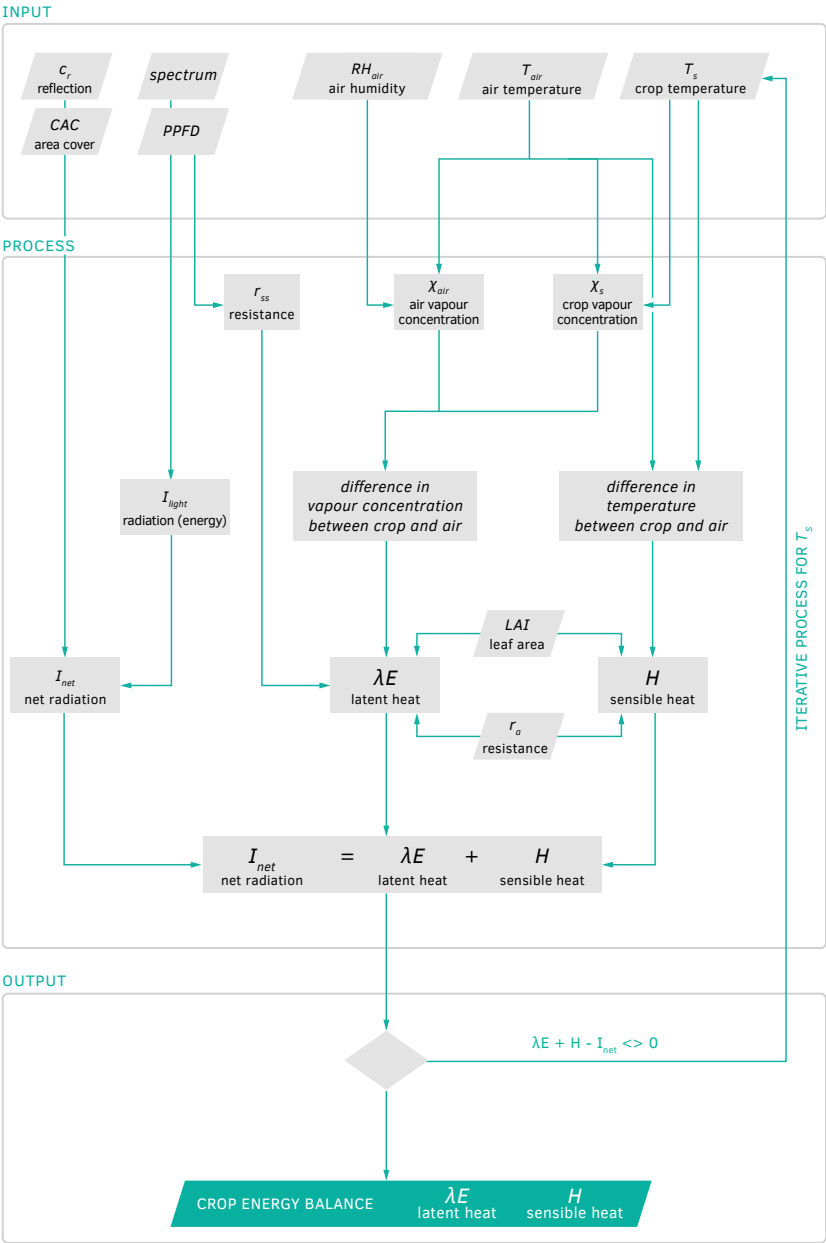


FIG. APP. 2A.1 Simplified model diagram to illustrate key processes and variables.

Reference list

- [1] Newcombe, K. & Nichols, E.H. (1979). An integrated ecological approach to agricultural policy-making with reference to the urban fringe: The case of Hong Kong. *Agricultural Systems*, 4(1), 1-27. doi:10.1016/0308-521x(79)90011-8
- [2] Rosenzweig, C. & Liverman, D. (1992). Predicted effects of climate change on agriculture: A comparison of temperate and tropical regions. In Majumdar, SK. (Ed.), *Global climate change: Implication, challenges and mitigation measures* (pp. 342-361). Philadelphia: Pennsylvania Academy of Sciences.
- [3] Kennedy, C., Cuddihy, J., & Engel-Yan, J. (2007). The changing metabolism of cities. *Journal of industrial ecology*, 11(2), 43-59. doi:10.1162/jiec.0.1107
- [4] Lambin, E. & Meyfroidt, P. (2011). Global land use change, economic globalization, and the looming land scarcity. *Proceedings of the National Academy of Sciences*, 108(9), 3465-3472. doi:10.1073/pnas.1100480108
- [5] Kozai, T. (2013). Resource use efficiency of closed plant production system with artificial light: Concept, estimation and application to plant factory. *Proceedings of the Japan Academy. Series B, Physical and biological sciences*, 89(10), 447-461. doi:10.2183/pjab.89.447
- [6] Kozai, T., Ohyama, K., & Chun, C. (2006). Commercialized closed systems with artificial lighting for plant production. *Acta Horticulturae*, 711, 61-70. doi:10.17660/actahortic.2006.711.5
- [7] Kozai, T. (2013). Sustainable plant factory: Closed plant production systems with artificial light for high resource use efficiencies and quality produce. *Acta Horticulturae*, 1004, 27-40. doi:10.17660/actahortic.2013.1004.2
- [8] Seginer, I. & Ioslovich, I. (1999). Optimal spacing and cultivation intensity for an industrialized crop production system. *Agricultural Systems*, 62(3), 143-157. doi:10.1016/s0308-521x(99)00057-8
- [9] Goto, E. (2012). Plant production in a closed plant factory with artificial lighting. *Acta Horticulturae*, 956, 37-49. doi:10.17660/actahortic.2012.956.2
- [10] Boulard, T. & Wang, S. (2000). Greenhouse crop transpiration simulation from external climate conditions. *Agricultural and forest Meteorology*, 100(1), 25-34. doi:10.1016/s0168-1923(99)00082-9
- [11] Sabe, N.C. (2007). *Evaluating and minimizing water use by greenhouse evaporative cooling systems in a semi-arid climate*. (PhD), University of Arizona, Tucson, AZ, USA.
- [12] Clum, H.H. (1926). The effect of transpiration and environmental factors on leaf temperatures II. light intensity and the relation of transpiration to the thermal death point. *American Journal of Botany*, 13(4), 217-230. doi:10.2307/2435312
- [13] Penman, H.L. (1947). Evaporation in nature. *Reports on progress in physics*, 11(1), 366. doi:10.1088/0034-4885/11/1/312
- [14] Schofield, R.K. & Penman, H.L. (1948). *The principles governing transpiration by vegetation*. Paper presented at the Conference on Biology and Civil Engineering, London, UK.
- [15] Penman, H.L. (1948). *Natural evaporation from open water, bare soil and grass*. Paper presented at the Royal Society of London, Series A: Mathematical and Physical Sciences, London, UK.
- [16] Monteith, J.L. (1965). *Evaporation and environment*. Paper presented at the Symposia of the Society for Experimental Biology.
- [17] Pollet, S., Bleyaert, P., & Lemeur, R. (2000). Application of the Penman-Monteith model to calculate the evapotranspiration of head lettuce (*Lactuca sativa* L. var. *capitata*) in glasshouse conditions. *Acta Horticulturae*, 519, 151-162. doi:10.17660/actahortic.2000.519.15
- [18] Stanghellini, C. (1987). *Transpiration of greenhouse crops. An aid to climate management*. (PhD), Wageningen University of Agriculture, Wageningen, the Netherlands. (2690)
- [19] Ado, Y., Asada, Y., Benemann, J. R., Kishimoto, M., Miyake, J., Miyamoto, K., & Nishio, N. (1997). *Renewable biological systems for alternative sustainable energy production* (Vol. 128). Rome, Italy: FAO.
- [20] Gates, D.M. (1965). Energy, plants, and ecology. *Ecology*, 46(1-2), 1-13. doi:10.2307/1935252
- [21] Boulard, T. & Baille, A. (1993). A simple greenhouse climate control model incorporating effects of ventilation and evaporative cooling. *Agricultural and forest Meteorology*, 65(3), 145-157. doi:10.1016/0168-1923(93)90001-x
- [22] Chalabi, Z.S. & Bailey, B.J. (1989). Simulation of the energy balance in a greenhouse. *Divisional Note DN.1516, AFRC Institute of Engineering Research, Silsoe (UK)*.
- [23] Aikman, D.P. & Houter, G. (1990). Influence of radiation and humidity on transpiration: implications for calcium levels in tomato leaves. *Journal of Horticultural Science*, 65(3), 245-253. doi:10.1080/00221589.1990.11516053

- [24] Jolliet, O. (1994). HORTITRANS, a model for predicting and optimizing humidity and transpiration in greenhouses. *Journal of Agricultural Engineering Research*, 57(1), 23-37. doi:10.1006/jaer.1994.1003
- [25] Alves, I. & Pereira, L.S. (2000). Modelling surface resistance from climatic variables? *Agricultural Water Management*, 42(3), 371-385. doi:10.1016/S0378-3774(99)00041-4
- [26] Alves, I., Perrier, A., & Pereira, L.S. (1998). Aerodynamic and surface resistances of complete cover crops: How good is the "big leaf"? *Transactions of the ASAE - American Society of Agricultural Engineers*, 41(2), 345-352. doi:10.13031/2013.17184
- [27] Frantz, J.M., Ritchie, G., Cometti, N.N., Robinson, J., & Bugbee, B. (2004). Exploring the limits of crop productivity: beyond the limits of tipburn in lettuce. *Journal of the American Society for Horticultural Science*, 129(3), 331-338.
- [28] Tei, F., Scaife, A., & Aikman, D.P. (1996). Growth of lettuce, onion, and red beet. 1. Growth analysis, light interception, and radiation use efficiency. *Annals of Botany*, 78(5), 633-643. doi:10.1006/anbo.1996.0171
- [29] Allen, R.G., Pereira, L.S., Raes, D., & Smith, M. (1998). Crop evapotranspiration - Guidelines for computing crop water requirements - FAO Irrigation and drainage paper 56. *FAO*, 300(9).
- [30] Jarvis, P.G. (1976). The interpretation of the variations in leaf water potential and stomatal conductance found in canopies in the field. *Philosophical Transactions of the Royal Society of London B: Biological Sciences*, 273(927), 593-610. doi:10.1098/rstb.1976.0035
- [31] Jolliet, O. & Bailey, B.J. (1992). The effect of climate on tomato transpiration in greenhouses: measurements and models comparison. *Agricultural and forest Meteorology*, 58(1), 43-62. doi:10.1016/0168-1923(92)90110-p
- [32] Wang, J., Lu, W., Tong, Y., & Yang, Q. (2016). Leaf morphology, photosynthetic performance, chlorophyll fluorescence, stomatal development of lettuce (*Lactuca sativa* L.) exposed to different ratios of red light to blue light. *Frontiers in plant science*, 7, 1-10. doi:10.3389/fpls.2016.00250
- [33] Perrier, A. (1975). Etude physique de l'évapotranspiration dans les conditions naturelles. III. Evapotranspiration réelle et potentielle des couverts végétaux (Study and modelling of mass and energy exchanges of vegetated surfaces). *Annales Agronomiques*, 26, 229-243.
- [34] Thom, A.S. (1975). Momentum, mass and heat exchange of plant communities. In Monteith, J.L. (Ed.), *Vegetation and the atmosphere, Volume 1: Principles* (pp. 57-109). London: Academic Press.
- [35] Monteith, J.L. & Unsworth, M.H. (1990). *Principles of environmental physics*. London: Edward Arnold. doi:10.1017/s0014479700001381
- [36] Fuchs, M. (1993). *Transpiration and foliage temperature in a greenhouse*. Paper presented at the International Workshop on Cooling Systems for Greenhouses, AGRITECH, Tel Aviv, Israel.
- [37] Tuzet, A., Perrier, A., & Leuning, R. (2003). A coupled model of stomatal conductance, photosynthesis and transpiration. *Plant, Cell & Environment*, 26(7), 1097-1116. doi:10.1046/j.1365-3040.2003.01035.x
- [38] Ohashi-Kaneko, K., Takase, M., Kon, N., Fujiwara, K., & Kurata, K. (2007). Effect of light quality on growth and vegetable quality in leaf lettuce, spinach and komatsuna. *Environmental Control in Biology*, 45(3), 189-198. doi:10.2525/ecb.45.189
- [39] MATLAB. (2016). MATLAB version R2016a (9.0.0.341360). Natick, Massachusetts, USA: The MathWorks, Inc. Retrieved from www.mathworks.com/products/matlab.html
- [40] Wheeler, R.M., Mackowiak, C.L., Sager, J.C., Yorio, N.C., Knott, W.M., & Berry, W.L. (1994). Growth and gas exchange by lettuce stands in a closed, controlled environment. *Journal of the American Society for Horticultural Science*, 119(3), 610-615.
- [41] Royal Philips N.V. (2015). Philips Horticulture LED solutions - GreenPower LED toplighting - high output. Retrieved 15 December 2016 http://images.philips.com/is/content/PhilipsConsumer/PDFDownloads/Global/ODLI20150701_001-UPD-en_AA-QIG_LED_Toplighting_HO_Philips_Horticulture_EN.pdf
- [42] Vermeulen, P.C.M. (2014). *Kwantitatieve Informatie voor de glastuinbouw: Kengetallen voor groenten – snijbloemen – pot- en perkplanten teelten. Rapport GTB-5067* (Vol. 23). Wageningen, the Netherlands: Wageningen UR Glastuinbouw.
- [43] KNMI. (2014). *KNMI '14 - klimaatscenario's voor Nederland; leidraad voor professionals in klimaatadaptatie*. de Bilt: KNMI (the Royal Netherlands Meteorological Institute).
- [44] Harbick, K. & Albright, L.D. (2016). Comparison of energy consumption: greenhouses and plant factories. *Acta Horticulturae*, 1134, 285-292. doi:10.17660/actahortic.2016.1134.38
- [45] Katsoulas, N., Sapounas, A., De Zwart, F., Dieleman, J.A., & Stanghellini, C. (2015). Reducing ventilation requirements in semi-closed greenhouses increases water use efficiency. *Agricultural Water Management*, 156, 90-99. doi:10.1016/j.agwat.2015.04.003

INTERMEZZO 2

Chapter 2 discussed the crop energy balance. There, the importance of the relation between sensible and latent heat exchange was presented as a design parameter and as an input into the total energy balance. The crop energy balance could then be effectively integrated into the plant factories' energy balances and their resource use could be investigated in greater detail.

In Chapter 3, the crop energy balance model was combined with existing models for crop growth and building energy to calculate resource use efficiency. The energy, electricity, water, CO₂ and land area use of plant factories was calculated and compared with those in greenhouses. Three different climates and latitudes were studied to illustrate the effect of external climate. Chapter 3 offered initial insight into the resource use efficiency of both production systems.



3 System evaluation

Plant factories versus greenhouses: Comparison of resource use efficiency
Graamans, L., Baeza, E., van den Dobbelsteen, A., Tsafaras, I., Stanghellini, C.
Agricultural Systems. 2018; 160: 31–43.
doi:10.1016/j.agsy.2017.11.003

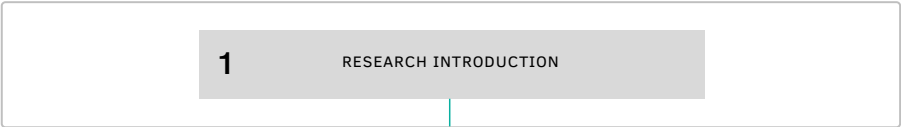
ABSTRACT Research on closed plant production systems, such as artificially illuminated and highly insulated plant factories, has offered perspectives for urban food production but more insight is needed into their resource use efficiency. This paper assesses the potential of this ‘novel’ system for production in harsh climates with either low or high temperatures and solar radiation levels.

The performance of plant factories is compared with cultivation in traditional greenhouses by analysing the use of resources in the production of lettuce. We applied advanced climate models for greenhouses and buildings, coupled with a lettuce model that relates growth to microclimate. This analysis was performed for three different climate zones and latitudes (24–68°N).

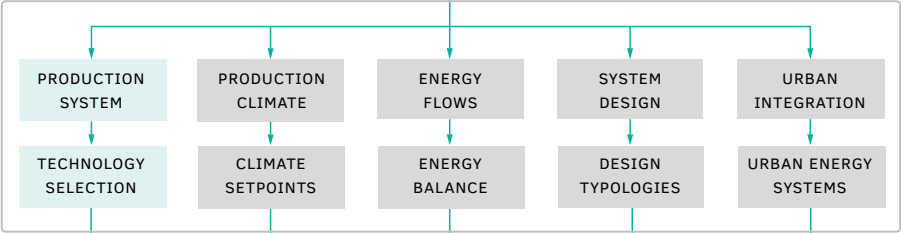
In terms of energy efficiency, plant factories (1411 MJ kg^{-1} dry weight) outperform even the most efficient greenhouse (Sweden with artificial illumination; 1699 MJ kg^{-1} dry weight). Additionally, plant factories achieve higher productivity for all other resources (water, CO_2 and land area). With respect to purchased energy, however, greenhouses excel as they use freely available solar energy for photosynthesis. The production of 1 kg dry weight of lettuce requires an input of 247 kWh_e in a plant factory, compared to 70, 111, 182 and 211 kWh_e in greenhouses in respectively the Netherlands, United Arab Emirates and Sweden (with and without additional artificial illumination).

The local scarcity of resources determines the suitability of production systems. Our quantitative analysis provides insight into the effect of external climate on resource productivity in plant factories and greenhouses. By elucidating the impact of the absence of solar energy, this provides a starting point for determining the economic viability of plant factories.

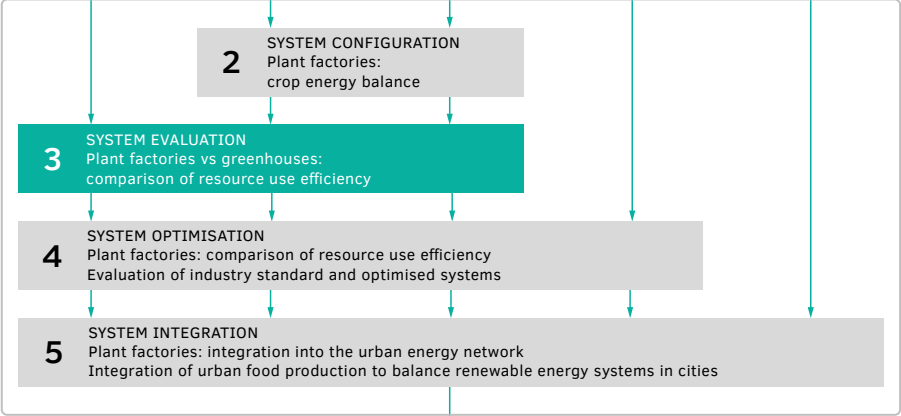
I. INTRODUCTION & METHODOLOGICAL FRAMEWORK



II. THEORETICAL FRAMEWORK



III. DESIGN & EXPERIMENTAL VALIDATION



IV. INTEGRATED DISCUSSION



3.1 Introduction

By midcentury, the number of people living in cities is likely to reach the level of the world's total population in 2002; the urban population is expected to increase from 3.6 billion in 2011 to 6.3 billion in 2050 [1]. The supply chains to feed the expanding cities will become increasingly complex, which will have a major impact on urban and rural areas [2-5]. It has often been suggested that urban agriculture could ensure a supply of locally produced, fresh food. Given the financial value of urban space, an economically viable venture would require exceptionally high productivity.

One proposed solution is the use of closed production systems such as plant factories and vertical farms [6-8]. A vertical farm can be considered as a multi-storey plant factory. Closed systems are designed to maximise production density, productivity and resource use efficiency [9]. High productivity is achieved by adapting the interior climate to achieve uniform lighting, temperature and relative humidity through minimising the interaction with the exterior climate. Limiting this interaction can also benefit the efficient use of energy, water and CO₂ [10].

The evident shortcoming of this typology is the high energy (electricity) demand for artificial illumination, which is needed for photosynthesis. Furthermore, the combination of high-density crop production, limited volume and lack of natural ventilation is likely to induce a high demand for cooling and vapour removal [11].

In contrast, greenhouse horticulture consists of a (semi-)controlled environment which uses primarily solar energy for photosynthesis as well as for heating. Excess energy can be discharged by ventilation and any deficits or surplus can be compensated by heating or cooling. The transparent, conductive design of greenhouses is a trade-off between solar energy and the influence of the exterior climate. The relation between the costs (heating and cooling) and benefits (solar radiation) of greenhouse production largely depends on the latitude and external climate conditions of the site [8]. It can be expected that at high latitudes solar radiation no longer offsets the energy being lost through the greenhouse cover. The opposite may occur at low latitudes, where the incoming solar energy cannot be discharged by natural ventilation. In these situations, evaporative and/or active cooling would become necessary.

Plant factories are now being used for the commercial production of leafy greens, but their potential remains uncertain. In order to achieve economic viability, the increased resource productivity and/or the value of additional services would have to outweigh the disadvantage of the absence of solar energy.

3.1.1 Objective

The objective of this study is to quantify the resource requirement for lettuce production in greenhouses and plant factories and to analyse how this requirement is affected by external climate conditions.

3.1.2 Outline

We couple an established model for lettuce growth with accepted models for the simulation of climate and resource requirements in either plant factories or greenhouses. Subsequently, we calculate and analyse the resource requirement of lettuce production in the two growing systems, each in three climates.

3.2 Methodology

This study consists of a performance analysis of plant factories and greenhouses at three different locations. To this end, we analyse resource expenditure for lettuce production. The resource expenditure of each facility is the result of internal and external gains as well as the use of electricity, water and CO₂. These figures were calculated and compared. Greenhouse and building simulation software had to be used, since the two typologies require a different format. Ultimately, the production output, climatic performance and related resource consumption were analysed for each facility.

3.2.1 Model selection

3.2.1.1 KASPRO for greenhouses

Given the differences in the construction of greenhouses and plant factories, different simulation models had to be applied. The design of greenhouses implies considerable interaction with the exterior climate. This causes substantial fluctuations in the

interior climate, since control actuators have limited capacity. Therefore, a dynamic model is needed to calculate these variations. In this study we used KASPRO [12], an advanced, dynamic model to calculate the climate in greenhouses. It consists of sub-models that are based on the energy and mass balance of the greenhouse elements. The model takes full account of the interdependence of the greenhouse characteristics and the various climate control actuators, accounting for their limited capacity. More details of this model are described by [12-15].

3.2.1.2 DesignBuilder for plant factories

Unlike greenhouses, plant factories are closed systems, consisting of a highly insulating and airtight structure [9]. Detailed dynamic greenhouse models, such as KASPRO, are less suitable for calculating the limited interaction between the interior and the exterior climate as well as the high internal heat loads. Furthermore, calculating the energetic requirements of plant factories in KASPRO would require considerable modification and validation of the energy balance. Therefore, we selected EnergyPlus in combination with DesignBuilder [16].

EnergyPlus is a building energy simulation program with three basic components – a simulation manager, a heat and mass balance simulation module and a building systems simulation module [17]. We used DesignBuilder [16] for simulating the energy consumption of the plant factory, as this program is considered the most complete graphic user interface for EnergyPlus.

DesignBuilder is not a dynamic simulation model. This is not a limitation, as plant factories have just two states (photo-/dark period), each with a constant climate throughout. It is essential to calculate the energetic behaviour of the crop in both states – how it transpires, reflects light and exchanges heat and radiation. Cooling and vapour removal are quite different processes and the relation between sensible and latent heat is a key factor in the energy demand. Therefore, the energy balance must be based on an accurate estimate of the crop transpiration coefficient, i.e. the fraction of the radiation load that is dissipated by the crop as latent heat. We have integrated the energetic behaviour into the simulations, following the method described by Graamans et al. [11]. We have taken into account an average LAI of 2.1, according to Tei et al. [18], in order to represent a facility where all stages of development are simultaneously present, as is common in actual practice.

The energetic behaviour of lettuce was calculated for the conditions of photo- and dark periods (Table 3.1). The various positive energetic fluxes were set as equipment gains in DesignBuilder; the negative sensible heat transfers were set as process gains. The cooling load for maintaining a constant temperature of the nutrient solution (Section 3.2.3.4) was calculated manually and integrated into the total sensible cooling load. We used Fourier's law of heat conduction to calculate the heat transfer across container and cover. For this calculation we assumed a constant temperature of the nutrient solution of 24°C, air temperatures of 30/24°C during photo-/dark periods, a conductive surface area of 2.2 m² per m² cultivation area, a thickness of 50 mm and a U-value of 0.03 W m⁻² K⁻¹. The conductive surface area is based on suspended, extruded containers with a rectangular cross section of 850 x 130 mm and a nutrient solution depth of 125 mm.

3.2.2 Lettuce production in relation to climate

Differences between the interior climates of greenhouses and plant factories result in differences in plant production. The production in both types of facility determines their respective energetic performances. To this end, the model described by van Henten [19] was implemented in computational software [20]. This is a dynamic growth model that simulates various physiological processes in butterhead lettuce (*Lactuca sativa* var. *capitata* L.). The model determines crop growth rate by distinguishing between growth of structural (e.g. glucose, sucrose, starch) and non-structural (e.g. cell walls, cytoplasm) dry weight. Non-structural dry weight is calculated as a function of gross canopy photosynthesis, respiration and transformation into structural material. Structural dry weight is a function of non-structural dry weight and canopy temperature. We took total dry matter (shoot and root) as the most adequate indicator of production in different conditions. This method negates the effects of commercial and crop management strategies, as well as possible variations in dry matter partitioning between root and shoot. In practice the roots contain approximately 8% of the total dry matter [21–23]. Furthermore, we assumed a fixed dry matter content of 7% [24, 25], an average LAI of 2.1 (Section 3.2.1.2) and an initial dry weight of 0.48 g m⁻² cultivation area.

The van Henten model [19] reduces the three-dimensional crop canopy to a single plane (cultivation area), though it does not address the plant density. This limitation inhibits modelling the transplanting and the respacing of crops. Respacing is done in plant factories and greenhouses to optimise light interception and minimise the required cultivation area.

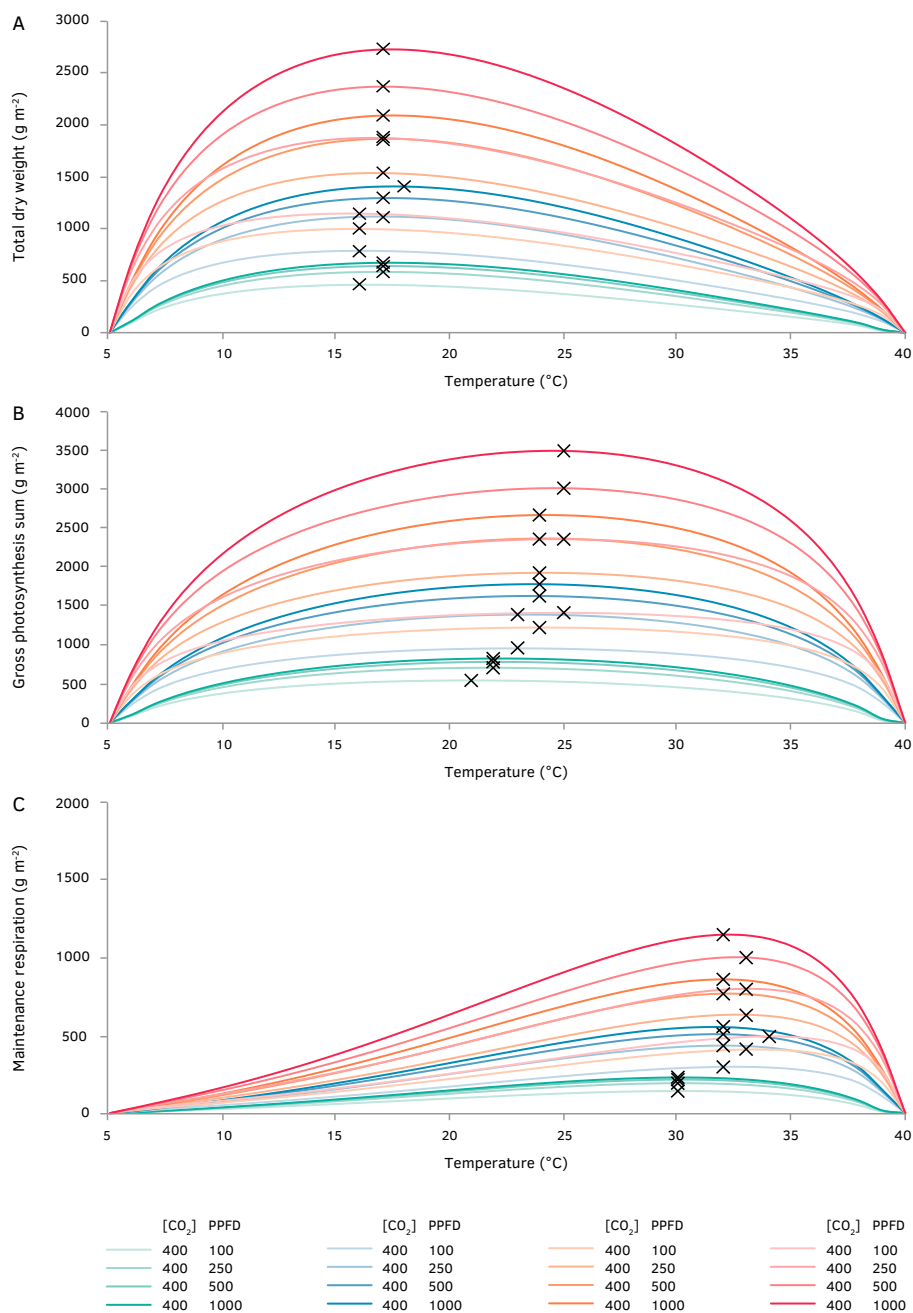


FIG. 3.1 The calculated total dry weight production (A), photosynthesis (B) and respiration (C) of lettuce at different leaf temperatures and combinations of CO₂ concentration (ppm) and PPFD ($\mu\text{mol m}^{-2} \text{s}^{-1}$). Calculations include a complete production cycle of 60 days, a photoperiod of 16 h d⁻¹, and a constant temperature during photo-/dark periods. The maximum value on each curve is indicated by X.

The climate variables affecting crop growth are temperature, photosynthetic photon flux density (PPFD) and CO₂ concentration. The effect of different combinations of temperature, PPFD and CO₂ concentration is illustrated in Figure 3.1. For this calculation we used cycles of 60 days with uniform conditions and a photoperiod of 16 h d⁻¹. Maximum photosynthesis is achieved at temperatures of 20-25°C. Respiration increases with temperature and reaches a maximum at 30-35°C. This results in a maximum dry matter production at approximately 16-17°C.

3.2.3 Model inputs

3.2.3.1 Location and typology

Three sites were selected to represent diverse latitudes and climates, namely Kiruna in Sweden (SWE: 67.8° N, 20.2° E), Amsterdam in the Netherlands (NLD: 52.0° N, 5.7° E) and Abu Dhabi in the United Arab Emirates (UAE: 24.5° N, 54.7° E). The hourly weather information for the simulations was retrieved from the EnergyPlus database [26-28]. This database was chosen for its comprehensiveness. Figure 3.2 shows a monthly summary of solar radiation and temperature.

3.2.3.2 Geometry

A simulation was done of greenhouses and plant factories with a footprint of 100 x 100 m, a size deemed sufficient to negate border effects. The model for the plant factory assumes five production layers and that for the greenhouse just one. The greenhouse is modelled as a Venlo type, consisting of 25 spans of 4 m, with a NorthSouth gutter, a gutter height of 6 m and a roof slope of 23°. The plant factory is modelled as a highly insulated opaque box that is illuminated by LEDs and has an overall height of 6 m. Key parameters of the model are given in Table 3.1.

In plant factories it is assumed that no air is exchanged with the exterior climate. Conversely, in greenhouses some air infiltration occurs, even with closed rooftop ventilators. The infiltration ($\text{m}^3 \text{m}^{-2}_{\text{GH}} \text{s}^{-1}$) is assumed to linearly increase with wind velocity (m s^{-1}) with a coefficient of 8E5.

3.2.3.3 Climate systems

All plant factories feature the same growing, lighting and climatisation system. The lighting system uses LEDs and its efficiency (the conversion of electric power into the irradiance of photosynthetically active radiation) was set at 52% [29]. The remaining power of 48% dissipates as sensible heat, which is extracted by water cooling to ensure optimal efficiency. It is assumed that the climatisation system has the capacity to ensure the required air temperature, humidity and CO₂ concentration.

Greenhouse climatisation systems, however, have fewer actuators and a limited capacity. The capacities and setpoints for the supply of heating, cooling and CO₂ are listed in Table 3.1. The use of identical hardware in greenhouses would not result in a viable growing system at each of the three locations. Therefore, the greenhouses in NLD and SWE were fitted with an energy-saving screen (nonporous, semi-transparent: 88% perpendicular light transmission), in accordance with current practice. Conversely, the greenhouse in UAE did not feature heating and screens. Artificial illumination has to be applied in the greenhouses in SWE to enable year-

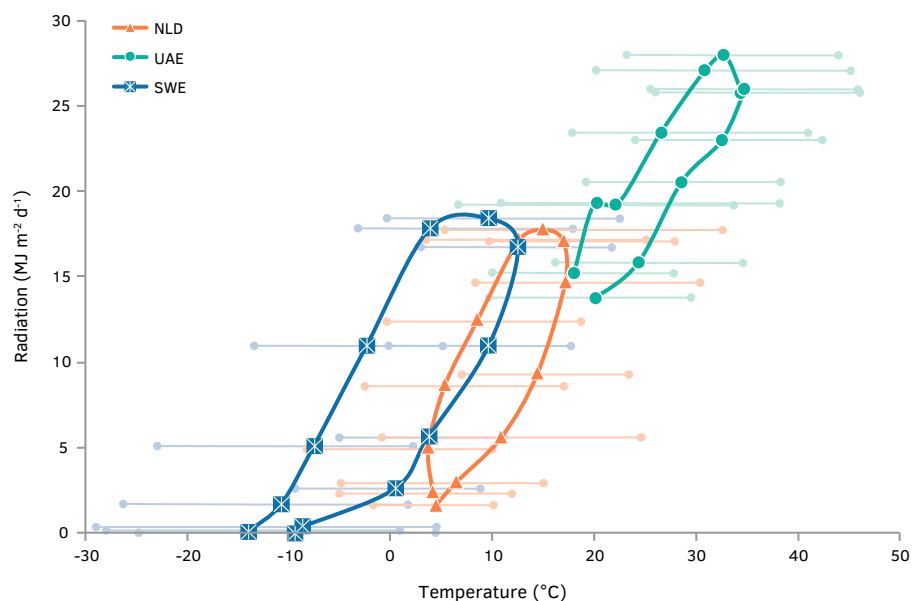


FIG. 3.2 Average daily radiation per month ($\text{MJ m}^{-2} \text{d}^{-1}$) and monthly average, minimum and maximum temperatures ($^{\circ}\text{C}$) for Kiruna (SWE, stars), Amsterdam (NLD, triangles) and Abu Dhabi (UAE, circles). January is the lower left data point in each cycle.

round production (Figure 3.3). This is achieved by supplementing the low levels of solar radiation (Figure 3.2). Our lighting system includes high-pressure sodium lamps with an average power of 55 W m^{-2} .

Similarly, there are differences in the greenhouse cooling systems. A high-pressure fogging system and natural ventilation are adequate to cool greenhouses in NLD and SWE. In the greenhouse in UAE the use of an active cooling installation is imperative, as evaporative cooling would require large amounts of water, which is scarce [30]. Additionally, the high relative humidity of the ambient air in UAE would make evaporative cooling ineffective. Fogging systems, however, are included to increase the ratio of latent to sensible heat. This, in turn, increases the efficiency of the total heat extraction.

3.2.3.4 Climate setpoints

Climate setpoints for each growing system had to be selected carefully, as the productivity of lettuce is mainly determined by the relationship between canopy temperature, PPFD, photoperiod and CO_2 concentration.

For the greenhouse models, we selected climate setpoints roughly in agreement with standard local practice (Table 3.1). Root zone temperature was considered to be equal to air temperature, as nutrient solution tanks are commonly placed within the greenhouse without temperature control. It was also assumed that the irrigation system is completely closed (drain water is recovered and re-used) and that water and nutrient supplies are non-limiting. With respect to lighting, we made two separate calculations for SWE to capture the greenhouse with and without artificial lighting. In these calculations we simulated supplemental lighting in order to match the amount of solar photosynthetically active radiation found in NLD. This facilitates comparison, even though in practice lighting systems would probably be used for longer periods.

The (low) setpoint for greenhouse air temperature would lead to an unrealistically high cooling requirement in plant factories. Therefore, the air temperature was limited to 30°C [31, 32] and the relative humidity was set at 65–90%. The root zone temperature in plant factories was limited to 24°C to ensure the formation of compact lettuce heads [21–23, 33]. With respect to lighting, we assumed a PPFD of $500 \mu\text{mol m}^{-2} \text{ s}^{-1}$ [31] and a photoperiod of 16 h in order to prevent premature bolting [34].

As there is no loss of CO₂ to the exterior climate in a plant factory, a smaller supply of CO₂ is sufficient to maintain a higher-than-ambient concentration. Therefore, the CO₂ concentration setpoint in plant factories exceeds the one in greenhouses (1200 versus 800 ppm).

Production in greenhouses commonly requires different cultivars and crop management than production in plant factories. The selection of slow-bolt cultivars can contribute to an efficient production at higher temperatures and longer photoperiods [35–37]. This study does not address the selection of cultivars but instead discusses total dry matter production, on which the cultivars have a limited effect.

3.2.4 Processing model output

The simulations focus on energy loads and on the use of electricity, water and CO₂. Dry matter production is calculated in relation to the production climate, as stated in Section 3.2.2. In order to represent a facility where all stages of development occur simultaneously, we calculated the moving average in all aspects of this study. Hereafter, in addition to the three-letter codes for the country, the acronym PF refers to plant factories, and GH and GH+ stand for greenhouses without and with artificial lighting, respectively.

3.2.4.1 Energetic loads

The system loads include artificial illumination by LED, LED cooling (Section 3.2.3.3), sensible cooling, dehumidification, heating and installed power. The output from DesignBuilder presents the energetic loads for individual systems. The KASPRO output contains the resources required by the climatisation systems. Subsequently, these values had to be converted to system loads, following the factors listed in Table 3.2. The heating load (Q_{heat}) in greenhouses, for instance, is determined by the gas use for heating ($V_{gas,heat}$) and its energy conversion efficiency (c_g) according to the formula:

$$Q_H = c_g \cdot V_{gas,heat} \quad [3.1]$$

Each greenhouse features a fogging system for cooling (Section 3.2.3.3). The evaporation of water extracts energy as sensible heat and converts it to latent heat.

These systems can therefore only be considered as sensible cooling when vents are opened to extract water vapour. Subsequently, the sensible cooling load ($Q_{cool, sen}$) can be determined by multiplying the amount of water evaporated from the fogging system when vents are opened ($w_{cool, fog}$) by the heat capacity of water (c_w) according to the formula:

$$Q_{cool, sen} = c_w \cdot w_{cool, fog} \quad [3.2]$$

The UAE-GH has a sensible and latent cooling load. The latent (dehumidification) load ($Q_{cool, lat}$) of this greenhouse is determined by multiplying the amount of vapour condensed by the heat exchanger ($w_{con, hex}$) by the heat capacity of water according to the formula:

$$Q_{cool, lat} = c_w \cdot w_{con, hex} \quad [3.3]$$

Subsequently, the sensible cooling load ($Q_{cool, sen}$) can be determined by subtracting $Q_{cool, lat}$ from the total load of the heat exchanger ($Q_{cool, hex}$). Then the energy load from the fogging system and from cooling the nutrient solution ($Q_{cool, ns}$) can be integrated in the following formula:

$$Q_{cool, sen} = c_w \cdot w_{cool, fog} + Q_{cool, ns} + Q_{cool, hex} - Q_{cool, lat} \quad [3.4]$$

3.2.4.2 Electricity

When calculating electricity use, we distinguish two categories: systems using only electricity and systems using other natural resources. The system loads (Q) for plant factories are converted to electricity use (E) following their respective coefficient of performance (COP) according to the formula:

$$E = \frac{Q}{COP} \quad [3.5]$$

The plant factories and the UAE-GH use electric heating and cooling (Section 3.2.3.3). In these models, the energetic loads can be converted to electricity use by using their COP, as listed in Table 3.3. These COPs were determined by taking the difference between supplied and exterior temperature, weighted for corresponding load [38].

The SWE-GH, SWE-GH+ and NLD-GH use heating by means of natural gas and cooling by means of water (fogging). Therefore, their energetic loads should not be converted using COPs. Instead, we consider the actual electricity use of the fogging system ($E_{cool,fog}$) as sensible cooling ($E_{cool,sen}$) when vents are opened for natural ventilation, which is calculated in KASPRO. Additionally, we consider that the conversion of natural gas into electricity use depends on the same conversion efficiency as heating, therefore $Q_{heat} = E_{heat}$. Electricity and light are not converted, therefore COP = 1.

The UAE-GH features a hybrid cooling system, where the electricity demand for latent and sensible cooling is determined by the heat pump, the heat exchanger + fans and the fogging system. Sensible and latent cooling in UAE are calculated by the aforementioned cooling loads, their respective energy requirement for the heat exchangers + fans ($E_{cool,fan}$), and the electricity use of the fogging system ($E_{cool,fog}$) according to the formulas:

$$E_{cool,lat} = \frac{Q_{cool,lat}}{COP} + \frac{Q_{cool,lat}}{Q_{cool,hex}} \cdot E_{cool,fan} \quad [3.6]$$

$$E_{cool,sen} = \frac{Q_{cool,ns} + Q_{cool,hex} - Q_{cool,lat}}{COP} + \frac{Q_{cool,hex} - Q_{cool,lat}}{Q_{cool,hex}} \cdot E_{cool,fan} + E_{cool,fog} \quad [3.7]$$

In order to determine the total electricity demand for plant factories (E_{PF}), we calculated the electricity demands for heating (E_H), dehumidification or latent cooling ($E_{cool,lat}$), and sensible cooling ($E_{cool,sen}$). Additionally, we calculated the energy required for powering (E_{LED}) and cooling ($E_{cool,LED}$) the LED fixtures. This is represented by the following formula:

$$E_{PF} = E_{heat} + E_{cool,lat} + E_{cool,sen} + E_{cool,LED} + E_{LED} \quad [3.8]$$

The calculation of total energy demand for greenhouses (E_{GH}) also includes total solar radiation. KASPRO calculates greenhouse transmissivity in relation to solar position. The radiation that is not transmitted ($E_{sol,nTrans}$), is subdivided into reflection and absorption by greenhouse elements to account for the warming effect of the latter. The transmitted radiation is subdivided into photosynthetically active radiation ($E_{sol,PAR}$) and near-infrared radiation ($E_{sol,NIR}$) according to the formula:

$$E_{GH} = E_{heat} + E_{cool,lat} + E_{cool,sen} + E_{LED} + E_{sol,nTrans} + E_{sol,PAR} + E_{sol,NIR} \quad [3.9]$$

3.2.4.3 Water

All water expenditure (w_{GH}) has been taken up by the crop, as we assumed that there is no water loss from the irrigation system. Most water is transpired by the crop and subsequently extracted through natural ventilation ($w_{air,out}$), or condensed at the greenhouse cover ($w_{con,fac}$) or the heat exchanger ($w_{con,hex}$). It is assumed that condensed water was retrieved, allowing for a loss of 10%. Finally, a small fraction is stored in the biomass of the crop (w_{fw-dw}). The water content in lettuce biomass can be estimated by making an assumption about the fixed dry matter content, for instance 7% [24, 25]. Water expenditure is given in the following formula:

$$w_{GH} = w_{fw-dw} + w_{air,out} + 0.1(w_{con,fac} + w_{con,hex}) \quad [3.10]$$

In this model condensation on surfaces other than the greenhouse cover or the cooler is not retrieved but re-evaporated. The water used in the fogging system is calculated separately in the KASPRO model. Plant factories are designed as closed systems and do not include water loss resulting from exfiltration and ventilation. Therefore, total water use in plant factories is assumed to be the water content of the produce (w_{fw-dw}).

3.2.4.4 CO₂

In greenhouses, ventilation limits the CO₂ concentration that can be maintained; in practice a certain CO₂ concentration is selected (simulation setpoint: 800 ppm). The concentration that is attained is the result of the supply capacity and the ventilation rate. KASPRO uses the dosage and operational time of the CO₂ supply system to calculate the total amount of supplied CO₂. Similar to water vapour, CO₂ is considered not to exit plant factories; all supplied CO₂ is assimilated. Therefore, the total amount of supplied CO₂ in plant factories is calculated as twice the accumulated dry weight. This results from the weight loss in the transformation from CO₂ to carbohydrates (68%) and the fixation efficiency of CO₂ (approximately 70%) and an assumed harvest index of 1 (ratio of yield dry matter to total dry matter, see Section 3.2.2) for lettuce.

TABLE 3.1 Key model parameters for the design of plant factories and greenhouses in Sweden (SWE), the Netherlands (NLD) and the United Arab Emirates (UAE).

Parameter	Plant factories	Greenhouse: SWE	Greenhouse: NLD	Greenhouse: UAE
Location	See Greenhouse	67.83° N, 20.34° E	51.99° N, 5.66° E	24.45° N, 54.65° E
ASHRAE/Köppen-Gelger climate classification	See Greenhouse	7/Dfc	4A/Cfb	1B/BWh
Typology	Closed system	Venlo type	Venlo type	Venlo type
Dimensions (m)	100 x 100 x 6	100 x 100 x 6	100 x 100 x 6	100 x 100 x 6
Production area (m ²)	50,000	10,000	10,000	10,000
Average transmissivity ^a (%)	0	61.5 / 60.0 ^b	63.8	60.0
Façade construction	Gypsum – PUR – Gypsum	Standard single glass cover ^d	Standard single glass cover ^d	Standard single glass cover ^d
Heat transfer coefficient (W m ⁻² K ⁻¹)	0.05 ^c	5.70	5.70	5.70
Heating setpoints photo-/dark period (°C)	24/24	12/9	12/9	N/A
Cooling/ventilation setpoints photo-/dark period (°C)	30/30	16/13	16/13	24/17
P-Band ventilation	N/A	(5;5);(15;4) ^e	(5;5);(15;4) ^e	N/A
Relative humidity setpoints photo-/dark period (%)	RH _{min} = 65/65 RH _{max} = 90/90	RH _{max} = 85/90 RH _{min} = 80	RH _{max} = 85/90 RH _{min} = 80	RH _{max} = 85/90 RH _{min} = 70
P-Band relative humidity	N/A	(5;10);(20;5) ^f	(5;10);(20;5) ^f	N/A
Heating system	HVAC (forced circulation)	Boiler (gas) Low metallic pipes	Boiler (gas) Low metallic pipes	N/A
Heating capacity (W m ⁻²)	N/A	150	100	N/A
Cooling system	HVAC (forced circulation) Fancoil unit Air cooled chiller	Natural ventilation Fogging system (H ₂ O)	Natural ventilation Fogging system (H ₂ O)	Natural ventilation Fogging system (H ₂ O) Heat exchanger Air cooled chiller
Active cooling capacity (W m ⁻²)	N/A	0	0	700
Fog system setpoints ^g	N/A	T _{min} = 20 °C (summer ^h) T _{min} = 22 °C (winter ^h) RH _{min} = 80%	T _{min} = 20 °C (summer ^h) T _{min} = 22 °C (winter ^h) RH _{min} = 80%	T _{min} = 25 °C RH _{min} = 70%
Fog system capacity (g m ⁻² h ⁻¹)	N/A	300	300	300

>>>

TABLE 3.1 Key model parameters for the design of plant factories and greenhouses in Sweden (SWE), the Netherlands (NLD) and the United Arab Emirates (UAE).

Parameter	Plant factories	Greenhouse: SWE	Greenhouse: NLD	Greenhouse: UAE
Energy saving screen setpoints ⁱ	N/A	(-20;300); (3;200); (4;10) T_{out} (max): 10 °C	(-20;300); (3;200); (4;10) T_{out} (max): 10 °C	N/A
CO ₂ levels ($\mu\text{mol mol}^{-1}$)	1200	800	800	800
CO ₂ dosing capacity ($\text{kg ha}^{-1} \text{h}^{-1}$)		180	180	150
Lighting system	LED	N/A / HPS ^j	N/A	N/A
Radiation ($\mu\text{mol m}^{-2} \text{s}^{-1}$)	500	Natural / Natural + 100 ^j	Natural	Natural
Duration photo-/dark period	16h/8h	Natural / Natural + artificial illumination ^j	Natural	Natural
Growth cycle (d)	30 ^k	60 ^l	60 ^l	60 ^l

^a Average transmissivity is defined as the average of greenhouse daytime transmission values for the entire year (Appendix 3A).

^b Average transmissivity without (GH) and with (GH+) shadows created by the lighting installation, respectively.

^c Standards for insulation and airtightness were exceeded to simulate a closed system [7, 9].

^d Optical properties are listed in Appendix 3A.

^e Vents are fully opened when interior temperature exceeds the setpoint by $\geq 5^\circ\text{C}$ at $T_{ex} < 5^\circ\text{C}$. Vents are also fully opened if interior temperature exceeds the setpoint by $\geq 4^\circ\text{C}$ at $T_{ex} \geq 15^\circ\text{C}$. In between, linear interpolation is used.

^f Vents are fully opened when interior relative humidity exceeds the setpoint by $\geq 10\%$ at $T_{ex} \leq 5^\circ\text{C}$. Vents are also fully opened when interior relative humidity exceeds the setpoint by $\geq 5\%$ at $T_{ex} \geq 20^\circ\text{C}$. In between, linear interpolation is used.

^g Fogging is activated when the interior climate exceeds the temperature setpoint or falls below the relative humidity setpoint.

^h Summer runs from 01 APR - 30 SEP and winter from 01 OCT - 31 MAR.

ⁱ Screens are closed at $-20^\circ\text{C} < T_{ex} < 3^\circ\text{C}$ if radiation is $< 300 \text{ W m}^{-2}$, at $3^\circ\text{C} < T_{ex} < 4^\circ\text{C}$ if radiation is $< 200 \text{ W m}^{-2}$ and at $4^\circ\text{C} < T_{ex} < 10^\circ\text{C}$. Screens are not used at $T_{ex} \geq 10^\circ\text{C}$. In between, linear interpolation is used.

^j Values without (GH) and with (GH+) artificial illumination, respectively. The intensity and duration of the artificial lighting (average power of 55 W m^{-2}) were calculated to supplement natural lighting in SWE (by 299.5 MJ m^{-2} of PAR, annually) to match the total PAR available in the NLD greenhouse.

^k This cycle duration already produced crops of marketable size in plant factories.

^l Actual practice by Dutch greenhouse lettuce growers [39].

TABLE 3.2 The energy potential of resources as used to determine system loads from KASPRO output.

	Zone heating	Latent cooling	Sensible cooling	Electric	Solar
Output KASPRO	Gas use ($\text{m}^3 \text{s}^{-1}$)	Condensed water (kg s^{-1})	Evaporated water (kg s^{-1})	Electricity (kWh)	Total PAR ($\mu\text{mol s}^{-1}$)
Factor	$3.17\text{E}7 \text{ (J m}^{-3}\text{)}$	$2.44\text{E}6 \text{ (J kg}^{-1}\text{)}$	$1.67\text{E}-2 \text{ (J kg}^{-1}\text{)}$	1.00	$4.57 \text{ (J } \mu\text{mol}^{-1}\text{)}$

TABLE 3.3 Coefficients of performance for the conversion of system loads in electric systems. These coefficients were determined using the Carnot efficiency of a heat pump, following the method presented by Meggers et al. [38] and using temperatures weighted for corresponding load.

	Heating	Dehumidification	Sensible cooling	LED cooling	(LED) Electric
SWE	3.4	10.0*	10.0*	10.0*	1
NLD	5.0	7.5	7.5	7.5	1
UAE	10.0*	3.7	3.7	3.7	1

* The use of a heat pump would be inappropriate in this situation, since the outside temperature is adequate in using (air/air) heat exchangers for heating/cooling. In these cases the COP was set at 10

3.3 Results

The production and the use of water and CO₂ are quite similar in the three plant factories. Therefore, we decided to specify and analyse only the results for the NLD-PF, unless stated differently. Results are normalised for cultivation area and for dry matter production.

The total dry matter production (Figure 3.3) and the corresponding resource use were calculated for each lettuce production system at the three sites. A dry matter content of 7% results in a fresh weight production of approximately 31 kg m⁻² in greenhouses in NLD. This corresponds closely with the usual Dutch greenhouse production, as reported by Vermeulen [40]. Figure 3.4 illustrates the annual energetic loads in MJ y⁻¹, broken down into the energy use for LED lighting, the cooling of the LED lamps, sensible cooling, dehumidification and heating. Solar radiation is included in the calculation in order to illustrate the total energy requirement. The annual electricity requirement for all systems was assessed according to the method described in Section 3.2.4.2. The energetic efficiency of the systems was determined by normalising the energy requirement for dry weight production (Figure 3.5). The use of water and CO₂ by each facility is illustrated in Figure 3.5-3.8. Finally, a brief overview of the resource use efficiency of each system is given in Figure 3.9.

3.4 Discussion

Figure 3.3 shows the most obvious benefit of a plant factory compared with a greenhouse or open field production: it enables a high and uniform production year-round. The optimisation and uniformity of the interior climate of plant factories result in a production of dry matter that is higher and more consistent than in greenhouses. The efficiency of this production, however, depends on a number of resources, as discussed below.

3.4.1 Energy use

Plant factories require a larger input of purchased energy than greenhouses for the production of lettuce. The energy efficiency of plant factories, however, is considerably higher. The calculated load of artificial illumination in plant factories exceeds all other loads for each facility at each location (Figure 3.4). Other notably high energy loads are heating for NLD-GH and SWE-GH(+) and sensible/latent cooling for UAE-GH and all plant factories. In plant factories this cooling load results from the relatively high internal heat load from crop transpiration and the inefficiency of the LED fixtures.

The total system loads per cultivation area are greater in plant factories than in most greenhouses, even when taking solar energy into account (Figure 3.4). The total amount of equivalent energy required for the production of dry matter in plant factories, however, is lower than in greenhouses at each location (Figure 3.4). The semi-closed, transparent and conductive nature of the greenhouse design is responsible for this inefficient use of resources.

The greenhouse clearly excels with respect to the use of freely available solar energy. Greenhouses require less purchased energy than plant factories (Figure 3.5). Compared with the dry matter production in greenhouses, the plant factory requires an additional input of $30 \text{ kWh}_e \text{ kg}^{-1}$ (+14%) for SWE-GH, $59 \text{ kWh}_e \text{ kg}^{-1}$ (+33%) for SWE-GH+, $176 \text{ kWh}_e \text{ kg}^{-1}$ (+251%) for NLD-GH and $158 \text{ kWh}_e \text{ kg}^{-1}$ (+142%) for UAE-GH (Figure 3.9A). Direct use of solar energy has a greater impact on the total energy requirement than an efficient use of energy.

Presumably plant factories are more suitable than greenhouses for lettuce production at higher latitudes. This is illustrated by the fact that the energetic

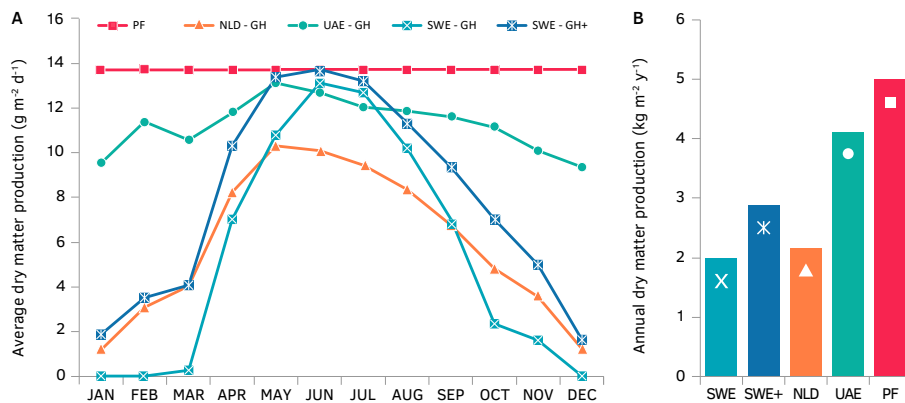


FIG. 3.3 Moving average of daily dry matter production ($\text{g m}^{-2} \text{d}^{-1}$) (A) and total annual dry weight production ($\text{kg m}^{-2} \text{y}^{-1}$) per cultivation area (B). Squares represent the plant factories, triangles represent greenhouses in NLD, circles represent greenhouses in the UAE, and crosses and stars represent greenhouses in SWE without and with artificial illumination, respectively.

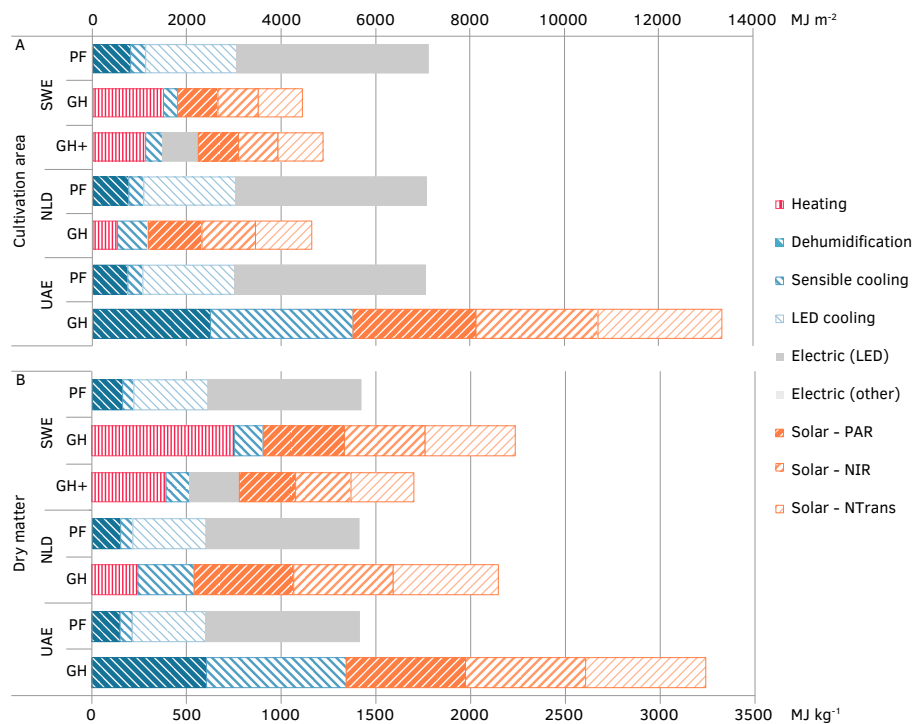


FIG. 3.4 Energy load of plant factories and greenhouses in UAE, NLD and SWE, normalised for cultivation area (MJ m^{-2}) (A) and for dry matter production ($\text{MJ kg}_{\text{dw}}^{-1}$) (B).

performance of SWE-GH+ considerably improves with artificial lighting. At even higher latitudes, heating is supposed to require more electricity than lighting. This supposition concurs with the idea that plant factories are effective in minimising electricity consumption in extremely dark/cold regions [8]. However, the idea that plant factories may also minimise electricity consumption in hot and arid regions seems to be erroneous, as suggested by the energetic efficiency of facilities in UAE. Here, freely available solar energy saves more electricity than is needed for cooling purposes.

3.4.2 Other resources: Water, CO₂ and land area

The viability of plant factories may depend on the efficient use of local resources; particularly water and land area may be scarce. At all three locations plant factories use these resources more efficiently than greenhouses.

The water use efficiency increases with lower ventilation requirements [13]. In this study we could confirm that (nearly) closed systems, such as UAE-GH and all plant factories, provide higher water use efficiencies than semi-open systems, such as NLD-GH and SWE-GH(+) (Figure 3.6–Figure 3.7). The water use in closed systems is presumed to approach the water content of the produce (Section 3.2.4.3). When assuming a harvest index of 1.0 (Section 3.2.2), the plant factory could have a theoretical water use efficiency of 100% [9]. Production in plant factories could reduce water use by 28% (UAE) to 95% (NLD) compared with greenhouses. Water use efficiency in relation to dry weight is demonstrated in Figure 3.9C.

Similar to water, the use of CO₂ is strongly influenced by the ventilation requirements of the facility (Figure 3.8). This is illustrated by SWE-GH where low temperatures during summer result in a lower requirement for natural ventilation compared with UAE-GH and NLD-GH. Concomitantly in SWE-GH a high retention rate and concentration of CO₂ is achieved, as well as an increased production. Production in plant factories could reduce CO₂ use by 67% (UAE) to 92% (NLD) compared with greenhouses. CO₂ use efficiency in relation to dry weight is illustrated in Figure 3.9B.

Finally, the land area can also be considered as a resource. Stacking production layers implies a linear increase in the production capacity. In this study we simulated five layers, but more are possible. In closed systems additional production layers should not affect the resource use efficiency. A high production density could overload the climatisation system, thereby decreasing efficiency and increasing energy expenditure. The densification of production, however, becomes more important in view of the variations in price and availability of land.

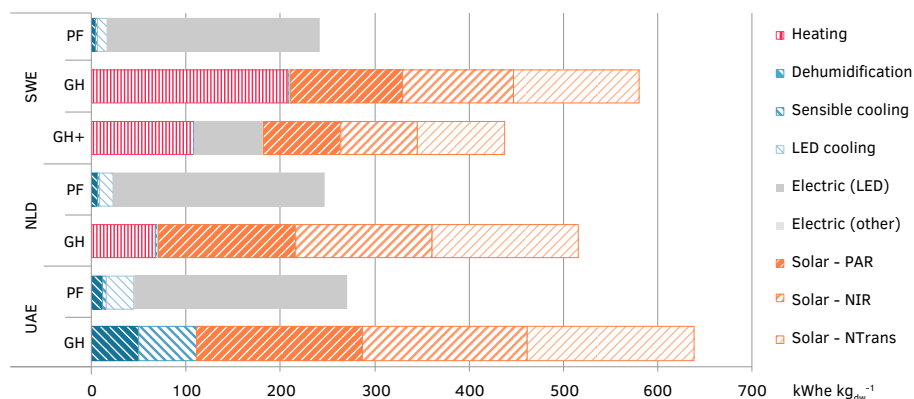


FIG. 3.5 Electricity use per kg lettuce dry matter production ($\text{kWh}_e \text{ kg}_{dw}^{-1}$) by end use. Electricity use has been calculated according to the methods described in Section 3.2.4.2.

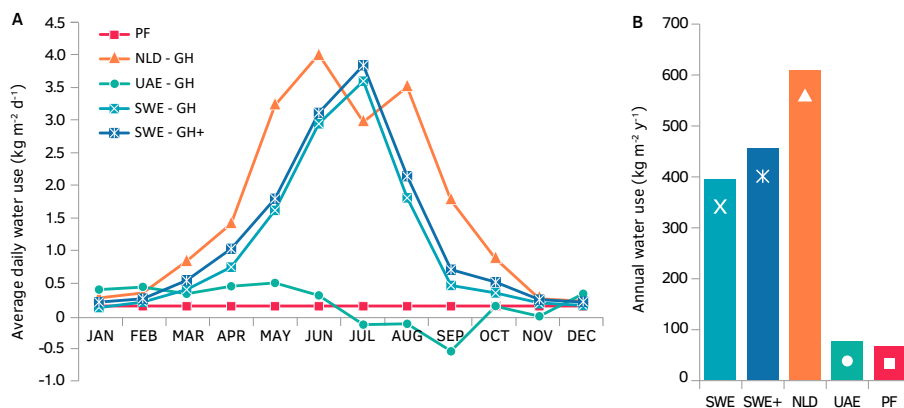


FIG. 3.6 Average daily water use ($\text{kg m}^{-2} \text{ d}^{-1}$) (A) and total annual water use per cultivation area ($\text{kg m}^{-2} \text{ y}^{-1}$) in plant factories and greenhouses (B). The negative values of UAE in summertime can be explained by the fact that the calculations include the influence of infiltration of water vapour. During the summer months the absolute vapour content of air is higher outside the greenhouse. This results in water vapour infiltrating the facility and consequently being condensed and retrieved.

3.4.3 Relevance of the assumptions

The production in each facility depends on interior climate, cultivar selection, crop production system and construction design. Production and energetic efficiency (calculations) could be improved by selecting a different growth model and by optimising the climate setpoints. In this study, the dry matter production of lettuce at higher temperatures (UAE-GH and PFs) was presumably underestimated by the van Henten model [19] due to a decrease in productivity at higher temperatures (Section 3.2.2). Additionally, we have not comprehensively optimised the climate setpoints with regard to maximum production at each location and for each typology. According to the model, the net dry matter production in plant factories could be increased by approximately 62% by lowering the production temperature to 19°C. As a consequence, the cooling requirements would increase. Higher temperature setpoints for greenhouses in colder climates could also raise the production, but this would inevitably lead to higher heating requirements. In addition to temperature, the optimisation of intensity, composition and duration of lighting could improve lettuce production.

Production and energetic efficiency could be further optimised by the design of the crop production system and facility construction. In this study crop production systems were not designed for optimal spacing and cultivation intensity, as the van Henten model [19] does not include transplanting or respacing (Section 3.2.2). The total amount of required cultivation area, intensity of cultivation and general production schedule should be improved by continuous or discontinuous spacing [6]. In this study we did not vary the construction design of the greenhouses and plant factories. In particular the performance of greenhouses could be improved by adjusting the design to each location. For instance, the use of double-layer covers or additional movable curtains could reduce the heating requirement by almost half in SWE-GH and NLD-GH (e.g. [41]).

In summary we are aware of the uncertainty that ensues from our assumptions. Uniformity in processing the data, however, allows for a more straightforward interpretation without significantly altering the main outcomes of this study. Presumably a minor effect on these outcomes can be achieved by selecting different lettuce models, hardware and/or climate setpoints.

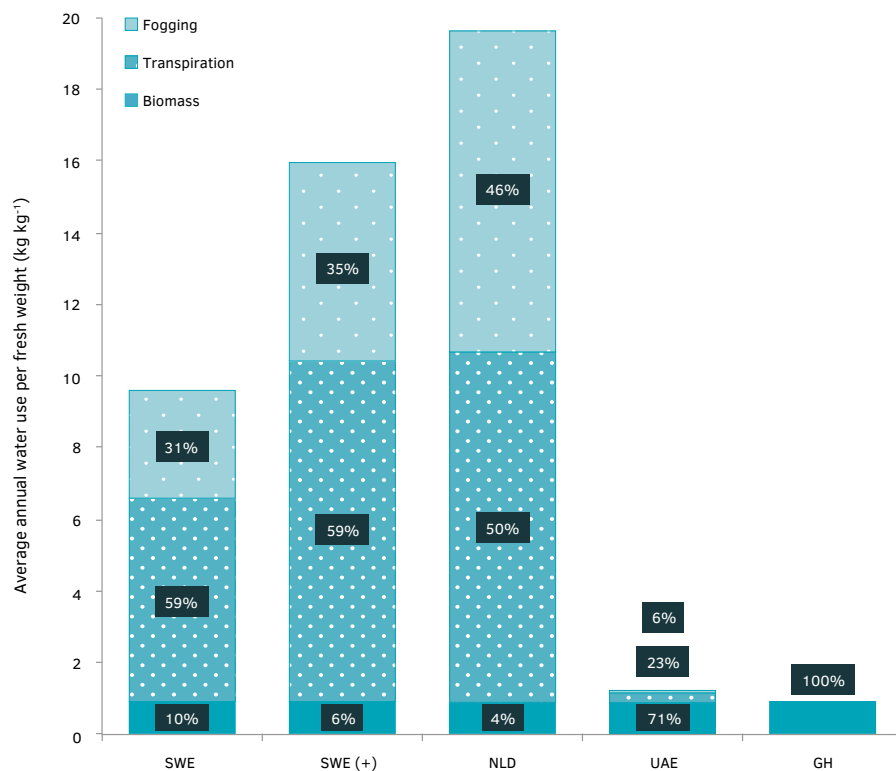


FIG. 3.7 Average annual water use per kg of fresh weight (kg kg^{-1}), divided for biomass and sources of water vapour. A dry matter content of 7% has been assumed throughout this study. The plant factory displays a theoretical water use efficiency of 1 to 1 [9].

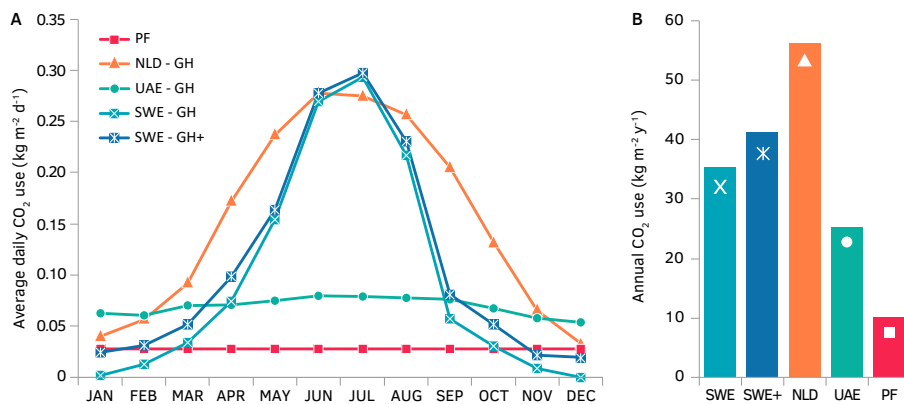


FIG. 3.8 Average daily CO₂ use ($\text{kg m}^{-2} \text{d}^{-1}$) (A) and total annual CO₂ use ($\text{kg m}^{-2} \text{y}^{-1}$) per cultivation area in plant factories and greenhouses (B).

In plant factories the predominance of artificial illumination in the total energy balance and the high total energy requirement are consistent with data from a wide range of production climates [42–44]. These issues are usually addressed by the technological advancement of LED systems and the integration of photovoltaic cells.

Indeed, the feasibility of plant factories largely depends on artificial illumination and its efficiency. When taking SWE-PF as an example, an increase of LED efficiency to 59% (Red:Blue = 80:20, $10.70 \text{ mol kWh}_e^{-1}$) could reduce electricity use for the production of dry matter to $210 \text{ kWh}_e \text{ kg}_{\text{dw}}^{-1}$, which is lower than in SWE-GH. When we consider a theoretical LED efficiency of 100% (Red:Blue = 80:20, $18.15 \text{ mol kWh}_e^{-1}$) the electricity use in NLD-PF and UAE-PF could be decreased to $132 \text{ kWh}_e \text{ kg}_{\text{dw}}^{-1}$ and $124 \text{ kWh}_e \text{ kg}_{\text{dw}}^{-1}$ respectively. The electricity use in the latter plant factories, however, would still be higher than in NLD-GH ($70 \text{ kWh}_e \text{ kg}_{\text{dw}}^{-1}$) and UAE-GH ($111 \text{ kWh}_e \text{ kg}_{\text{dw}}^{-1}$). The technological advancement in LED efficiency is of paramount importance, but presumably this is not sufficient to ensure the feasibility of plant factories.

Photovoltaic cells could be used to supply plant factories with renewable electricity. Modern monocrystalline silicon photovoltaic cells are able to reach efficiencies as high as 23% [45]. In practice, however, the efficiency of photovoltaic arrays does not exceed 17% [46]. When taking the roof of NLD-PF as an example (global solar radiation of $3.54 \text{ GJ m}^{-2} \text{ y}^{-1}$ [47], a photovoltaic array of $10,000 \text{ m}^2$ with an efficiency of 17% would be able to produce 1.67 GWh y^{-1} . This equals 2.71% of the plant factory's total annual electricity requirement. For lighting purposes direct solar energy is more efficient than artificial illumination powered by photovoltaic arrays. This can be illustrated by successively calculating the current efficiencies of photovoltaic cells (17%) and LED systems (52%, Section 3.2.3.3).

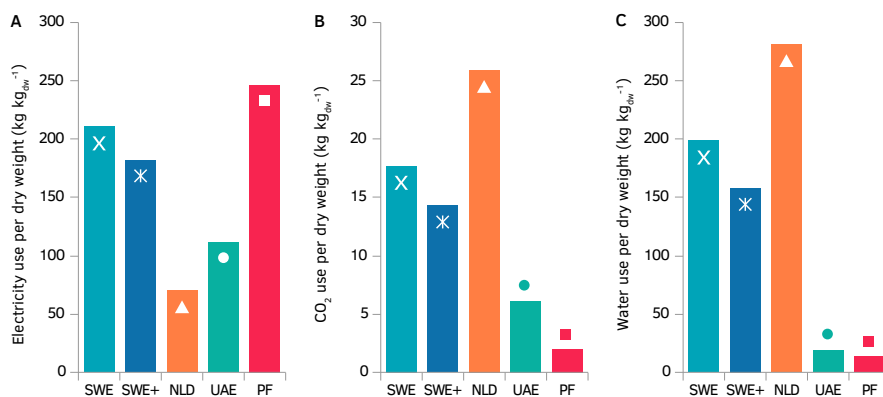


FIG. 3.9 Resource use for electricity (A), CO_2 (B) and water (C) of the plant factory (PF) and greenhouses (SWE, SWE(+), NLD and UAE), normalised for total dry matter production (kg_{dw}).

3.5 Outlook

At all three locations the greenhouse is more efficient in terms of purchased energy. It may be surprising that the benefits of solar energy exceed the need for climatisation even in the harsh environments of Kiruna and Abu Dhabi. This study demonstrates that the turnover point, where plant factories may be more energy efficient than greenhouses, lies in even more extreme environments. However, greenhouses in our most extreme locations (Kiruna and Abu Dhabi) were not viable without incorporating features of plant factories, such as artificial lighting and active cooling, respectively. This suggests that there is not a specific turnover point. Instead there is probably a gradual shift from a nearly natural to a fully controlled interior production climate. A shift in applicability of each typology is closely related to the energy use efficiency in greenhouses versus plant factories. The ratio of required input of energy can be estimated on the basis of KöppenGeiger climate zones and latitude. This may determine the suitability of plant factories compared with greenhouses (Figure 3.10).

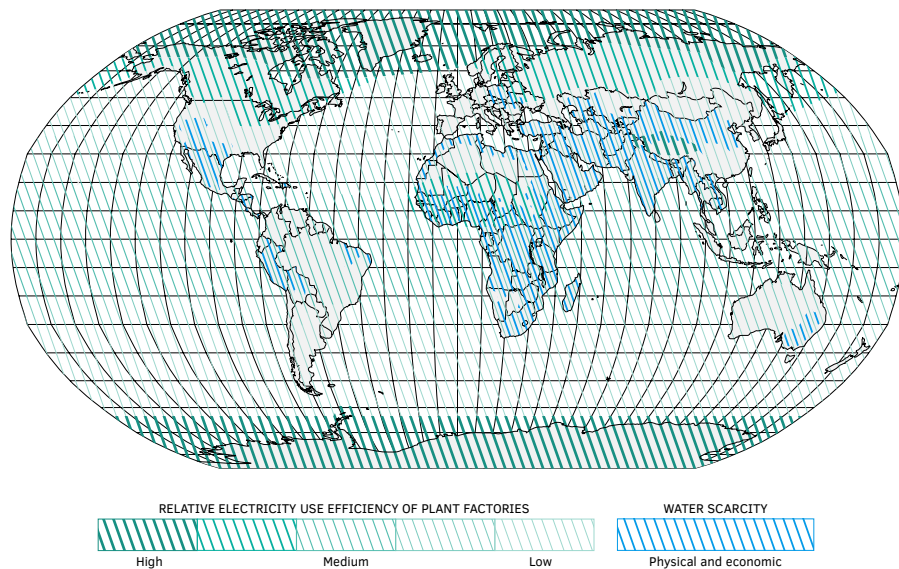


FIG. 3.10 Estimation of the advantages of plant factories versus greenhouses based on relative electricity use efficiency (red) and water scarcity (blue). Water scarcity is subdivided into (approaching) physical and economic scarcity [48].

In reality, the viability of the system as a whole does not solely depend on energetic performance. The efficiency of production and climatisation systems is directly related to the availability of resources. At locations with scarce resources plant factories offer opportunities by assuring an efficient use of water and CO₂ as well as a high production density (Figure 3.10).

Additional marketing advantages could also offset higher operational costs. A high and constant level of production allows the customer to reduce the number of contracted producers and to avoid the risk of asynchronous or insufficient supply. Moreover, the closed production environment of plant factories minimises the risk of pathogen infiltration and the need for protective chemicals. These side effects can increase the market value of the crop.

3.6 Concluding remarks

This study investigates the energetic requirements for the production of lettuce in different climate regions within either plant factories or greenhouses. The input and output were calculated, analysed and compared with respect to diverse latitudes and climates: Northern Sweden, the Netherlands and the United Arab Emirates. The results provide insight into the influence of the exterior climate on the production requirements and the performance of greenhouses and plant factories.

The outcome that plant factories would require a higher (purchased) energy input due to artificial lighting might have been foreseen. This study, however, offers detailed insights into the different interior and exterior exchanges and their influence on the production and the energy balance. Plant factories may offer many other advantages, such as a high retention of resources, uniformity of interior climate and density and quality of production. The disadvantage remains the high energetic demand due to the need for artificial lighting.

To forgo solar energy has a negative impact on the economic viability of a facility. This analysis enabled us to quantify this effect and determine the required offset. Additionally, it gave an indication of the productivity of various resources. Future research could use this approach for more comprehensive analyses and calculations on the financial and logistic viability of urban agricultural production in closed systems.

Acknowledgements

This work was supported jointly by the EUH2020 project “Ground Demonstration of Plant Cultivation Technologies and Operation in Space for Safe Food Production on-board ISS and Future Human Space Exploration Vehicles and Planetary Outposts” (EDEN-ISS, grant 636501) and by the Dutch Top Sector Tuinbouw & Uitgangsmaterialen (EU-2016-01). However, no endorsement of the results and conclusions by the European Commission or by the Dutch Ministry of Economic Affairs and Climate Policy is hereby implied. Thanks are due to Willem van der Spoel for his expert examination of the DesignBuilder model.

APPENDIX 3A

Optical properties and average transmissivity of the combination of a standard glass cover and the Venlo greenhouse structure.

The table shows the direct transmission values for a specific solar azimuth and elevation. Additionally, this table lists the hemispherical greenhouse transmission (tr_{diff}), specific heat of glass ($c_{p, glass}$) and type of cover (type). These values can be used to calculate the thermal exchange between the greenhouse and the surrounding climate.

direct	transmission	Diffuse transmission				tr_diff:										
		Specific heat per m material				$c_{p, glass}$:										
		Single or double cover				type:										
azimuth	elevation	2	4	6	8	10	15	20	25	30	40	50	60	70	80	90
0	0	0	0.060	0.136	0.212	0.284	0.437	0.553	0.635	0.694	0.763	0.799	0.819	0.832	0.842	0.850
5	0	0.020	0.082	0.153	0.220	0.288	0.438	0.551	0.634	0.692	0.760	0.797	0.818	0.831	0.841	0.850
10	0	0.026	0.131	0.204	0.275	0.327	0.445	0.551	0.632	0.690	0.760	0.798	0.817	0.831	0.841	0.850
15	0	0.030	0.149	0.241	0.318	0.381	0.477	0.556	0.630	0.687	0.759	0.796	0.818	0.830	0.841	0.850
20	0	0.032	0.162	0.273	0.351	0.415	0.525	0.577	0.632	0.685	0.756	0.796	0.817	0.829	0.840	0.850
25	0	0.033	0.169	0.289	0.381	0.440	0.553	0.614	0.643	0.685	0.754	0.794	0.816	0.832	0.840	0.850
30	0	0.041	0.172	0.300	0.394	0.476	0.573	0.641	0.670	0.690	0.752	0.793	0.817	0.831	0.840	0.850
35	0	0.033	0.192	0.307	0.405	0.477	0.588	0.655	0.694	0.704	0.751	0.792	0.816	0.831	0.840	0.850
40	0	0.045	0.182	0.313	0.414	0.488	0.601	0.666	0.709	0.724	0.751	0.791	0.816	0.831	0.840	0.850
45	0	0.030	0.186	0.317	0.421	0.497	0.629	0.675	0.716	0.740	0.752	0.790	0.816	0.831	0.840	0.850
50	0	0.026	0.190	0.322	0.428	0.505	0.639	0.683	0.723	0.750	0.756	0.790	0.816	0.833	0.843	0.850
55	0	0.048	0.194	0.356	0.435	0.513	0.630	0.691	0.729	0.756	0.763	0.791	0.816	0.833	0.844	0.850
60	0	0.017	0.213	0.368	0.443	0.521	0.638	0.699	0.735	0.761	0.773	0.791	0.817	0.833	0.844	0.850
65	0	0.011	0.242	0.379	0.451	0.529	0.646	0.721	0.741	0.766	0.783	0.793	0.817	0.834	0.844	0.850
70	0	0.005	0.254	0.362	0.461	0.539	0.655	0.732	0.748	0.771	0.791	0.794	0.818	0.835	0.845	0.850
75	0	0.044	0.267	0.370	0.471	0.549	0.664	0.741	0.754	0.777	0.798	0.797	0.820	0.836	0.845	0.850
80	0	0.055	0.282	0.383	0.484	0.561	0.673	0.749	0.761	0.782	0.804	0.799	0.821	0.837	0.845	0.850
85	0	0.054	0.287	0.390	0.492	0.571	0.684	0.758	0.768	0.788	0.809	0.802	0.823	0.838	0.846	0.850
90	0	0.055	0.291	0.393	0.495	0.574	0.688	0.766	0.775	0.794	0.814	0.805	0.825	0.839	0.847	0.850

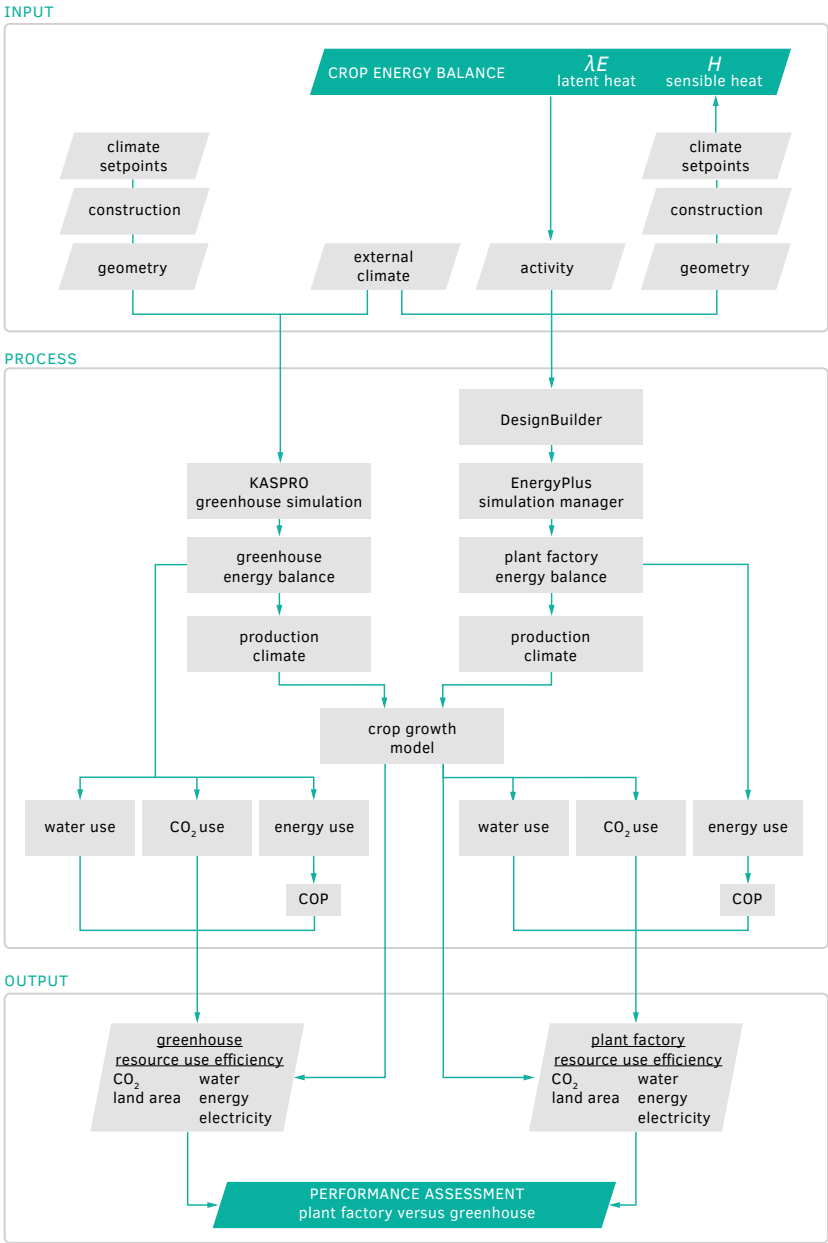


FIG. APP. 3B.1 Simplified model diagram to illustrate key processes and variables.

Reference list

- [1] United Nations. (2014). *World urbanization prospects: The 2014 revision, highlights*. New York: United Nations – Department of Economic and Social Affairs – Population division. doi:10.18356/527e5125-en
- [2] Newcombe, K. & Nichols, E.H. (1979). An integrated ecological approach to agricultural policy-making with reference to the urban fringe: The case of Hong Kong. *Agricultural Systems*, 4(1), 1-27. doi:10.1016/0308-521x(79)90011-8
- [3] Rosenzweig, C. & Liverman, D. (1992). Predicted effects of climate change on agriculture: A comparison of temperate and tropical regions. In Majumdar, SK. (Ed.), *Global climate change: Implication, challenges and mitigation measures* (pp. 342-361). Philadelphia: Pennsylvania Academy of Sciences.
- [4] Kennedy, C., Cuddihy, J., & Engel-Yan, J. (2007). The changing metabolism of cities. *Journal of industrial ecology*, 11(2), 43-59. doi:10.1162/jiec.0.1107
- [5] Lambin, E. & Meyfroidt, P. (2011). Global land use change, economic globalization, and the looming land scarcity. *Proceedings of the National Academy of Sciences*, 108(9), 3465-3472. doi:10.1073/pnas.1100480108
- [6] Seginer, I. & Ioslovich, I. (1999). Optimal spacing and cultivation intensity for an industrialized crop production system. *Agricultural Systems*, 62(3), 143-157. doi:10.1016/s0308-521x(99)00057-8
- [7] Kozai, T., Ohya, K., & Chun, C. (2006). Commercialized closed systems with artificial lighting for plant production. *Acta Horticulturae*, 711, 61-70. doi:10.17660/actahortic.2006.711.5
- [8] Kozai, T. (2013). Sustainable plant factory: Closed plant production systems with artificial light for high resource use efficiencies and quality produce. *Acta Horticulturae*, 1004, 27-40. doi:10.17660/actahortic.2013.1004.2
- [9] Kozai, T. (2013). Resource use efficiency of closed plant production system with artificial light: Concept, estimation and application to plant factory. *Proceedings of the Japan Academy. Series B, Physical and biological sciences*, 89(10), 447-461. doi:10.2183/pjab.89.447
- [10] Goto, E. (2012). Plant production in a closed plant factory with artificial lighting. *Acta Horticulturae*, 956, 37-49. doi:10.17660/actahortic.2012.956.2
- [11] Graamans, L., van den Dobbelsteen, A., Meinen, E., & Stanghellini, C. (2017). Plant factories; crop transpiration and energy balance. *Agricultural Systems*, 153, 138-147. doi:10.1016/j.agry.2017.01.003
- [12] De Zwart, H.F. (1996). *Analyzing energy-saving options in greenhouse cultivation using a simulation model*. (PhD), Wageningen University & Research, Wageningen, the Netherlands.
- [13] Katsoulas, N., Sapounas, A., De Zwart, F., Dieleman, J.A., & Stanghellini, C. (2015). Reducing ventilation requirements in semi-closed greenhouses increases water use efficiency. *Agricultural Water Management*, 156, 90-99. doi:10.1016/j.agwat.2015.04.003
- [14] Luo, W.H., de Zwart, H.F., Dai, J.F., Wang, X.H., Stanghellini, C., & Bu, C.X. (2005). Simulation of greenhouse management in the subtropics, Part I: Model validation and scenario study for the winter season. *Biosystems Engineering*, 90(3), 307-318. doi:10.1016/j.biosystemseng.2004.11.008
- [15] Luo, W.H., Stanghellini, C., Dai, J.F., Wang, X.H., de Zwart, H.F., & Bu, C.X. (2005). Simulation of greenhouse management in the subtropics, Part II: Scenario study for the summer season. *Biosystems Engineering*, 90(4), 433-441. doi:10.1016/j.biosystemseng.2004.12.002
- [16] DesignBuilder. (2016). DesignBuilder version 4.7.0.027. Gloucestershire, UK: DesignBuilder Software Ltd. Retrieved from www.designbuilder.co.uk/index.php
- [17] Crawley, D.B., Lawrie, L.K., Winkelmann, F.C., Buhl, W.F., Huang, Y.J., Pedersen, C.O., Strand, R.K., Liesen, R.J., Fisher, D.E., Witte, M.J., & Glazer, J. (2001). EnergyPlus: creating a new-generation building energy simulation program. *Energy and buildings*, 33(4), 319-331. doi:10.1016/s0378-7788(00)00114-6
- [18] Tei, F., Scaife, A., & Aikman, D.P. (1996). Growth of lettuce, onion, and red beet. 1. Growth analysis, light interception, and radiation use efficiency. *Annals of Botany*, 78(5), 633-643. doi:10.1006/anbo.1996.0171
- [19] Van Henten, E.J. (1994). Validation of a dynamic lettuce growth model for greenhouse climate control. *Agricultural Systems*, 45(1), 55-72. doi:10.1016/S0308-521X(94)90280-1
- [20] MATLAB. (2016). MATLAB version R2016a (9.0.0.341360). Natick, Massachusetts, USA: The MathWorks, Inc. Retrieved from www.mathworks.com/products/matlab.html

- [21] He, J. & Lee, S.K. (1998). Growth and photosynthetic responses of three aeroponically grown lettuce cultivars (*Lactuca sativa* L.) to different rootzone temperatures and growth irradiances under tropical aerial conditions. *Journal of Horticultural Science and Biotechnology*, 73(2), 173-180. doi:10.1080/14620316.1998.11510961
- [22] He, J. & Lee, S.K. (1998). Growth and photosynthetic characteristics of lettuce (*Lactuca sativa* L.) under fluctuating hot ambient temperatures with the manipulation of cool root-zone temperature. *Journal of Plant Physiology*, 152(4), 387-391. doi:10.1016/s0176-1617(98)80252-6
- [23] Frantz, J.M., Ritchie, G., Cometti, N.N., Robinson, J., & Bugbee, B. (2004). Exploring the limits of crop productivity: beyond the limits of tipburn in lettuce. *Journal of the American Society for Horticultural Science*, 129(3), 331-338.
- [24] Koudela, M. & Petříková, K. (2008). Nutrients content and yield in selected cultivars of leaf lettuce (*Lactuca sativa* L. var. *crispa*). *Horticultural Science*, 35(3), 99-106.
- [25] Gent, M.P.N. (2014). Effect of daily light integral on composition of hydroponic lettuce. *HortScience*, 49(2), 173-179.
- [26] EnergyPlus. (2016). EnergyPlus weather data by location - Amsterdam 062400 (IWE). Retrieved 26 October 2016 https://energyplus.net/weather-location/europe_wmo_region_6/NLD//NLD_Amsterdam.062400_IWE
- [27] EnergyPlus. (2016). EnergyPlus weather data by location - Kiruna 020440 (IWE). Retrieved 30 November 2016 https://energyplus.net/weather-location/europe_wmo_region_6/SWE//SWE_Kiruna.020440_IWE
- [28] EnergyPlus. (2016). EnergyPlus weather data by location - Bandar Abass 408750 (ITMY). Retrieved 30 November 2016 https://energyplus.net/weather-location/asia_wmo_region_2/IRN//IRN_Bandar.Abass.408750_ITMY
- [29] Royal Philips N.V. (2015). Philips Horticulture LED solutions - GreenPower LED toplighting - high output. Retrieved 15 December 2016 http://images.philips.com/is/content/PhilipsConsumer/PDFDownloads/Global/ODLI20150701_001-UPD-en_AA-QIG_LED_Toplighting_HO_Philips_Horticulture_EN.pdf
- [30] Sabe, N.C., Giacomelli, G.A., & Kubota, C. (2011). Water use in a greenhouse in a semi-arid climate. *Transactions of the ASABE - American Society of Agricultural and Biological Engineers*, 54(3), 1069-1077. doi:10.13031/2013.37098
- [31] Hall, A.E. (1979). A model of leaf photosynthesis and respiration for predicting carbon dioxide assimilation in different environments. *Oecologia*, 43(3), 299-316. doi:10.1007/bf00344957
- [32] Farquhar, G.D., von Caemmerer, S., & Berry, J.A. (1980). A biochemical model of photosynthetic CO₂ assimilation in leaves of C3 species. *Planta*, 149(1), 78-90. doi:10.1007/bf00386231
- [33] Thompson, H.C., Langhans, R.W., Both, A.J., & Albright, L.D. (1998). Shoot and root temperature effects on lettuce growth in a floating hydroponic system. *Journal of the American Society for Horticultural Science*, 123(3), 361-364.
- [34] Waycott, W. (1995). Photoperiodic response of genetically diverse lettuce accessions. *Journal of the American Society for Horticultural Science*, 120(3), 460-467.
- [35] Zhao, X. & Carey, E.E. (2009). Summer production of lettuce, and microclimate in high tunnel and open field plots in Kansas. *HortTechnology*, 19(1), 113-119.
- [36] Silva, E.C., Maluf, W.R., Leal, N.R., & Gomes, L.A.A. (1999). Inheritance of bolting tendency in lettuce *Lactuca sativa* L. *Euphytica*, 109(1), 1-7. doi:10.1023/A:1003698117689
- [37] Simonne, A., Simonne, E., Eitenmiller, R., & Coker, C.H. (2002). Bitterness and composition of lettuce varieties grown in the southeastern United States. *HortTechnology*, 12(4), 721-726.
- [38] Meggers, F., Ritter, V., Goffin, P., Baetschmann, M., & Leibundgut, H. (2012). Low exergy building systems implementation. *Energy*, 41(1), 48-55. doi:10.1016/j.energy.2011.07.031
- [39] Vermeulen, P.C.M. (2016). *Kwantitatieve Informatie voor de glastuinbouw 2016-2017: Kengetallen voor groenten – snijbloemen – pot- en perkplanten teelten. Rapport GTB-5121* (Vol. 25). Wageningen, the Netherlands: Wageningen UR Glastuinbouw.
- [40] Vermeulen, P.C.M. (2014). *Kwantitatieve Informatie voor de glastuinbouw: Kengetallen voor groenten – snijbloemen – pot- en perkplanten teelten. Rapport GTB-5067* (Vol. 23). Wageningen, the Netherlands: Wageningen UR Glastuinbouw.
- [41] Kempkes, F. (2017). Gasverbruik in onderzoekskassen onder 40% van praktijkgemiddeld: Aan energiebesparing zit een harde grens. *Vakblad onder Glas*, 14, 48-50.

- [42] Nishimura, M., Kozai, T., Kubota, C., & Chun, C. (2001). Analysis of electric energy consumption and its cost for a closed-type transplant production system. *Journal of Society of High Technology in Agriculture*, 14(3), 204-209.
- [43] Tong, Y., Yang, Q., & Shimamura, S. (2013). *Analysis of electric-energy utilization efficiency in a plant factory with artificial light for lettuce production*. Paper presented at the International Symposium on New Technologies for Environment Control, Energy-Saving and Crop Production in Greenhouse and Plant Factory - Greensys 2013.
- [44] Harbick, K. & Albright, L.D. (2016). Comparison of energy consumption: greenhouses and plant factories. *Acta Horticulturae*, 1134, 285-292. doi:10.17660/actahortic.2016.1134.38
- [45] Green, M.A., Emery, K., Hishikawa, Y., Warta, W., & Dunlop, E.D. (2015). Solar cell efficiency tables (Version 45). *Progress in photovoltaics: research and applications*, 23(1), 1-9. doi:10.1002/pip.2573
- [46] Tyagi, V.V., Rahim, N.A.A., Rahim, N.A., & Selvaraj, J.A.L. (2013). Progress in solar PV technology: Research and achievement. *Renewable and Sustainable Energy Reviews*, 20(C), 443-461. doi:10.1016/j.rser.2012.09.028
- [47] KNMI. (2014). *KNMI '14 - klimaatscenario's voor Nederland; leidraad voor professionals in klimaatadaptatie*. de Bilt: KNMI (the Royal Netherlands Meteorological Institute).
- [48] United Nations. (2012). *The United Nations world water development report 4: managing water under uncertainty and risk* (Vol. 1). Paris: United Nations.

INTERMEZZO 3

Chapter 3 provided an overview of the resource use efficiency of lettuce production in plant factories and in greenhouses in three different climates. Plant factories demonstrated a higher resource use efficiency for water and CO₂ as a result of their closed nature, as well as for land area due to the high crop yield per production area and stackable production layers. The electricity use efficiency, however, was notably lower in plant factories across the three climates. This primarily results from the predominance of artificial illumination in the total energy balance and to a lesser extent from the high internal heat loads.

Chapter 4 investigated the systems design of the plant factory in terms of the capacity to improve its energy use efficiency. The impact of the façade and cooling system design was analysed in detail. The system was designed to reduce the high energy demand of plant factories resulting from high internal heat loads and forgoing freely available solar energy.

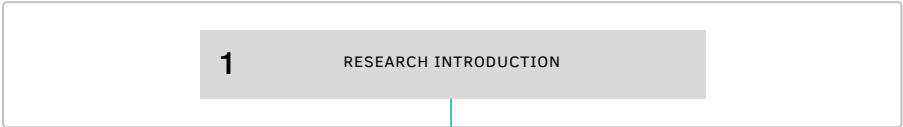


4 System optimisation

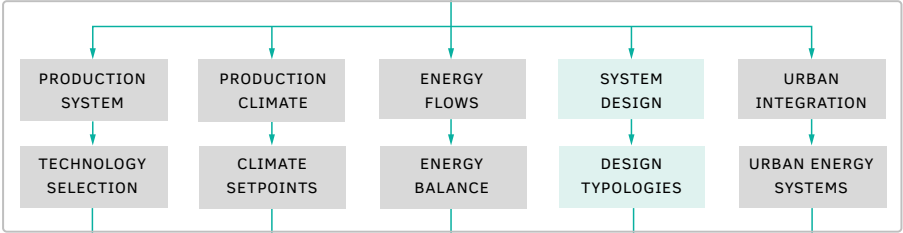
Plant factories: Reducing energy demand at high internal heat loads through façade design
Graamans, L., Tenpierik, M., van den Dobbelsteen, A., Stanghellini, C.
Applied energy. 2020; 262: 114544.
[doi:10.1016/j.apenergy.2020.114544](https://doi.org/10.1016/j.apenergy.2020.114544)

ABSTRACT The increase in global food demand has led to the introduction of new food production systems. One key example is the plant factory. Plant factories face the same challenge as many high-tech building functions: high energy demands resulting from high internal heat loads. In this study we investigate how this energy demand can be reduced through façade design. Energy efficient design closely follows function, façade construction and local climate. Therefore, we analysed the effects of façade properties on the energy use in plant factories for three disparate climate zones: Sweden (Dfc), the Netherlands (Cfb) and the United Arab Emirates (BWh). We coupled the building energy simulation program EnergyPlus with a crop transpiration model to calculate the lighting, sensible cooling, latent cooling, and heating demand from the energy balance. In terms of energy demand (kWh m^{-2}), opaque façades with high U-values and optimised albedo can reduce the facilities' cooling demand by 18.8%, 30.0% and 30.4%, and their energy demand by 6.1%, 12.5% and 9.5%, for the United Arab Emirates, the Netherlands and Sweden, respectively. In terms of electricity use ($\text{kWh}_e \text{m}^{-2}$), transparent façades are more efficient, as they allow the use of freely available solar energy instead of artificial light. These façades can reduce electricity use by 9.4%, 7.6% and 7.4%, for the United Arab Emirates, the Netherlands and Sweden, respectively. The presented façade design strategies can significantly reduce energy demand in plant factories. The investigation provides a foundation for the energy efficient design of high-tech buildings, tailored to local climate.

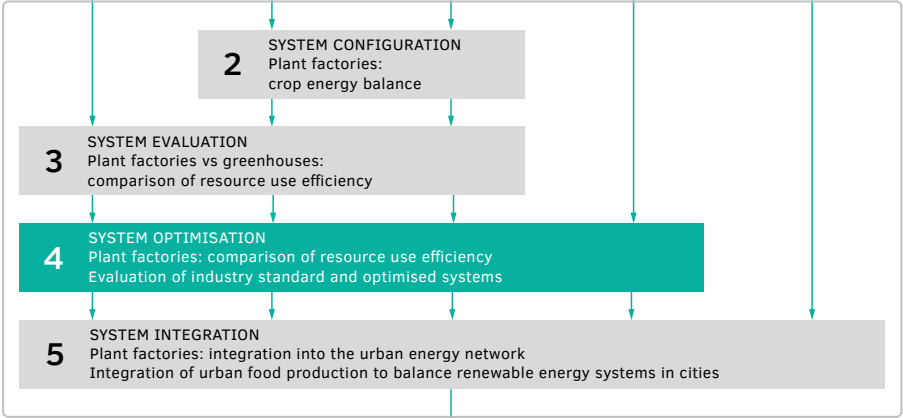
I. INTRODUCTION & METHODOLOGICAL FRAMEWORK



II. THEORETICAL FRAMEWORK



III. DESIGN & EXPERIMENTAL VALIDATION



IV. INTEGRATED DISCUSSION



4.1 Introduction

4.1.1 Background

Studies on urban climate resilience have resulted in the development of building typologies with new functions and improved performances. There is a growing interest in technologically advanced facilities for urban agriculture, such as plant factories and vertical farms⁵ [1]. These facilities are suggested to increase urban resiliency by ensuring the local supply of fresh food in the face of expanding urban populations. Food is generally supplied to large cities via the global food supply network, but the sustainability and resiliency of this network is questionable [2]. The predominance and complexity of that network will increase further as a result of the projected increase in the global urban population [3] to 6.3 billion by 2050 [4].

An exceptionally high productivity is a prerequisite for the (economic) viability of urban agriculture in view of local food demand and the financial value of urban space. Plant factories are closed production systems which are designed to maximise production density [5], crop productivity [6] and resource use efficiency [7]. Their aim is to increase productivity by stacking production layers and by optimising the interior climate with uniform lighting, temperature, CO₂ concentration and relative humidity. Uniformity is achieved by minimising the interaction with the exterior climate. This limited interaction could also contribute to the efficient (re-)use of energy [8], water [6] and CO₂ [9] in the plant factory, particularly in comparison with standard greenhouses [8].

The evident shortcoming of this typology is the high electricity requirement for artificial illumination to drive photosynthesis. Furthermore, the combination of high-density crop production, limited volume and lack of natural ventilation is likely to result in a high demand for cooling and vapour removal [10]. Sensible cooling, dehumidification and illumination account for approximately 32%, 11% and 57% of the total energy demand, respectively [8]. The high internal heat load and the demand for cooling in plant factories resemble the energy profile of modern data centres [11]. Improving the façade design can reduce the energy demand of plant

⁵ As a working definition, a vertical farm can be regarded as a plant factory with multiple building storeys.

factories and of other facilities with high internal heat loads. It has already been demonstrated that optimising insulation factors can limit HVAC system energy use [12] and that optimising window properties in conjunction with building form can increase the total energy efficiency of office buildings [13].

Façade design is directly related to context as well as to building design. Contextual factors include location, exterior climate and user behaviour; design factors include the building's shape, orientation, volume, zoning, compartmentalisation and envelope. Energy performance is predominated by the transfer of heat (e.g. insulation: U-value), and solar energy (e.g. solar heat gain coefficient: SHGC).

4.1.2 Problem statement

The façade design in plant factories differs from that for office buildings and housing, due to the high internal heat load and vapour production associated with plant production. Until now façade research typically has been concerned with the reduction of energy transfer across the façade, in order to limit cooling demands in warm climates [14] or heating demands in cold climates [15], whilst maintaining a certain level of transparency. On the other hand, research in the field of plant factories has been largely concerned with fully opaque, highly insulated and airtight structures [7]. Finally, research on building functions with comparatively high internal heat loads has predominantly focussed on the cooling systems in data centres. Examples range from reviewing the various thermal management techniques [16], to the impact of local climate on cooling system efficiency [17], and the integration of renewable energy [18] in data centres.

Little research has been done on the façade design of buildings with high internal heat loads, such as plant factories or data centres. To bridge that gap, this study addresses the interrelationship between façade properties and total energy demand in plant factories. Moreover, it formulates a rule-of-thumb for façade engineering at high internal heat loads, taking latitude and external conditions into account.

4.1.3 Objective

The main objective of this study is to quantify the effect of façade construction on the cooling, dehumidification, heating and lighting demand for lettuce production in plant factories, and to analyse how this demand is affected by the external climate.

4.1.4 Outline and framing

In this study, we have coupled established models for crop transpiration and energy balance to calculate and analyse the energy requirement for lettuce production in closed systems. A total of 54 variations (18 different façade constructions for three different building form factors) have been calculated for three disparate climate zones.

This study seeks to contribute to the energy efficiency of modern buildings. The analyses provide a foundation for the energy efficient design of plant factories and other building functions with high internal heat loads, such as data centres or other industrial functions. To the authors' knowledge, there are numerous studies on active measures to regulate these internal loads, but little is known about passive methods. Additionally, this study seeks to contribute to the field of sustainable food and energy supply. The energetic performance and optimisation of food production in plant factories and their potential integration into metropolitan areas have not yet been investigated in a quantitative manner. In short, this study seeks not only to contribute to the field of building energy efficiency but also to provide perspective on sustainable energy systems, the environmental footprint of cities and potentially climate change mitigation.

4.2 Materials and methods

The energy use of plant factories in three different locations was analysed. The energy demand of each facility consists of the system demands for dehumidification, sensible cooling, heating and artificial illumination, all of which are influenced by internal and external gains. These demands are calculated and compared using building simulation software.

4.2.1 Model selection

4.2.1.1 Building energy simulation

The energy loads and demands were calculated by means of EnergyPlus, using DesignBuilder v5.3. EnergyPlus is a dynamic building energy simulation program that consists of three basic components – a simulation manager, a heat and mass balance simulation module and a building systems simulation module [19]. Formal independent testing has been integral to the development of the model [20]. Afterwards, the model has been used in numerous studies to calculate building energy performance and has been extensively validated, i.e. for the calculation of energy use in large buildings [12], the effect of façade design on the energy use in highrise buildings [21], the calculation of zone climate loads [22], the simulation of energy flows through windows [23], the use of standard window performance indices to model window energy impacts [24], the impact of normalized energy profiles on hourly building energy consumption [25], as well as the temperature and velocity of air in a double-skin ventilated façade [26]. Furthermore, the climate in EnergyPlus for the selected locations is based on typical meteorological years, in order to guarantee a close representation of typical weather patterns [27]. It should still be realised, however, that “there is no such thing as a completely validated building energy simulation computer program. All building models are simplifications of reality” [28].

DesignBuilder [29] was used to generate input and visualise output, as it is considered the most complete graphic user interface for EnergyPlus. DesignBuilder does not allow for the integration of dynamic processes in order to calculate the effects of plants on the interior climate in real time, such as advanced greenhouse simulation models e.g. KASPRO [30]. This is not a limitation, however, as plant factories have just two states (photoperiod and dark period), each with constant climate setpoints throughout. In order to adequately calculate the interior energetic fluxes, it is essential to calculate the crop energy balance in both states – how it transpires, reflects light and exchanges heat and radiation.

4.2.1.2 Crop energy balance

The crop energy balance is a key factor in the internal heat load and should therefore be based on an accurate estimate of the crop transpiration coefficient,

i.e. the fraction of the radiation flux dissipated by the crop as latent heat. Cooling and vapour removal are quite different processes and the relation between sensible and latent heat is included in the calculation of energy demand. The energetic behaviour of crops was integrated into the simulations, following the method, model and assumptions described previously [10]. This model was validated for climate setpoints similar to those used in this study (Table 4.3). An average leaf area index of 2.1 was taken into account for the crop energy balance [31], in order to simulate that all stages of crop development are simultaneously present. The various positive energetic fluxes were set as equipment gains in DesignBuilder; the negative sensible heat fluxes were set as process gains, following the method described in [8].

The inefficiency of the LED-lighting system produces sensible heat, which was also set as an equipment gain. Assuming a system with an efficiency of $2.70 \mu\text{mol J}^{-1}$ and a red:blue distribution of 80:20, the waste heat is calculated as 48% of the electricity input (in W). The simulated plant factory features a lighting intensity of $250 \mu\text{mol m}^{-2} \text{s}^{-1}$, which translates to 46.15 W m^{-2} sensible heat per production layer.

4.2.1.3 Crop production

Minor differences in the interior climate of plant factories can result in differences in plant production and energetic performance. To allow for comparing data across studies, plant production should be calculated. There are several crop models available for the calculation of dry matter production, ranging from extensive and complex (i.e. 3D crop models, incorporating leaf angles and illumination ray tracing [32]), to pure photosynthetic assimilation (i.e. CO_2 assimilation in leaves [33]). To this end, the crop model described by van Henten [34] was selected and implemented in the computational software MATLAB [35] to calculate plant production, as described earlier [8] and presented in Appendix 4A. This model reduces the three-dimensional crop canopy to a single plane (cultivation area) and incorporates the fundamental photosynthesis processes as described by the Farquhar model [33]. This reduction increases workability and computational efficiency and is also considered sufficient for the required level of detail for this study.

The crop model was intensively investigated for its key parameters [36] that have been validated using experiments in Dutch greenhouses [34], which feature lower temperatures than are common in plant factories. The potential underestimation of dry matter production at higher temperatures has been investigated and quantified

[8]. Therefore, energy demand is normalised for area (m^2) and not for plant production (kg dry matter) throughout most of this study, in order to minimise the effect of this underestimation and to enhance the applicability of the presented findings within the broader field of energy systems engineering.

4.2.2 Fixed model inputs

4.2.2.1 Location and typology

Three representative sites of disparate latitudes and climates were selected, namely Kiruna in Sweden (67.8° N , 20.2° E ; SWE), Amsterdam in the Netherlands (52.0° N , 5.7° E ; NLD) and Abu Dhabi in the United Arab Emirates (24.5° N , 54.7° E ; UAE). The hourly weather information for the simulations was retrieved from the EnergyPlus database [37–39], which was selected for its extensiveness and precision. Figure 4.1 shows a monthly summary for solar radiation and temperature.

4.2.2.2 Interior climate setpoints

This study addresses the climate setpoints that directly influence dry matter production and it does not take the cultivars or other physiological factors into account. The climate setpoints for plant factories had to be carefully selected, as the productivity of lettuce is mainly determined by the relationship between canopy temperature, root zone temperature, photosynthetic photon flux density, photoperiod and CO_2 concentration. The photosynthetic photon flux density (PPFD) describes the number of photons in the photosynthetically active spectrum per square metre per second ($\mu\text{mol m}^{-2} \text{ s}^{-1}$), whereas the photoperiod (h d^{-1}) describes its diurnal duration.

This study uses PPFD of $250 \mu\text{mol m}^{-2} \text{ s}^{-1}$ as this should result in a high net photosynthetic rate of lettuce leaves [40] and a high light use efficiency [41]. The PPFD is combined with a photoperiod of 16 h d^{-1} to ensure adequate crop production, which is optimised for net photosynthetic rate [40], plant growth [42], light use efficiency [43] and thus for energy consumption. Furthermore, restricting the photoperiod to 16 h d^{-1} should prevent premature bolting (Waycott, 1995), which would render the crop unmarketable.

In greenhouses lettuce is usually grown at low temperatures, e.g. 12/9°C for day-/night-time in the Netherlands. In plant factories a low setpoint for air temperature would lead to an unrealistically high cooling demand, due to their high internal heat loads. Therefore, air temperature was maintained between 24°C and 30°C as this allows for the highest CO₂ assimilation at the selected PPFD and CO₂ concentration [44]. The relative humidity was maintained at between 75-85%. The root zone temperature was set to 24°C to ensure adequate plant production under elevated air temperatures, i.e. fresh weight production and the formation of compact heads [45]. Total production, colour, thickness and root structure were superior at this root zone temperature, at each air temperature [46].

The typical elevated CO₂ concentration setpoint in plant factories of 1200 ppm was used, in line with [47]. A small supply of CO₂ is considered sufficient to maintain this concentration, as the loss of CO₂ to the exterior climate is minimised in an airtight plant factory.

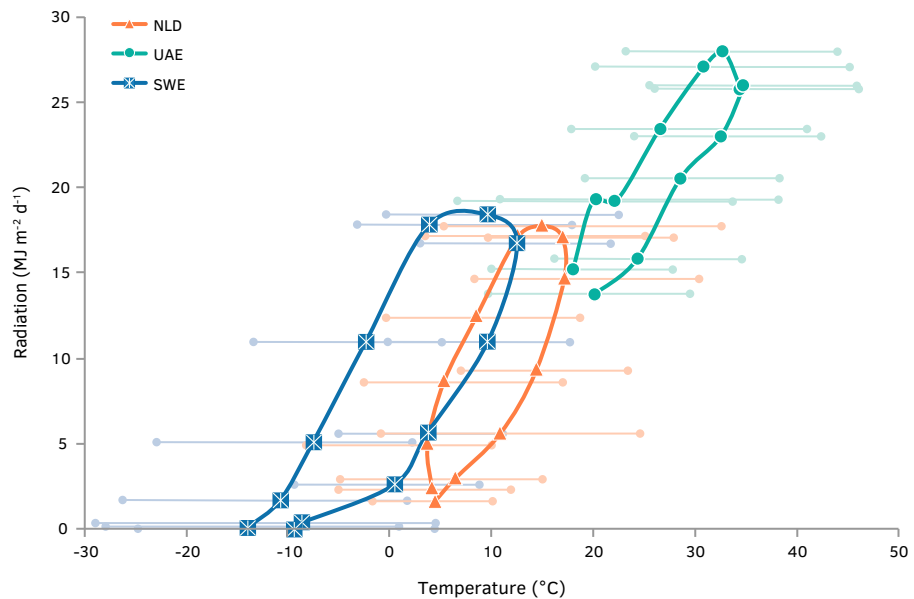


FIG. 4.1 Average daily radiation per month ($\text{MJ m}^{-2} \text{d}^{-1}$) and monthly average, minimum and maximum temperatures ($^{\circ}\text{C}$) for Kiruna (SWE, stars), Amsterdam (NLD, triangles) and Abu Dhabi (UAE, circles). January is the lower left data point in each cycle. Adapted from Graamans et al. [8].

4.2.2.3 Geometry

In this study we consider one building type with wall-to-floor ratios (W/F ratios) of 0.39, 0.49 and 0.65 (Table 4.1). The building height was kept constant at 3.5 m and contains five layers of crop production. This represents a common set-up for contemporary plant factories [7]. The properties of the various building components are listed in Table 4.2.

4.2.3 Variable model inputs

This study focuses on the static façade components and the ratio of wall-to-floor area; we consider 18 façade constructions (opaque and transparent) and three W/F ratios (Table 4.1–4.2). The analysis uses single factor variation to illustrate the impact of each factor and to prevent the exclusion of design combinations. This approach allows for an investigation of fundamental aspects that relate to the energy requirements of this novel building typology.

4.2.3.1 Opaque façade constructions: insulation and albedo

Two parameters of the opaque façade elements were considered: U-value and surface albedo. The opaque façade was modelled as aluminium panels encapsulating polyurethane foam, as in the construction of cold stores. This is standard practice in plant factories [6].

Insulation: The U-values were set at 0.05, 0.20 and 5.75 W m⁻² K⁻¹. These values were selected to represent a vacuum insulation panel [48], a standard insulated masonry façade [49] and a thermally conductive metal sheet [50], respectively. A single metal sheet is not considered feasible as a façade construction. However, this construction was selected in order to achieve the same U-values as single layer clear glazing (see Section 4.2.3.2). Heat transmission is limited by increasing the insulator thickness, as is common practice with conventional insulation materials. A more space-efficient, innovative method to increase the performance of the building skin would consist of more efficient insulation materials, such as vacuum insulation panels [51], aerogels [52] or nanomaterials [53].

Surface albedo: The albedo values were set at 0.10, 0.50 and 0.90. Surface albedo is defined as the ratio of the irradiance reflected from a surface to the irradiance

received by that surface. In warm areas, low albedo values can result in high surface temperatures. The selected values represent the available range for building materials [54]. To be able to distinguish between results, the impact of albedo was calculated for a U-value of $5.75 \text{ W m}^{-2} \text{ K}^{-1}$.

Roof: The albedo and U-value of the roof are in accordance with the façade for each simulation. The effect of this approach is discussed in Section 4.4.5.

Operation: The daily photoperiod inside was in counter phase with the natural photoperiod (photoperiods last from 18:00-10:00⁺¹) in order to maximise heat transmission across the façade. This schedule maximises the temperature difference between the interior and exterior during both photoperiods and dark periods. During photoperiods, the high internal heat load corresponds with exterior night-time temperatures to maximise heat loss. During dark periods, the elevated exterior daytime temperatures can reduce heating demands.

4.2.3.2 Transparent façade constructions: insulation and solar heat gain coefficient

Two parameters of the transparent façade elements were considered: U-value and solar heat gain coefficient (SGHC). The U-value and SGHC of the façade constructions have a double influence on the interior climate. Fully transparent façades increase the penetration of solar radiation, which can contribute to crop production. Conversely, they increase solar heat gains and thermal emission, thereby increasing the cooling and heating requirements, respectively. The transparent façade was modelled as a curtain wall system with glass panels consisting of single or multiple layers, using the simple glazing method of DesignBuilder [24].

Insulation: The U-values were set at 0.50, 1.25 and $5.75 \text{ W m}^{-2} \text{ K}^{-1}$, representing triple, double and single glazing, respectively [49]. They take the frame and connection between glazing and frame into account.

SHGC: The SHGC of the transparent façade was set at 0.30, 0.55 and 0.80. The SHGC is the ratio of the transmitted solar radiation to the incident solar radiation on the entire glass façade, including the window frames. Emissivity and transmissivity of the façade are included in SHGC (total transmission) when using the simple glazing method and are not independently defined [55, 56].

Roof: The roof was modelled as an opaque element, featuring the medium albedo and U-values of 0.5 and 0.20 W m⁻² K⁻¹, respectively. This was done to prevent modelling a structure akin to a greenhouse.

Operation: Contrary to the opaque façade, the daily photoperiod follows the natural exterior photoperiod to maximise the use of photosynthetically active solar radiation; photoperiods last from 04:00-20:00.

Integrating natural and artificial illumination: The daily photoperiod inside follows the natural photoperiod (photoperiods last from 05:00-21:00). A combination of artificial illumination and solar radiation must be taken into account, as solar radiation is neither continuous nor capable of fully penetrating the building structures. In this study it was assumed that solar illumination levels were continuously supplemented to 250 µmol m⁻² s⁻¹. The calculated solar gains were subtracted from the lighting requirement and the consequent sensible cooling requirement when processing the hourly simulation data.

4.2.3.3 Form factor: wall-to-floor area ratio

The geometrical form affects the relative surface area and consequently the influence of the façade on the building energy balance. Therefore, this study took three rectangular W/F ratios (Table 4.1) into account to obtain a fundamental understanding of this influence. The floor and roof surface area remained constant. The production and logistic aspects of the facility layouts were not taken into consideration.

4.2.4 Climate systems – Energy demand and electricity use

The individual energy demands for the climate systems are a direct output from DesignBuilder. The system demands are converted to electricity use by using their respective coefficients of performance (COP). The COP of a climate system is the ratio of the generated flux (i.e. sensible heat or refrigeration) to the net input of work (electricity) required to achieve that effect.

The COP for heating (COP_{heat}) was determined using the Carnot efficiency of a heat pump. This theoretical optimum efficiency was multiplied by 0.4 to achieve realistic efficiencies, following [57].

In addition, the COP was determined for sensible and latent cooling, as these play a central role in the total energy balance of plant factories. To reduce electricity use, cooling is achieved through a combination of active and ‘free’ cooling. ‘Free’ cooling uses the temperature difference between the interior and the exterior climate and bypasses the need for compressors [58]. The exterior climate naturally determines the number of hours that free cooling can be used [11].

In this study, active cooling was realised by a vapour compression refrigeration cycle. Air-to-air heat exchangers were used to minimise the use of vapour compression cooling and consequently the electricity demand for cooling and dehumidification (Figure 4.2). The methods for calculating the air extraction, heat exchanger and vapour compression cooling systems are detailed in Appendix 4C. An indirect system is used as this causes no direct disturbance to the indoor air quality and does not introduce vapour or other volatiles into the production climate.

The potential of natural circulation using a thermosyphon was investigated, as it has the capability to transport heat at high rates without needing pumping devices [59]. The system, however, was not considered suitable for this study due to numerous uncertainties: the dimensioning of components [60], the heat transfer limit due to pressure drops [61], the impact of pipe dimensions [62], the limited experimentally validated cooling capacities [63], and the overall refrigerant flow stability [64].

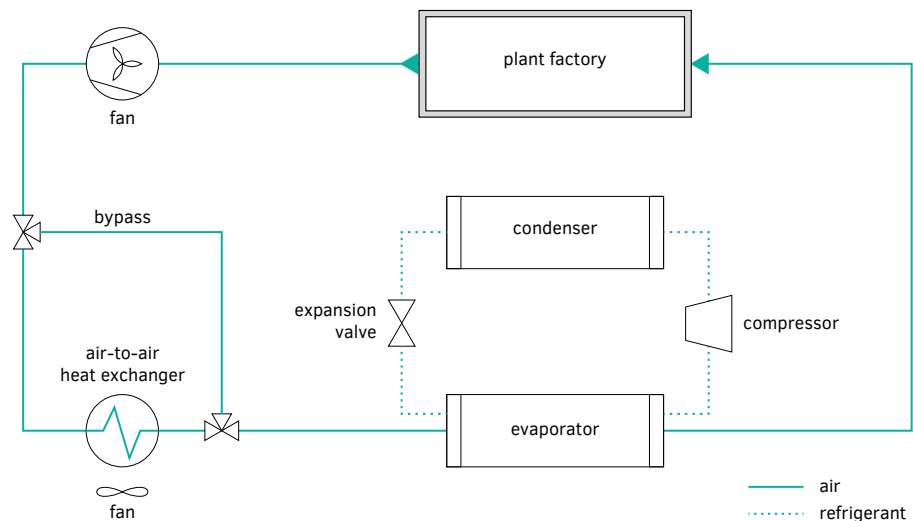


FIG. 4.2 Schematic representation of the cooling system design. A continuous line represents the flow of air and a dashed line the flow of the refrigerant.

Electricity demand

The total electricity demand for plant factories (E_{PF}) is comprised of the electricity demand for heating (E_{heat}), dehumidification or latent cooling ($E_{cool,lat}$) and sensible cooling ($E_{cool,sen}$). Additionally, the energy required for cooling the nutrient solution ($E_{cool,ns}$) and for powering the LED fixtures (E_{LED}) were included.

$$E_{PF} = E_{heat} + E_{cool,lat} + E_{cool,sen} + E_{cool,ns} + E_{LED} \quad [4.1]$$

The system demands (Q) for plant factories are converted to electricity use (E) following their respective COP (COP) according to the formula:

$$E = \frac{Q}{COP} \quad [4.2]$$

The electricity demand E_{heat} , $E_{cool,lat}$ and $E_{cool,sen}$ are calculated using the COP for heating (COP_{heat}) and cooling (COP_{cool}), respectively. Additionally, the required electrical fan power (E_{fans}) is included, weighted for the relative share of the heating flux (Q_{heat}), latent cooling flux ($Q_{cool,lat}$) or sensible cooling flux ($Q_{cool,sen}$) in the combined energy demand ($Q_{heat} + Q_{cool,lat} + Q_{cool,sen}$).

$$E_{heat} = \frac{Q_{heat}}{COP_{heat}} + \frac{Q_{heat}}{Q_{heat} + Q_{cool,lat} + Q_{cool,sen}} \cdot E_{fans} \quad [4.3]$$

Additionally, the required electrical fan power from the heat exchanger ($E_{fans,hex}$) is included and weighted for the latent and sensible flux in the heat exchanger ($Q_{hex,lat}$ and $Q_{hex,sens}$, respectively).

$$E_{lat} = \frac{Q_{lat}}{COP_{cool}} + \frac{Q_{cool,lat}}{Q_{heat} + Q_{cool,lat} + Q_{cool,sen}} \cdot E_{fans} + \frac{Q_{hex,lat}}{Q_{hex,lat} + Q_{hex,sens}} \cdot E_{fans,hex} \quad [4.4]$$

$$E_{sens} = \frac{Q_{sens}}{COP_{cool}} + \frac{Q_{cool,sen}}{Q_{heat} + Q_{cool,lat} + Q_{cool,sen}} \cdot E_{fans} + \frac{Q_{hex,sens}}{Q_{hex,lat} + Q_{hex,sens}} \cdot E_{fans,hex} \quad [4.5]$$

4.2.5 Presentation of the results

The analysis of energy-saving potential was carried out by comparing several scenarios. As a starting point, simulations were carried out considering the industry standard: an opaque, highly insulated ($U = 0.05 \text{ W m}^{-2} \text{ K}^{-1}$), moderately reflective ($A = 0.50$), square ($W/F = 0.39$) plant factory. Results are reported in absolute and relative values on an annual basis ($\text{kWh m}^{-2} \text{ y}^{-1}$).

TABLE 4.1 Geometry of simulation models.

W/F ratio	-	0.39	0.49	0.65
Length	m	36.00	72.00	108.00
Width	m	36.00	18.00	12.00
Height	m	3.50	3.50	3.50
Floor area	m^2	1296.00	1296.00	1296.00
Wall area	m^2	504.00	630.00	840.00

TABLE 4.2 Parameters for annual energy demand simulations. Middle values are typically aligned with the current accepted building practice. Variables not considered in a specific simulation set (#) are marked by X. The variables are expanded upon in Section 4.2.3.

#	Type	Form factor	Façade properties				Roof properties	
		W/F ratio (-)	U-value (opaque) (W m ⁻² K ⁻¹)	Albedo (-)	U-value (transparent) (W m ⁻² K ⁻¹)	Solar heat gain coeffi- cient (-)	U-value roof (opaque) (W m ⁻² K ⁻¹)	Albedo (-)
O1	Opaque – insulation	0.39	0.05 / 0.20 / 5.75	0.50	X	X	0.05 / 0.20 / 5.75	0.50
O2	Opaque – albedo	0.39	5.75	0.10 / 0.50 / 0.90	X	X	5.75	0.10 / 0.50 / 0.90
O3	Opaque – W/F – insulation	0.39 / 0.49 / 0.65	0.05 / 0.20 / 5.75	0.50	X	X	0.05 / 0.20 / 5.75	0.50
O4	Opaque – W/F – albedo	0.39 / 0.49 / 0.65	5.75	0.10 / 0.50 / 0.90	X	X	5.75	0.10 / 0.50 / 0.90
T1	Transparent – insulation	0.39	X	X	0.50 / 0.20 / 5.75	0.55	0.20	0.50
T2	Transparent – SHGC	0.39	X	X	5.75	0.30 / 0.50 / 0.80	0.20	0.50
T3	Transparent – W/F – insulation	0.39 / 0.49 / 0.65	X	X	0.50 / 0.20 / 5.75	0.55	0.20	0.50
T4	Transparent – W/F – SHGC	0.39 / 0.49 / 0.65	X	X	5.75	0.30 / 0.50 / 0.80	0.20	0.50

TABLE 4.3 Constant model input for annual energy demand simulations.

Climate setpoints		Climate systems		Building components	
Parameter	Input	Parameter	Input	Parameter	Input
Location	SWE: 67.83° N, 20.34° E NLD: 51.99° N, 5.66° E UAE: 24.45° N, 54.65° E	HVAC system (template)	Fancoil unit Air cooled chiller	Façade construction (opaque)	1-Layers Aluminium ^c – PUR ^d – Aluminium
ASHRAE/Köppen- Geiger climate classification	SWE: 7/Dfc NLD: 4A/Cfb UAE: 1B/BWh	Lighting system	LED	Façade lay-out (opaque)	No glazing
Heating setpoints photo-/dark period (°C)	24/24 ^a	HVAC – Fuel heating	1-Electricity from grid	Façade construction (transparent)	2-Simple glazing ^e
Cooling/ventilation setpoints photo-/dark period (°C)	30/30 ^a	HVAC – Fuel cooling	1-Electricity from grid	Façade lay-out (transparent)	100% fitted glazing
Relative humidity setpoints photo-/dark period (%)	RH _{min} = 75/75 ^a RH _{max} = 85/85 ^a	HVAC – COP heating	1.00 ^b	Ground floor	150 mm concrete slab 30 mm XPS
CO ₂ levels (μmol mol ⁻¹)	1200 ^a	HVAC – COP cooling	1.00 ^b	Internal floor	300mm concrete slab
Radiation (μmol m ⁻² s ⁻¹)	250 ^a	HVAC – Humidification	2-Humidistat	Internal thermal mass	300mm concrete slab
Duration photo-/ dark period	16h/8h ^a	HVAC – Dehumidification	2-Humidistat	Air tightness	Model infiltration off ^f

^a The interior climate setpoints are expanded upon in Section 4.2.2.2.

^b COPs were calculated separately (see Section 4.2.4).

^c Exterior surface properties were varied to achieve desired albedo (see Section 4.2.3.1).

^d PUR Polyurethane board (diffusion tight). Thickness was varied to achieve desired U-value.

^e Glazing properties were varied to achieve desired solar heat gain coefficient and U-value. Light transmission was fixed at 0.70.

^f Standards for airtightness were exceeded to simulate a fully closed system [7].

4.3 Results

The results have been normalised for cultivation area (Section 4.4) and for dry matter production (Appendix 4A). The total annual energetic demands for opaque and transparent façades are specified in Figure 4.3 and Figure 4.4, respectively.

The energy requirements were calculated for each plant factory and specify the energy use for LED lighting, sensible cooling, dehumidification and heating. The total energy use is reduced in opaque and transparent façades by increasing U-values. SHGC reduces the total energy use at varying intensities in different locations, whereas the effect of albedo is more closely related to location. Figure 4.5 and Figure 4.6 illustrate the impact of form factor (W/F ratio) on the total annual energetic demands for opaque and transparent façades, respectively. Increasing the W/F ratio consequently increases the impact of the façade components on the total energy use. This impact can result in additional energy savings. Total energy use is closely related to the differences between the interior and the exterior climate. Finally, Figure 4.7 gives an overview of the energy and electricity use of the most efficient analysed systems. The COP of the different systems is used to convert energy demand to electricity use. The predominance of electricity required for artificial illumination is illustrated.

4.4 Discussion

The following section discusses the calculated energy demands per cultivation area (kWh m^{-2}). The figures illustrate the impact of each single variable for each location.

4.4.1 Opaque façade constructions

4.4.1.1 Opaque façade constructions – insulation values

The effects of the opaque façades' insulation and albedo on the total energy demand are illustrated in Figure 4.3. The plant factories show a decrease in energy demand resulting from higher U-values. Increasing the façades' U-value from 0.05 to $5.75 \text{ W m}^{-2} \text{ K}^{-1}$ changes the facility's total cooling demand by 12.1% (UAE), 30.0% (NLD) and 31.6% (SWE) and its total energy demand by 6.1% (UAE), 9.5% (SWE) and 12.5% (NLD).

The decrease in sensible cooling demands indicates an increased heat transmittance from the interior to the exterior climate. These effects are most pronounced in the decrease of total energy demand in cooler climates, such as NLD and SWE, but are also seen in UAE. In all locations the savings related to the sensible cooling demand were notably higher than the increase in heating demand.

4.4.1.2 Opaque façade constructions – albedo values

The effect of the albedo of total energy demand is closely related to the facility's location and the façade's U-value (Figure 4.3). The albedo value had hardly any effect at the medium U-value, as the thermal insulation limits most heat transmittance across the façade. However, increasing the albedo value from 0.1 to 0.9 at the highest U-value resulted in maximum changes in total energy demand of +0.8% (SWE), 0.5% (NLD) and 7.5% (UAE).

The effect of the albedo value is visible in the heating and sensible cooling demands and is notably dependent on location. In general, lower albedo values will increase the exterior surface temperature, which results in a decreased heat transmittance to the exterior and a higher sensible cooling demand. Concomitantly, at lower albedo values the heating demand is reduced due to the increased heat gain from the exterior walls. The most notable decrease in total energy demand is achieved at the maximum albedo value in UAE, as the high exterior temperatures in UAE reduce the need for heating. The high internal heat load and temperature setpoints still allow for the dissipation of energy. In contrast, albedo has a clearer effect on the heating demand than on the sensible cooling demand in SWE.

The façade albedo values have a smaller impact on the total energy demand than the insulation values, but they show distinct trends related to the exterior climate. This observation allows for additional fine-tuning of the façade construction to the local climate, aiming at a further reduction of the total energy demand.

4.4.2 Transparent façade constructions

In all locations the energy demands calculated for artificial illumination exceed all other demands (Figure 4.3). This predominance of artificial illumination in the total energy balance is consistent with data from a wide range of production climates (i.e. 50.1% [65], 72.0-86.0% [66], 75.0-80.0% [67], 42.8-52.6% [68], and

57.0–57.4% [8]). Transparent façades may serve to reduce electricity costs by directly using solar energy and limiting artificial illumination. In reality, the values for insulation and SHGC are largely linked. However, greater insight into the energetic behaviour can be achieved by independently assessing both factors.

4.4.2.1 Transparent façade constructions – insulation values

The effects of the transparent façades' insulation and SHGC on the total energy demand are illustrated in Figure 4.4. Plant factories show a decrease in total energy demand following higher U-values for transparent façades; increasing the U-value from 0.50 to 5.75 W m⁻² K⁻¹ results in a change in energy demand of 4.2% (UAE), 6.3% (NLD) and 6.4% (SWE).

The lower energy demand at higher U-values is caused by decreased sensible cooling demands, comparable with the situation in the opaque façade structures. The internal heat is partially dissipated across the façade to the exterior climate. In comparison with the opaque structures, the sensible cooling demand changes slightly in UAE (+43%) but notably in NLD (+512%) and in SWE (+1025%) at a U-value of 5.75 W m⁻² K⁻¹. The combination of the additional solar heat gains and the regular production schedule resulted in an increased transmission of heat across the façade to the interior.

4.4.2.2 Transparent façade constructions – solar heat gain coefficient

The impact of SHGC on the total energy demand is related to location and follows the same trend, regardless of the insulation value (Figure 4.4). Increasing the SHGC from 0.3 to 0.8 at a high U-value changes the total energy demand by -2.3% (SWE), -2.4% (NLD) and -3.6% (UAE).

The higher SHGC allows for an increased transmittance of solar radiation, which most notably reduces the need for LED illumination. The savings in total energy demand directly follow the savings in LED energy demand, as the influence on LED was notably higher than the influence on sensible cooling, dehumidification and heating in all locations.

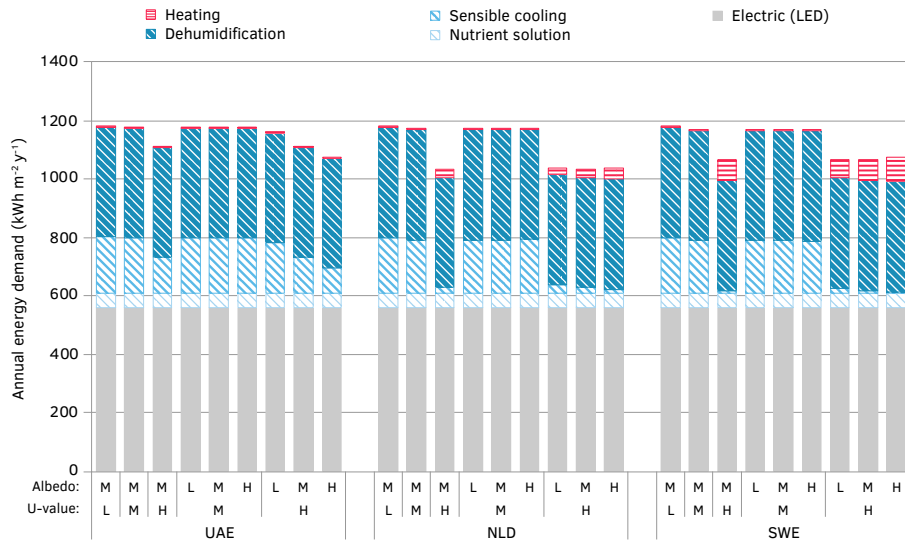


FIG. 4.3 Annual energy demand (kWh m⁻² y⁻¹) of plant factories featuring opaque façades in UAE, SWE and NLD, as a result of variation in insulation (U-value in W m⁻² K⁻¹) and reflection of solar radiation (albedo). Values are indicated by L (low: A=0.10, U=0.05), M (medium: A=0.50, U=0.20) and H (high: A=0.90, U=5.75) and refer to values listed in Table 4.2. Presented simulations feature a W/F ratio of 0.39 and face north.

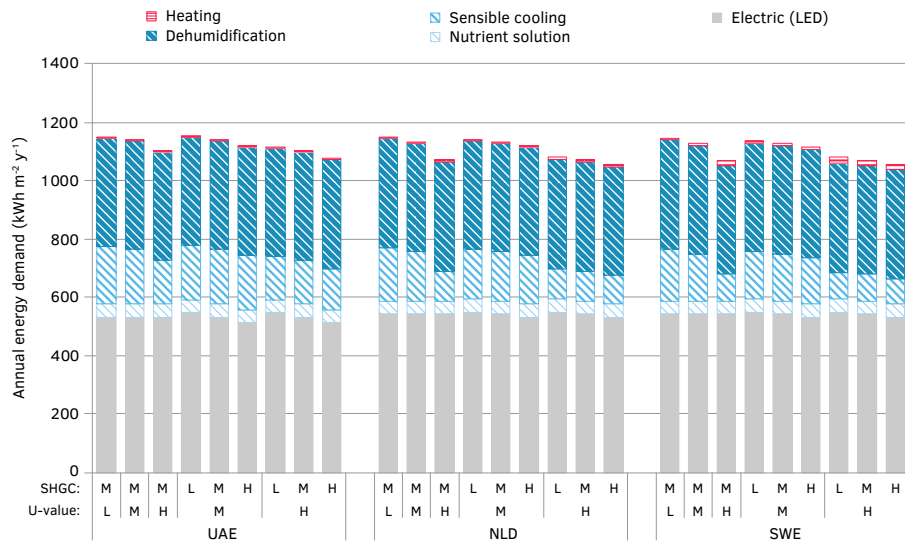


FIG. 4.4 Annual energy demand (kWh m⁻² y⁻¹) of plant factories featuring transparent façades in UAE, SWE and NLD, as a result of variation in insulation (U-value in W m⁻² K⁻¹) and solar heat gain coefficient (SHGC). Values are indicated by L (low: SHGC=0.30, U=0.50), M (medium: SHGC=0.55, U=1.25) and H (high: SHGC=0.80, U=5.75) and refer to the values listed in Table 4.2. Presented simulations feature a W/F ratio of 0.39 and face north.

4.4.3 Geometry – wall-to-floor ratio

In the previous calculations the opaque façade exceeded the transparent façades in energetic performance for SWE and NLD, despite the free availability of solar radiation for photosynthesis. These calculations used a model with a square footprint and minimal relative façade area, which consequently minimised the effect of design variations. The effect of different W/F ratios on the total energy demand in opaque and transparent constructions was addressed. Firstly, the effect of different U-values was analysed; secondly, the impact of albedo value or SHGC was analysed. The W/F ratio of 0.39 (square footprint) was taken as the baseline for comparison.

4.4.3.1 Geometry - opaque façade constructions

The effect of the W/F ratio on the total energy demand in opaque plant factories depends strongly on the location (Figure 4.5). Higher W/F ratios and U-values result in a notably higher total energy demand in NLD and SWE, whereas only minimal differences were seen in UAE. The determining factor for opaque façades is the thermal transmission, which increases at greater temperature differences. These differences are considerably larger in SWE and NLD than in UAE, as is evident in the increased heating demand in NLD and SWE.

In opaque constructions an increase in the W/F ratio generally results in an increase in total energy demand, except in UAE. There, in combination with a high U-value and albedo, the larger façade surface area facilitates additional heat loss during night-time and changes the total energy demand by -0.7%. In UAE the reduction in sensible cooling is greater than the increase in heating, whereas in NLD and SWE the increase in heating remain dominant over the reduction in cooling.

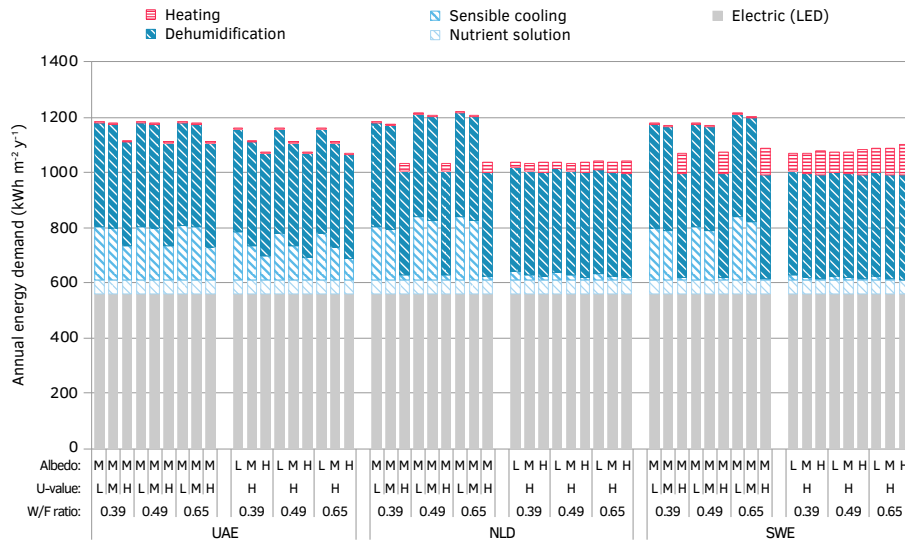


FIG. 4.5 Annual energy demand (kWh m⁻² y⁻¹) of plant factories in UAE, NLD and SWE featuring opaque façades, as a result of variation in insulation (U-value in W m⁻² K⁻¹) and reflection of solar radiation (albedo) in combination with W/F ratio. Values are indicated by L (low: A=0.10, U=0.05), M (medium: A=0.50, U=0.20) and H (high: A=0.90, U=5.75) and refer to values listed in Table 4.2. The long façade faces north in presented simulations.

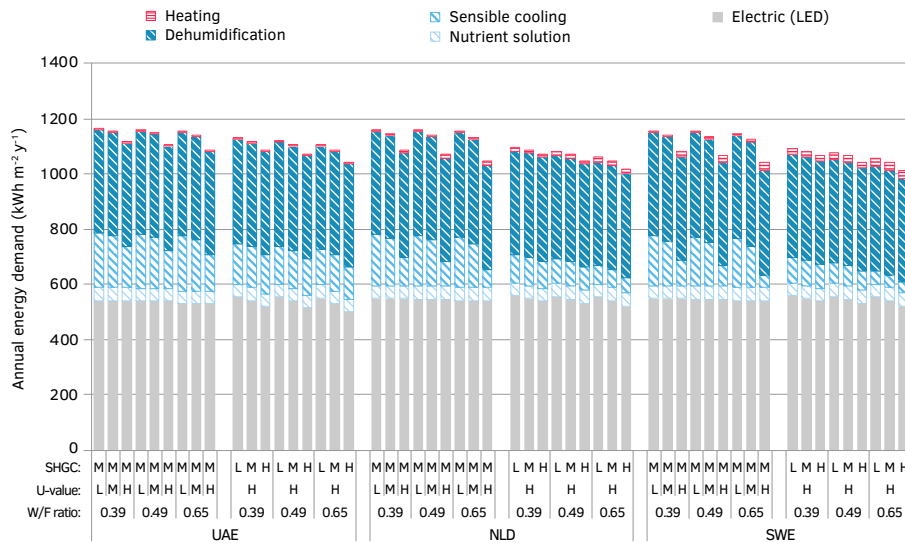


FIG. 4.6 Annual energy demand (kWh m⁻² y⁻¹) of plant factories in UAE, NLD and SWE featuring transparent façades, as a result of variation in insulation (U-value in W m⁻² K⁻¹) and solar heat gain coefficient (SHGC) in combination with W/F ratio. Values are indicated by L (low: SHGC=0.30, U=0.50), M (medium: SHGC=0.55, U=1.25) and H (high: SHGC=0.80, U=5.75) and refer to the values listed in Table 4.2. The long façade faces north in presented simulations.

4.4.3.2 Geometry - transparent façade constructions

A higher W/F ratio results in a decrease in total energy use in the calculated variants, where the longest façade faces north. This effect is more evident in transparent than in opaque constructions, due to the benefits of direct solar radiation. The total energy demand is most notably reduced in the cases focusing on SHGC. Increasing the W/F ratio resulted in a relative change in energy demand of 4.2% for UAE, 5.0% for NLD and 5.2% for SWE with respect to their base value. These energy savings are the result of the lower energy demand for LEDs and lower sensible cooling demands.

The W/F ratio has the highest absolute and relative impact on lighting demand in UAE, followed by SWE and then NLD; the sensible cooling demand was reduced primarily in SWE, followed by NLD and UAE. This decrease in sensible cooling demand at higher SHGCs seems unexpected based on increased solar heat gains. However, the production temperature is higher than the average exterior temperature, which ensures the transfer of heat across the façade. This large decrease in sensible cooling outweighs the absolute increase in heating requirements.

4.4.4 Comparison of results and sensitivity analysis

The analysed design variables have been applied to minimise the total use of energy and electricity (Table 4.4 and Figure 4.7). These designs might not be economically feasible, but they present the highest potential for energy savings. Additionally, a sensitivity analysis using single variable variation provides insight into the key design factors (Figure 4.8).

4.4.4.1 Comparison of façade properties

The ranges of reduction in annual energy demand are given in Table 4.4. The table lists the effect of each façade property on the annual energy demand of plant factories at the W/F ratios. The delta is relative to the annual energy demand of the baseline facility, which features the listed properties. Among the analysed variables, the U-value brought about the largest reduction in energy demand, followed by SHGC. The constructions in each location required a high U-value to maximise the dissipation of the internal heat and a high SHGC to minimise LED energy use. However, they notably differ with respect to the W/F ratio and the albedo value. The

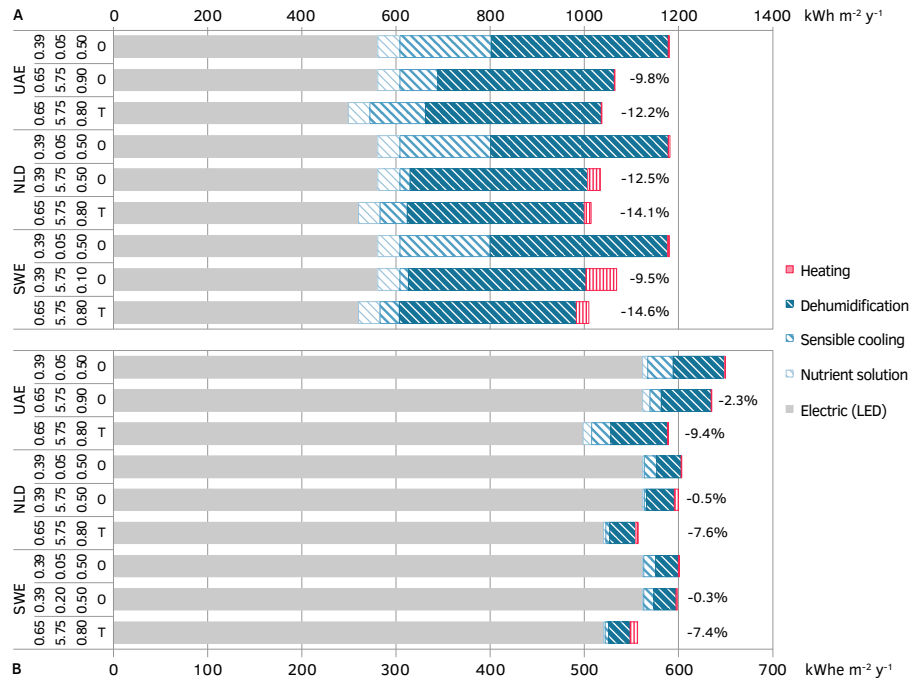


FIG. 4.7 Energy demand (A) in $kWh m^{-2} y^{-1}$ and final electricity use (B) in $kWh m^{-2} y^{-1}$ for the most efficient opaque and transparent constructions in each location. The relative delta (%) illustrates the difference with the industry-standard plant factory in the specific location (opaque, $U=0.05 W m^{-2} K^{-1}$, $A=0.55$, $W/F=0.39$). The y-axis lists location, W/F ratio (-), U-value ($W m^{-2} K^{-1}$), SGHC (-) or albedo (-) (dependent on transparency), and transparency (O for opaque and T for transparent) from left to right. The long façade faces north in presented simulations.

positive effects of albedo were most evident in UAE and rather minimal in NLD and SWE. The advantage of transparent versus opaque constructions depends on which outcome measure is selected, total energy demand or final electricity use. The latter depends on the COPs of the subsystems.

If energy demand is considered as the outcome measure, the transparent constructions offer the best performance by a narrow margin (Figure 4.7A). The opaque constructions already offer a notable reduction in total energy demand. The relatively high external temperature and solar radiation in UAE require a high W/F ratio to allow for (night-time) dissipation of heat and a high albedo to minimise solar heat gains, respectively. In contrast, a small W/F ratio impedes excessive heat losses to the exterior in the colder climates of NLD and SWE. Moreover, medium and lower albedo values allow for increased solar heat gains that minimise heating demands at a U-value of $5.75 W m^{-2} K^{-1}$ in NLD and SWE, respectively.

If final electricity use is considered as the outcome measure (Figure 4.7B), transparent constructions offer the best perspective. The role of illumination becomes more predominant in the final electricity use because of the system COPs. Consequently, this increased predominance increases the relative effects of solar radiation on electricity use. The final electricity use decreases inversely to the W/F ratio and the SHGC as both factors increase the solar gains.

TABLE 4.4 Range of effects of façade properties on the annual energy demand of plant factories. Colour intensity illustrates the relative effect in comparison with the baseline per location. The characteristics of these baselines are given by listing their U-value (U), albedo or solar heat gain coefficient (A or SHGC), and wall-to-floor ratios (W/F). In addition, the transparency (T) is listed and indicated by transparent (T) or opaque (O). The effect of orientation is relative to the north-facing orientation for each W/F ratio (Δ).

Façade construction	Base				UAE			NLD			SWE		
	U	A or SHGC	W/F	T	0.39	0.49	0.65	0.39	0.49	0.65	0.39	0.49	0.65
Opaque: U-value (0.05-5.75)	0.05	0.50	0.39	O	0.0% - 6.1%	+ 0.1% - 6.2%	+ 0.3% - 6.4%	0.0% - 12.5%	+ 2.9% - 12.5%	- 3.0% - 12.3%	0.0% - 9.5%	0.0% - 8.9%	+ 3.0% - 7.8%
Opaque: Albedo (0.10-0.90)	5.75	0.10	0.39	O	0.0% - 7.5%	- 0.1% - 7.7%	+ 0.1% - 8.1%	0.0% - 0.5%	0.0% - 0.5%	+ 0.4% - 0.3%	+ 0.8% 0.0%	+ 1.6% + 0.6%	+ 3.0% + 1.8%
Opaque: Orientation (0°-135°)	5.75	0.50	Δ	O	0.0% 0.0%	+ 0.2% 0.0%	+ 0.3% 0.0%	0.0% 0.0%	+ 0.1% 0.0%	+ 0.1% 0.0%	0.0% 0.0%	+ 0.1% 0.0%	+ 0.1% 0.0%
Transparent: U-value (0.50-5.75)	0.50	0.55	0.39	T	0.0% - 4.2%	- 0.2% - 5.1%	- 0.6% - 6.7%	0.0% - 6.3%	- 0.3% - 7.7%	- 0.8% - 9.8%	0.0% - 6.4%	- 0.3% - 7.9%	- 0.8% - 10.1%
Transparent: SHGC (0.30-0.80)	5.75	0.30	0.39	T	0.0% - 3.6%	- 0.8% - 5.0%	- 1.9% - 7.6%	0.0% - 2.4%	- 1.3% - 4.3%	- 3.1% - 7.2%	0.0% - 2.3%	- 1.4% - 4.4%	- 3.3% - 7.4%
Transparent: Orientation (0°-135°)	5.75	0.80	Δ	T	0.0% 0.0%	0.0% - 0.7%	0.0% - 1.4%	+ 0.1% 0.0%	0.0% 0.0%	+ 0.1% 0.0%	0.0% 0.0%	+ 0.1% 0.0%	+ 0.2% 0.0%

4.4.4.2 Sensitivity analysis of key variables

The sensitivity analysis provides insight into the variations in total energy demand as a result of the variation in key variables. This sensitivity is closely related to location (Figure 4.8). The investigated variables are U-value and SHGC in the case of transparent constructions and LED efficiency, U-value and albedo in the case of opaque constructions. Total energy demand is most sensitive to LED efficiency, followed by U-value.

The impact of LED efficiency was calculated in combination with an opaque façade ($U=5.75 \text{ W m}^{-2} \text{ K}^{-1}$, $A=0.50$). Increasing LED efficiency had a direct effect on the

energy demand of illumination and an indirect effect on the sensible cooling and heating demand. Differences in sensitivity across locations illustrate the influence of local climate. The high exterior temperatures in UAE limit the required increase in heating demand, even at reduced internal heat gains. In contrast, the lower exterior temperatures in SWE and NLD result in a decline in sensitivity as LED efficiency increases, because of a larger heating demand.

The impact of U-value was calculated for transparent and opaque constructions. Opaque constructions showed greater variation at U-values varying between 0.05 and $5.75 \text{ W m}^{-2} \text{ K}^{-1}$. The sensitivity is minimal in UAE due to the relatively limited thermal exchange as a result of high interior temperatures. In contrast, SWE and NLD show greater sensitivity to U-value because of their colder exterior climates. The sensitivity in SWE indicates an optimum U-value (around $4.33 \text{ W m}^{-2} \text{ K}^{-1}$) due to the shift in predominance of sensible cooling to heating demand. This shift in predominance is responsible for a decline in sensitivity at higher U-values.

The impact of albedo on the total energy demand may be rather small but was clearly influenced by the external climate. Facilities at low latitudes require a high albedo (UAE), moderate latitudes a moderate albedo (NLD) and high latitudes a low albedo (SWE).

In short, the sensitivity analysis illustrates that the general trends are similar for each location. However, the slope and optimum of each variable are closely related to the external climate and warrant future optimisation studies.

4.4.5 Additional factors affecting energetic performance

Several additional factors that affect the energetic performance of plant factories can be identified. The impact of these factors is described below.

- *The roof as the fifth façade:* In this study, the roof can be regarded as the fifth façade, as it follows the characteristics of the opaque façade. This design approach mirrors the current building practice for plant factories but inhibits the direct extrapolation of the results to a facility with multiple building layers, a vertical farm. To simulate a multi-layered facility, it would be necessary to exclude heat transfer across floors and roofs by modelling them as adiabatic. These additional calculations were beyond the scope of this study.

- *Opaque roof in combination with transparent façades:* In the analysis of transparent façade constructions, the roof was modelled as an opaque element, featuring the medium albedo and U-values of 0.5 and 0.20 W m⁻² K⁻¹, respectively. However, the analysis of opaque structures indicated the benefits of a roof construction with a U-value of 5.75 W m⁻² K⁻¹. Additional calculations would be required to assess this combination but were beyond the scope of this study.
- *Orientation of the building:* The beneficial effects of solar radiation can be increased by taking the combination of the W/F ratio and the spatial orientation of the building into account. Changing the orientation from north with 45° increments resulted in maximum changes in total energy demand of –1.4% (UAE) in the case of a transparent plant factory (U=5.75, SHGC=0.8, W/F=0.65). The decrease in LED lighting exceeds the increase in sensible cooling demand in this case. Building orientation has a small influence on total energy use in comparison with façade construction, particularly in NLD and SWE. However, it remains an interesting variable, as it can reduce energy demand but has a negligible effect on the investment costs.
- *Coefficients of performance:* The COPs achieved in practice will strongly influence the final electricity use of the plant factory. The coefficient was calculated for each case (Section 4.2.4). The COP for cooling in UAE is relatively high due to small differences between the required source temperature and the temperature inside the plant factory. The counter phase production schedule warrants low exterior air temperatures that can be used for passive cooling during night-time. Cooling in SWE might be problematic due to frost on the air chiller during winter time; this would result in a lower COP.
- *LED efficiency:* The sensitivity analysis illustrates the impact of the efficiency of artificial illumination on the total energy demand and consequently the technoeconomic feasibility of plant factories (Figure 4.8). The technological advancement of LED efficiency is of paramount importance, but presumably this is not sufficient to guarantee feasibility. It has to be taken into account that the maximum attainable efficiency ($W_{\text{Output}}/W_{\text{Electricity}}$) of LEDs is limited [69].
- *Local production of energy:* Photovoltaic cells could be a source of renewable electricity for plant factories. However, the direct use of solar energy is more efficient for crop illumination compared to artificial illumination powered by photovoltaic arrays. This can be illustrated by successively calculating the current efficiencies of photovoltaic arrays at approximately 17% [70] and of LED systems at approximately 52% [71].

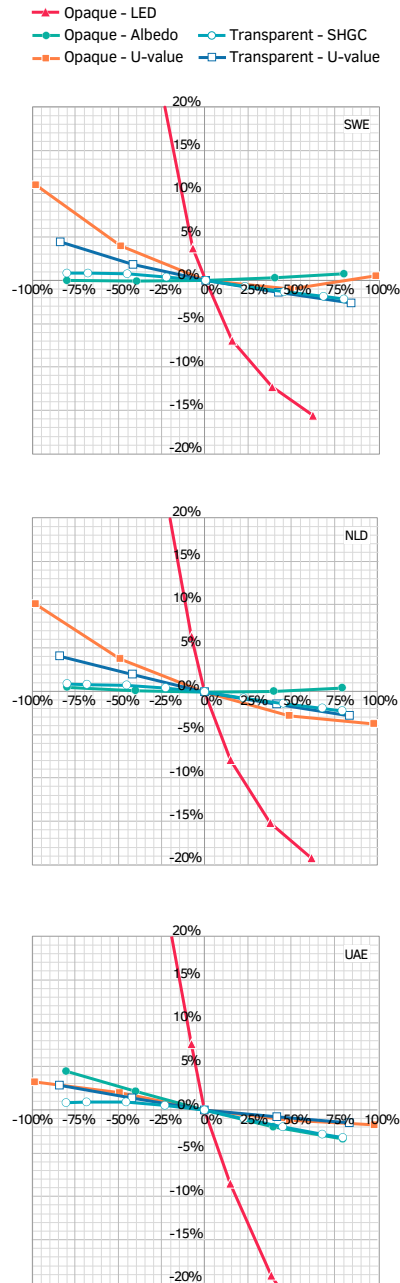


FIG. 4.8 Sensitivity analysis illustrating the relative change in total energy demand (y-axis) as a result of relative change in LED efficiency, U-value, and albedo or SHGC, respectively (x-axis) in UAE, NLD and SWE. The base values for these parameters are 52% LED efficiency (red:blue=80:20, $2.70 \mu\text{mol J}^{-1}$) for opaque - LED efficiency, $2.90 \text{ W m}^{-2} \text{ K}^{-1}$ for opaque - Uvalue, 0.50 for opaque - albedo, $3.215 \text{ W m}^{-2} \text{ K}^{-1}$ for transparent - U-value, and 0.55 for transparent - SHGC.

4.4.6 Additional considerations

DesignBuilder exhibited anomalous behaviour in the simulation of simple glazing systems, which resulted in an apparent connection between the U-value of single glass and the transmitted solar gains. This is the result of the glazing 2-Simple method option, where DesignBuilder uses the EnergyPlus object *WindowMaterial:SimpleGlazingSystem*. This object accesses a model that turns simple performance indices into a more extensive model of the glazing system. The overall glazing system is defined using just three parameters: U-value, solar heat gain coefficient, and visible transmittance [56], following the method outlined in [24]. Within the scope of this study, this resulted in a difference of 5.4% between solar gains transmitted through single glazing ($U=5.75 \text{ W m}^{-2} \text{ K}^{-1}$) and double/triple glazing ($U=0.50/1.25 \text{ W m}^{-2} \text{ K}^{-1}$) at a SHGC of 0.80. The simulation of a broader range of U-values ($0.10\text{--}7.00 \text{ W m}^{-2} \text{ K}^{-1}$) demonstrated that this anomaly arose at U-values from $5.75 \text{ W m}^{-2} \text{ K}^{-1}$ on. It was corrected by substituting the solar gains of insulated glass ($U=0.50/1.25 \text{ W m}^{-2} \text{ K}^{-1}$) by those of uninsulated glass ($U=5.75 \text{ W m}^{-2} \text{ K}^{-1}$). As a result, the transmission of solar gains exclusively corresponds with SHGC.

4.5 Conclusions

Research on buildings with a high internal heat load generally concerns the optimisation of equipment efficiency to improve the facility's energy efficiency as a whole. However, the potential of building design and engineering are important as well, as they can contribute to substantial savings with respect to total building energy use. Therefore, this work investigated the total energy demand of plant factories in relation to façade design and exterior climate. Their energy demand was calculated with respect to diverse latitudes and climates: Sweden, the Netherlands and the United Arab Emirates.

On average, the energy demand consists of 50% for lighting, 2% for heating, 34% for dehumidification and 14% for sensible cooling. The insulation (U-value) was found to be the most effective in reducing the total energy demand at every wall-to-floor ratio and in each location (Table 4.4). In opaque constructions the increase in U-value from 0.05 to $5.75 \text{ W m}^{-2} \text{ K}^{-1}$ can change the total energy use by 7.1% to 12.5%. Varying the albedo between 0.1 and 0.9 can result in additional change

of 0.3% to 8.1%, depending on location. In transparent constructions an increase in U-value from 0.50 to 5.75 W m⁻² K⁻¹ can contribute 4.2% to 10.1%. Increasing the solar heat gain coefficient from 0.3 to 0.8 was found to change the total energy demand by an additional -2.3% to 7.6%.

The standard practice for plant factories has focused on achieving high insulation values to improve energy use efficiency, regardless of the local climate. Conversely, this study shows that a decentralised dissipation of the internal heat load through the façade can result in a lower total energy demand in each climate that was investigated.

The standard practice for sustainable building focuses on producing compact buildings to minimise both the surface area and the influence of the façade in the total energy balance. Conversely, this study shows that altering the wall-to-floor ratio of the building can amplify the targeted positive effects of the façade construction in certain locations. This strategy will influence operational and financial aspects, in addition to energetic expenditures. Additional studies are required to determine the relevance of these aspects.

4.6 Outlook

Plant factories are just one example of trends in the development of novel (urban) functions that feature high internal heat loads. The presented study enabled us to quantify the role of façade construction in the total energy balance in plant factories and the potential for reduction of their energy use. The dissipation of heat across the façade proved to be the most efficient design strategy in terms of energy expenditure in the three locations. This passive approach limits the need for forced air extraction and cooling via climate systems and consequently reduces the electricity demand of such systems. In short, optimising the façade for the dissipation of the internal heat load results in the same total amount of heat being exhausted, but at a lower energy expenditure. The reuse of the excess energy for other (urban) functions is recommended as a topic for future study.

Acknowledgements

This study was funded by the EU European Regional Development Fund “Kansen voor West” with the programme “Fieldlab FreshTeq”. The authors wish to thank Staaïj Food Group and Westland Infra for their support. Finally, the authors would like to express their gratitude to Mark Dornhelm for his advice on vapour compression cooling cycles and Dirk Hoogterp for his advice on heat exchangers.

APPENDIX 4A

Resource use efficiency

Crop production should be calculated to ensure a clear comparison of resources expended for crop production, the resource use efficiency (Fig. 4A.1). These values differ from the values in Figure 6B due to the differences in plant production. The model described by Van Henten [34] was used to calculate plant production, following each interior climate. The implementation of this model was described by [8] and the presented calculations follow their assumptions on dry weight, root/shoot-ratio and dry matter content. The production cycle that yields the highest annual dry weight production per square metre was calculated for each interior climate dataset. A key boundary condition was a minimum fresh weight of 300 g per crop.

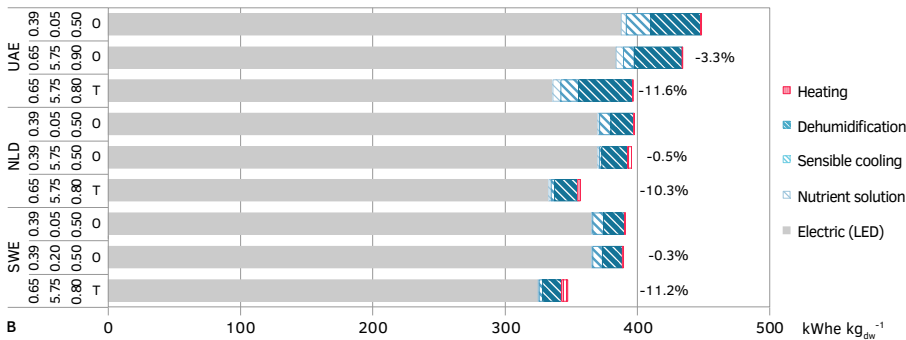


FIG. APP. 4A.1 Final electricity use for dry matter production ($\text{kWh kg}_{\text{dw}}^{-1}$) for the most efficient opaque and transparent constructions in each location. The relative delta (%) illustrates the difference with the industry-standard plant factory in the specific location (opaque, $U=0.05 \text{ W m}^{-2} \text{ K}^{-1}$, $A=0.55$, $W/F=0.39$). The y-axis lists location, W/F ratio (-), U-value ($\text{W m}^{-2} \text{ K}^{-1}$), SGHC (-) or albedo (-) (dependent on transparency), and transparency (O for opaque and T for transparent) from left to right. The long façade faces north in presented simulations.

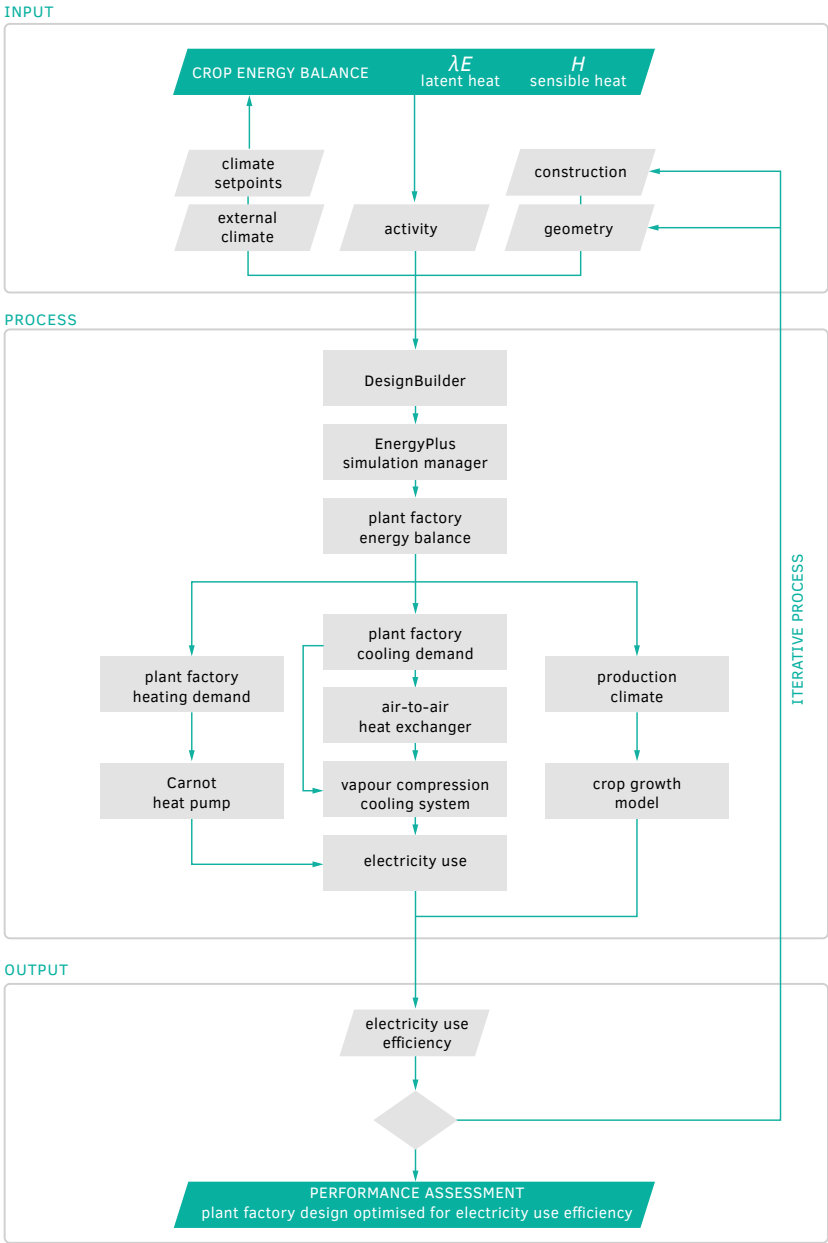


FIG. APP. 4B.1 Simplified model diagram to illustrate key processes and variables.

Coefficients of performance

This section specifies the methodology applied to calculate the electricity requirement for cooling. The projected combination of active and 'free' cooling (Section 4.2.4) is explained and each individual technique is expanded upon. Active cooling was realised by a vapour compression refrigeration cycle and 'free' cooling was realised by an air-to-air heat exchanger. Other methods for 'free' cooling were considered unsuitable for this study, due to the direct disturbance to the indoor air quality (direct airside free cooling) or the need for elements closely tied to location, such as a large body of open water or a geothermal source (direct/indirect waterside free cooling).

The presented methodology is formulated as a general approach, limiting the need for technical details and system characteristics where possible. As input, the model uses the latent and sensible cooling load and the heating load from DesignBuilder. Additionally, the model requires the temperature and relative humidity of the supply air, the return air, and the exterior air. The calculations for the vapour compression cooling systems (4B.1), the heat exchanger (4B.2) and the forced air extraction (4B.3) are detailed below.

Vapour compression refrigeration cycle

In its most basic form, a vapour compression refrigeration system consists of an evaporator, a compressor, a condenser, a throttling device (which is usually an expansion valve or capillary tube) and the connecting tubing. The working fluid is the refrigerant, which goes through a thermodynamic cycle.

For each individual process type (and temperature range) there is a wide span of design parameters and configuration options, which should be evaluated in order to calculate the best available technology for the assignment in light of performance and investment [72]. As this level of detail would go beyond the scope of this particular study, a model is constructed to calculate the performances under different operating conditions for the vapour compression model. This model is based on the fundamental principles of vapour compression cooling, as described by King [73], Zietlow [74] and Moran et al. [75] and is explained in greater detail hereafter.

The calculation of the vapour compression cycle has four degrees of freedom: the superheat, subcooling, the condenser temperature and the evaporator temperature. The optimisation of the condenser and evaporator temperature offset does not

entirely depend on the refrigeration cycle itself but depends on the ambient temperatures as well, due to the heat exchange [76].

TABLE APP. 4C.1 Assumptions for vapour compression cycle

Symbol	Value	Description	Source
T_{sup}	+ 5.0 K	Evaporator superheating	[72, 77, 78]
ΔT_{evap}	– 8.0 K	Evaporator temperature off-set	[79]
T_{sub}	– 9.0 K	Condenser subcooling	[80, 81]
ΔT_{cond}	+ 15.0 K	Condenser temperature off-set	[73, 81]
η_c	0.8	Compressor isentropic efficiency	[72, 75]
R -	134A	Selected refrigerant	[75]

Step 1: Fixing principal states

The heat transfers between the refrigerant and the warm and cold regions are not accomplished reversibly: the refrigerant temperature in the evaporator is lower than the cold region temperature ($T_{1s} < T_{evap,in}$) and the refrigerant temperature in the condenser is greater than the warm region temperature ($T_{3s} > T_{cond,in}$). An evaporator temperature difference (ΔT_{evap}) of 8 K with the interior air ($T_{evap,in}$) is assumed (see Table 4B.1).

$$T_{1s} = T_{evap,in} + \Delta T_{evap} \quad [4C.1]$$

The refrigerant is superheated (T_{sup}) beyond its boiling point to T_1 to ensure the quality of the vapour entering the compressor. T_{sup} is assumed to be 5 K.

$$T_1 = T_{1s} + T_{sup} \quad [4C.2]$$

The enthalpy (h_1) and entropy (s_1) of the refrigerant entering the compressor can be determined following T_1 and the quality (X), which is a saturated vapour.

$$h_1 = h(T_1, X) \quad [4C.3]$$

$$s_1 = s(T_1, X) \quad [4C.4]$$

Step 2: Calculating the increase in entropy using compressor efficiency

A greater temperature difference between the condenser (T_{3s}) and the ambient air ($T_{cond,in}$) is required with an air-cooled condenser, to partially offset poor heat transfer through the air film. A temperature difference (ΔT_{cond}) of 15 K is assumed.

$$T_{3s} = T_{cond,in} + \Delta T_{cond} \quad [4C.5]$$

The refrigerant is subcooled (T_{sub}) below its boiling point to T_3 to ensure the quality of the liquid refrigerant entering the expansion device. T_{sub} is assumed to be -9 K.

$$T_3 = T_{3s} + T_{sub} \quad [4C.6]$$

The pressure at state-point 2 (p_2) is the same as the pressure at state-point 3 (p_3), which is the saturation pressure in the condenser, since constant pressure heat rejection in the condenser is assumed. The saturation pressure can be found using a property relationship as a function of the saturation temperature (T_{3s}).

$$p_2 = p_3 = p(T_{3s}) \quad [4C.7]$$

In an isentropic process, which assumes an ideal compression, the entropy remains constant ($s_{2s}=s_1$). The enthalpy of the superheated vapour (h_{2s}) can then be determined using its entropy (s_1) and pressure (p_2) by:

$$h_{2s} = h(s_1, p_2) \quad [4C.8]$$

In reality, the adiabatic compression process results in an increase in specific entropy from compressor inlet to exit due to irreversibilities. The isentropic compressor efficiency is given by:

$$\eta_c = \frac{h_{2s} - h_1}{h_2 - h_1} \therefore h_2 = \frac{h_{2s} - h_1}{\eta_c} + h_1 \quad [4C.9]$$

The isentropic efficiency is one of the several parameters that typically has to be determined experimentally [82]. The presented model uses an efficiency of 0.8 (Table 4B.1). State 2 is then fixed by the value of specific enthalpy h_2 and the pressure p_2 , which makes it possible to determine the specific entropy (s_2):

$$s_2 = s(h_2, p_2) \quad [4C.10]$$

Step 3: Determining condenser exit conditions, assuming a constant pressure

The quantity of refrigerant in the vapour compression cycle will determine the condition at the exit of the condenser. We assume that the amount of refrigerant provides a saturated liquid condition at the condenser exit and that pressure is kept constant. The specific enthalpy can then be approximated by the saturated liquid value. That is:

$$h(T, p) \approx h_f(T) \therefore h_3 \approx h_f(T_3) \quad [4C.11]$$

The entropy of the saturated liquid exiting the condenser (h_3) can be approximated by the saturated liquid value at the given temperature.

$$s(T, p) \approx s_f(T) \therefore s_3 \approx s_f(T_3) \quad [4C.12]$$

Step 4: Throttling process in expansion valve

The conservation of energy around the expansion device is used to find the specific enthalpy at state-point 4 (h_4) as a function of the specific enthalpy at state-point 3 (h_3). The expansion valve is considered adiabatic, so the throttling of the refrigerant at the expansion valve is considered to be isenthalpic [75].

$$h_4 = h_3 \quad [4C.13]$$

The quality of the fluid-vapour mixture after the expansion valve can be calculated as follows:

$$X_4 = \frac{h_4 - h_{f4}}{h_{g4} - h_{f4}} \quad [4C.14]$$

The enthalpy of saturated fluid is represented by h_f and h_g is the enthalpy of the saturated vapour. The specific entropy of the vapour-fluid mixture after the throttling valve (s_4) can then be calculated using the entropy of a saturated liquid (s_{f4}), a saturated gas (s_{g4}) and the quality of the vapour-fluid mixture (X_4):

$$s_4 = s_{f4} + X_4 \cdot (s_{g4} - s_{f4}) \quad [4C.15]$$

Step 5: Calculating cooling cycle characteristics

The required refrigerant mass flow rate (\dot{m}) is linked to the refrigeration capacity (Q_{rc}) required for the total cooling demand (Q_{tot}) and the change in enthalpy over the evaporator (h_1-h_4).

$$Q_{rc} = \dot{m} \cdot (h_1 - h_4) \therefore \dot{m} = \frac{Q_{rc}}{(h_1 - h_4)} \quad [4C.16]$$

$$Q_{rc} = Q_{tot} \quad [4C.17]$$

The mass flow rate and the heat of compression (h_2-h_1) can then be used to calculate the compressor power (W_c).

$$W_c = \dot{m} \cdot (h_2 - h_1) \quad [4C.18]$$

The final coefficient of performance (COP) can be calculated using the refrigeration effect and the heat of compression.

$$COP = \frac{h_1 - h_4}{h_2 - h_1} \quad [4C.19]$$

The total amount of heat rejected to the surrounding air is the heat lost in the condenser, Q_{cond} [81]. The amount of heat lost can be calculated using the refrigerant mass flow rate and the decrease in enthalpy (h_2-h_3).

$$Q_{cond} = \dot{m} \cdot (h_2 - h_3) \quad [4C.20]$$

Step 6: Approximating physical system characteristics

From the conductance form of the equation it is possible to illustrate the relationship between the heat flux (Q_{cond} or Q_{evap}), the temperature difference ($T_{3s}-T_{cond,in}$ or $T_{1s}-T_{evap,in}$) and the design of the condenser or evaporator, as described in [74].

$$Q_{cond} = U_{cond} \cdot A_{cond} \cdot (T_{3s} - T_{cond,in}) \therefore U_{cond} \cdot A_{cond} = \frac{Q_{cond}}{(T_{3s} - T_{cond,in})} \quad [4C.21]$$

$$Q_{evap} = U_{evap} \cdot A_{evap} \cdot (T_{1s} - T_{evap,in}) \therefore U_{evap} \cdot A_{evap} = \frac{Q_{evap}}{(T_{1s} - T_{evap,in})} \quad [4C.22]$$

The overall conductance is the product of the overall heat transfer coefficient and the relevant heat transfer surface area ($U \cdot A$), the latter comprising the exterior surface of the channels and fins. The overall heat transfer coefficient is fixed for a given cross-section of the channel, fin type, fin density and flow rates. An attempt to maximise the COP or minimize the irreversibilities results in the sizes of the heat exchangers approaching infinity [74]. These variables need to be determined by applying optimisation techniques which lie beyond the scope of this paper. The flow rates and expended energy for the forced ventilation are discussed in Section B.3.

APP. 4C.2 Free cooling: Air-to-air heat exchanger

An air-to-air heat exchanger is applied to make use of the exterior temperature as a cold source. For the vast majority of regions, the exterior temperature provides favourable conditions for free cooling for extended periods during the year [83]. Indirect air exchange takes advantage of favourable outdoor conditions without introducing outside air into the plant factory. The outside air which cools the extracted air is circulated through an independent loop, allowing for greater control of humidity and air quality [11].

Similar to the vapour compression cycle, there is a wide span of design parameters and configuration options. Providing this level of detail, however, would go beyond the scope of this study. A model is constructed to calculate the heat exchange under different operating conditions and is explained in greater detail hereafter.

TABLE APP. 4C.2 Assumptions for heat exchanger and ventilation

Symbol	Value	Description	Source
n_{hex}	20	Number of parallel heat exchanger arrays	-
λ_{tube}	$380 \text{ W m}^{-1} \text{ K}^{-1}$	Thermal conductivity of copper tube	[50]
d_{tube}	0.0015 m	Tube wall thickness	-
$Q_{cool,ref}$	750 kW	Reference volume air flow	Output: maximum cooling demand
$u_{air,max}$	15 m s^{-1}	Maximum air speed in vents	[84]

Step 1: Determining ventilation requirement

The air volume flow extracted from the plant factory can be calculated using the total cooling demand (Q_{tot}), the density ($\rho_{air,in}$) and specific heat capacity ($c_{p,air,in}$) of the interior air, as well as the difference in enthalpy with the exterior air (Δh_{air}). The flow velocity ($u_{air,in}$) is determined by the hydraulic inner radius of the cylindrical tube (R_{in}) and the volume air flow (V_{air}).

$$V_{air} = \frac{Q_{tot}}{\rho_{air,in} \cdot \Delta h_{air}} \quad [4C.23]$$

$$u_{air,in} = \frac{V_{air}}{\pi \cdot (R_{in})^2} \quad \therefore R_{in} = \sqrt{\frac{V_{air}}{u_{air,in} \cdot \pi}} \quad [4C.24]$$

$$V_{air,hex,ref} = \frac{Q_{cool,ref}}{\Delta h_{evap,ref} \cdot \rho_{air,ref} \cdot n_{hex}} \quad [4C.25]$$

The required R_{in} can be estimated taking a reference volume air flow ($V_{air,hex,ref}$), a maximum $u_{air,in}$, the difference in enthalpy between supply air and return air ($\Delta h_{evap,ref}$) and the number of parallel heat exchanger arrays (n_{hex}) (see also Table 4B.2). The enthalpy of moist air (h_{air}) is determined using air temperature (T_{air}), the specific heat of air and water ($c_{p,air}$ and $c_{p,w}$ respectively) and the evaporation heat of water (h_{we}), as described in [85].

$$h_{air} = c_{p,air} \cdot T_{air} + x_{air} \cdot (h_w + c_{p,w} \cdot T_{air}) \quad [4C.26]$$

In order to prevent excessive u_{air} it is recommended to split the extracted V_{air} over multiple vents. This also minimises vent diameters.

Step 2: Calculating heat transfer inside the tube

In order to calculate the total heat transfer it is necessary to determine the transfer from the air inside the tube to the tube itself, as well as the transfer from the tube surface to the surrounding air. Firstly, the exchange between the interior medium and the tube is calculated. The turbulence of the flow is dependent on the Reynolds number (Re_{in}), which is comprised of $\rho_{air,in}$, $u_{air,in}$, and the dynamic viscosity of the air in the tube (μ_{in}), after [86].

$$Re_{in} = \frac{\rho_{air,in} \cdot u_{air,in} \cdot 2 \cdot R_{in}}{\mu_{air,in}} \quad [4C.27]$$

The heat transfer between the medium inside the tube and the tube surface under turbulent flow regime is governed by the Nusselt number (Nu_{in}), which is a function of the Prandtl (Pr) and Reynolds (Re) numbers. Pr is the product of the kinematic viscosity (ν) and the thermal diffusivity (α) of air [87]. The function for turbulent flow in a smooth tube is given by [88].

$$Pr = \frac{\nu}{\alpha} \quad [4C.28]$$

$$Nu_{in} = 0.023 \cdot Re_{in}^{0.8} \cdot Pr^{0.4} \quad [4C.29]$$

The heat transfer coefficient between the air inside the tube and the tube surface (α_{in}) is determined using Nu_{in} , R_{in} and the thermal conductivity of the interior air ($\lambda_{air,in}$).

$$\alpha_{in} = \frac{Nu_{in} \cdot \lambda_{air,in}}{2 \cdot R_{in}} \quad [4C.30]$$

Step 3: Calculating heat transfer from the tube

Secondly, the heat transfer between the tube surface and the surrounding air is calculated. The heat transfer coefficient is determined by Nu , as in Equation 4B.30, which depends on the Reynolds (Re_{ex}) and Prandtl (Pr_{ex}) numbers, accounting for the exterior air characteristics $\rho_{air,ex}$, $u_{air,ex}$ and μ_{ex} , and the exterior tube radius (R_{ex}).

$$Re_{ex} = \frac{\rho_{air,ex} \cdot u_{air,ex} \cdot 2R_{ex}}{\mu_{ex}} \quad [4C.31]$$

Assuming that external air is not under pressure, Pr_{ex} can be regarded as constant, and is incorporated into the coefficient of the corresponding formula in Equation 4B.29 [89].

$$Nu_{ex} = 0.023 \cdot Re_{ex}^{0.8} \quad [4C.32]$$

The heat transfer coefficient between the tube surface and the surrounding air (α_{ex}) is determined as in Equation 4B.30, using Nu_{ex} , R_{ex} and the thermal conductivity of the exterior air ($\lambda_{air,ex}$).

$$\alpha_{ex} = \frac{Nu_{ex} \cdot \lambda_{air,ex}}{2 \cdot R_{ex}} \quad [4C.33]$$

Step 4: Calculating total heat transfer

The heat transfer (Φ) in W m^{-1} can be calculated following the temperature difference between the air temperature at position l in the tube (T_l) and the exterior air ($T_{air,ex}$), the various thermal conductivities and the tube dimensions.

$$\Phi = \frac{(T_l - T_{air,ex})}{\frac{1}{\alpha_{in} \cdot 2 \cdot \pi \cdot R_{in}} + \frac{1}{\alpha_{ex} \cdot 2 \cdot \pi \cdot R_{ex}} + \frac{\ln(R_{ex} / R_{in})}{2 \cdot \pi \cdot \lambda}} \quad [4C.34]$$

The temperature of the air after tube length l (T_l) can be calculated using the various resistances, the air temperature at the start of the tube (T_0), the tube length l , the surface area of the cross-section, as well as the air characteristics.

$$T_l = T_{air,ex} + (T_0 - T_{air,ex}) \cdot e^{-\frac{l}{R' \cdot \rho_{c,air,in} \cdot c_{p,air,in} \cdot u_{air,in} \cdot \pi \cdot (R_{in})^2}} \quad [4C.35]$$

where:

$$R' = \frac{1}{\alpha_{in} \cdot 2 \cdot \pi \cdot R_{in}} + \frac{1}{\alpha_{ex} \cdot 2 \cdot \pi \cdot R_{ex}} + \frac{\ln(R_{ex} / R_{in})}{2 \cdot \pi \cdot \lambda} \quad [4C.36]$$

Where l is either the maximum tube length ($l_{max} = 40$ m, see Table 4B.2) or the required tube length (l_{req}) to reach the temperature setpoint for the supply air (18 °C). Variable l_{req} is determined by:

$$l_{req} = -\ln \frac{T_{l,set} - T_{air}}{T_0 - T_{air}} \cdot \left(R' \cdot \rho_{c,in} \cdot c_{p,air} \cdot u_{air} \cdot \pi \cdot (R_{in})^2 \right) \quad [4C.37]$$

The latent and sensible component ($Q_{hex,lat}$ and $Q_{hex,sen}$, respectively) of the energy exchanged are determined as follows:

$$Q_{hex,lat} = \Delta x_{air,hex} \cdot h_{we} \cdot \rho_{c,air} \cdot V_{air} \quad [4C.38]$$

$$Q_{hex,sen} = \Delta h_{air,hex} \cdot \rho_{c,air} \cdot V_{air} - Q_{hex,lat} \quad [4C.39]$$

The presented model can be used to calculate the potential heat transfer to the surrounding environment, without requiring active cooling. The total heat transfer is dominated by the exchange with the surrounding air, which is facilitated by forced ventilation (see Section 4B.3). The emissivity to the night's sky is not considered as

heat exchangers are typically built to be compact, decreasing the relative importance of radiation in the cooling process.

APP. 4C.3

Active and free cooling: Forced ventilation

Air circulation fans are required for an adequate exchange between the evaporator, the condenser, the heat exchanger and the surrounding air. These fans represent a notable share in the total electricity requirement for cooling [58]. The required electricity for forced ventilation (fan power) was determined based on [81]. The methodology is specified hereafter.

The power input of (condenser) fans ($P_{fan,elec}$) means the total power of the fan(s) staged at a given operating condition. The necessary mechanical fan power ($P_{fan,mech}$) can be determined from the volume flow of air (V_{air}) and the pressure difference (Δp), assuming an incompressible flow [77].

$$P_{fan,mech} = V_{air} \cdot \Delta p \quad [4C.40]$$

In order to include both the sensible and the latent component, we use the difference in enthalpy to determine V_{air} , as is shown in Equation 4B.23. To prevent excessive fan dimensions, it is recommended to split the extracted V_{air} over multiple fans. The Δp can be found using the Bernoulli equation, air characteristics and the friction loss (Δp_{fl}).

$$\Delta p = \frac{u_{air}^2 \cdot \rho_{c,air}}{2} + \Delta p_{fl} \quad [4C.41]$$

The Δp_{fl} can be defined as a function of u_{air} [77]:

$$\Delta p_{fl} = 3.4 \cdot u_{air}^2 + 4.9 \cdot u_{air} \quad [4C.42]$$

The expended electrical power (E_{fans}) can then be calculated when introducing a fan efficiency (c_{fan}).

$$E_{fans} = \frac{V_{air}}{c_{fan}} \cdot \frac{\rho_{c,air} \cdot u_{air}^2}{2} + \Delta p_{fl} \quad [4C.43]$$

In the presented calculations c_{fan} was assumed to be 65%, in line with [77]. The electricity expenditure of the fans ($E_{fans,x}$) is specified for heating and sensible and latent cooling by its relative share (Q_a) in the total energy demand.

$$E_{fans,x} = \frac{Q_a}{Q_{cool,lat} + Q_{cool,sen} + Q_{heat}} \cdot E_{fans} \quad [4C.44]$$

A similar method is applied to specify the electricity expenditure of the heat exchanger fans ($E_{fans,hex,a}$) for sensible and latent cooling ($Q_{hex,sen}$ and $Q_{hex,lat}$, respectively).

$$E_{fans,hex,x} = \frac{Q_x}{Q_{cool,lat} + Q_{cool,sen}} \cdot E_{fans,hex} \quad [4C.45]$$

Reference list

- [4] Benis, K. & Ferrão, P. (2018). Commercial farming within the urban built environment – Taking stock of an evolving field in northern countries. *Global Food Security*, 17, 30–37. doi:10.1016/j.gfs.2018.03.005
- [5] Kennedy, C., Cuddihy, J., & Engel-Yan, J. (2007). The changing metabolism of cities. *Journal of industrial ecology*, 11(2), 43–59. doi:10.1162/jiec.0.1107
- [6] Newcombe, K. & Nichols, E.H. (1979). An integrated ecological approach to agricultural policy-making with reference to the urban fringe: The case of Hong Kong. *Agricultural Systems*, 4(1), 1–27. doi:10.1016/0308-521x(79)90011-8
- [7] United Nations. (2014). *World urbanization prospects: The 2014 revision, highlights*. New York: United Nations - Department of Economic and Social Affairs - Population division. doi:10.18356/527e5125-en
- [8] Seginer, I. & Ioslovich, I. (1999). Optimal spacing and cultivation intensity for an industrialized crop production system. *Agricultural Systems*, 62(3), 143–157. doi:10.1016/s0308-521x(99)00057-8
- [9] Kozai, T., Ohyama, K., & Chun, C. (2006). Commercialized closed systems with artificial lighting for plant production. *Acta Horticulturae*, 711, 61–70. doi:10.17660/actahortic.2006.711.5
- [10] Kozai, T. (2013). Resource use efficiency of closed plant production system with artificial light: Concept, estimation and application to plant factory. *Proceedings of the Japan Academy. Series B, Physical and biological sciences*, 89(10), 447–461. doi:10.2183/pjab.89.447
- [11] Graamans, L., Baeza, E., van den Dobbelsteen, A., Tsafaras, I., & Stanghellini, C. (2018). Plant factories versus greenhouses: Comparison of resource use efficiency. *Agricultural Systems*, 160, 31–43. doi:10.1016/j.agry.2017.11.003
- [12] Kozai, T. (2013). Sustainable plant factory: Closed plant production systems with artificial light for high resource use efficiencies and quality produce. *Acta Horticulturae*, 1004, 27–40. doi:10.17660/actahortic.2013.1004.2
- [13] Graamans, L., van den Dobbelsteen, A., Meinen, E., & Stanghellini, C. (2017). Plant factories; crop transpiration and energy balance. *Agricultural Systems*, 153, 138–147. doi:10.1016/j.agry.2017.01.003
- [14] Daraghmeh, H.M. & Wang, C.C. (2017). A review of current status of free cooling in datacenters. *Applied Thermal Engineering*, 114, 1224–1239. doi:10.1016/j.applthermaleng.2016.10.093
- [15] Boyano, A., Hernandez, P., & Wolf, O. (2013). Energy demands and potential savings in European office buildings: Case studies based on EnergyPlus simulations. *Energy and buildings*, 65, 19–28. doi:10.1016/j.enbuild.2013.05.039
- [16] Ihara, T., Gustavsen, A., & Jelle, B.P. (2015). Effect of facade components on energy efficiency in office buildings. *Applied energy*, 158, 422–432. doi:10.1016/j.apenergy.2015.08.074
- [17] Hien, W.N., Liping, W., Chandra, A.N., Pandey, A.R., & Xiaolin, W. (2005). Effects of double glazed facade on energy consumption, thermal comfort and condensation for a typical office building in Singapore. *Energy and buildings*, 37(6), 563–572. doi:10.1016/j.enbuild.2004.08.004
- [18] Thalfeldt, M., Pikas, E., Kurnitski, J., & Voll, H. (2013). Facade design principles for nearly zero energy buildings in a cold climate. *Energy and buildings*, 67, 309–321. doi:10.1016/j.enbuild.2013.08.027
- [19] Khalaj, A.H. & Halgamuge, S.K. (2017). A review on efficient thermal management of air-and liquid-cooled data centers: From chip to the cooling system. *Applied energy*, 205, 1165–1188. doi:10.1016/j.apenergy.2017.08.037
- [20] Cho, J. & Kim, Y. (2016). Improving energy efficiency of dedicated cooling system and its contribution towards meeting an energy-optimized data center. *Applied energy*, 165, 967–982. doi:10.1016/j.apenergy.2015.12.099
- [21] Oró, E., Depoorter, V., Pflugradt, N., & Salom, J. (2015). Overview of direct air free cooling and thermal energy storage potential energy savings in data centres. *Applied Thermal Engineering*, 85, 100–110. doi:10.1016/j.applthermaleng.2015.03.001
- [22] Crawley, D.B., Lawrie, L.K., Winkelmann, F.C., Buhl, W.F., Huang, Y.J., Pedersen, C.O., Strand, R.K., Liesen, R.J., Fisher, D.E., Witte, M.J., & Glazer, J. (2001). EnergyPlus: creating a new-generation building energy simulation program. *Energy and buildings*, 33(4), 319–331. doi:10.1016/s0378-7788(00)00114-6
- [23] Witte, M.J., Henninger, R.H., Glazer, J., & Crawley, D.B. (2001). *Testing and validation of a new building energy simulation program*. Paper presented at the 7th International Building Performance Simulation Association Conference, Rio de Janeiro, Brazil.

- [24] Raji, B., Tenpierik, M., & van den Dobbelsteen, A. (2016). An assessment of energy-saving solutions for the envelope design of high-rise buildings in temperate climates: A case study in the Netherlands. *Energy and buildings*, 124, 210-221. doi:10.1016/j.enbuild.2015.10.049
- [25] Shrestha, S.S. & Maxwell, G. (2011). *Empirical validation of building energy simulation software: EnergyPlus*. Paper presented at the 12th Conference of International Building Performance Simulation Association, Sydney, Australia.
- [26] Loutzenhiser, P.G., Manz, H., Moosberger, S., & Maxwell, G.M. (2009). An empirical validation of window solar gain models and the associated interactions. *International Journal of Thermal Sciences*, 48(1), 85-95. doi:10.1016/j.ijthermalsci.2008.01.011
- [27] Arasteh, D., Kohler, C., & Griffith, B. (2009). Modeling windows in energy plus with simple performance indices. doi:10.2172/975375
- [28] Fumo, N., Mago, P., & Luck, R. (2010). Methodology to estimate building energy consumption using EnergyPlus Benchmark Models. *Energy and buildings*, 42(12), 2331-2337. doi:10.1016/j.enbuild.2010.07.027
- [29] Andelković, A.S., Mujan, I., & Dakić, S. (2016). Experimental validation of a EnergyPlus model: Application of a multi-storey naturally ventilated double skin façade. *Energy and buildings*, 118, 27-36. doi:10.1016/j.enbuild.2016.02.045
- [30] Crawley, D.B. (1998). Which weather data should you use for energy simulations of commercial buildings? *ASHRAE Transactions*, 104, 498-515.
- [31] ASHRAE. (2011). ASHRAE Standard 140-2011. Standard method of test for the evaluation of building energy analysis computer programs. Atlanta, USA: ASHRAE - American Society of Heating, Refrigerating and Air-Conditioning Engineers.
- [32] DesignBuilder. (2018). DesignBuilder version 5.3.0.014. Gloucestershire, UK: DesignBuilder Software Ltd. Retrieved from www.designbuilder.co.uk/index.php
- [33] De Zwart, H.F. (1996). *Analyzing energy-saving options in greenhouse cultivation using a simulation model*. (PhD), Wageningen University & Research, Wageningen, the Netherlands.
- [34] Tei, F., Scaife, A., & Aikman, D.P. (1996). Growth of lettuce, onion, and red beet. 1. Growth analysis, light interception, and radiation use efficiency. *Annals of Botany*, 78(5), 633-643. doi:10.1006/anbo.1996.0171
- [35] De Visser, P.H.B., van der Heijden, G., & Buck-Sorlin, G. (2014). Optimizing illumination in the greenhouse using a 3D model of tomato and a ray tracer. *Frontiers in plant science*, 5, 48. doi:10.3389/fpls.2014.00048
- [36] Farquhar, G.D., von Caemmerer, S., & Berry, J.A. (1980). A biochemical model of photosynthetic CO₂ assimilation in leaves of C3 species. *Planta*, 149(1), 78-90. doi:10.1007/bf00386231
- [37] Van Henten, E.J. (1994). Validation of a dynamic lettuce growth model for greenhouse climate control. *Agricultural Systems*, 45(1), 55-72. doi:10.1016/S0308-521X(94)90280-1
- [38] MATLAB. (2018). MATLAB version R2018a (9.4.0.813654). Natick, Massachusetts, USA: The MathWorks, Inc. Retrieved from www.mathworks.com/products/matlab.html
- [39] Van Henten, E.J. & Van Straten, G. (1994). Sensitivity analysis of a dynamic growth model of lettuce. *Journal of Agricultural Engineering Research*, 59(1), 19-31. doi:10.1006/jaer.1994.1061
- [40] EnergyPlus. (2018). EnergyPlus weather data by location - Abu Dhabi 412170 (IWE). Retrieved 30 April 2018 https://energyplus.net/weather-download/asia_wmo_region_2/ARE//ARE_Abu.Dhabi.412170_IWE/
- [41] EnergyPlus. (2018). EnergyPlus weather data by location - Amsterdam 062400 (IWE). Retrieved 26 April 2018 https://energyplus.net/weather-location/europe_wmo_region_6/NLD//NLD_Amsterdam.062400_IWE/
- [42] EnergyPlus. (2018). EnergyPlus weather data by location - Kiruna 020440 (IWE). Retrieved 30 April 2018 https://energyplus.net/weather-location/europe_wmo_region_6/SWE//SWE_Kiruna.020440_IWE/
- [43] Zhang, X., He, D.X., Niu, G.H., Yan, Z.N., & Song, J.X. (2018). Effects of environment lighting on the growth, photosynthesis, and quality of hydroponic lettuce in a plant factory. *International Journal of Agricultural and Biological Engineering*, 11(2), 33-40. doi:10.25165/j.ijabe.20181102.3240
- [44] Fu, W.G., Li, P.P., & Wu, Y.Y. (2012). Effects of different light intensities on chlorophyll fluorescence characteristics and yield in lettuce. *Scientia Horticulturae*, 135, 45-51. doi:10.1016/j.scienta.2011.12.004
- [45] Hiroki, R., Shimizu, H., Ito, A., Nakashima, H., Miyasaka, J., & Ohdoi, K. (2013). *Identifying the optimum light cycle for lettuce growth in a plant factory*. Paper presented at the International Symposium on New Technologies for Environment Control, Energy-Saving and Crop Production in Greenhouse and Plant Factory - Greensys 2013.

- [46] Lee, H.I. & Kim, Y.H. (2013). Utilization efficiencies of electric energy and photosynthetically active radiation of lettuce grown under red LED, blue LED and fluorescent lamps with different photoperiods. *Journal of Biosystems Engineering*, 38(4), 279-286. doi:10.5307/jbe.2013.38.4.279
- [47] Hall, A.E. (1979). A model of leaf photosynthesis and respiration for predicting carbon dioxide assimilation in different environments. *Oecologia*, 43(3), 299-316. doi:10.1007/bf00344957
- [48] He, J. & Lee, S.K. (1998). Growth and photosynthetic responses of three aeroponically grown lettuce cultivars (*Lactuca sativa* L.) to different rootzone temperatures and growth irradiances under tropical aerial conditions. *Journal of Horticultural Science and Biotechnology*, 73(2), 173-180. doi:10.1080/14620316.1998.11510961
- [49] Thompson, H.C., Langhans, R.W., Both, A.J., & Albright, L.D. (1998). Shoot and root temperature effects on lettuce growth in a floating hydroponic system. *Journal of the American Society for Horticultural Science*, 123(3), 361-364.
- [50] Frantz, J.M., Ritchie, G., Cometti, N.N., Robinson, J., & Bugbee, B. (2004). Exploring the limits of crop productivity: beyond the limits of tipburn in lettuce. *Journal of the American Society for Horticultural Science*, 129(3), 331-338.
- [51] Tenpierik, M.J., Cauberg, J.J.M., & Thorsell, T.I. (2007). Integrating vacuum insulation panels in building constructions: an integral perspective. *Construction Innovation*, 7(1), 38-53. doi:10.1108/14714170710721287
- [52] Engineering ToolBox. (2004). Transmission heat loss through building elements. Retrieved 21 May 2019 https://www.engineeringtoolbox.com/heat-loss-transmission-d_748.html
- [53] Engineering ToolBox. (2005). Thermal conductivity of metals, metallic elements and alloys. Retrieved 19 August 2019 https://www.engineeringtoolbox.com/thermal-conductivity-metals-d_858.html
- [54] Jelle, B.P., Gustavsen, A., & Baetens, R. (2010). The path to the high performance thermal building insulation materials and solutions of tomorrow. *Journal of Building Physics*, 34(2), 99-123. doi:10.1177/1744259110372782
- [55] Ihara, T., Gao, T., Grynning, S., Jelle, B.P., & Gustavsen, A. (2015). Aerogel granulate glazing facades and their application potential from an energy saving perspective. *Applied energy*, 142, 179-191. doi:10.1016/j.apenergy.2014.12.053
- [56] Gao, T., Jelle, B.P., Sandberg, L.I.C., & Gustavsen, A. (2013). Monodisperse hollow silica nanospheres for nano insulation materials: synthesis, characterization, and life cycle assessment. *ACS applied materials & interfaces*, 5(3), 761-767. doi:10.1021/am302303b
- [57] Engineering ToolBox. (2012). Materials - Light reflecting factors. Retrieved 22 December 2019 https://www.engineeringtoolbox.com/light-material-reflecting-factor-d_1842.html
- [58] United States - Department of Energy. (2015). *EnergyPlus documentation - Engineering reference*. Berkeley, CA (USA).
- [59] United States - Department of Energy. (2018). *EnergyPlus documentation - Input output reference*. Berkeley, CA (USA).
- [60] Meggers, F., Ritter, V., Goffin, P., Baetschmann, M., & Leibundgut, H. (2012). Low exergy building systems implementation. *Energy*, 41(1), 48-55. doi:10.1016/j.energy.2011.07.031
- [61] Bieliński, H. & Mikielawicz, J. (2011). Natural circulation in single and two phase thermosyphon loop with conventional tubes and minichannels. In Belmiloudi, A. (Ed.), *Heat transfer - Mathematical modelling, numerical methods and information technology*: Intech. doi:10.5772/569
- [62] Sabharwall, P., Patterson, M., & Gunnerson, F. (2008). *Theoretical design of thermosyphon for process heat transfer from NGNP to hydrogen plant*. Paper presented at the ASME 4th International Topical Meeting on High Temperature Reactor Technology, Washington, D.C., USA.
- [63] Haider, S.I., Joshi, Y.K., & Nakayama, W. (2002). A natural circulation model of the closed loop, two-phase thermosyphon for electronics cooling. *Journal of heat transfer*, 124(5), 881-890. doi:10.1115/1.1482404
- [64] Milanez, F. & Mantelli, M.B.H. (2010). Heat transfer limit due to pressure drop of a two-phase loop thermosyphon. *Heat Pipe Science and Technology, An International Journal*, 1(3). doi:10.1615/heatpipesci.2011003082
- [65] Zhang, H., Shao, S., Xu, H., Zou, H., Tang, M., & Tian, C. (2017). Simulation on the performance and free cooling potential of the thermosyphon mode in an integrated system of mechanical refrigeration and thermosyphon. *Applied energy*, 185, 1604-1612. doi:10.1016/j.apenergy.2016.01.053

- [66] Lee, S., Kang, H., & Kim, Y. (2009). Performance optimization of a hybrid cooler combining vapor compression and natural circulation cycles. *International Journal of Refrigeration*, 32(5), 800-808. doi:10.1016/j.ijrefrig.2008.12.008
- [67] Gartia, M.R., Vijayan, P.K., & Pilkhwal, D.S. (2006). A generalized flow correlation for two-phase natural circulation loops. *Nuclear Engineering and Design*, 236(17), 1800-1809. doi:10.1016/j.nucengdes.2006.02.004
- [68] Nishimura, M., Kozai, T., Kubota, C., & Chun, C. (2001). Analysis of electric energy consumption and its cost for a closed-type transplant production system. *Journal of Society of High Technology in Agriculture*, 14(3), 204-209.
- [69] Ohyama, K., Kozai, T., Kubota, C., Chun, C., Hasegawa, T., Yokoi, S., & Nishimura, M. (2002). Coefficient of performance for cooling of a home-use air conditioner installed in a closed-type transplant production system. *Shokubutsu Kojo Gakkaishi*, 14(3), 141-146. doi:10.2525/jshita.14.141
- [70] Tong, Y., Yang, Q., & Shimamura, S. (2013). *Analysis of electric-energy utilization efficiency in a plant factory with artificial light for lettuce production*. Paper presented at the International Symposium on New Technologies for Environment Control, Energy-Saving and Crop Production in Greenhouse and Plant Factory - Greensys 2013.
- [71] Harbick, K. & Albright, L.D. (2016). Comparison of energy consumption: greenhouses and plant factories. *Acta Horticulturae*, 1134, 285-292. doi:10.17660/actahortic.2016.1134.38
- [72] Pattison, PM., Hansen, M., & Tsao, JY. (2018). LED lighting efficacy: Status and directions. *Comptes Rendus Physique*, 19(3), 134-145. doi:10.1016/j.crhy.2017.10.013
- [73] Tyagi, V.V., Rahim, N.A.A., Rahim, N.A., & Selvaraj, J.A.L. (2013). Progress in solar PV technology: Research and achievement. *Renewable and Sustainable Energy Reviews*, 20(C), 443-461. doi:10.1016/j.rser.2012.09.028
- [74] Royal Philips N.V. (2018). Philips GreenPower LED production module. Retrieved 15 October 2018 <http://www.lighting.philips.com/main/products/horticulture/products/greenpower-led-production-module>
- [75] Ommen, T., Jensen, J.K., Markussen, W.B., Reinholdt, L., & Elmegaard, B. (2015). Technical and economic working domains of industrial heat pumps: Part 1–Single stage vapour compression heat pumps. *International Journal of Refrigeration*, 55, 168-182. doi:10.1016/j.ijrefrig.2015.02.012
- [76] King, G.R. (1971). *Modern refrigeration practice*: McGraw-Hill Companies.
- [77] Zietlow, D.C. (2014). *Optimization of vapor compression cycles*. Paper presented at the American Society for Engineering Education, Indianapolis, IN, USA.
- [78] Moran, M.J., Shapiro, H.N., Boettner, D.D., & Bailey, M.B. (2015). *Principles of Engineering Thermodynamics, 8th Edition - SI Version*: John Wiley & Sons.
- [79] Larsen, L.S. & Thybo, C. (2004). *Potential energy savings in refrigeration systems using optimal set-points*. Paper presented at the IEEE International Conference on Control Applications.
- [80] Sahlsten, A. & Heinerud, V. (2016). *Natural refrigerants in data center cooling with thermosiphon application*. (MSc), KTH, Stockholm, Sweden.
- [81] Kim, D.H., Park, H.S., & Kim, M.S. (2013). Optimal temperature between high and low stage cycles for R134a/R410A cascade heat pump based water heater system. *Experimental thermal and fluid science*, 47, 172-179. doi:10.1016/j.exthermflusci.2013.01.013
- [82] Maivel, M. & Kurnitski, J. (2015). Heating system return temperature effect on heat pump performance. *Energy and buildings*, 94, 71-79. doi:10.1016/j.enbuild.2015.02.048
- [83] Pottker, G. & Hrnjak, P. (2015). Effect of the condenser subcooling on the performance of vapor compression systems. *International Journal of Refrigeration*, 50, 156-164. doi:10.1016/j.ijrefrig.2014.11.003
- [84] Chan, K.T. & Yu, F.W. (2004). Optimum setpoint of condensing temperature for air-cooled chillers. *HVAC&R Research*, 10(2), 113-127. doi:10.1080/10789669.2004.10391095
- [85] Zsebinszki, G., de Gracia, A., Moreno, P., Rovira, R., González, M.A., & Cabeza, L.F. (2017). A novel numerical methodology for modelling simple vapour compression refrigeration system. *Applied Thermal Engineering*, 115, 188-200. doi:10.1016/j.applthermaleng.2016.12.059
- [86] Zhang, H., Shao, S., Xu, H., Zou, H., & Tian, C. (2014). Free cooling of data centers: A review. *Renewable and Sustainable Energy Reviews*, 35, 171-182. doi:10.1016/j.rser.2014.04.017
- [87] Engineering ToolBox. (2005). Air duct velocities. Retrieved 21 August 2019 https://www.engineeringtoolbox.com/duct-velocity-d_928.html
- [88] Engineering ToolBox. (2004). Enthalpy of moist air. Retrieved 21 August 2019 https://www.engineeringtoolbox.com/enthalpy-moist-air-d_683.html

- [89] Rattner, A. & Bohren, J. (2008). Heat and mass correlations. from University of Pennsylvania
- [90] Van Wijngaarden, L. (1971). Warmte- en stromingsleer - deel 1b. from Universiteit Twente
- [91] Holman, J.P. (1997). *Heat transfer - 8th edition*. New York, NY, USA: McGraw-Hill.
- [92] Kutateladze, S.S. (1963). *Fundamentals of heat transfer*. London, UK: Edward Arnold.

INTERMEZZO 4

Chapter 4 provided insight into the effects of operation schedule, cooling system design, form factor and façade design on the energy and electricity use of plant factories. We analysed the effects of transparency, insulation, albedo, solar heat gain coefficient and wall-to-floor ratio on total energy use. The chapter illustrated the potential of passive measures to reduce energy use, such as the dissipation of internal heat through the façade. This passive approach reduces the energy use for climate systems and increases the energy use efficiency of the plant factory.

Excess heat is generally discharged to the ambient air in both passive and active climatisation and may contribute to the urban heat island effect. If this residual heat could be recovered and reused, however, it would represent a significant heat source. In Chapter 5 we investigated the potential for heat recovery and reuse in the urban energy system. Utilising this source of residual heat can contribute to balancing the urban energy system. This chapter provided insight into the role of urban food production and the food-energy interface.



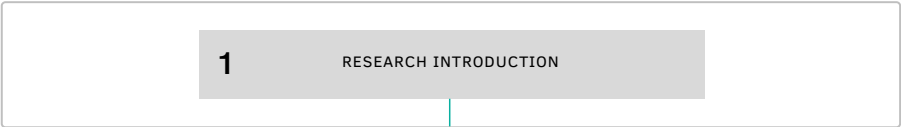
5 System integration

Plant factories: Integrating food production to balance the renewable energy system in cities
Graamans, L., Tenpierik, M., van den Dobbelsteen, A., Stanghellini, C.
Applied energy. 2020; submitted.

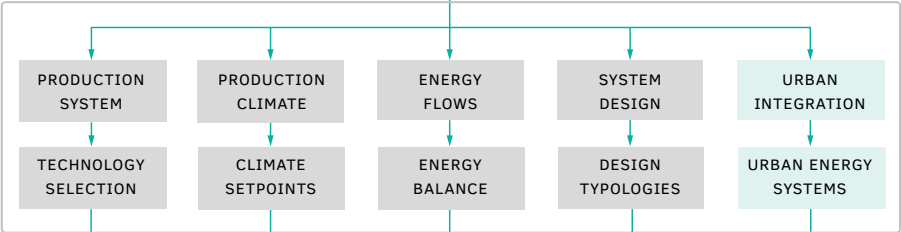
ABSTRACT Large cities strive to increase their resilience by integrating renewable energy production and reducing their dependence on global food networks. Shifting to intermittent renewable energy sources leads to imbalance between hourly production and demand. Balance is typically achieved by relying on the surrounding region for the exchange of electricity via the public grid. Food resilience can be achieved by implementing new food production systems, such as plant factories. These present the same challenge as many high-tech building functions: high internal heat loads resulting in considerable amounts of residual heat.

This study investigates how plant factories can serve as flexible heat production units to reduce the imbalance in energy production and demand. To this end, we calculated the energy demand and renewable energy distribution for a simulated city in three disparate climate zones: Sweden (subarctic), the Netherlands (temperate oceanic) and the United Arab Emirates (hot desert). We worked out nine scenarios, each incorporating a particular energy distribution, residual heat production capacity and thermal energy storage capacity. Utilising residual heat from plant factories proved to be an effective strategy in locations with high heating demands. The integration of plant factories could increase the primary energy supply by 47.0%, 28.6% and 11.0% for Sweden, the Netherlands and the United Arab Emirates and could decrease energy imbalance by 38.9%, 41.3% and 11.8% respectively. The presented strategies can reduce energy imbalance and provide a foundation for an integrated energy system design tailored to the local climate.

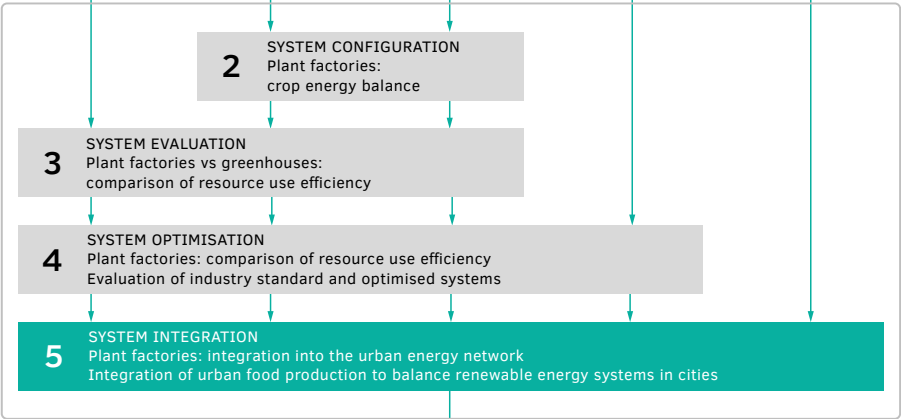
I. INTRODUCTION & METHODOLOGICAL FRAMEWORK



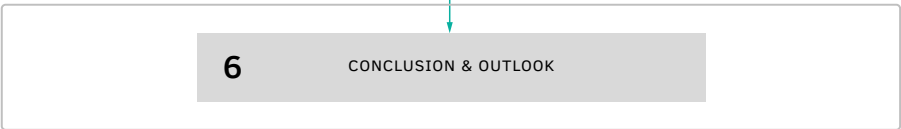
II. THEORETICAL FRAMEWORK



III. DESIGN & EXPERIMENTAL VALIDATION



IV. INTEGRATED DISCUSSION



5.1 Introduction

5.1.1 Background

Cities rely on several essential flows: energy, food, water, supplies and data. Extensive urbanisation, technological advancement and shifts in the global market have markedly affected these flows, confronting cities with complex challenges. In this study, we focus on energy and food. Firstly, the urban energy demand and supply are shifting. On the one hand, the energy demand of buildings is being reduced by sustainable building and renovation practices (i.e. [1]). Meanwhile, new (high-tech) building functions with high energy use and disparate usage profiles (i.e. data centres) are changing the distribution of the total energy demand in cities. On the other hand, the production of energy is shifting from fossil fuels to renewable energy sources (RES) in an attempt to reduce carbon emissions [2]. RES are typically subject to climate conditions that vary per minute, per hour, even over years. Energy production then becomes intermittent, following fluctuations in the weather [3]. The key challenge in energy is therefore to integrate a high share of intermittent RES in the energy system and to balance production and demand [4-9]. Resolving the energy imbalance via import and export makes demands on the neighbouring regions which may not be met [7] and diminishes resilience. Secondly, large cities generally obtain food via the global food supply network, but the sustainability and resilience of this network is questionable [10]. The predominance and complexity of this network is projected to increase even further as a result of the expanding urban population [11]. A key challenge in food supply is therefore to ensure resilience to changes in this supply network and introduce independence.

The independence and resilience of cities can be increased by shifting energy production to RES and by localising food production. However, the consequences of such a strategy for the urban energy requirement and balance are largely unknown. New technologies are often investigated from a sectoral or single technology focus with little regard for the broader energy system. The goal of analysis is to identify innovative solutions in which all sectors can contribute to feasible 100% renewable energy systems [4]. This study investigates how a food production system could be integrated into an advanced urban energy network in order to address the imbalance in renewable energy supply and demand.

The production system selected for this investigation is the plant factory or vertical farm⁶, which is intended for urban or peri-urban food production in the form of fresh fruit and vegetable crops [12]. Plant factories are closed production systems that allow for full artificial control of the interior climate, with uniform lighting, temperature, CO₂ concentration and relative humidity [13]. They are designed for high-density crop production [14] with efficient use of water [15], CO₂ [16] and other resources [17]. The closed nature of such a system and the use of artificial light result in a high electricity demand, high internal heat loads and consequently considerable generation of residual heat, particularly in comparison with other crop production systems [18].

The future energy systems are intended to balance the energy production and demand through the interaction of intermittent RES, production units, energy storage and energy demand [19]. Advanced energy networks provide an important infrastructure to integrate new, flexible technologies in order to improve the effectiveness of the energy system as a whole [20, 21]. Energy storage is an important component in addressing the integration of intermittent RES as it can bridge the gap between energy generation and use. Electrical energy can be stored directly (e.g. in batteries) or converted (e.g. to compressed air, hydro-electric power, heat) at varying efficiency and cost. One established strategy to shift energy loads from high-peak to off-peak production hours is converting electrical energy to thermal energy that can be stored [22]. Thermal energy is vastly more cost-effective to store than even the cheapest form of large-scale electricity storage, namely hydro-electric storage [23]. In a thermal system the plant factory could convert energy to heat, with a useful by-product.

The question is whether such an integrated system can improve the energy balance while increasing the food resilience of the city. To what extent can plant factories and other functions with large internal heat loads serve as flywheels in urban energy systems that rely on RES? Exploring the impact of food production on the energy balance can provide insight into the complexity and viability of food-resilient cities and contribute to the development of cities that operate on 100% renewable energy.

⁶ As a working definition, a vertical farm can be regarded as a plant factory with multiple storeys.

5.1.2 Problem statement and framing

This study focuses on the interface between energy and food where the differences in energy demand and renewable energy production are bridged by urban food production in plant factories.

The literature on energy systems demonstrates the effects of incorporating high shares of RES in the total primary energy supply and the import/export of energy [4]. Numerous studies have investigated how the broader energy balance is affected by various pathways: i.e. flexible technologies [6], combined heat and power [8], heat pumps [24], data centres for dynamic flexibility [25], implementing heat savings [26], limiting biomass [27], and incorporating residual heat from process industry [28] or data centres [29]. Research on closed food production has primarily focused on optimising the efficient use of resources through growth recipes for various crops (e.g. [30]) or the systems design of individual facilities [31]. Finally, the literature on urban food production consists largely of qualitative investigations into their viability [12], business models [32], stakeholder perspectives [33] or the sustainability of supply chains [34].

Little research has been done on reducing the imbalance between energy supply and demand by utilising waste heat from high-tech functions, such as plant factories or data centres. To bridge that gap, we investigated the integration of plant factories in the urban energy system. With this study we seek to contribute to the sustainable energy transition, the environmental footprint of cities and potential directions for climate change mitigation and adaptation.

5.1.3 Objective

The main objective of this study is to quantify the effect of localising food production in plant factories on the energy balance of a metropolitan city running on renewable energy. We explore the role plant factories can play in balancing primary energy demand and supply.

5.1.4 Outline

In our research, we have coupled established models for the energy demand of buildings, electricity demand and heat production from plant factories, energy

production from RES and advanced energy systems. This approach provides insight into each component of the energy balance. A total of 27 scenarios (nine scenarios for three disparate climate zones) have been worked out and analysed for primary energy use and energy imbalance.

5.2 Theoretical background

The following overview of potential challenges and solutions for sustainable energy systems contains the starting points for the selection of technologies, key variables and boundary conditions for our methods.

5.2.1 Challenges to the future urban energy system

The urban energy system can be (re)designed to be more effective, using the *New Stepped Strategy* [35, 36]. First, the initial energy demand should be *reduced* by intelligent design. Then remaining energy fluxes should be *reused* for other purposes. Only when this is no longer possible, the remaining energy demand should be *produced* using renewable sources. Applied to the energy demand of cities, this strategy generally entails:

- Increase in efficiency of building energy use and installations (reduce);
- Efficient redistribution of residual energy (reuse); and
- Renewable energy sources for energy production (produce).

The question is whether plant factories can perform an integral role in this future energy system balancing the production of surplus electricity with the demand for heat over time. The viability of this approach depends on several factors: how extensive integration of intermittent renewable energy affects the network; the actual imbalance in energy generation and demand; the efficient distribution of energy in an urban system; the ability to reuse heat from low-temperature sources; and finally, the energy required to operate existing, renovated and new buildings. The following sections expand on these factors and their interrelations.

5.2.2 Intermittent renewable energy supply

The integration of renewable energy sources (RES), such as wind power and solar energy, poses challenges for the energy system. It may result in electricity production, exceeding demand in a given area [9]. The storage of this surplus is generally associated with high costs and low efficiencies. Solving the imbalance between energy supply and demand at the individual building level is not economically feasible when compared to the aggregate level [37]. Firstly, fluctuations in energy demand of individual buildings with different urban functions are already levelled out at the aggregate urban level. Secondly, economies of scale tend to favour investing in and operating larger (storage/production) facilities versus numerous smaller ones. Thirdly, the energy imbalance spans various time frames, from sub-hourly to seasonal [3].

Network flexibility has to increase in order to balance the demand and supply of energy [8, 9, 19, 38, 39]. Matching the supply of electricity to the energy demand is a fundamental requirement for maintaining the adequate, efficient, secure and reliable operation of the total power system. Intermittent RES introduce additional variability and uncertainty that will ultimately require an overhaul of the conversion and storage of electricity. In a power system run on 100% RES, any demand not directly supplied by intermittent RES must be provided by one of the dispatchable RES generation technologies (hydro, bioelectricity, et cetera), or come from electrical or thermal storage [39]. The nature and availability of this flexible generation and storage naturally play a crucial role in the associated cost (e.g. locations with insufficient elevation differences for hydro storage) [40]. The integration of these technologies makes it necessary to investigate the most suitable and future-proof energy networks.

5.2.3 District heating networks

District heating (DH) is an established system with potential for integrating energy generation and demand at the urban scale. Large DH networks enable centralised solutions for the integration of renewable energy that would otherwise not be feasible for individual buildings [41, 42]. Research has shown that a substantial reduction in fuel demand, carbon emissions and costs can be achieved by converting to DH using non-fossil energy sources [20, 26, 43]. The use of DH was found to be beneficial for existing energy systems as well as future scenarios aiming at 100% renewable energy supply and 75% reduction in heating demand [20]. Current

research focuses on climate system design, low-temperature solutions, utilisation of new heat sources, energy storage, power-to-heat concepts and network efficiency.

A key aspect of DH networks is their temperature range. Current DH networks operate around 75–120°C, depending on the exterior air temperature [20]. There is a gradual shift towards low-temperature district heating (LTDH) networks, because low temperatures reduce transportation losses and improve prospects for heat storage [23]. LTDH networks typically rely on a supply of approximately 25–45°C. Lower temperatures enhance the efficiency of residual heat sources and of heat pumps, which facilitates their implementation [24, 41, 43–46]. Heat losses can be further reduced by optimising pipe insulation, dimensions, design and routing [23, 42, 43, 47].

The financial feasibility of these networks depends on economies of scale. Expanding the infrastructure will spread capital cost investments and risk [28, 42] and will decrease sensitivity to variations in temperature or distance [23]. The costs are to be offset by substantially lower costs for heat production and lower grid losses [43].

5.2.4 Energy storage

Extensive storage of thermal and electrical energy can reduce the imbalance between demand and generation by intermittent RES. The selection of a thermal energy storage (TES) system is typically based on temperature operative range, storage duration and field of application. TES systems can be classified as sensible (temperature only), latent (phase change) and thermochemical (endo-/exothermic chemical reaction) heat storage. Examples include storage in thermally stratified tanks, aquifers, boreholes and rock caverns (sensible), an array of phase change materials (latent) and several reversible thermochemical reactions, mainly using metal oxides/metals (thermochemical). The applicability of these technologies for long-term thermal storage has been reviewed by several authors [22, 48, 49]. They state that latent and thermochemical storage are able to achieve far higher energy storage densities than sensible storage and are less sensitive to heat loss, which would reduce the required storage volume and increase efficiency and duration. However, the two technologies are still in the early stages of material investigation and have not yet been applied on a larger scale. In contrast, the combination of intermittent RES and thermal storage, including seasonal storage, has already been shown to offer perspectives for the total energy system [43, 50].

The selection of an electrical energy storage (EES) system is based on storage duration, response time, storage efficiency, power-related costs and storage-related costs. Examples include batteries, flow batteries, compressed air energy storage, pumped hydro, electrolysis combined with fuel cells, and electric vehicles used as a distributed energy storage. The applicability of these systems has been investigated from a technical and economic standpoint (e.g. [51–53]), as well as from the standpoint of energy systems (e.g. [38, 54]). Long-term (several days to seasonal) storage is only possible using compressed air, pumped hydro or electrolysis combined with hydrogen storage [38]. The round-trip efficiencies of long-term EES technologies would make them less fuel- and cost-effective than other technologies [4]. As long-term EES technologies have not been implemented on a large scale and have geographic limitations, an interesting alternative may be to convert electricity to heat. The storage of thermal energy is a more mature technology and has been applied on a larger scale. This approach also coincides with the energy demand of cities, which is often dominated by space heating and domestic hot water (DHW) (e.g. ~64% in New York City [55, 56]).

Another approach for dealing with surplus production would be the export and import of electricity, effectively using surrounding countries as a buffer. However, the cost of avoiding critical surplus production by investing in grid flexibility (e.g. by means of heat pumps, heat storages and the regulation of combined heat and power (CHP) plants) is much lower than investing in high-voltage transmission lines for the export of electricity [9].

In short, it will most likely be necessary to store energy in media (batteries, hydropower, etc.), as the conversion to other fuels is rather inefficient. The conversion of electricity to heat and its subsequent storage/distribution is of interest due to its practicality and feasibility.

5.2.5 Residual heat and heat pumps

Residual heat⁷ in a DH network can replace peak load production, minimise fossil fuel use and related CO₂ emissions and potentially replace the need for investing in new heat production capacity. The challenges of using residual heat in space and water heating include greater system complexity, resilience of the system to minimise

⁷ Residual heat refers to energy that is generated in (industrial) processes without being put to practical use. Typically, this energy is wasted and released into the environment.

any downtime, possible maintenance and security issues, as well as adequate temperature management. Feasibility is greater in regions with a higher population density, where buildings have high heat demands [57]. Furthermore, the connection between the production and utilisation of waste heat should be as short as possible. That could make the integration of residual heat sources more feasible than alternate heating strategies, such as local fuel boilers [8, 23, 58].

Heat pumps can be integrated into the LTDH to increase temperatures as central or individual heat supply [41]. They can also be integrated as heat boosters for residual heat [59] or DH grid temperatures [24, 47, 60, 61]. Finally, individual heat pumps can supply heat directly to dwellings. Individual heat pumps provide an adequate alternative to DH for short-term renewable energy scenarios, as their fuel efficiency, CO₂ emissions and costs are similar [20, 62]. In a 100% RES system, fuel efficiency is high and the cost of individual heat pumps is comparative to district heating. For long-term scenarios, however, their relative cost is closely (and inversely) related to the distance to district heating grids. This distance factor limits their cost-efficiency in cities with high densities and existing DH networks.

5.2.6 Data centres and plant factories as sources of residual heat

Heat recovery should be seen as an energy-effectiveness measure, even though it is often categorised as a renewable energy source. In general, low-temperature heat sources are widely available. The main technologies for the reuse of this waste heat include domestic space and water heating, district heating, absorption cooling, direct power generation (piezoelectric and thermoelectric), biomass co-location and desalination. Heat sources for DH range from industry and data centres [29, 58, 59, 63] to transport [64], power generation [8, 57] and waste incineration [65].

The potential of plant factories is illustrated here by data centres (DCs), as they too have a high internal heat load while providing a broader body of knowledge (e.g. [57, 66-69]). The reuse of residual heat is governed by its temperature and its quantity. Firstly, the temperature of captured heat is influenced by the facility's cooling method. Heat at higher temperature (50-70°C) can be captured from liquid-cooled data centres, which may be used for the preheating of power plant water (60-100°C), absorption cooling (70-90°C), electricity production via organic Rankine cycles (32-65°C), biofuel production via drying/burning plant materials to produce steam or anaerobic digestion to produce biogas (>60°C). Lower temperature heat (25-45°C) is captured from air-cooled data centres and is limited to space heating and DHW production [63].

Secondly, the quantity of available residual heat is determined by the internal heat load of the facility. DCs are often listed as requiring 1000 W m^{-2} of power, but Mitchell-Jackson et al. [70] found that they actually feature a computer power density of 169 W m^{-2} ($\sim 50\%$ of the total energy use) and HVAC load of 134 W m^{-2} ($\sim 38\%$). Plant factories feature a higher HVAC load at regular production densities, at approximately 430 W m^{-2} and 890 W m^{-2} at light levels of 250 and $500 \mu\text{mol m}^{-2} \text{ s}^{-1}$, respectively [18]. Since a significant component in plant factories is latent energy, direct liquid cooling is not possible. An advantage, however, is that plant factories allow for a more flexible operation, whereas data centres are required to operate without any interruptions [25, 71].

5.2.7 Energy demand of buildings

Buildings account for a substantial part of the national energy demand. Their energy use typically consists of four main components: plug electricity and lighting, DHW supply, space heating and space cooling. The development of sustainable buildings plays an important role in minimising this energy use, particularly for heating and cooling. The energy efficiency and carbon footprint of the total urban system can be improved by integrating buildings into the local energy system [21, 43]. In this case, it is necessary for the climate systems and the network to be designed specifically for low distribution temperatures [29, 44, 45, 72].

Improvements in insulation and airtightness allow for new buildings to be heated using lower temperatures ($25\text{--}40^\circ\text{C}$), often via underfloor heating systems or electric heating. Underfloor heating will remain rather inefficient with respect to COP [20] and exergy, and CO_2 benefits depend on local energy supply. DHW, on the other hand, requires more attention to be incorporated with LTDH, due to its higher temperature demands. The DHW system's energy efficiency is mainly influenced by DH supply and return temperature, heat losses from heat exchanger, storage tank and pipes, and thermal bypass setpoint. Comfort and hygienic DHW temperatures can be achieved with LTDH [43, 45, 73, 74] but may occasionally require a temperature boost.

5.2.8 Summary

In short, whether plant factories can perform an integral role in future energy systems will depend on a number of technological factors. Increased shares of intermittent RES will require an adaptation of the technical and building

infrastructure to reduce the energy imbalance. LTDH networks can minimise network losses, limit the use of high exergy fuels for pure heat generation and allow for the redistribution of excess heat, all improving the efficiency and effectiveness of the total energy system [75]. The demand side should be designed/renovated for low-temperature heating [29, 45] and the connection between heat production and utilisation should be as short as possible [58]. Several functions could serve as a source of residual heat for DH production, but plant factories have the additional benefit of flexible operation and of food production. Finally, energy storage is required to reduce the imbalance in the demand for energy and the generation by intermittent RES. Thermal energy storage offers a practical strategy considering the efficiency and capacity of electricity storage and fuel conversion.

5.3 Materials and methods

The urban energy balance was analysed for multiple scenarios in three different locations: the north of Sweden (SWE), the Netherlands (NLD) and the United Arab Emirates (UAE). Several of the scenarios incorporate plant factories. Firstly, the design of a synthetic city is formulated to enable comparison between locations. Secondly, the fresh food demand of this city is calculated. This demand is linked to the plant factory area, electricity demand and heat production. Thirdly, the model for calculating the energy demand of the synthetic city is described. Fourthly, the calculation of the energy production and storage from various RES is discussed. Fifthly, the simulation scenarios combining the energy demand, food demand and energy production are listed. Finally, the calculation of these scenarios in the total energy system using EnergyPLAN is outlined. The outcome indicators are the annual energy demand, as well as the required energy import and export.

5.3.1 Urban design

A synthetic, high-density, mixed-use metropolitan area (hereafter SynCity) was modelled to ensure a fair comparison between disparate climates. SynCity features a fixed number of inhabitants and distribution of floor area per building function (Table 1), amounts based on data gathered from New York City (NYC). Information on the NYC building stock is stored in a geo-rectified database, named PLUTO,

which is maintained and updated annually by the Department of City Planning [76]. The building floor area for each tax lot in PLUTO is placed into building categories and each lot is given a building class code to describe the main use. These class designations and the floor area categories were used to allocate floor area, following Howard et al. [77]. The total floor area, number of units, number of floors and building measurements per function were used to approximate representative building dimensions, weighted for floor area. The total building area is calculated as the sum of all building footprints and is $1.42 \cdot 10^8 \text{ m}^2$. The total number of inhabitants is 8,550,971 [78].

TABLE 5.1 Building characteristics per building function from PLUTO 2019 v1 [76]. The calculated averages are weighted for the floor area of each building.

	PLUTO 2019 v1			Calculated average (weighted for floor area)			
	Total floor area	Share	Units	Unit area	Building floors	Building length	Building width
	(m ²)	(%)	(n)	(m ² n ⁻¹)	(n)	(m)	(m)
Residential S (1-2 families)	93,867,288	21	854,569	110	2.2	6.9	13.0
Residential M (3-6 families)	37,980,871	8	493,815	77	3.0	8.5	18.1
Residential L (>6 families)	191,144,656	42	2,211,964	86	12.4	38.0	35.6
Office	48,254,411	11	228,282	211	26.1	44.0	55.8
Retail	22,262,320	5	250,307	89	7.3	35.9	41.2
Education	21,260,027	5	5,944	3,577	4.9	64.9	57.8
Warehouses & industry	17,338,315	4	27,965	620	2.6	54.2	63.2
Health	9,864,202	2	12,631	781	8.3	45.3	46.9
Other	12,446,674	2	38,357	324	4.1	33.0	41.1

5.3.2 Urban food demand and plant factories

Food demand

The total amount of production area directly influences the balancing capacity of the plant factories. However, this area greatly depends on the local diet and the efficiency of production. For this study, we took into account the most recent dietary

guidelines for a “healthy eating pattern” published by the USDA [79]. The guidelines recommend a daily intake of approximately 400 g of assorted vegetables and 320 g of fruit. The required production area for each category of vegetables was calculated using crop production data from closed systems, as was investigated by NASA [80]. The production area to meet the fruit and vegetable demand is calculated as approximately 8.2 m² per inhabitant of SynCity, or 7.01·10⁷ m² in total.

Plant factories electricity demand and heat production

To calculate the amount of heat produced and electricity required by plant factories, it is necessary to determine the crop energy balance. This is the main internal heat load and it was calculated according to the method and assumptions described by [81]. The crop behaviour was then integrated into the building energy model following the method and assumptions described by [18], in which the various energetic fluxes are set as process gains in DesignBuilder.

Another important internal heat load is the inefficiency of the LED lighting system, which produces sensible heat. Taking into account a system that produces an intensity of 500 μmol m⁻² s⁻¹ with an efficiency of 3.00 μmol J⁻¹ and a red:blue distribution of 80:20, the LED inefficiency (sensible heat) can be calculated as 44.2% of the electricity input (in W), or 73.6 W per m² production layer. During photoperiods (“ON”), the simulated plant factory features a lighting intensity of 500 μmol m⁻² s⁻¹, which translates to 89.8 W m⁻² of latent heat and 4.6 W m⁻² of sensible heat per crop layer. During dark periods (“OFF”), the crop transpiration results in approximately 14.0 W m⁻² of latent heat and -14.0 W m⁻² of sensible heat per crop layer. Cooling of the nutrient solution requires an additional 7.9 W m⁻². The residual heat produced when “OFF” is set as industrial waste heat and the energy use as additional electricity use in EnergyPLAN. Residual heat production and electricity when “ON” are set as an heat pump with specific thermal capacity and COP.

5.3.3 Urban energy demand

Model selection

Representative building sections containing a number of standardised units were modelled in DesignBuilder for each building function (Table C1–C2). The energy loads and demands were calculated by means of EnergyPlus [82] using

DesignBuilder [83]. EnergyPlus is a dynamic building energy simulation program that consists of three basic components – a simulation manager, a heat and mass balance simulation module and a building systems simulation module [84]. The model has been formally and independently tested during its development [85] and has been extensively validated since. Examples of validation are listed in [31]. It should be realised, however, that “all building models are simplifications of reality” [86]. DesignBuilder was used to generate input and visualise output, as it is considered the most complete graphic user interface for EnergyPlus.

The energy demand was analysed for three representative locations of disparate latitudes and climates, namely Kiruna in Sweden (67.8° N, 20.2° E; subarctic climate; SWE), Amsterdam in the Netherlands (52.0° N, 5.7° E; temperate oceanic climate; NLD) and Abu Dhabi in the United Arab Emirates (24.5° N, 54.7° E; hot desert climate; UAE). The climate in EnergyPlus for the selected locations is based on typical meteorological years in order to guarantee a close representation of typical weather patterns [87]. The hourly weather information for the simulations was retrieved from the EnergyPlus database [88-90], which was selected for its extensiveness and precision.

Energy demand per building function (hourly)

The model is set up using reported values for the distribution of energy use [55] and the total energy use [56] per building function in NYC. Reported data on domestic hot water (DHW), lighting and plug electricity are used, whereas heating and cooling demands follow occupation and local climate. The hourly profiles for occupation, DHW, lighting and plug electricity for each building function are based on ASHRAE standards. In reality, human behaviour can lead to significant variation in the (timing of) heating demand and peak demands, creating a smoother aggregate profile [42]. However, these considerations are beyond the scope of this study. The occupation profiles and the energy demand for DHW, lighting and plug electricity are assumed to be the same for the three locations, to facilitate comparison. Climate systems were adapted to their respective climate via economisers. The incremental energetic improvements of the building stock until 2050 are simulated by applying current building standards to all buildings. The detailed settings are listed in Tables C1-C2. The calculated energy demand for space heating (E_{heat}), DHW (E_{DHW}), space cooling (E_{cool}), plug electricity (E_{elec}) and lighting (E_{light}) were used as input data in the energy system.

5.3.4 Energy production and storage

Additional attention is given to variability in the distribution of variable RES as to not overestimate their capacity. This is a common oversimplification in modelling tools for energy systems with large shares of variable RES [91]. The RES production is calculated by electricity from wind power using wind speed, and by heat and electricity from solar power using solar radiation. The resulting hourly power distributions were used as input data for calculating the energy balance in EnergyPLAN (Section 5.3.6). The annual energy generation is set as equal to the annual energy demand, in order to assess the imbalance with respect to timing and to facilitate comparison.

Wind energy

Wind power generation of a wind farm largely depends on wind speed distribution and on the installed capacity [40]. Firstly, the stochastic wind speed distribution is calculated using a Markov chain model to accurately incorporate the variability of wind and to extend the applicability of this study. This model is used to generate synthetic climate state time series, different from the observational data, but with the same statistical properties. Secondly, the power generation is calculated as a function of flow speed, taking into account a cut-in speed, exponential segment, rated speed and a cut-out speed. Finally, the installed capacity of the wind farms (P_{wind}) was calculated using the total annual energy demand, the number of hours at capacity ($t_{wind,full}$), a safety factor (c_{safe}) and the installed capacity of the other RES, photovoltaic (P_{pv}) and wave energy (P_{wave}). The c_s is set at 1.0.

$$P_{wind} = \frac{E_{heat} + E_{DHW} + E_{cool} + E_{elec} + E_{light}}{t_{wind,full}} \cdot c_{safe} - P_{pv} - P_{wave} \quad [5.1]$$

Net generation from a wind farm would normally also include highly specific losses that vary greatly from one wind farm/period to another, such as maintenance [3]. However, these considerations are beyond the scope of this study. The methodology is described in greater detail in Appendix 5B.

Solar energy

Solar power generation of a photovoltaic array largely depends on solar energy distribution, photovoltaic efficiency and the installed capacity. The distribution

of solar energy throughout the year is notably less stochastic than that of wind. Therefore, the distribution in solar energy is based on typical meteorological years, in order to guarantee a close representation of typical annual weather patterns [87]. The installed capacity of the photovoltaic arrays was calculated using the available share of roof space (c_{roof}), total roof surface area (A_{roof}), efficiency of the array (c_{pv}) and the maximum solar radiation ($I_{sol,max}$).

$$P_{pv} = c_{roof} \cdot A_{roof} \cdot c_{pv} \cdot I_{sol,max} \quad [5.2]$$

The A_{roof} of SynCity was calculated as $1.42 \cdot 10^8 \text{ m}^2$ (see Section 5.3.1), c_{roof} was set at 0.2 and c_{pv} was set at 0.15 [92].

Other technologies

The installed capacity of the other energy production technologies (P_x) was calculated using the calculated energy production (E_x) and the full-capacity-equivalent hours achieved ($t_{x,full}$) of the respective technologies.

$$P_x = \frac{E_x}{t_{x,full}} \quad [5.3]$$

Storage of thermal energy

The amount of available storage of thermal energy ($E_{th,st}$) is assumed to be a fixed share (c_{st}) of the total annual heat demand ($E_{heat} + E_{DHW}$). The c_{st} is set at 0.15 for all scenarios containing thermal storage.

$$E_{th,st} = (E_{heat} + E_{DHW}) \cdot c_{st} \quad [5.4]$$

5.3.5 Simulation scenarios

The urban energy balance was analysed for multiple scenarios in each location. Several of these scenarios incorporate plant factories. Each scenario investigates the effectiveness of the energy system to supply the calculated energy demand. The distribution of energy production, heating technologies and the operation and area of plant factories are varied.

Four scenarios serve as baseline scenarios (B1-B4) and five incorporate food production (F1-F5). Each one was analysed for the three locations of disparate latitudes and climates, namely Sweden (SWE), the Netherlands (NLD) and the United Arab Emirates (UAE). For each scenario several assumptions were made regarding the energy demand and production units.

Two baseline scenarios are formulated to illustrate the energy imbalance by exclusively incorporating intermittent RES without any form of energy storage (B1-B2), the latter scenario with limited supply. The primary RES is wind-powered generation, as it has proven to be the most economical alternative [93]. Scenarios F1-F3 incorporate food production and thermal energy storage into scenario B1. In scenario F1 plant factory area is scaled to ensure adequate food production (Section 5.3.2) and operation follows a fixed schedule, without flexibility. A flexible operation to increase potential synergy is introduced in scenarios F2 and F3. In the latter, production area is upscaled to cover the peak heat demand of SynCity, resulting in surplus food production. The flexible operation follows direct heating demand from SynCity or thermal storage.

The other two baseline scenarios use a more realistic, diverse energy production distribution (B3-B4). For B3 the distribution of CEESA 2050 [94] was selected as representative of best practice, as it incorporates advanced renewable technologies and optimises its climatological impact based on LCA studies [95]. For scenario B4 the use of biomass was reduced from the original CEESA 2050 because its availability may be limited and it is considered dispensable for cost-effective DH systems [27]. To this end, CHP using biomass are replaced with electric heat pumps. The original distribution of RES for electricity is maintained and production is maximised to replace the biomass requirement. Industrial waste heat and thermal storage are not included [94]. Scenarios F4 and F5 incorporate food production and thermal energy storage into scenarios B3 and B4, respectively. The scenarios are listed below and their model input is listed in Tables D1-D2.

B1. Baseline

Base scenario to determine surplus production and import in a system using 100% intermittent RES based on solar and wind. Their production capacities are calculated using Equations 5.1 and 5.2. Thermal storage is excluded.

B2. Variable baseline

Scenario B1 with variable production. In practice, critical surplus electricity production is controlled by lowering production, i.e. shutting down wind turbines [5]. This variable base scenario illustrates the full-capacity-equivalent hours achieved in this strategy. Thermal storage is excluded.

B3. CEESA 2050

This base scenario follows the diverse energy production of the 100% renewable energy scenario in CEESA 2050 [94]. The energy generation and processing follow CEESA 2050 and are scaled for the energy demand. Thermal storage is excluded [94].

B4. CEESA 2050 (Wind)

Scenario B3 with maximised wind-powered generation and use of central heat pumps, replacing CHP. The shares of renewable energy production from wind, wave and photovoltaic power are increased to replace biomass. Thermal storage is excluded [94].

F1. Standard food production

Scenario B1 with the introduction of plant factories. The plant factory is dimensioned to cover the annual fruit and vegetable demand of the inhabitants of SynCity, resulting in $7.01 \cdot 10^7$ m² of production area (see Section 5.3.4). Operation is consistent and maintains production cycles of 16-hours photoperiod (“ON”) and 8-hours dark period (“OFF”) throughout the year. The ON period is counterphase to the diurnal cycle and runs from 18:00-10:00⁺¹. Thermal storage is included.

F2. Flexible food production

Scenario B1 with the introduction of plant factories. They feature $7.01 \cdot 10^7$ m² of production area. The operation of the plant factories is flexible: they are only operational when there is a surplus electricity production from intermittent renewable sources. Thermal storage is included.

F3. Food production for peak heat demand

Scenario B1 with the introduction of plant factories. The production area of the plant factory is scaled to cover the peak heat demand of SynCity, resulting in $9.54 \cdot 10^7$, $1.56 \cdot 10^8$ and $2.21 \cdot 10^8$ m² for UAE, NLD and SWE, respectively. The operation of the plant factories is flexible: they are only operational when there is a surplus electricity production from intermittent renewable sources. Thermal storage is included.

F4. Combination flexible food production with CEESA 2050

Scenario B3 with the introduction of plant factories. They feature $7.01 \cdot 10^7$ m² of production area. The operation of the plant factories is flexible: they are only operational when there is a surplus electricity production from intermittent renewable sources. Thermal storage is included.

F5. Combination flexible food production with CEESA 2050 (Wind)

Scenario B4 with the introduction of plant factories. They feature $7.01 \cdot 10^7 \text{ m}^2$ of production area. The operation of the plant factories is flexible: they are only operational when there is a surplus electricity production from intermittent renewable sources. Thermal storage is included.

The scenarios described above do not represent a comprehensive identification of the optimal solution of a full renewable energy system for each location. The scenarios serve as a framework for analysing the impact of food production and residual heat in future renewable energy systems. It is a technical, quantitative analysis, without taking account of any financial and/or logistic issues.

5.3.6 Urban energy system

The scenarios are calculated by means of EnergyPLAN [96]. This model is able to calculate the production and demand of renewable, thermal and electrical energy for domestic and industrial processes, as well as its conversion and storage in national and regional systems. The model is a deterministic input/output tool, in which inputs are energy demands, energy production (from RES), energy technology capacities, costs and a number of optional regulation strategies for import/export and excess electricity production [97]. Outputs are energy balances and resulting annual production, fuel consumption, import/export of electricity and total costs [97]. The accuracy and relevance of the input data is important [98]. The methodology presented above ensures accurate estimates for the key model inputs: the capacities of energy technologies and their hourly distribution. The full input data is detailed in Tables D1-D2.

EnergyPLAN was selected for its applicability in the integration of RES into the energy system as well as district heating. It has been used and validated in multiple studies with varying degrees of renewable energy [99]. Additional examples of validation are listed in [97]. The model is deemed particularly suitable for analysing radical changes in energy systems and RES with high intermittency [20]. The model provides a solid combination of accuracy and computational efficiency, as calculations use time-steps of 1 hour, but require little calculation time. Finally, it is freely available and user-friendly [97]. For a full, detailed description of the model, please consult [100].

5.4 Results and discussion: Energy production and demand

The following section discusses the urban energy demand per function (kWh per m² building floor area) and in total (TWh). In addition, it lists the calculated distribution of energy generated by RES. These values are input data for the urban energy balance and the model in EnergyPLAN.

5.4.1 Urban energy demand in present-day New York City

The annual distribution for the calculated and reported energy demand per building function in NYC is illustrated in Figure 5.1A. The calculated total annual energy use adequately matched reported values, with a deviation of 8.5%. The main discrepancy between the calculated and reported data stems from heating and cooling demand, where the calculated total annual energy use deviates by 17.5% from reported values. The extent of this deviation varies per building function and can likely be attributed to assumptions made in the model geometry, as well as to differences between the simulated and actual weather patterns. Additionally, several factors listed in [55] may have played a role, such as potential inaccuracies in the (reporting of) meter values, the COP of climate systems, the airtightness of the building façade, fuel sources and installed electric capacity.

The main differences between the source data and our calculations are an underestimation of heating requirement and an overestimation of cooling requirement for most functions. This is likely the result of the installed electric capacity, because the reported heating/cooling values can be matched by ignoring 80% of the internal heat load produced by the installed electric capacity. This discrepancy may be caused by inaccurate reporting of the installed electric capacity or of the cooling/ventilation energy required to process this internal heat load. The model was not calibrated further to match the reported values exactly, as this would have introduced a significant bias and would render results between different locations incomparable. Furthermore, the focus of the study lies on the integration of plant factories into urban energy systems and not on the exact calculation of urban energy demand.

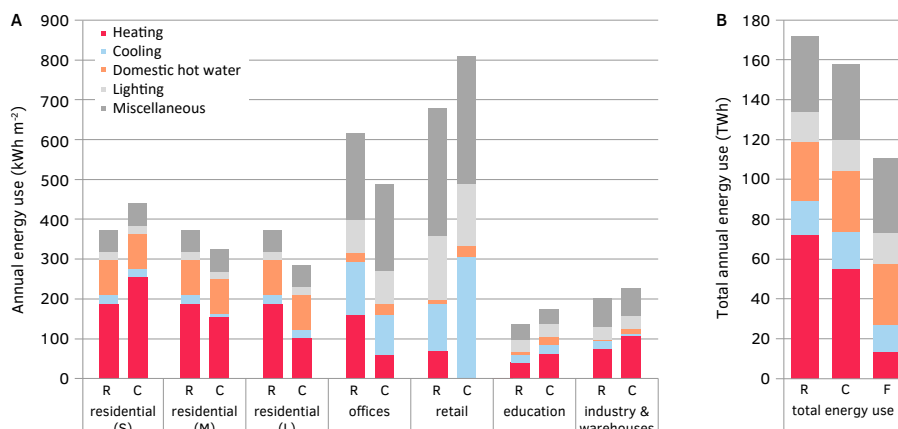


FIG. 5.1 Comparison between reported (R) and calculated (C) values for annual energy use per building function (A in kWh m⁻²) and total annual energy use (B in TWh) for New York City. The calculated total energy use after improvement of the building stock is also listed (F). Residential (S) and (M) and (L) denote buildings housing 1-2, 3-6 or more than 6 families, respectively (Table 5.1).

5.4.2 Future urban energy demand

In the SynCity model, the building stock was improved in comparison with present-day NYC to better represent future cities. Improving insulation and airtightness values to current building standards reduces heating demand and moderately increases cooling demand for most functions. In the case of NYC, heating and cooling demand was decreased by 63% and heating demand alone was decreased by 75% (Figure 5.1B). This reduction exceeds other suggested least-cost heating reduction strategies (~53% [101]) but is considered reasonable in light of the current age and characteristics of NYC's building stock [76].

The SynCity model was used to calculate the energy use for three locations, taking into account the aforementioned improvement of the building stock (Figure 5.2). The model provides a detailed overview of hourly and annual energy demand in subarctic SWE, NLD and UAE. Major variations in heating and cooling requirement arise following local climate, which result in a total annual energy demand of 122.8 (SWE), 96.8 (NLD) and 170.8 (UAE) TWh for SynCity. The combined share of DHW and space heating in the total energy demand is 56.9% for SWE, 42.1% for NLD and 18.1% for UAE.

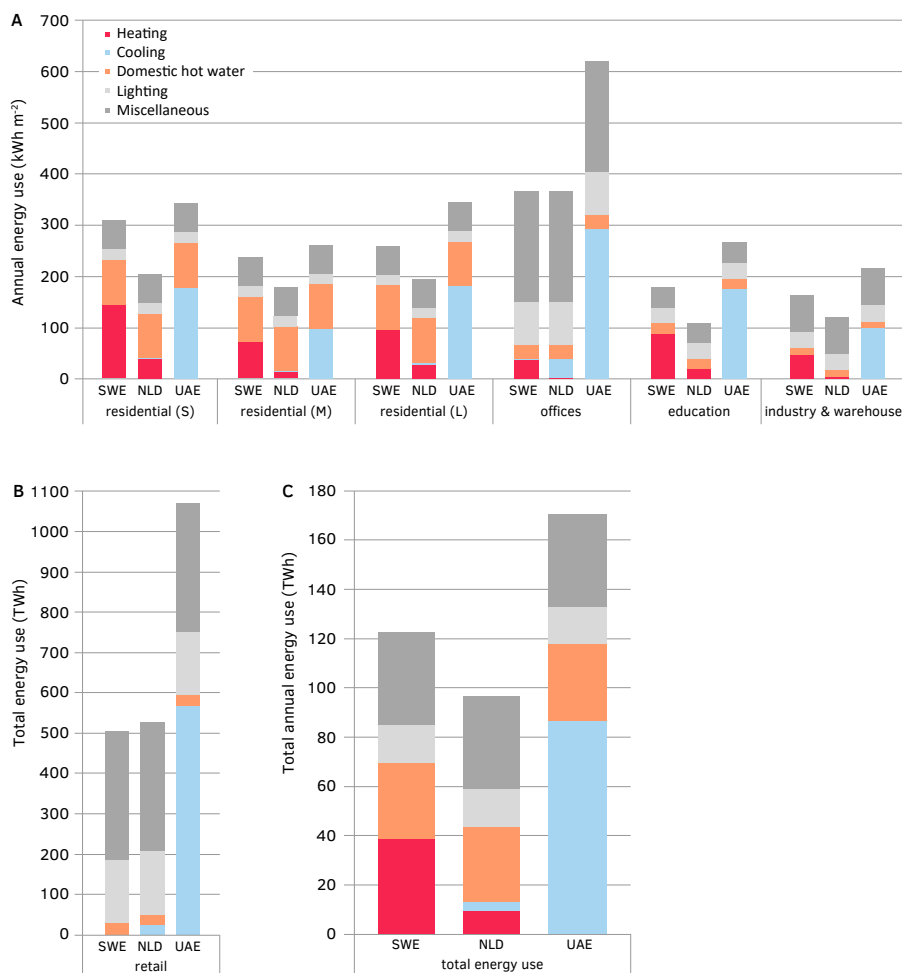


FIG. 5.2 Calculated annual energy consumption in SynCity. Energy consumption is presented per building function (A and B in kWh m⁻²) and total annual energy use (C in TWh) for Sweden (SWE), the Netherlands (NLD) and the United Arab Emirates (UAE). Please note the different yaxes for each graph.

The presented calculation method provides comparable, detailed, hourly energy demand profiles that serve as input for EnergyPLAN. The divergent energy demand profiles present different challenges in balancing the energy system. Furthermore, they allow for a more comprehensive investigation of integrating food production into the urban energy system.

Renewable energy sources

The presented calculation method provided a detailed overview of hourly distribution for wind power. The distribution of solar energy was based on typical meteorological years. The distribution of wave energy production was standardised in this study and was not extensively calculated for each location, due to its minute share in the total energy balance and a lack of observational data. The distribution series was used in EnergyPLAN to calculate energy generation per hour (Figure 5.3).

The Markov chain model was able to produce a synthetic, stochastic wind series. The calculation was performed for each month to adequately capture seasonal variations. The corresponding power generation was calculated and is illustrated in Figure 5.3. Unsurprisingly, the distribution in solar energy showed larger differences between seasons at higher latitudes. This impacted both solar thermal and photovoltaic generation.

Heat production from plant factories

The heat production and energy use from plant factories was calculated for both operation modes (ON/OFF) for all three locations. The resulting energy fluxes are listed in Table 5.2.

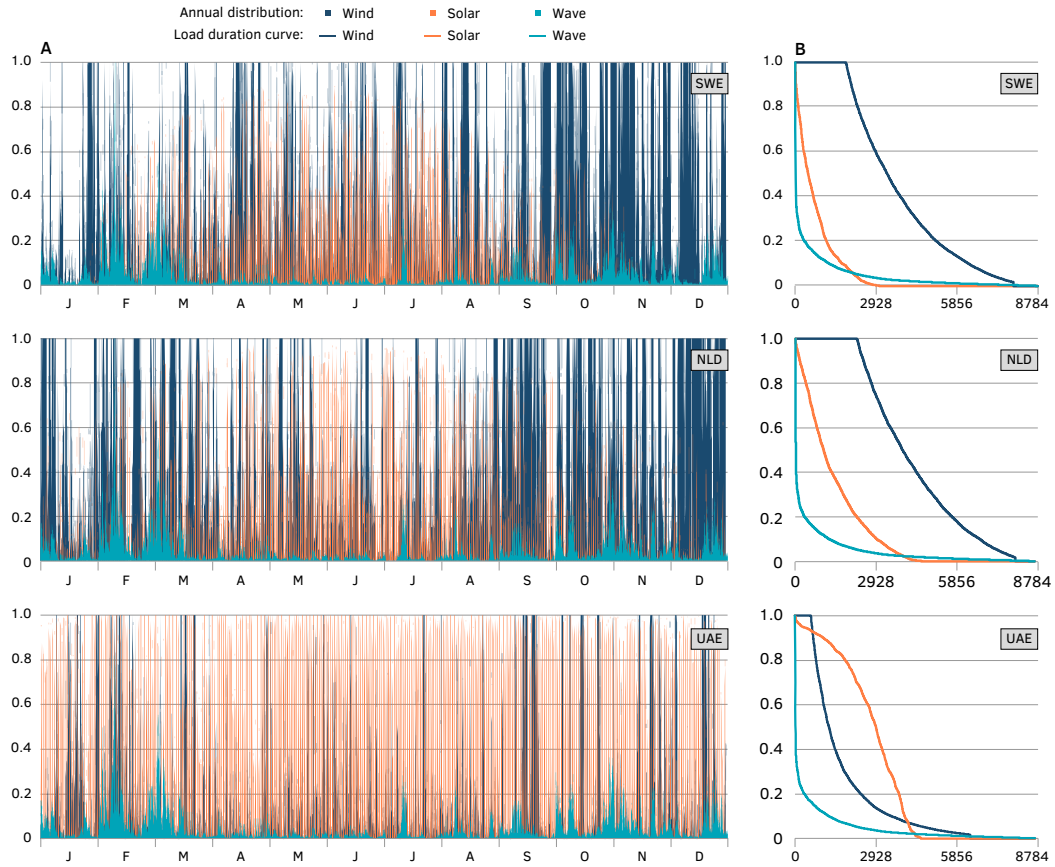


FIG. 5.3 Annual energy distribution (A) and load duration curve (B) for wind, solar and wave energy for subarctic Sweden (SWE), the Netherlands (NLD) and the United Arab Emirates (UAE). The annual energy distribution illustrates the share of total capacity realised per hour and is ordered chronologically. The load duration curve illustrates the capacity utilisation for each increment of the total energy generation and is shown in descending order of magnitude.

TABLE 5.2 Electricity use and residual heat production of plant factories in Sweden (SWE), the Netherlands (NLD) and the United Arab Emirates (UAE). Values are given per m² of production area (in W m⁻²) and for the total production area of 7.01·10⁷ m² (in MW).

	SWE		NLD		UAE	
	On	Off	On	Off	On	Off
Heat production (W m ⁻²)	177.6	21.9	177.7	21.9	178.1	21.9
Electricity use (W m ⁻²)	184.4	3.3	190.4	3.7	214.8	6.3
Heat production (MW)	12453.7	1535.1	12462.5	1538.9	12486.5	1538.7
Electricity use (MW)	12931.7	233.1	13348.0	257.3	15061.1	440.3

5.5 Results and discussion: Urban energy balance

The following section discusses the calculated urban energy balance, specified for primary energy supply (TWh) and energy imbalance (TWh). Primary energy supply was defined as the net energy use in the system (energy generated + import - export) (Figure 5.4). The energy imbalance was defined as the sum of export and import (Figure 5.5).

5.5.1 Baseline energy supply and imbalance

Nine scenarios were calculated for each of the three locations (Figures 5.4-5). The reference base scenarios (B1 and B2) provide a clear indication of the primary energy supply (Figure 5.4) and the energy imbalance over time (Figure 5.5A). This supply is 81.0, 72.4 and 152.4 TWh for SWE, NLD and UAE, respectively. The imbalance in electricity is highest in UAE at 190.2 TWh, medium in SWE at 88.9 TWh and lowest in NLD at 62.6 TWh. The most effective way to minimise this imbalance is to reduce production capacity during moments of excess production, as illustrated in B2. This strategy is not economic as it implies a large amount of downtime of expensive installations dimensioned for the peak demand.

From the outset it is evident that utilising residual heat from food production can reduce this imbalance (scenarios F2-F3), but results in a higher primary energy supply compared to the base scenarios. This largely results from the lower efficiencies for heat production in comparison with the heat pumps.

5.5.2 The effect of residual heat from plant factories

The effects of integrating plant factories on the annual energy supply and imbalance are illustrated in Figure 5.4 and the hourly imbalances are illustrated in Figure 5.5. In scenario F1 the operation and linked residual heat production are not flexible. Production is counterphase to urban electricity and heat demand in an attempt to level out the aggregate demand. However, the cyclic electricity demand and heat production still reduce flexibility and place additional pressure on the system in all

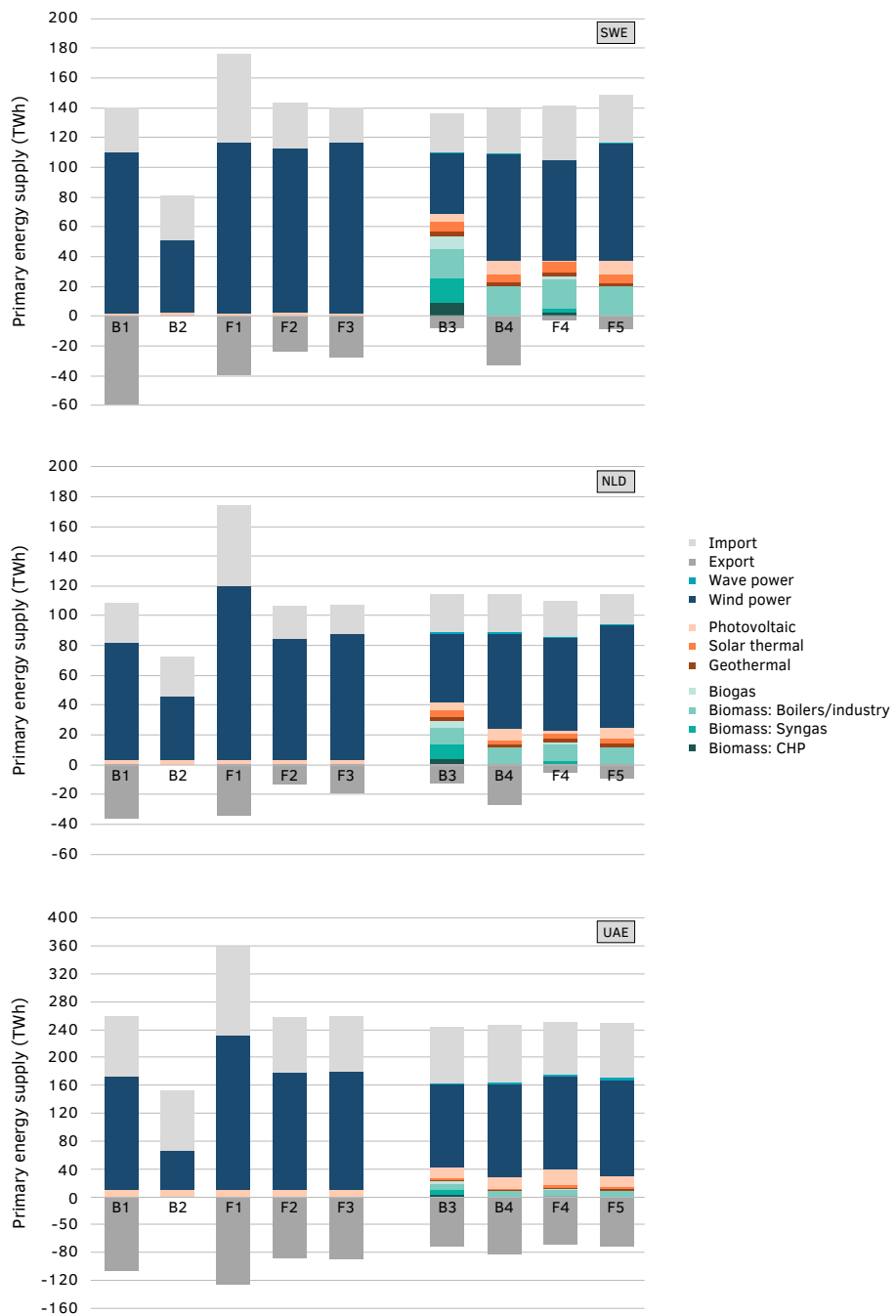


FIG. 5.4 Primary energy use for all scenarios in Sweden (SWE), the Netherlands (NLD) and the United Arab Emirates (UAE) in TWh.

locations, increasing both their energy supply and imbalance (Figure 5.4). The use of thermal storage is not sufficient to compensate for this effect. As a result, the required import is increased by 98.3% (SWE), 104.3% (NLD) and 51.3% (UAE), in comparison with B1.

The opposite effect is illustrated in scenarios F2 and F3, where the operation is flexible. There the energy balance shows a decrease in energy imbalance following the integration of flexible plant factories. Scenario F2 reduces imbalance with respect to B1 by 38.9% (SWE), 43.1% (NLD) and 11.8% (UAE). This comes at the expense of a higher primary energy supply, which is increased by 47.0% (SWE), 28.6% (NLD) and 11.0% (UAE). This increase is caused by the lower efficiency of utilising residual heat versus that of a central heat pump. Additionally, the flexible operation in F2 resulted in only 4477 (SWE), 2407 (NLD) and 1537 (UAE) full-capacity-equivalent hours of operation per year, which reduced food production.

The lower energy imbalance of F2 versus B1 is mainly caused by a decrease in export and, to a lesser extent, a decrease in import. Excess electricity production is shifted from export to heat production at a lower efficiency and may also be supplied to storage. In NLD-F2 and SWE-F2 this notably reduces imbalance over the year and leads to concentrated seasonal peaks (Figure 5.5A). In UAE-F2 only minor improvements can be found, due to the predominance of cooling in the total energy demand. Similar effects can be seen in scenario F3, where a larger share of the heating demand is covered by residual heat, either directly or via storage. Excess electricity production is used to generate heat for storage, reducing instances of import and increasing export during periods of low heat demand.

5.5.3 The effect of diversified energy distributions

Diversification of the energy distribution generally leads to a more balanced energy system. Implementing the diverse distribution of CEESA did indeed reduce the total imbalance, but it also increased the primary energy supply in comparison with scenario B1 (Figures 5-4 and 5-5, B3). Incorporating this distribution resulted in a primary energy supply of 128.7 (+58.8%), 101.7 (+40.5%) and 174.4 (+14.4%) TWh for SWE, NLD and UAE, respectively. The impacts of integrating CEESA followed the share of heating in the total energy demand and are therefore highly dependent on location. Biomass consumption also varied considerably between locations and follows CHP heat production. SWE consumed the largest relative and absolute amount of biomass, due to the large share of space heating in the total energy balance. While it has a relatively low efficiency, the constant availability of biomass

allowed for a close response to heating demand. This is clearly visible in the energy imbalance, which decreased by 61.5% (SWE), 40.6% (NLD) and 20.6% (UAE), in comparison with B1.

Minimising the use of biomass and increasing the share of intermittent RES in scenario B4 therefore increased the imbalance but reduced total primary energy supply. The energy imbalance increased slightly in UAE (+9.7%), but notably in NLD (+39.9%) and SWE (+84.1%), in comparison with B3 (Figure 5.4, B4). The combination of a high share of heating and the shift towards intermittent RES resulted in an increase of export throughout the year (Figure 5.5B, B4). Biomass consumption was reduced by approximately half (53.5-55.5%) for all locations.

5.5.4 **Combination of diversification and plant factories**

The combined effects of diversified energy distributions and plant factories were investigated in scenarios F4 and F5. Here the primary energy supply increased to approximately 139 (SWE), 105 (NLD) and 178 (UAE) TWh for scenarios F4 and F5. The greatest effects of utilising residual heat and thermal storage can be seen in systems with more intermittent RES, such as CEESA Wind. Here the imbalance was reduced by 35.2% from 62.9 to 40.7 TWh (SWE), by 43.4% from 52.0 to 29.4 TWh (NLD) and by 10.9% from 165.5 to 147.4 TWh (UAE), when comparing scenario B4 to F5. The only investigated scenario where energy imbalance actually increased is SWEF4. Here the imbalance was shifted to import in the early months, as the plant factory area was insufficient in meeting the high heating demand (Figure 5.5B).

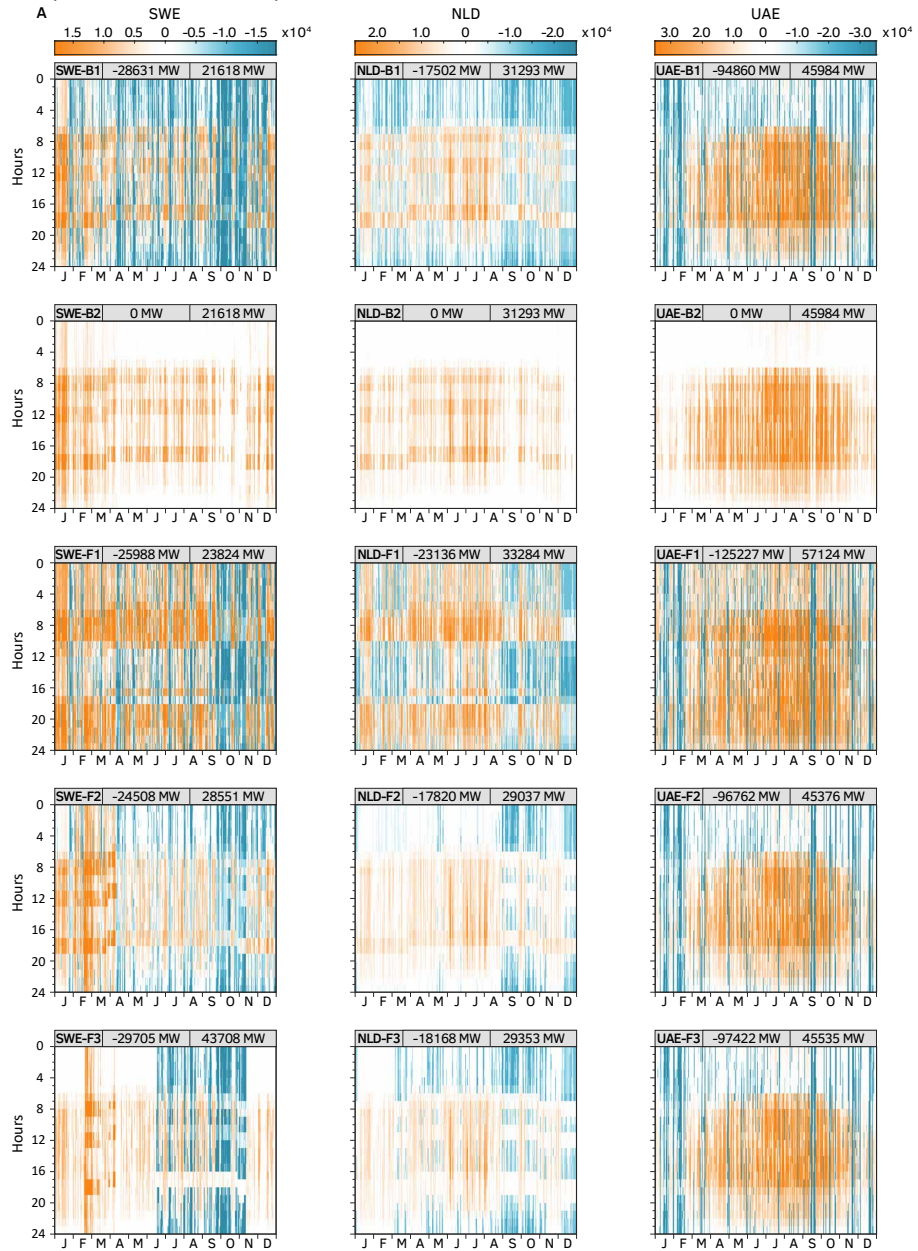
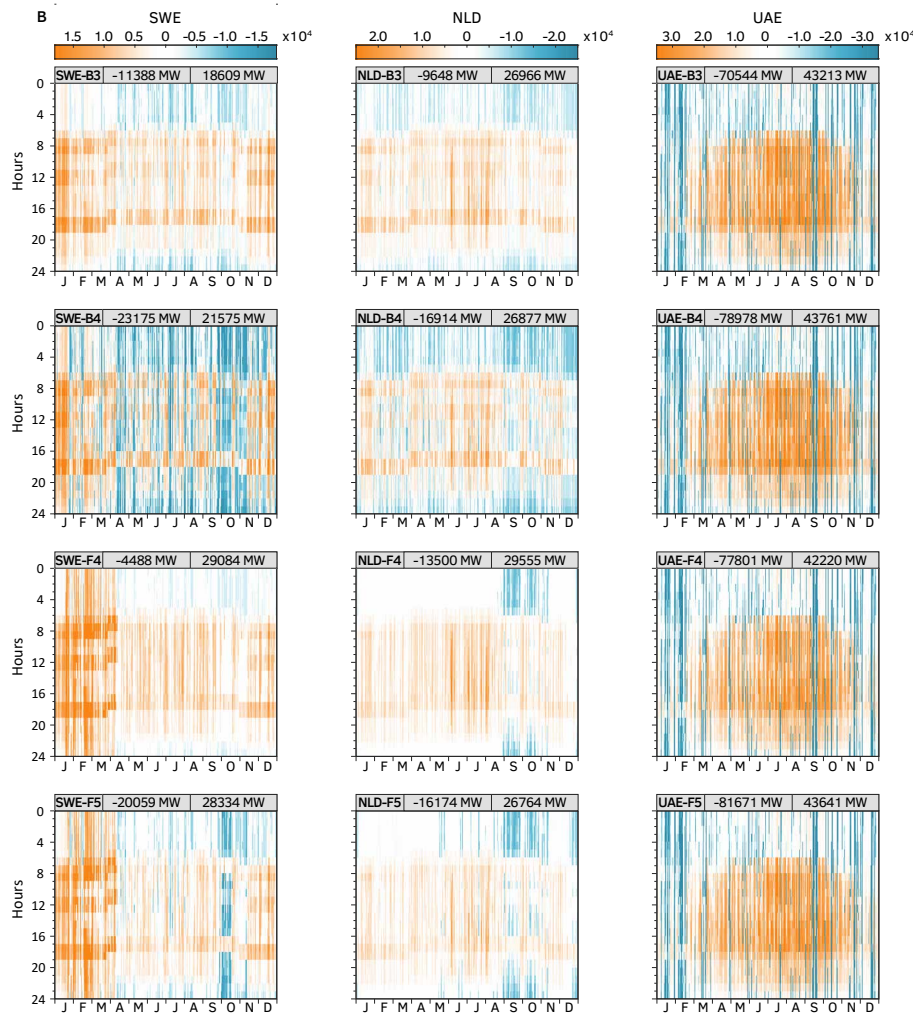


FIG. 5.5 Hourly distribution profile of the energy imbalance (in MW) in Sweden (SWE), the Netherlands (NLD) and the United Arab Emirates (UAE). Scenarios B1-B2 and F1-F3 exclusively use intermittent RES (A) and scenarios B3-B4 and F4-F5 feature a more diverse energy production distribution (B). Positive values (orange) represent import and negative values (blue) represent export.



5.5.5 Sensitivity analysis of key variables

The sensitivity analysis provides insight into the variations in total energy imbalance as a result of the variation in key variables (Figure 5.6). Scenario F2 was used as the baseline for comparison. The investigated variables are plant factory area (m^2), thermal storage capacity (GWh), generated wind energy (TWh) and LED efficiency ($\mu\text{mol J}^{-1}$). Total energy imbalance is generally found to be the most sensitive to the share of wind energy in the RES. The sensitivity of the investigated variables clearly varies per location.

The generated wind energy in the RES distribution shows the greatest sensitivity and is most notably influenced by location. The decrease in wind energy is supplemented by an increase in solar energy, which follows a more cyclic distribution. The annual distribution of solar energy determines the optimal distribution of both RES: the large difference between winter and summer generation in SWE favours a low share of solar energy, whereas the more even distribution in UAE favours a high share to reduce imbalance (see also Figure 5.3). Additionally, cooling demand follows a distribution similar to solar energy production throughout the year in UAE, whereas heating demand and solar energy production are antiphase in SWE.

The impact of total plant factory areas varies between locations and follows total heating demand. Lower plant factory areas lead to a smaller share of the immediate heating demand being covered and to a smaller production of excess heat for thermal storage. One might then presume that the optimal area exceeds the maximum hourly heating demand, in which case excess capacity is simply not used. However, the plant factory requires electricity even when switched “OFF”, which leads to a (minor) increase in energy supply and imbalance with an increase of area. This is visible at higher capacities in NLD and UAE, but not in SWE as the highest illustrated production area does not cover the maximum heat demand.

The impact of thermal storage capacity primarily follows the annual distribution of heating demand. When heating demand is lower or more evenly distributed throughout the year, such as in UAE and to a certain extent NLD, the thermal storage capacity is used to bridge smaller time steps between generation and demand. In these situations, a smaller thermal storage can suffice and will not be depleted at any moment throughout the year. In SWE the plant factory heat production is insufficient to reach this balance, which explains the curve tapering off at higher storage capacities.

The impact of LED efficiency is closely related to the total heating capacity of the plant factories. Increasing LED efficiency directly decreases the energy demand

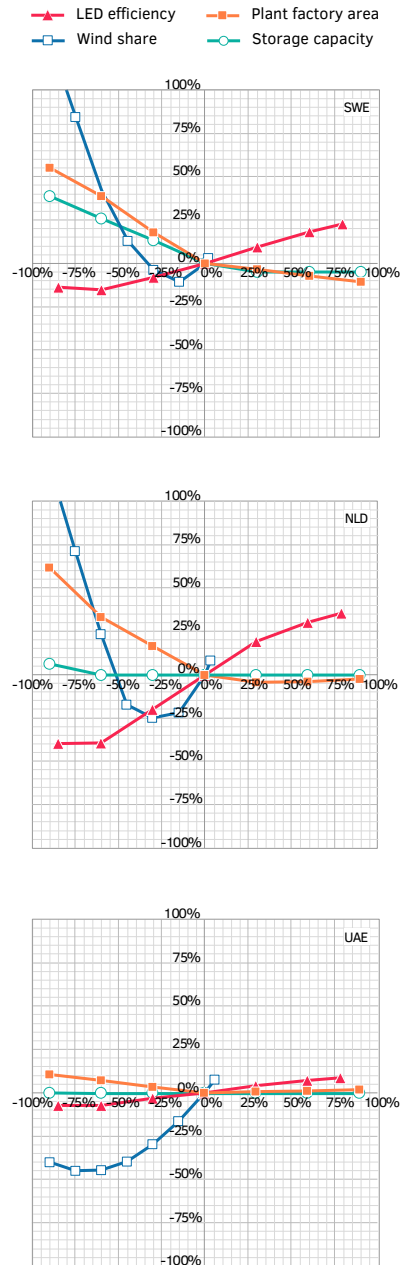


FIG. 5.6 Sensitivity analysis illustrating the relative change in energy imbalance (y-axis) as a result of relative change in LED efficiency, plant factory area, share of wind in RES production and thermal storage capacity. The base values for these parameters match Scenario F2 (Table 5C.1). The locations are Sweden (SWE), the Netherlands (NLD) and the United Arab Emirates (UAE).

for illumination and indirectly the residual heat production capacity. At higher LED efficiencies residual heat production is decreased and DH production is shifted to heat pumps, lowering total energy demand and consequently increasing export. At lower LED efficiencies, this increase in residual heat capacity cannot always be utilised. When combined with minor changes in plant factory efficiency, this leads to levelled or even slightly increased energy imbalance compared to higher LED efficiencies. The sensitivity in SWE is reduced due to a simultaneous increase in export and decrease in import as LED efficiency increases; this is caused by insufficient thermal storage and consequent reliance on heat pumps.

In short, the sensitivity analysis illustrates that most trends show similar patterns for each location. However, the slope and optimum of each variable are closely related to the external climate and warrant future optimisation studies. Key results of the analysis for the energy imbalance are listed below.

- 1 Increasing plant factory production area over a certain limit offers no benefits with respect to energy imbalance. An increase beyond assumed values yields little to no benefit.
- 2 The integration of plant factories presents little value in locations dominated by cooling demands.
- 3 An increase in thermal storage capacity beyond assumed values gives little to no benefit. With the exception of SWE, thermal storage capacity may even be decreased.
- 4 The current trend toward increasing LED efficiency diminishes the future value of plant factories in balancing the energy network.
- 5 The optimal distribution of solar and wind energy in the distribution of RES can be identified, but it greatly depends on local climate, annual distribution of solar energy and annual energy demand profiles.

5.5.6 Comparison of results and alternative strategies

The integration of residual heat from plant factories and thermal storage offers the best perspective for reducing the energy imbalance. The introduction of flexible heat generation in plant factories would improve the imbalance for almost every situation, particularly at higher shares of heating and intermittent RES. The combination of a diverse RES distribution and plant factories results in the lowest energy imbalances

for each location (F4), except for SWE. The RES distribution and plant factory area can be optimised to further reduce the imbalance for each location.

The integration of central heat pumps and thermal storage can provide an alternative strategy [6] to that of residual heat and thermal storage (Table D3). The higher efficiencies of heat pumps would reduce primary energy supply to 80.9 (SWE), 71.3 (NLD) and 151.6 (UAE) TWh, which are the lowest values found out of all investigated scenarios (B1-F5). When compared to F2, import of electricity can be reduced to 16.0 (-47.5%), 18.1 (-18.3%) and 75.49 (5.2%) TWh for SWE, NLD and UAE, respectively (Figure 5.7). The RES capacity and distribution can then be optimised to reduce export and consequently the energy imbalance too. When compared to B1 (heat pumps without thermal storage) it becomes clear that integrating a certain capacity of thermal storage is important for each location in order to reduce energy imbalance and import. Heat pumps produce district heating and cooling without any other valuable by-products and their economic feasibility will remain closely connected to their hours of operation. A focus on residual heat from industrial processes can increase the hourly operation value by introducing a valuable by-product, such as data services from data centres or vegetable and fruit production from plant factories. These economic considerations require future investigation.

Another strategy to balance the energy system would be to stabilise and reduce the urban energy demand via building innovations and renovations beyond those described in Section 5.3.3. In this case, the reduced heating demands can be more readily met by residual heat from food production. The residual heat from scenario

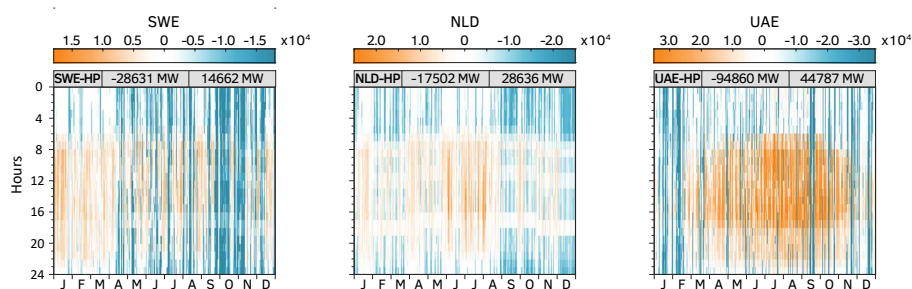


FIG. 5.7 Hourly distribution profile of the energy imbalance (in MW) following the integration of central heat pumps and thermal storage in Sweden (SWE), the Netherlands (NLD) and the United Arab Emirates (UAE), as described in Section 5.5.6. The positive values (orange) represent import and negative values (blue) represent export.

F2 can already cover space heating demands in NLD and UAE, but the demand would need to be reduced by 42.8% in SWE. Peak total heating demand would need to be reduced by 70.6% (SWE), 58.3% (NLD) and 47.4% (UAE). The residual heat from standard production (F1) can cover the total heating demands of UAE and NLD, but the demand would need to be reduced by approximately 14.4% for SWE. The transition to low supply temperature heating in buildings will likely play a role in this development.

5.5.7 Additional considerations

The technical and economic feasibility of the proposed integration is also influenced by numerous factors that have not been taken into account in this study, ranging from the energy system design to crop production. Several of these factors are discussed below and should be further investigated in the future.

- *Optimised energy distribution:* The CEESA 2050 distribution was selected for each location. Additional calculations are required to assess the optimal distribution of RES for each location, as well as for the integration of plant factories.
- *Impact of transport on urban carbon footprint:* The local production of food will partially eliminate food transport miles and will change the carbon footprint of the city. The impact of transportation and resource use efficiency in shorter supply chains has been extensively debated [102]. The effects will be case-specific and will depend on the footprints for food production, processing, handling and transport.
- *Integration of transport and energy systems:* The integration of the transport sector and its fuel demand will require a shift in energy distribution and will likely need to combine biofuels with other technologies [103]. The sector can also contribute to the effective use of intermittent RES and biomass resources, e.g. by using electric vehicles for storage during excess electricity production [27].
- *Systems design for capturing and reusing residual heat:* The design and specifications of the thermal management systems for residual heat sources will determine the quantity and quality of captured heat [63] and the design of the DH networks will determine that of delivered heat [23, 29]. Both components will determine the technical and financial feasibility.
- *Reusing residual heat for cooling:* The use of residual heat for cooling on an urban scale has not been investigated. The residual heat can be utilised by adsorption

cooling systems, which may serve as viable alternatives to electricity-driven vapour compression refrigeration systems [104].

- *Operational hours of the plant factory:* The plant factory operation was controlled by excess electricity production and heat demand without a minimum operation time, apart from F1. In F2 this resulted in only 4477 (SWE), 2407 (NLD) and 1537 (UAE) full-capacity-equivalent hours of operation per year, which means that the projected production was not achieved. Operational flexibility that incorporates a set minimum operation is recommended to ensure adequate crop production and to potentially increase financial feasibility.
- *Crop production under intermittent operation:* The flexible operation of the plant factories may have negative consequences for food production. A stochastic time distribution of artificial light negatively affects different processes in the crop [105], ranging from photosynthetic induction to gene expression and starch breakdown rate. This may severely limit photosynthetic assimilation of CO₂ and consequently long-term crop production [106].

5.6 Conclusions

This study analysed the integration of food production in plant factories with large-scale thermal storage into the energy system. The plant factory was used for the flexible generation of residual heat and thermal storage was used for bridging gaps between energy demand and production, also known as the energy imbalance. In the end, the effects of this integration on the energy imbalance (energy import + export) of a synthetic city relying exclusively on renewable energy sources was quantified for three disparate climates. The energetic consequences of urban food resilience were analysed, as well as the potential of flexible heat generation for balancing the energy system. The main conclusions from this study are listed below.

- District heating networks can facilitate the integration of large-scale residual heat sources, renewable heat sources, heat pumps, thermal storage and other technologies.
- The residual heat production from plant factories designed for food resilience (8.2 m² production area per inhabitant) can cover heating demand in moderate and warm climates but is too low for colder climates.

- The aforementioned plant factories can balance the energy system by operating during hours with excess electricity production combined with heat demand or available thermal storage capacity. However, this flexible operation reduces the plant factories' annual full-capacity-equivalent hours and consequently reduces annual food production.
- The plant factories can be operated according to a fixed schedule to ensure sufficient food production. However, this cyclic operation reduces flexibility and places additional pressure on the system, which consequently increases the energy imbalance.
- In subarctic climates the flexible generation of residual heat can be used to effectively balance the energy system. However, the plant factories do not produce enough residual heat to cover the high heating demand in this type of climate. Additionally, a high thermal storage capacity is required to bridge the large seasonal differences. In Sweden, for example, the integration of plant factories reduces the energy imbalance by 38.9% (from 88.9 to 54.3 TWh) and the optimal thermal storage capacity is higher than in locations with a lower heating demand.
- In temperate (oceanic) climates the flexible heat generation from plant factories has the largest effect on the energy imbalance. The moderate heating demand can be covered by the residual heat from the plant factories. Less thermal storage is required compared to colder climates, due to the lower seasonal variations and peaks in heating demand. For the Netherlands, the integration of plant factories reduces the energy imbalance by 43.1% (from 62.6 to 35.6 TWh).
- In hot desert climates the integration of plant factories offers little benefit to the energy balance. The imbalance between the energy production and the high cooling demands in these climates cannot be reduced using residual heat. Furthermore, the slight heating demand can easily be covered by the plant factories, which results in few operational hours. Little thermal storage capacity is required, as heating demand mainly fluctuates on an hourly and not a seasonal basis. This is all illustrated in the United Arab Emirates, where the energy imbalance is calculated to decrease by 11.8% (from 190.2 to 167.7 TWh) and thermal storage does not drop below 85% of its capacity.
- The combination of central heat pumps and thermal storage can provide flexibility similar to that of utilising residual heat from plant factories, but at a higher coefficient of performance. The plant factory produces a valuable industrial by-product.

- A flexible (sub-)hourly operation of heating technologies is important for balancing the energy system. However, a minimum operation in terms of full-capacity-equivalent hours per year is required to ensure their technical and financial feasibility.

This study provides a first step in identifying the impact of food production on the urban energy balance in a search for food-resilient cities. It illustrates how plant factories could balance energy systems that rely on intermittent renewable sources. Naturally, plant factories are just one example of (urban) industrial functions that produce considerable amounts of residual heat. The integration of other sources with thermal storage may also prove to be an effective strategy in reducing the imbalance in systems that operate on 100% renewable energy. The manner in which that is achieved depends strongly on local climate and energy demand and should be researched in greater depth.

Acknowledgements

This study was funded by the EU European Regional Development Fund “Kansen voor West” with the programme “Fieldlab FreshTeq”. This work was partly supported by the EU-H2020 project “Food systems in European Cities - FoodE” (FoodE, grant 862663). However, no endorsement from the European Commission of the results and conclusions is hereby implied.

The authors wish to thank Staaï Food Group and Westland Infra for their support. Finally, the authors would like to express their gratitude to Andrei David Korberg from Aalborg University for his advice on energy system modelling in EnergyPLAN.

Model overview

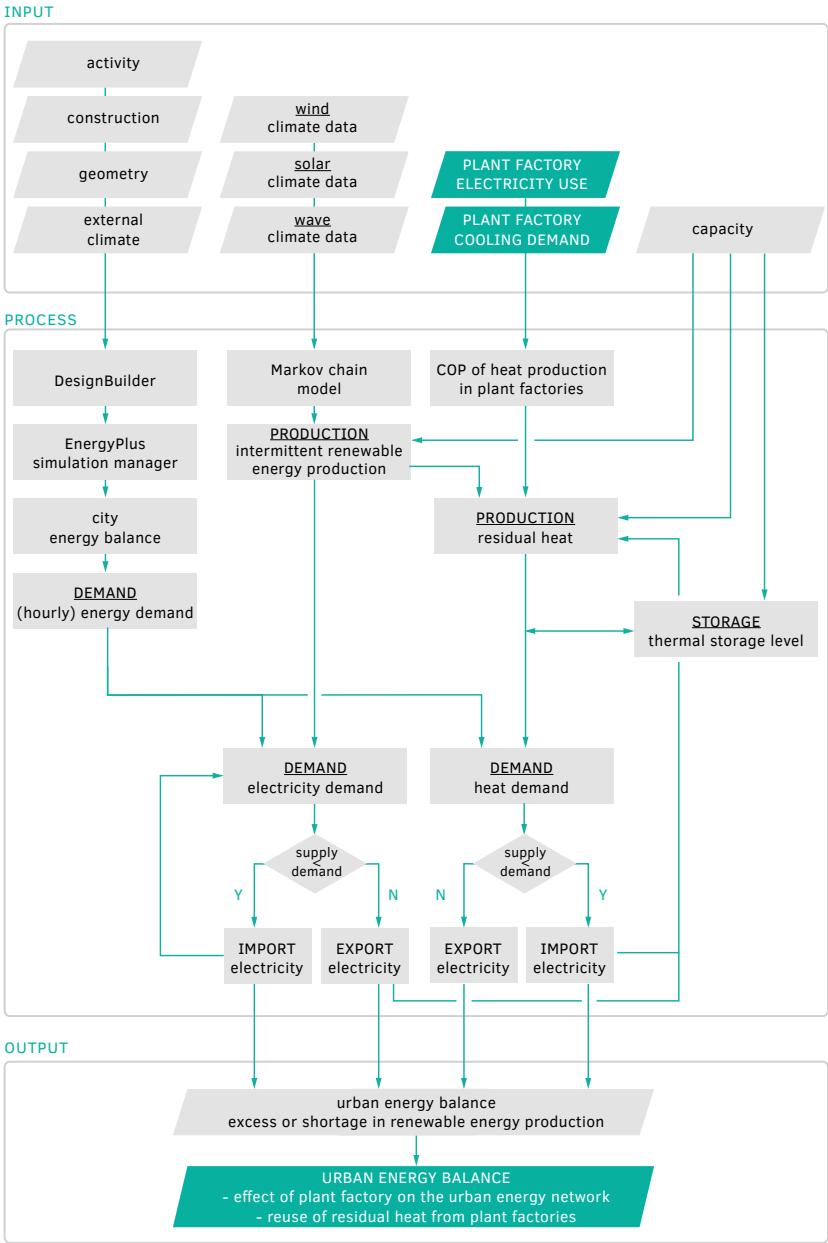


FIG. APP. 5A.1 Simplified model diagram to illustrate key processes and variables.

Modelling wind energy production

Wind power generation largely depends on the wind speed distribution and on the installed capacity of wind farms [40]. The stochastic wind speed distribution is calculated using a Markov chain model, to accurately incorporate the variability of wind and to extend the applicability of this study. This model is used to generate synthetic climate state time series, different from the observational data, but with similar statistical properties. The installed capacity was set following annual energy demand.

The Markov chain model is a discrete stochastic process which uses the Markov property. In short, the model determines the future condition based on the condition directly preceding it. Stochastic transitions are used to generate synthetic climate state time series, different from the observational data, but with the same statistical properties. The method is described in greater detail by [107].

In this study, the transitions were calculated for each month to increase accuracy. Observational data were retrieved for the period 2000–2018 from representative offshore weather stations in the Gulf of Bothnia for Sweden [108, 109], the North Sea for the Netherlands [110, 111] and the Persian Gulf for the United Arab Emirates [112]. A discrete setting was applied for workability and computational efficiency: the resolutions for wind speed and time were $\Delta u = 0.5 \text{ m s}^{-1}$ and $\Delta t = 1 \text{ h}$, respectively. This discrete nature is considered the drawback of the Markov chain model. However, the level of detail and accuracy achieved in practice has been proven to be adequate [107, 113] and is deemed sufficient for the scale of this study.

The distribution of power generation is determined as a function of the flow speed that the blades receive. The power generation is dominated by a cut-in wind speed (no generation below), an exponential segment, the rated wind speed (maximum generation) and a cut-out wind speed (no generation above). The flow speed at hub height (80–120 m) is used to determine power generation, but weather stations typically provide wind speeds at 10 m (u_{10m}). The wind speed at 100 m (u_{100m}) can be obtained by applying the power law using a shearing exponent of $\beta = 0.143$ for land and $\beta = 0.110$ for water [3].

$$u_{100m} = u_{10m} \cdot \frac{100}{10}^{\beta} = \begin{matrix} u_{10m} \cdot 1.39 & \text{over land} \\ u_{10m} \cdot 1.29 & \text{over sea} \end{matrix} \quad [5B.1]$$

The power generation in the exponential segment can be determined using various methods. The exponential and the cubic power curves show the best behaviour in terms of the energy density error, mean power error and the lowest standard deviation [114]. Generated power (q) can then be determined as a function of u_{100m} , density of the air (ρ_{air}), swept area of the turbine (A), and power coefficient (c_{pw}) [115, 116].

$$q(u) = \frac{1}{2} \cdot \rho_{air} \cdot A_{tur} \cdot c_{pw} \cdot u_{100m}^3 \quad [5B.2]$$

Wind turbine data from [114] for turbines with a capacity greater than 5 MW are used to fix the average radius (blade length) of the wind turbine at 62.5 m, the c_{pw} at 0.43, the cut-in speed at 3.5 m s^{-1} , the rated wind speed at 13.5 m s^{-1} , and the cut-out wind speed at 30 m s^{-1} . The resulting hourly power distributions were used as input data in EnergyPLAN. Considerations such as maintenance and other highly specific losses are beyond the scope of this study.

TABLE APP. 5C.1 SynCity model input for dwellings, offices and retail buildings

			Dwelling (SML)	Office	Retail	Unit
Profile	Occupancy		Residential Occ	Occupancy - Office	Occupancy - Retail	-
	DHW		Residential kitchen loads	Service hot water - office	Service hot water - retail	-
	Electricity		Residential light	Occupancy - Office	HVAC availability - Retail (EDITED: Misc.)	
	Lighting		Residential light	Occupancy - Office	HVAC availability - Retail (EDITED: lighting)	-
	HVAC		HtgClgSPSB_default	HtgClgSPSB_default	HtgClgSPSB_default	-
Input	DHW	Daily	5.6894	2.2313	1.8973	l m ⁻² d ⁻¹
		COP	1.5151	1.5151	1.5151	W W ⁻¹
	Plug load	Installed	9.11 ^a	9.11 ^a	47.03	W m ⁻²
	Lighting	Installed	3.29	31.40	32.51	W m ⁻²
	T_cool	Setpoint	26	24	24	°C
	T_heat	Setpoint	20	20	20	°C
	Occupancy	Persons	0.0261	0.11	0.08	n m ⁻²
Profiles	Activity	Profile	Residential - Dwelling unit (with kitchen)	Office buildings - Office - Open plan	Retail - Supermarket	-
Schedules	Profile		Married_Couple_Two_Children	Office work/ Standing/Walking	Walking around	-
	Misc. gains		Residential light	Occupancy - Office	HVAC availability - Retail (EDITED: Miscellaneous)	-
	Lighting		Residential light	Occupancy - Office	HVAC availability - Retail (EDITED: lighting)	-
	DHW		Residential kitchen loads	Service hot water - office	Service hot water - retail	-
	Cooling		HtgClgSPSB_default	HtgClgSPSB_default	HtgClgSPSB_default	-
	Heating		HtgClgSPSB_default	HtgClgSPSB_default	HtgClgSPSB_default	-
	Ventilation		Residential Occ	Occupancy - Office	Occupancy - Retail	-

>>>

TABLE APP. 5C.1 SynCity model input for dwellings, offices and retail buildings

			Dwelling (SML)	Office	Retail	Unit
Construction (Standard)	Shading	Type	Blind with medium reflectivity	Blind with high reflectivity	OFF	-
		Control	8 - Cooling	8-Cooling	-	-
	HVAC	Type	VAV, Air-cooled Chiller, Reheat	Fan coil unit (4-pipe), air cooled chiller	Fan coil unit (4-pipe), air cooled chiller	-
	DHW	Type	Dedicated hot water boiler	Dedicated hot water boiler	Dedicated hot water boiler	-
	Natural vent.		ON	OFF	OFF	-
Construction (present)	Insulation		Uninsulated	Uninsulated	Uninsulated	-
	Thermal mass		Medium	Medium	Medium	-
	Model infiltration		1	1	1	ac h ⁻¹
	Glazing	Type	Single glazing, clear, no shading	Single glazing, clear	Single glazing, clear, no shading	-
		Lay-out	30% - preferred height	Curtain wall, 85% glazed	Curtain wall, 85% glazed	-
Construction (Future)	Insulation		Energy Code	Energy Code	Energy code	-
	Thermal mass		Medium	Medium	Medium	-
	Model infiltration		0.3	0.3	0.3	ac h ⁻¹
	Glazing	Type	Best practice	Best practice	Best practice	-
		Lay-out	30% - preferred height	Curtain wall, 85% glazed	Curtain wall, 85% glazed	-
	Economizer	ON/OFF	OFF	ON	ON	-
		Control	-	3-Differential enthalpy	3-Differential enthalpy	-

^a The plug loads as reported by NYC [55, 56] are excessive for the functions residential (L), offices, and retail, resulting in extraordinarily high internal heat loads. The maximum internal heat load for offices was reduced to match the maximum load factor for offices with a high level of installed appliances [117].

TABLE APP. 5C.2 Model input for warehouses and educational buildings

			Warehouse	Education	Unit
Profile	Occupancy		Occupancy - Warehouse	Occupancy - School	-
	DHW		Service hot water - Warehouse	Service hot water - School	-
	Electricity		HVAC availability - Warehouse	Lighting receptacle - School	-
	Lighting		HVAC availability - Warehouse	Lighting receptacle - School	-
	HVAC		HtgClgSPSB_default	HtgClgSPSB_default	-

>>>

TABLE APP. 5C.2 Model input for warehouses and educational buildings

			Warehouse	Education	Unit
Input	DHW	Daily	1.0040	1.7849	$\text{l m}^{-2} \text{d}^{-1}$
		COP	1.5151	1.5151	W W^{-1}
	Basic Electricity	Installed	23.78	14.18	W m^{-2}
	Lighting	Installed	10.98	11.47	W m^{-2}
	T_cool	Setpoint	26	26	$^{\circ}\text{C}$
	T_heat	Setpoint	20	20	$^{\circ}\text{C}$
	Occupancy	Persons	0.005	0.35	n m^{-2}
Profiles	Activity	Profile	Misc. Spaces - Warehouse	Educational Facilities - Classroom (9+)	-
Schedules	Profile		Occupancy - Warehouse	Writing	-
	Misc.		HVAC availability - Warehouse	Lighting receptacle - School	-
	General lighting		HVAC availability - Warehouse	Lighting receptacle - School	-
	DHW		Service hot water - Warehouse	Service hot water - School	-
	Cooling		HtgClgSPSB_default	HtgClgSPSB_default	-
	Heating		HtgClgSPSB_default	HtgClgSPSB_default	-
	Ventilation		Occupancy - Warehouse	Occupancy - School	-
Construction (Constant)	Glazing	Type	No windows	Best practice	-
		Lay-out	-	30% - preferred height	-
	Shading	Type	None	Blind with high reflectivity slats	-
		Control	-	8-Cooling	-
	HVAC	Type	Fan coil unit (4-pipe), air cooled chiller	Fan coil unit (4-pipe), air cooled chiller	-
	DHW	Type	Dedicated hot water boiler	Dedicated hot water boiler	-
	Natural ventilation		ON	ON	-
Construction (Present)	Insulation		Uninsulated	Typical ref	-
	Thermal mass		Medium	Medium	-
	Model infiltration		1	1	ac h^{-1}
Construction (Future)	Insulation		Energy code	Energy code	-
	Thermal mass		Medium	Medium	-
	Model infiltration		0.3	0.3	ac h^{-1}

EnergyPLAN model input

TABLE APP. 5D.1 EnergyPLAN input for scenarios B1-B2 and F1-F3

SWE		B1	B2	F1	F2	F3	Unit
Demand	Electricity demand	52.8082	52.8082	52.8082	52.8082	52.8082	TWh y ⁻¹
	Additional electricity	0	0	76.4104 ^a	2.0472 ^b	6.4381 ^b	TWh y ⁻¹
	DH	84.1831	84.1831	84.1831	84.1831	84.1831	TWh y ⁻¹
	Network losses ^c	0.17	0.17	0.17	0.17	0.17	-
	Cooling	0.1621	0.1621	0.1621	0.1621	0.1621	TWh y ⁻¹
	Cooling COP	1.00	1.00	1.00	1.00	1.00	-
Supply	Wind power	28908	28908	30651	29454	30624	MW
	Photovoltaic	3824	3824	3824	3824	3824	MW
	Stabilisation shares	0.3	0.3	0.3	0.3	0.3	-
	Compression HP	13556	13556	0	12699 ^d	39935 ^d	MWe
	COP	3.0	3.0	0	0.8598 ^d	0.8598 ^d	-
	Thermal capacity	40668	40668	0	10919 ^d	34337 ^d	MJ s ⁻¹
	Industrial excess heat	0	0	77.4 ^e	13.5 ^f	42.4 ^f	TWh y ⁻¹
Balancing & storage	Grid stabilisation share ^c	0.3	0.3	0.3	0.3	0.3	-
	CEEP regulation	0	167	0	0	0	-
	Thermal storage	0	0	10481	10481	10481	GWh
	Days of optimising	0	0	366	366	366	d
	Thermal storage regulation	Seasonal	Seasonal	Seasonal	Seasonal	Seasonal	-

>>>

TABLE APP. 5D.1 EnergyPLAN input for scenarios B1-B2 and F1-F3

NLD		B1	B2	F1	F2	F3	Unit
Demand	Electricity demand	52.8082	52.8082	52.8082	52.8082	52.8082	TWh y ⁻¹
	Additional electricity	0	0	78.9193 ^a	2.2601 ^b	5.0338 ^b	TWh y ⁻¹
	DH	49.1443	49.1443	49.1443	49.1443	49.1443	TWh y ⁻¹
	Network losses ^c	0.17	0.17	0.17	0.17	0.17	-
	Cooling	3.1783	3.1783	3.1783	3.1783	3.1783	TWh y ⁻¹
	Cooling COP	1.00	1.00	1.00	1.00	1.00	-
Supply	Wind power	18208	18208	27015	18730	19371	MW
	Photovoltaic	4142	4142	4142	4142	4142	MW
	Stabilisation shares	0.3	0.3	0.3	0.3	0.3	-
	Compression HP	9910	9910	0	13091 ^d	29156 ^d	MWe
	COP	3.0	3.0	0	0.8345 ^d	0.8345 ^d	-
	Thermal capacity	29729	29729	0	10924 ^d	24329 ^d	MJ s ⁻¹
	Industrial excess heat	0	0	77.5 ^e	13.5 ^f	30.1 ^f	TWh y ⁻¹
Balancing & storage	Grid stabilisation share ^c	0.3	0.3	0.3	0.3	0.3	-
	CEEP regulation	0	167	0	0	0	-
	Thermal storage	0	0	6118	6118	6118	GWh
	Days of optimising	0	0	366	366	366	d
	Thermal storage regulation	Seasonal	Seasonal	Seasonal	Seasonal	Seasonal	-

>>>

TABLE APP. 5D.1 EnergyPLAN input for scenarios B1-B2 and F1-F3

UAE		B1	B2	F1	F2	F3	Unit
Demand	Electricity demand	52.8082	52.8082	52.8082	52.8082	52.8082	TWh y ⁻¹
	Additional electricity	0	0	89.4868 ^a	3.8677 ^b	5.2643 ^b	TWh y ⁻¹
	DH	37.1630	37.1630	37.1630	37.1630	37.1630	TWh y ⁻¹
	Network losses ^c	0.17	0.17	0.17	0.17	0.17	-
	Cooling	87.1910	87.1910	87.1910	87.1910	87.1910	TWh y ⁻¹
	Cooling COP	1.00	1.00	1.00	1.00	1.00	-
Supply	Wind power	95588	95588	129958	97855	98674	MW
	Photovoltaic	4545	4545	4545	4545	4545	MW
	Stabilisation shares	0.3	0.3	0.3	0.3	0.3	-
	Compression HP	8233	8233	0	14621 ^d	19900 ^d	MWe
	COP	3.0	3.0	0	0.7488 ^d	0.7488 ^d	-
	Thermal capacity	24698	24698	0	10948 ^d	14901 ^d	MJ s ⁻¹
	Industrial excess heat	0.0	0.0	77.6 ^e	13.5 ^f	18.4 ^f	TWh y ⁻¹
Balancing & storage	Grid stabilisation share ^c	0.3	0.3	0.3	0.3	0.3	-
	CEEP regulation	0	167	0	0	0	-
	Thermal storage	0.0	0.0	4627	4627	4627	GWh
	Days of optimising	0.0	0.0	366	366	366	d
	Thermal storage regulation	Seasonal	Seasonal	Seasonal	Seasonal	Seasonal	-

^a Total annual electricity use of the plant factory during fixed operation schedule

^b Electricity use of plant factory when switched "OFF", see Section 5.3.2.

^c Assumptions concerning energy network are in line with [62].

^d The plant factory is modelled as a compression heat pump, with its COP representing the residual heat production versus required electricity input when switched "ON", see Section 5.3.2.

^e Total annual residual heat production by the plant factory during fixed production schedule.

^f Heat production by plant factory when switched "OFF", see Section 5.3.2.

TABLE APP. 5C.2 EnergyPLAN input for scenarios B3-B4 and F4-F5

	SWE				
	B3	B4	F4	F5	
Electricity demand	528.082	528.082	528.082	528.082	
Additional electricity	0	0	2.0472 ^a	2.0472 ^a	
DH	841.831	841.831	841.831	841.831	
Network losses ^b	0.17	0.17	0.17	0.17	
Cooling	0.1621	0.1621	0.1621	0.1621	
Cooling COP	1	1	1	1	
Biomass: industry	202.095	202.095	202.095	202.095	
CHP electricity	1642	0	339	0	
CHP heat	4442	0	917	0	
>Electric efficiency	0.27	0	0.27	0	
>Thermal efficiency	0.73	0	0.73	0	
Wind power	10972	19117	17986	20839	
Photovoltaic	9321	16241	2227	17704	
Wave power	1530	2665	274	2665	
Stabilisation shares	0.3	0.3	0.3	0.3	
Solar thermal	66.011	52.151	66.647	52.136	
Compression HP	13556	13556	12699 ^c	12699 ^c	
COP	3	3	0.8598 ^c	0.8598 ^c	
Thermal capacity	40668	40668	10919 ^c	10919 ^c	
> Ngas	1.00	0	1	0	
> Biomass	0.483412	0	0.483412	0	
> Biomass	16.1	0	3.32	0	
> Coldgas efficiency	0.83	0	0.83	0	
Biogases: Biogas plant	8.02	0	1.66	0	
> CHP and boilers	900	0	185.86	0	
> Fuel efficiency	0.6694	0	0.6694	0	
Hydrogen storage	2031	0	419	0	
Geothermal	34.529	27.279	34.861	27.271	
Industrial excess heat	0	0	13.4847 ^d	13.4847 ^d	
Grid stabilisation share ^b	0.3	0.3	0.3	0.3	
CEEP regulation	0	0	0	0	
Thermal storage	0	0	10481	10481	
Days of optimising	0	0	366	366	
Thermal storage regulation	Seasonal	Seasonal	Seasonal	Seasonal	

	NLD				UAE				Unit
	B3	B4	F4	F5	B3	B4	F4	F5	
	528.082	528.082	528.082	528.082	528.082	528.082	528.082	528.082	TWh y ⁻¹
	0	0	2.2601 ^a	2.2601 ^a	0	0	3.8677 ^a	3.8677 ^a	TWh y ⁻¹
	491.443	491.443	491.443	491.443	37.163	37.163	37.163	37.163	TWh y ⁻¹
	0.17	0.17	0.17	0.17	0.17	0.17	0.17	0.17	-
	31.783	31.783	31.783	31.783	87.191	87.191	87.191	87.191	TWh y ⁻¹
	1	1	1	1	1	1	1	1	-
	117.982	117.982	117.982	117.982	89.218	89.218	89.218	89.218	TWh y ⁻¹
	959	0	156	0	725	0	128	0	MWe
	2593	0	423	0	1961	0	347	0	MW
	0.27	0	0.27	0	0.27	0	0.27	0	-
	0.73	0	0.73	0	0.73	0	0.73	0	-
	10583	14705	14474	15703	70063	77973	78110	80901	MW
	8118	11280	1792	12046	6456	7184	9671	7454	MW
	1702	2365	221	2365	4441	4942	1190	4942	MW
	0.3	0.3	0.3	0.3	0.3	0.3	0.3	0.3	-
	38.537	30.445	38.908	30.437	29.142	23.023	29.422	23.016	TWh y ⁻¹
	9910	9910	13091 ^c	13091 ^c	8233	8233	14621 ^c	14621 ^c	MW-e
	3	3	0.8345 ^c	0.8345 ^c	3	3	0.7488 ^c	0.7488 ^c	
	29729	29729	10924 ^c	10924 ^c	24698	24698	10948 ^c	10948 ^c	MJ s ⁻¹
	1	0	1	0	1	0	1	0	-
	0.483412	0	0.483412	0	0.483412	0	0.483412	0	-
	9.4	0	1.53	0	7.11	0	1.26	0	TWh y ⁻¹
	0.83	0	0.83	0	0.83	0	0.83	0	-
	4.68	0	0.76	0	3.54	0	0.63	0	TWh y ⁻¹
	561.39	0	85.66	0	441.31	0	70.3	0	MW-e
	0.6694	0	0.6694	0	0.6694	0	0.6694	0	-
	1186	0	193	0	897	0	159	0	GWh
	20.158	15.925	20.352	15.921	15.243	12.043	1.539	12.039	TWh y ⁻¹
	0	0	13.5176 ^d	13.5176 ^d	0	0	13.5162 ^d	13.5162 ^d	TWh y ⁻¹
	0.3	0.3	0.3	0.3	0.3	0.3	0.3	0.3	-
	0	0	0	0	0	0	0	0	-
	0	0	6118	6118	0	0	4627	4627	GWh
	0	0	366	366	0	0	366	366	d
	Seasonal	Seasonal	Seasonal	Seasonal	Seasonal	Seasonal	Seasonal	Seasonal	-

TABLE APP. 5C.3 EnergyPLAN input for the integration of central HPs and thermal storage

Heat pumps		SWE	NLD	UAE	Unit
Demand	Electricity demand	52.8082	52.8082	52.8082	TWh y ⁻¹
	Additional electricity	0	0	0	TWh y ⁻¹
	DH	84.1831	49.1443	37.1630	TWh y ⁻¹
	Network losses ^b	0.17	0.17	0.17	-
	Cooling	0.1621	3.1783	87.1910	TWh y ⁻¹
	Cooling COP	1.00	1.00	1.00	-
Supply	Wind power	28908	18208	95588	MW
	Photovoltaic	3824	4142	4545	MW
	Stabilisation shares	0.3	0.3	0.3	-
	Compression HP	16333	11939	8233	MWe
	COP	3.0	3.0	3.0	-
	Thermal capacity	48998	35818	24698	MJ s ⁻¹
	Industrial excess heat	0	0	0	TWh y ⁻¹
Balancing & storage	Grid stabilisation share ^a	0.3	0.3	0.3	-
	CEEP regulation	0	0	0	-
	Thermal storage	10481	6118	4627	GWh
	Days of optimising	366	366	366	d
	Thermal storage regulation	Seasonal	Seasonal	Seasonal	-

^a Electricity use of plant factory when switched "OFF", see Section 5.3.2.

^b Assumptions concerning energy network are in line with [62].

^c The plant factory is modelled as a compression heat pump, with its COP representing the residual heat production versus required electricity input when switched "ON", see Section 5.3.2.

^d Heat production by plant factory when switched "OFF", see Section 5.3.2.

Reference list

- [1] Li, D.H.W., Yang, L., & Lam, J.C. (2013). Zero energy buildings and sustainable development implications—A review. *Energy*, 54, 1–10. doi:10.1016/j.energy.2013.01.070
- [2] Mathiesen, B.V., Lund, H., & Karlsson, K. (2011). 100% Renewable energy systems, climate mitigation and economic growth. *Applied energy*, 88(2), 488–501. doi:10.1016/j.apenergy.2010.03.001
- [3] Lledó, L.I., Torralba, V., Soret, A., Ramon, J., & Doblas-Reyes, F.J. (2019). Seasonal forecasts of wind power generation. *Renewable energy*, 143, 91–100. doi:10.1016/j.renene.2019.04.135
- [4] Mathiesen, B.V., Lund, H., Connolly, D., Wenzel, H., Østergaard, P.A., Möller, B., Nielsen, S., Ridjan, I., Karnøe, P., Sperling, K., & Hvelplund, F.K. (2015). Smart Energy Systems for coherent 100% renewable energy and transport solutions. *Applied energy*, 145, 139–154. doi:10.1016/j.apenergy.2015.01.075
- [5] Lund, H. (2005). Large-scale integration of wind power into different energy systems. *Energy*, 30(13), 2402–2412. doi:10.1016/j.energy.2004.11.001
- [6] Mathiesen, B.V. & Lund, H. (2009). Comparative analyses of seven technologies to facilitate the integration of fluctuating renewable energy sources. *IET Renewable Power Generation*, 3(2), 190–204. doi:10.1049/iet-rpg:20080049
- [7] Østergaard, P.A. (2006). Ancillary services and the integration of substantial quantities of wind power. *Applied energy*, 83(5), 451–463. doi:10.1016/j.apenergy.2005.04.007
- [8] Sorknæs, P., Lund, H., & Andersen, A.N. (2015). Future power market and sustainable energy solutions – The treatment of uncertainties in the daily operation of combined heat and power plants. *Applied energy*, 144, 129–138. doi:10.1016/j.apenergy.2015.02.041
- [9] Lund, H. & Münster, E. (2003). Management of surplus electricity—production from a fluctuating renewable-energy source. *Applied energy*, 76(1–3), 65–74. doi:10.1016/S0306-2619(03)00048-5
- [10] Kennedy, C., Cuddihy, J., & Engel-Yan, J. (2007). The changing metabolism of cities. *Journal of industrial ecology*, 11(2), 43–59. doi:10.1162/jiec.0.1107
- [11] Newcombe, K. & Nichols, E.H. (1979). An integrated ecological approach to agricultural policy-making with reference to the urban fringe: The case of Hong Kong. *Agricultural Systems*, 4(1), 1–27. doi:10.1016/0308-521x(79)90011-8
- [12] Benis, K. & Ferrão, P. (2018). Commercial farming within the urban built environment – Taking stock of an evolving field in northern countries. *Global Food Security*, 17, 30–37. doi:10.1016/j.gfs.2018.03.005
- [13] Goto, E. (2012). Plant production in a closed plant factory with artificial lighting. *Acta Horticulturae*, 956, 37–49. doi:10.17660/actahortic.2012.956.2
- [14] Seginer, I. & Ioslovich, I. (1999). Optimal spacing and cultivation intensity for an industrialized crop production system. *Agricultural Systems*, 62(3), 143–157. doi:10.1016/s0308-521x(99)00057-8
- [15] Kozai, T., Ohya, K., & Chun, C. (2006). Commercialized closed systems with artificial lighting for plant production. *Acta Horticulturae*, 711, 61–70. doi:10.17660/actahortic.2006.711.5
- [16] Kozai, T. (2013). Sustainable plant factory: Closed plant production systems with artificial light for high resource use efficiencies and quality produce. *Acta Horticulturae*, 1004, 27–40. doi:10.17660/actahortic.2013.1004.2
- [17] Kozai, T. (2013). Resource use efficiency of closed plant production system with artificial light: Concept, estimation and application to plant factory. *Proceedings of the Japan Academy. Series B, Physical and biological sciences*, 89(10), 447–461. doi:10.2183/pjab.89.447
- [18] Graamans, L., Baeza, E., van den Dobbelsteen, A., Tsafaras, I., & Stanghellini, C. (2018). Plant factories versus greenhouses: Comparison of resource use efficiency. *Agricultural Systems*, 160, 31–43. doi:10.1016/j.agry.2017.11.003
- [19] Lund, H. (2006). Large-scale integration of optimal combinations of PV, wind and wave power into the electricity supply. *Renewable energy*, 31(4), 503–515. doi:10.1016/j.renene.2005.04.008
- [20] Lund, H., Möller, B., Mathiesen, B.V., & Dyrrelund, A. (2010). The role of district heating in future renewable energy systems. *Energy*, 35(3), 1381–1390. doi:10.1016/j.energy.2009.11.023
- [21] Lund, H., Werner, S., Wiltshire, R., Svendsen, S., Thorsen, J.E., Hvelplund, F.K., & Mathiesen, B.V. (2014). 4th Generation District Heating (4GDH): Integrating smart thermal grids into future sustainable energy systems. *Energy*, 68, 1–11. doi:10.1016/j.energy.2014.02.089
- [22] Arteconi, A., Hewitt, N.J., & Polonara, F. (2012). State of the art of thermal storage for demand-side management. *Applied energy*, 93, 371–389. doi:10.1016/j.apenergy.2011.12.045

- [23] Kavvadias, K.C. & Quoilin, S. (2018). Exploiting waste heat potential by long distance heat transmission: Design considerations and techno-economic assessment. *Applied energy*, 216, 452–465. doi:10.1016/j.apenergy.2018.02.080
- [24] Østergaard, P.A. & Andersen, A.N. (2016). Booster heat pumps and central heat pumps in district heating. *Applied energy*, 184, 1374–1388. doi:10.1016/j.apenergy.2016.02.144
- [25] Alaperä, I., Honkapuro, S., & Paananen, J. (2018). Data centers as a source of dynamic flexibility in smart grids. *Applied energy*, 229, 69–79. doi:10.1016/j.apenergy.2018.07.056
- [26] Connolly, D., Lund, H., Mathiesen, B.V., Werner, S., Möller, B., Persson, U., Boermans, T., Trier, D., Østergaard, P.A., & Nielsen, S. (2014). Heat Roadmap Europe: Combining district heating with heat savings to decarbonise the EU energy system. *Energy Policy*, 65, 475–489. doi:10.1016/j.enpol.2013.10.035
- [27] Mathiesen, B.V., Lund, H., & Connolly, D. (2012). Limiting biomass consumption for heating in 100% renewable energy systems. *Energy*, 48(1), 160–168. doi:10.1016/j.energy.2012.07.063
- [28] Kapil, A., Bulatov, I., Smith, R., & Kim, J.K. (2012). Process integration of low grade heat in process industry with district heating networks. *Energy*, 44(1), 11–19. doi:10.1016/j.energy.2011.12.015
- [29] Wahlroos, M., Pärssinen, M., Manner, J., & Syri, S. (2017). Utilizing data center waste heat in district heating – Impacts on energy efficiency and prospects for low-temperature district heating networks. *Energy*, 140, 1228–1238. doi:10.1016/j.energy.2017.08.078
- [30] Massa, G.D., Kim, H.H., Wheeler, R.M., & Mitchell, C.A. (2008). Plant productivity in response to LED lighting. *HortScience*, 43(7), 1951–1956. doi:10.21273/HORTSCI.43.7.1951
- [31] Graamans, L., Tenpierik, M., van den Dobbelsteen, A., & Stanghellini, C. (2020). Plant factories: Reducing energy demand at high internal heat loads through façade design. *Applied energy*, 262, 114544. doi:10.1016/j.apenergy.2020.114544
- [32] Pölling, B., Mergenthaler, M., & Lörleberg, W. (2016). Professional urban agriculture and its characteristic business models in Metropolis Ruhr, Germany. *Land use policy*, 58, 366–379. doi:10.1016/j.landusepol.2016.05.036
- [33] Specht, K., Zoll, F., Schümann, H., Bela, J., Kachel, J., & Robischon, M. (2019). How will we eat and produce in the cities of the future? From edible insects to vertical farming—A study on the perception and acceptability of new Approaches. *Sustainability*, 11(16), 4315. doi:10.3390/su11164315
- [34] Schmitt, E., Galli, F., Menozzi, D., Maye, D., Touzard, J.M., Marescotti, A., Six, J., & Brunori, G. (2017). Comparing the sustainability of local and global food products in Europe. *Journal of cleaner production*, 165, 346–359. doi:10.1016/j.jclepro.2017.07.039
- [35] van den Dobbelsteen, A. (2008). *Towards closed cycles - New strategy steps inspired by the Cradle to Cradle approach*. Paper presented at the 25th Conference on Passive and Low Energy Architecture, Dublin, Ireland.
- [36] Tillie, N., van den Dobbelsteen, A., Doepel, D., Joubert, M., De Jager, W., & Mayenburg, D. (2009). Towards CO₂ neutral urban planning: presenting the Rotterdam Energy Approach and Planning (REAP). *Journal of Green Building*, 4(3), 103–112. doi:10.3992/jgb.4.3.103
- [37] Lund, H., Marszal, A., & Heiselberg, P. (2011). Zero energy buildings and mismatch compensation factors. *Energy and buildings*, 43(7), 1646–1654. doi:10.1016/j.enbuild.2011.03.006
- [38] Hedegaard, K. & Meibom, P. (2012). Wind power impacts and electricity storage – A time scale perspective. *Renewable energy*, 37(1), 318–324. doi:10.1016/j.renene.2011.06.034
- [39] Zappa, W., Junginger, M., & van den Broek, M. (2019). Is a 100% renewable European power system feasible by 2050? *Applied energy*, 233, 1027–1050. doi:10.1016/j.apenergy.2018.08.109
- [40] Albadi, M.H. & El-Saadany, E.F. (2010). Overview of wind power intermittency impacts on power systems. *Electric power systems research*, 80(6), 627–632. doi:10.1016/j.epsr.2009.10.035
- [41] Østergaard, P.A. (2013). Wind power integration in Aalborg Municipality using compression heat pumps and geothermal absorption heat pumps. *Energy*, 49, 502–508. doi:10.1016/j.energy.2012.11.030
- [42] Dalla Rosa, A. & Christensen, J.E. (2011). Low-energy district heating in energy-efficient building areas. *Energy*, 36(12), 6890–6899. doi:10.1016/j.energy.2011.10.001
- [43] Lund, H., Østergaard, P.A., Chang, M., Werner, S., Svendsen, S., Sorknæs, P., Thorsen, J.E., Hvelplund, F.K., Mortensen, B.O.G., Mathiesen, B.V., Bojesen, C., Duic, N., Zhang, X.L., & Möller, B. (2018). The status of 4th generation district heating: Research and results. *Energy*. doi:10.1016/j.energy.2018.08.206
- [44] Rämä, M. & Wahlroos, M. (2018). Introduction of new decentralised renewable heat supply in an existing district heating system. *Energy*, 154, 68–79. doi:10.1016/j.energy.2018.03.105
- [45] Schmidt, D., Kallert, A., Blesl, M., Svendsen, S., Li, H., Nord, N., & Sipilä, K. (2017). Low temperature district heating for future energy systems. *Energy Procedia*, 116, 26–38. doi:10.1016/j.egypro.2017.05.052

- [46] Ozgener, L., Hepbasli, A., & Dincer, I. (2005). Energy and exergy analysis of geothermal district heating systems: an application. *Building and Environment*, 40(10), 1309-1322. doi:10.1016/j.buildenv.2004.11.001
- [47] Dalla Rosa, A., Li, H.W., & Svendsen, S. (2011). Method for optimal design of pipes for low-energy district heating, with focus on heat losses. *Energy*, 36(5), 2407-2418. doi:10.1016/j.energy.2011.01.024
- [48] Hedegaard, K., Mathiesen, B.V., Lund, H., & Heiselberg, P. (2012). Wind power integration using individual heat pumps – Analysis of different heat storage options. *Energy*, 47(1), 284-293. doi:10.1016/j.energy.2012.09.030
- [49] Xu, J., Wang, R.Z., & Li, Y. (2014). A review of available technologies for seasonal thermal energy storage. *Solar Energy*, 103, 610-638. doi:10.1016/j.solener.2013.06.006
- [50] Olsthoorn, D., Haghighat, F., & Mirzaei, P.A. (2016). Integration of storage and renewable energy into district heating systems: A review of modelling and optimization. *Solar Energy*, 136, 49-64. doi:10.1016/j.solener.2016.06.054
- [51] Divya, K.C. & Østergaard, J. (2009). Battery energy storage technology for power systems - An overview. *Electric power systems research*, 79(4), 511-520. doi:10.1016/j.epsr.2008.09.017
- [52] Ibrahim, H., Ilinca, A., & Perron, J. (2008). Energy storage systems - Characteristics and comparisons. *Renewable and Sustainable Energy Reviews*, 12(5), 1221-1250. doi:10.1016/j.rser.2007.01.023
- [53] Luo, X., Wang, J., Dooner, M., & Clarke, J. (2015). Overview of current development in electrical energy storage technologies and the application potential in power system operation. *Applied energy*, 137, 511-536. doi:10.1016/j.apenergy.2014.09.081
- [54] Castillo, A. & Gayme, D.F. (2014). Grid-scale energy storage applications in renewable energy integration: A survey. *Energy Conversion and Management*, 87, 885-894. doi:10.1016/j.enconman.2014.07.063
- [55] Urban Green Council. (2016). *New York City's energy and water use - 2013 report*. New York City, NY, USA: The City of New York's Mayor's Office of Sustainability.
- [56] Urban Green Council. (2017). *New York City's energy and water use - 2014 and 2015 report*. New York City, NY, USA: The City of New York's Mayor's Office of Sustainability.
- [57] Rezaie, B. & Rosen, M.A. (2012). District heating and cooling: Review of technology and potential enhancements. *Applied energy*, 93, 2-10. doi:10.1016/j.apenergy.2011.04.020
- [58] Wahlroos, M., Pärssinen, M., Rinne, S., Syri, S., & Manner, J. (2018). Future views on waste heat utilization– Case of data centers in Northern Europe. *Renewable and Sustainable Energy Reviews*, 82, 1749-1764. doi:10.1016/j.rser.2017.10.058
- [59] Davies, G.F., Maidment, G.G., & Tozer, R.M. (2016). Using data centres for combined heating and cooling: An investigation for London. *Applied Thermal Engineering*, 94, 296-304. doi:10.1016/j.applthermaleng.2015.09.111
- [60] Ommen, T., Thorsen, J.E., Markussen, W.B., & Elmegaard, B. (2017). Performance of ultra low temperature district heating systems with utility plant and booster heat pumps. *Energy*, 137, 544-555. doi:10.1016/j.energy.2017.05.165
- [61] Ommen, T., Markussen, W.B., & Elmegaard, B. (2016). Lowering district heating temperatures–Impact to system performance in current and future Danish energy scenarios. *Energy*, 94, 273-291. doi:10.1016/j.energy.2015.10.063
- [62] Connolly, D. & Mathiesen, B.V. (2014). A technical and economic analysis of one potential pathway to a 100% renewable energy system. *International Journal of Sustainable Energy Planning and Management*, 1, 7-28. doi:10.5278/ijsepm.2014.1.2
- [63] Ebrahimi, K., Jones, G.F., & Fleischer, A.S. (2014). A review of data center cooling technology, operating conditions and the corresponding low-grade waste heat recovery opportunities. *Renewable and Sustainable Energy Reviews*, 31, 622-638. doi:10.1016/j.rser.2013.12.007
- [64] Davies, G.F., Boot-Handford, N., Curry, D., Dennis, W., Ajileye, A., Revesz, A., & Maidment, G.G. (2019). Combining cooling of underground railways with heat recovery and reuse. *Sustainable cities and society*, 45, 543-552. doi:10.1016/j.scs.2018.11.045
- [65] Persson, U. & Münster, M. (2016). Current and future prospects for heat recovery from waste in European district heating systems: A literature and data review. *Energy*, 110, 116-128. doi:10.1016/j.energy.2015.12.074
- [66] ASHRAE. (2016). *2016 ASHRAE Handbook - HVAC Systems and Equipment*: American Society of Heating, Refrigeration and Air-conditioning Engineers.

- [67] Ebrahimi, K., Jones, G.F., & Fleischer, A.S. (2015). Thermo-economic analysis of steady state waste heat recovery in data centers using absorption refrigeration. *Applied energy*, 139, 384-397. doi:10.1016/j.apenergy.2014.10.067
- [68] Lu, T., Lü, X.S., Remes, M., & Viljanen, M. (2011). Investigation of air management and energy performance in a data center in Finland: Case study. *Energy and buildings*, 43(12), 3360-3372. doi:10.1016/j.enbuild.2011.08.034
- [69] Marcinichen, J.B., Olivier, J.A., & Thome, J.R. (2012). On-chip two-phase cooling of datacenters: Cooling system and energy recovery evaluation. *Applied Thermal Engineering*, 41, 36-51. doi:10.1016/j.enbuild.2011.08.034
- [70] Mitchell-Jackson, J., Koomey, J.G., Nordman, B., & Blazek, M. (2003). Data center power requirements: measurements from Silicon Valley. *Energy*, 28(8), 837-850. doi:10.1016/S0360-5442(03)00009-4
- [71] Pärssinen, M., Wahlroos, M., Manner, J., & Syri, S. (2019). Waste heat from data centers: An investment analysis. *Sustainable cities and society*, 44, 428-444. doi:10.1016/j.scs.2018.10.023
- [72] Østergaard, D.S. & Svendsen, S. (2016). Replacing critical radiators to increase the potential to use low-temperature district heating – A case study of 4 Danish single-family houses from the 1930s. *Energy*, 110, 75-84. doi:10.1016/j.energy.2016.03.140
- [73] Yang, X.C., Li, H.W., & Svendsen, S. (2016). Decentralized substations for low-temperature district heating with no Legionella risk, and low return temperatures. *Energy*, 110, 65-74. doi:10.1016/j.energy.2015.12.073
- [74] Yang, X.C., Li, H.W., & Svendsen, S. (2016). Alternative solutions for inhibiting Legionella in domestic hot water systems based on low-temperature district heating. *Building services engineering research and technology*, 37(4), 468-478. doi:10.1177/0143624415613945
- [75] Persson, U. & Werner, S. (2011). Heat distribution and the future competitiveness of district heating. *Applied energy*, 88(3), 568-576. doi:10.1016/j.apenergy.2010.09.020
- [76] New York City Department of City Planning. (2019). PLUTO. Retrieved 1 November 2019 <https://www1.nyc.gov/site/planning/data-maps/open-data.page#pluto>
- [77] Howard, B., Parshall, L., Thompson, J., Hammer, S., Dickinson, J., & Modi, V. (2012). Spatial distribution of urban building energy consumption by end use. *Energy and buildings*, 45, 141-151. doi:10.1016/j.enbuild.2011.10.061
- [78] The City of New York & Department of City Planning. (2013). New York City population projections by age/sex & borough, 2010–2040.
- [79] United States - Department of Health and Human Services & United States - Department of Agriculture. (2015). *2015–2020 Dietary guidelines for Americans*: US Department of Health and Human Services, US Department of Agriculture.
- [80] Hanford, A.J. (2006). Advanced life support baseline values and assumptions document. *Technical Reports*, (3). <http://docs.lib.purdue.edu/nasatr/3/>
- [81] Graamans, L., van den Dobbelsteen, A., Meinen, E., & Stanghellini, C. (2017). Plant factories; crop transpiration and energy balance. *Agricultural Systems*, 153, 138-147. doi:10.1016/j.agsy.2017.01.003
- [82] EnergyPlus. (2016). EnergyPlus 8.6: United States – Department of Energy. Retrieved from www.EnergyPlus.net
- [83] DesignBuilder. (2018). DesignBuilder version 5.3.0.014. Gloucestershire, UK: DesignBuilder Software Ltd. Retrieved from www.designbuilder.co.uk/index.php
- [84] Crawley, D.B., Lawrie, L.K., Winkelmann, F.C., Buhl, W.F., Huang, Y.J., Pedersen, C.O., Strand, R.K., Liesen, R.J., Fisher, D.E., Witte, M.J., & Glazer, J. (2001). EnergyPlus: creating a new-generation building energy simulation program. *Energy and buildings*, 33(4), 319-331. doi:10.1016/S0378-7788(00)00114-6
- [85] Witte, M.J., Henninger, R.H., Glazer, J., & Crawley, D.B. (2001). *Testing and validation of a new building energy simulation program*. Paper presented at the 7th International Building Performance Simulation Association Conference, Rio de Janeiro, Brazil.
- [86] ASHRAE. (2011). ASHRAE Standard 140-2011. Standard method of test for the evaluation of building energy analysis computer programs. Atlanta, USA: ASHRAE - American Society of Heating, Refrigerating and Air-Conditioning Engineers.
- [87] Crawley, D.B. (1998). Which weather data should you use for energy simulations of commercial buildings? *ASHRAE Transactions*, 104, 498-515.
- [88] EnergyPlus. (2018). EnergyPlus weather data by location - Abu Dhabi 412170 (IWEC). Retrieved 30 April 2018 https://energyplus.net/weather-download/asia_wmo_region_2/ARE//ARE_Abu.Dhabi.412170_IWEC/ARE_Abu.Dhabi.412170_IWEC

- [89] EnergyPlus. (2018). EnergyPlus weather data by location - Amsterdam 062400 (IWECC). Retrieved 26 April 2018 https://energyplus.net/weather-location/europe_wmo_region_6/NLD//NLD_Amsterdam.062400_IWECC
- [90] EnergyPlus. (2018). EnergyPlus weather data by location - Kiruna 020440 (IWECC). Retrieved 30 April 2018 https://energyplus.net/weather-location/europe_wmo_region_6/SWE//SWE_Kiruna.020440_IWECC
- [91] Ringkjøb, H.K., Haugan, P.M., & Solbrekke, I.M. (2018). A review of modelling tools for energy and electricity systems with large shares of variable renewables. *Renewable and Sustainable Energy Reviews*, 96, 440-459. doi:10.1016/j.rser.2018.08.002
- [92] Tyagi, V.V., Rahim, N.A.A., Rahim, N.A., & Selvaraj, J.A.L. (2013). Progress in solar PV technology: Research and achievement. *Renewable and Sustainable Energy Reviews*, 20(C), 443-461. doi:10.1016/j.rser.2012.09.028
- [93] Boccard, N. (2009). Capacity factor of wind power realized values vs. estimates. *Energy Policy*, 37(7), 2679-2688. doi:10.1016/j.enpol.2009.02.046
- [94] Lund, H., Hvelplund, F.K., Mathiesen, B.V., Østergaard, P.A., Christensen, P., Connolly, D., Schaltz, E., Pillay, J.R., Nielsen, M.P., & Felby, C. (2011). *Coherent energy and environmental system analysis*: Department of Development and Planning, Aalborg University.
- [95] Kwon, P.S. & Østergaard, P.A. (2012). Comparison of future energy scenarios for Denmark: IDA 2050, CEESA (coherent energy and environmental system analysis), and climate commission 2050. *Energy*, 46(1), 275-282. doi:10.1016/j.energy.2012.08.022
- [96] EnergyPLAN. (2019). EnergyPLAN 15.0. Aalborg, Denmark: Sustainable Energy Planning Research Group, Aalborg University. Retrieved from www.EnergyPLAN.eu
- [97] Connolly, D., Lund, H., Mathiesen, B.V., & Leahy, M. (2010). A review of computer tools for analysing the integration of renewable energy into various energy systems. *Applied energy*, 87(4), 1059-1082. doi:10.1016/j.apenergy.2009.09.026
- [98] Connolly, D. (2015). Finding and inputting data into EnergyPLAN (the FIDE guide): Aalborg University.
- [99] Østergaard, P.A. (2015). Reviewing EnergyPLAN simulations and performance indicator applications in EnergyPLAN simulations. *Applied energy*, 154, 921-933. doi:10.1016/j.apenergy.2015.05.086
- [100] Lund, H. & Zinck Thellufsen, J. (2019). EnergyPLAN - Advanced energy systems analysis computer model - Documentation version 15.
- [101] Lund, H., Thellufsen, J.Z., Aggerholm, S., Wittchen, K.Bj., Nielsen, S., Mathiesen, B.V., & Möller, B. (2014). Heat saving strategies in sustainable smart energy systems. *International Journal of Sustainable Energy Planning and Management*, 4, 3-16. doi:10.5278/ijsepm.2014.4.2
- [102] Mundler, P. & Rumpus, L. (2012). The energy efficiency of local food systems: A comparison between different modes of distribution. *Food Policy*, 37(6), 609-615. doi:10.1016/j.foodpol.2012.07.006
- [103] Mathiesen, B.V., Lund, H., & Nørgaard, P. (2008). Integrated transport and renewable energy systems. *Utilities Policy*, 16(2), 107-116. doi:10.1016/j.jup.2007.11.007
- [104] Choudhury, B., Saha, B.B., Chatterjee, P.K., & Sarkar, J.P. (2013). An overview of developments in adsorption refrigeration systems towards a sustainable way of cooling. *Applied energy*, 104, 554-567. doi:10.1016/j.apenergy.2012.11.042
- [105] Kaiser, E., Morales, A., Harbinson, J., Kromdijk, J., Heuvelink, E., & Marcelis, L.F.M. (2015). Dynamic photosynthesis in different environmental conditions. *Journal of experimental botany*, 66(9), 2415-2426. doi:10.1093/jxb/eru406
- [106] Kaiser, E., Zhou, D., Heuvelink, E., Harbinson, J., Morales, A., & Marcelis, L.F.M. (2017). Elevated CO₂ increases photosynthesis in fluctuating irradiance regardless of photosynthetic induction state. *Journal of experimental botany*, 68(20), 5629-5640. doi:10.1093/jxb/erx357
- [107] Hagen, B., Simonsen, I., Hofmann, M., & Muskulus, M. (2013). A multivariate Markov weather model for O&M simulation of offshore wind parks. *Energy Procedia*, 35, 137-147. doi:10.1016/j.egypro.2013.07.167
- [108] NOAA. (2019). National Oceanic and Atmospheric Administration (NOAA) - Station 028630 (Kemi I Lighthouse, Finland). Retrieved 15 December 2019 <https://gis.ncdc.noaa.gov/maps/ncei/cdo/hourly>
- [109] FMI. (2019). Finnish Meteorological Institute (FMI) - Station 028630 (Kemi I Lighthouse, Finland). Retrieved 15 December 2019 <https://en.ilmatieteenlaitos.fi/download-observations#!/>
- [110] KNMI. (2019). Royal Netherlands Meteorological Institute (KNMI) - Station 062050 (A12-CPP, the Netherlands). Retrieved 15 December 2019 https://www.knmi.nl/nederland-nu/klimatologie/uurgegevens_Noordzee

- [111] NOAA. (2019). National Oceanic and Atmospheric Administration (NOAA) - Station 062050 (A12-CPP, the Netherlands). Retrieved 15 December 2019 <https://gis.ncdc.noaa.gov/maps/ncei/cdo/hourly>
- [112] NOAA. (2019). National Oceanic and Atmospheric Administration (NOAA) - Station 412165 (Sir Abu Nair, the United Arab Emirates). Retrieved 15 December 2019 <https://gis.ncdc.noaa.gov/maps/ncei/cdo/hourly>
- [113] Scheu, M.N., Matha, D., & Muskulus, M. (2012). *Validation of a Markov-based weather model for simulation of O&M for offshore wind farms*. Paper presented at the 22nd International Offshore and Polar Engineering Conference, Rhodes, Greece.
- [114] Carrillo, C., Obando Montaño, A.F., Cidrás, J., & Díaz-Dorado, E. (2013). Review of power curve modelling for wind turbines. *Renewable and Sustainable Energy Reviews*, 21, 572-581. doi:10.1016/j.rser.2013.01.012
- [115] Engineering ToolBox. (2009). Wind Power. Retrieved 15 December 2019 https://www.engineeringtoolbox.com/wind-power-d_1214.html
- [116] Royal Academy of Engineering. (2010). Wind turbine power calculations. from RWE npower renewables <https://www.raeng.org.uk/publications/other/23-wind-turbine>
- [117] ASHRAE. (2017). *2017 ASHRAE Handbook - Fundamentals (SI Version)*: American Society of Heating, Refrigeration and Air-conditioning Engineers.

INTERMEZZO 5

To achieve technical and economic viability, the high energy requirement of plant factories has to be offset by increased productivity of other resources and/or services. Chapter 5 illustrated the potential for recovery and reuse of heat from plant factories in the urban energy system. The integration of the urban and horticultural systems provides opportunities for the exchange of resources, a reduction in the total energy demand and the modulation of electricity use to match fluctuations in the supply of renewable energy.

On the one hand, a flexible operation of plant factories is important to adequately match the fluctuations of an energy system that predominantly or exclusively relies on intermittent energy sources. On the other hand, for plant factories to be feasible they must operate above a minimum amount of hours per year. The technical manner in which urban and horticultural systems can be integrated will depend highly on local climate, energy demand and energy production. In the end, the sophistication and integration of the essential networks will determine the resilience of cities in the future.

Chapter 6 synthesises the results obtained throughout this study. It will give the main conclusions and recommendations for future development and potential applications.



6 Conclusions and outlook

6.1 Conclusions

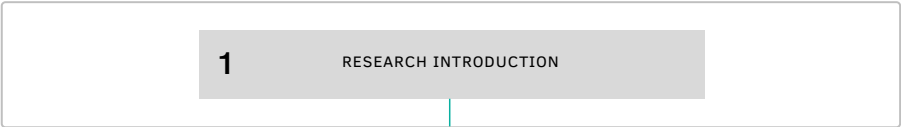
Exploring alternative methods for food production is imperative. Such methods could offer perspective on resilience to climate change and on meet the rising demand for food by a growing (urban) population. Plant factories provide means to extensively control the production climate, independently of exterior climate or location. Closed production systems have already been used successfully in research settings and are gaining a foothold in industry. However, it is necessary to quantify the resource use efficiency of plant factories to determine their effectiveness as a method for urban food production. To this end, this study has analysed their performance across different scales, from leaf to facility to city. Performance was calculated for a variety of climates, from subarctic (Kiruna, Sweden) to temperate oceanic (Amsterdam, the Netherlands) to hot desert (Abu Dhabi, the United Arab Emirates). An important first step was to accurately model the crop energy balance, as the closed nature of plant factories limits the influence of the exterior climate and will amplify the impact of the internal energy loads.

6.1.1 System configuration

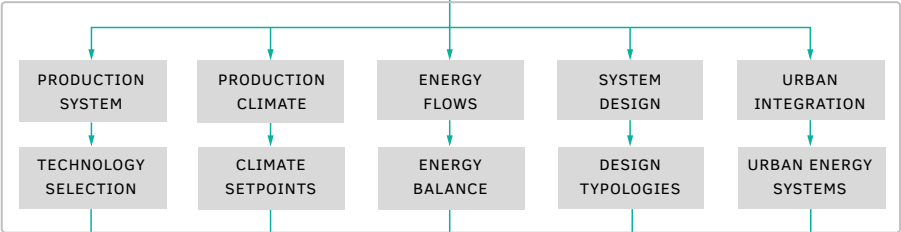
How can the crop energy balance be calculated using the production climate in order to determine the vapour production and energy exchange by the crop canopy?

Firstly, the crop energy balance of plant factories was formulated. To this end, the Penman-Monteith crop transpiration model, or the 'big leaf' model, was used

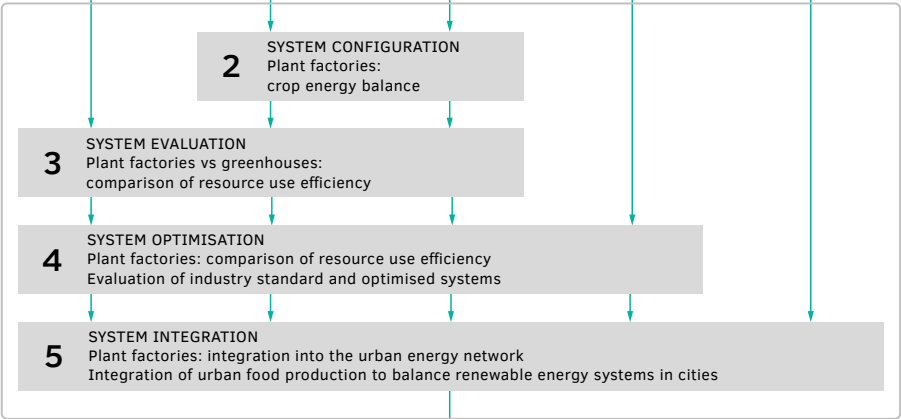
I. INTRODUCTION & METHODOLOGICAL FRAMEWORK



II. THEORETICAL FRAMEWORK



III. DESIGN & EXPERIMENTAL VALIDATION



IV. INTEGRATED DISCUSSION



to calculate the crop energy balance and explicate the energetic fluxes. Penman demonstrated that crop transpiration is primarily a physical process, and Monteith explicitly identified the parameters that are affected by the crop. The three-dimensional crop canopy was reduced to a one-dimensional 'big leaf' where net radiation is absorbed, heat is exchanged and water vapour escapes. By formulating net radiation, aerodynamic resistance and surface resistance, the model could be used in a predictive setting. The formulated model was able to calculate the distribution of radiation converted to sensible heat and latent heat, as well as the corresponding vapour production. Experimental validation showed that the model predicted the transpiration of the lettuce crop with great accuracy for different lighting intensities, air humidity levels and stages of development (cultivation area cover and leaf area index).

Given these results, the model is considered suitable for a realistic simulation of the vapour flux associated with the production of lettuce in plant factories. It does not require extensive empirical data and can therefore readily provide an accurate estimate for a range of closed production climates. Transpiration can be integrated effectively as a design parameter and the total energy profile of plant factories can be assessed in detail. The model was therefore used throughout this study to analyse and optimise the design of plant factories.

6.1.2 System evaluation

What is the resource use efficiency of water, energy, CO₂ and land area for crop production in plant factories in comparison to greenhouses?

Secondly, the performance of plant factories for crop production was analysed in comparison with greenhouses. Performance was calculated as the combined resource use efficiency for electricity, water, CO₂ and land area. The required input and output for food production were calculated, analysed and compared for the three aforementioned climates, to determine the influence of the exterior climate on the production requirements and the relative performance of plant factories. In practice, the suitability of a production system will not be determined only by a single resource use efficiency but in part by the local availability of each resource.

The results indicated that fully closed plant factories did indeed achieve higher resource use efficiencies for water, CO₂, land area and energy than greenhouses. They also indicated that the greenhouses were more efficient with respect to purchased energy (read: electricity) in all three climates: The advantages of

transparent facades outweighed their disadvantages. The advantage is free solar energy and the disadvantages are the increased need for cooling in hot desert climates and the need for heating in subarctic climates. The advantages were smallest in subarctic climates, where the difference in electricity use efficiency between greenhouses and plant factories was minimal. Separate calculations at a lower PPFD ($250 \mu\text{mol m}^{-2} \text{s}^{-1}$) and higher LED efficiency ($3 \mu\text{mol J}^{-1}$) even found that the plant factory could achieve a better electricity use efficiency than the greenhouses.

Greenhouses in the most extreme climates (subarctic and hot desert climates) were not viable without advanced techniques for climate control, such as artificial lighting and active cooling. The optimal system would likely show a gradual shift aligned with latitude and exterior climate, from a nearly natural to a fully controlled interior production climate. The applicability of each system is closely related to the electricity use efficiency, which will in part determine the suitability of plant factories compared with greenhouses. In short, plant factories already offer opportunities for food production in locations where water, CO_2 or land area are scarce. The biggest disadvantage is their low electricity use efficiency.

6.1.3 System optimisation

How can façade and climate system design reduce the resource requirement for crop production in plant factories?

Thirdly, the energy and electricity use efficiency of plant factories were improved by optimising the building and systems design. The energy use for food production was calculated, analysed and compared for the three selected climates. The annual energy demand consisted of 50% for lighting, 2% for heating, 34% for dehumidification and 14% for sensible cooling, when averaging all investigated variants. Understandably, the existing literature was primarily focused on improving lighting equipment efficiency to reduce total VF energy use. Little to no research existed on improving the building design and systems engineering for high internal heat loads.

From this perspective, the dissipation of heat across conductive façades proved to be the most effective design strategy to reduce energy expenditure in all three climates. This passive approach limited the need for forced air extraction and cooling via the HVAC system and consequently reduced the total energy demand (-9.5 to 12.5%) and electricity demand (-0.3 to -2.3%). From the perspective of electricity use,

minimising the energy requirement for crop photosynthesis proved most effective. This suggested that the technological advancement of LED photosynthetic efficacy is paramount, but not the only available strategy. Transparent façades and solar radiation directly reduced the operation of the LED system and consequently the total electricity use of the facility (-7.4 to -9.4%).

Standard practice for both plant factories and sustainable buildings has been focused on minimising excessive heat gain or loss via the façade. In plant factories this is achieved through high insulation values, regardless of the local climate; in buildings it is generally achieved through compact geometries. Conversely, this study showed that dissipation of internal heat through the façade can result in a lower total energy demand in each investigated climate. Furthermore, altering the wall-to-floor ratio of the building can amplify the targeted positive effects of the façade in certain climates. In short, optimising the façade for the dissipation of the internal heat resulted in a given amount of heat being exhausted from plant factories at a significantly lower electricity expenditure. This study has thereby offered perspective for facilities with high internal heat loads but also presented a new challenge: the reuse of residual heat.

6.1.4 System integration

How can plant factories be integrated in the urban energy network to exchange resource streams with surrounding urban functions and reduce the resource requirement of the joint system?

Finally, the residual heat from plant factories was integrated into the urban energy network of cities of the future. That network prioritised local food production and energy from renewable sources. Production from renewable sources varies with weather conditions, resulting in an intermittent energy supply. This study investigated how plant factories could serve as flexible heat production units to reduce the imbalance between energy production and demand. To this end, the energy demand, renewable energy distribution and energy imbalance were calculated for a simulated city in the aforementioned three climates.

The results indicated that adjusting the distribution of solar and wind energy to the local climate was the most effective way to reduce energy imbalance in all climates. The use of residual heat from plant factories was an effective strategy to balance the energy system in climates with high heating demands, but it was of little benefit in climates with low heating demands. The cultivation area necessary for local fruit

and vegetable demand produced sufficient heat for most locations. Integrating plant factories and thermal storage decreased energy imbalance by 41.3%, 38.9% and 11.8% for a city in a temperate oceanic, subarctic and hot desert climate, respectively. The hot desert climate featured high cooling demands, which could not effectively be met using residual heat, as well as low heating demands, which were readily covered by the plant factory with few operational hours.

The operation strategy of the integrated plant factories greatly influenced their merits. On the one hand, a flexible operation allowed for greater balancing of the energy system but reduced the number of fullcapacityequivalent hours per year, which would in turn negatively impact food production. On the other hand, a consistent, cyclic operation would likely benefit food production. However, it was shown to reduce flexibility, increase imbalance and to put additional pressure on the energy system. This calls for a compromise between a flexible operation to minimise energy system imbalance and a consistent operation to maximise food production. In short, plant factories can balance the energy system by operating during hours with excess electricity production to produce heat directly for the city or for available thermal storage capacity. However, this strategy is only effective in climates dominated by considerable heating demand.

6.1.5 **STACKED method**

The main objective of this research was to quantify the resource use efficiency of plant factories and explore their potential as a system for urban food production and ultimately, to improve it. Research on and in closed production systems, such as plant factories, had been around for decades, but a clear method to assess their broader potential had not yet been formulated. The STACKED method developed here is comprised of various modules, or sub-models for crop energy balance, crop production, climate system performance, facility energy use, urban energy use, synthetic climate time series and urban energy systems (Figure 6.1). Naturally, each sub-model represents a compromise between realism and simplicity, requiring numerous assumptions. The novelty and strength of the STACKED method lies in the integration and contextualisation of the modules across multiple scales. In the future, the various sub-models can be further validated, updated, expanded or replaced in accordance with technological advances or specialist insights.

Using the STACKED method, plant factories were calculated to achieve a significantly higher water use efficiency and CO₂ use efficiency than most greenhouses. However, because the systems are fully closed, the electricity use efficiency is lower. In a plant

factory, all energy has to be introduced and extracted from the system, requiring electricity. Several strategies were investigated to reduce this energy and electricity use in plant factories, but the most effective strategy was to include a key feature of greenhouses: the use of sunlight for photosynthesis. The key advantage of plant factories with respect to resource use efficiency is the density of production and the resulting land use efficiency. The advanced climate control allows for a high production capacity per cultivation area, as well as for predictable crop cycles.

Among all food production systems, plant factories show the greatest potential for producing food in cities, due to their independence from the external climate, their production capacity and the possible advantageous integration in urban energy systems. However, they are not the most efficient production system to address the projected increase in global food demand with respect to electricity use and environmental impact. For the future, the likely solution lies in combining systems, each optimised for extensive (high caloric) crops and intensive (fresh) crops.

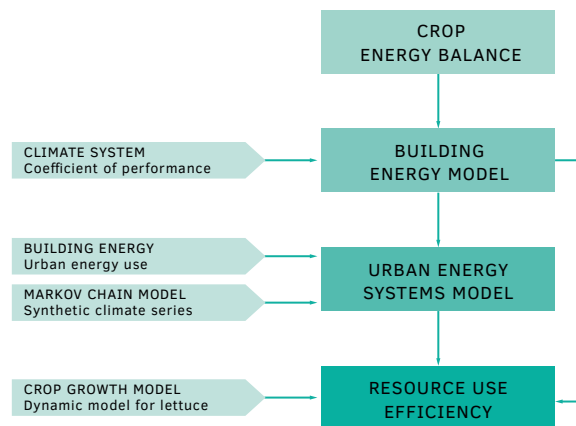


FIG. 6.1 Simplified overview of the method and modules.

6.2 Method evaluation

A model has to find a compromise between realism and simplicity, and this one was no exception. This section addresses the key strengths, weaknesses, simplifications and exclusions of the method.

6.2.1 System configuration

The crop energy balance model was designed for the simulation of plant factories. In the model, microclimate influences transpiration rate primarily through the available shortwave radiation, the ambient temperature and humidity. Select processes were simplified and certain aspects were not included. For example, the performance of the transpiration model can still be improved by integrating crop growth, e.g. incorporating a dynamic LAI and cultivation area cover. This would allow for a more accurate simulation throughout the different crop stages and crop respacing. The accuracy of the model could be increased by incorporating more sophisticated sub-models for determining stomatal and aerodynamic resistance.

The model described in Chapter 2 provided a solid foundation for future simulations of plant factories by offering insight into the role of plant processes in the total energy balance. In theory, the model can be applied to different crops and production climates. Additional validation is deemed necessary for a broader range of climate conditions and for crops with different morphologies. Within the scope of this study, the model provided a realistic simulation of the crop energy balance associated with the production of lettuce.

6.2.2 System evaluation

The performance of plant factories was analysed and compared with that of greenhouses. The analysis integrated the crop energy balance model with a lettuce growth model and advanced climate models for greenhouses and buildings. It did not include certain aspects. Firstly, the system design and climate set-points were not optimised for maximum production in each climate. Optimisation could have improved the performance of greenhouses in particular. Secondly, the sensitivities of the crop growth model to air temperature were not addressed.

The crop growth model was extensively validated for greenhouses but not for the elevated temperatures of plant factories, which presumably resulted in an underestimation of production. Thirdly, the energetic behaviour of the crop was not calculated dynamically. Rather, it was standardised for the climate setpoints during photoperiods and dark periods. The dynamic calculation of a linked production climate and crop energy balance would increase the accuracy of both. The impact was minimal, as the closed production environment was closely aligned with the set conditions. Finally, an extensive validation of the integrated model was not possible due to insufficient data on plant factories.

The model described in Chapter 3 provided insight into the resource use of plant factories and greenhouses. The outcome that plant factories would require higher (purchased) energy input due to artificial lighting might have been foreseen but had never been quantified in detail. In the future, the model can be applied to additional locations and incorporate the suggested improvements listed above. Within the scope of this study, the analysis indicated that designs should be optimised for the local scarcity of resources. Furthermore, it quantified the main challenge of plant factories: low electricity use efficiency.

6.2.3 System optimisation

The energy use efficiency of plant factories was improved by optimising the building and systems design. The effects of passive climate control and façade design on energy use for cooling, dehumidification, heating and lighting were investigated. The analysis incorporated a detailed model for the climate system to accurately calculate passive cooling, as well as the coefficient of performance and electricity use of active cooling. Numerous assumptions had to be made in the design of the cooling system. A literature study on the standard design and operation of vapour compression refrigeration cycles and heat exchangers informed these assumptions. Specialised insight and models would be needed to further optimise the performance of the climate system.

With respect to lighting, transparent façades and solar radiation were shown to reduce the operation time of the LED system and, as a result, to reduce electricity use. The increased influence of the exterior climate on the production climate was included in the model, but local disturbances and their potential effect on crop development were not quantified.

The model described in Chapter 4 was able to calculate the resource use of plant factories in greater detail and explore various system designs. Its modular approach (depicted in Figure 6.1) allows technological advancement and specialised models to be integrated with relative ease. Within the scope of this study, it illustrated how plant factory designs could be optimised for their climate and location.

6.2.4 System integration

The residual heat from plant factories was integrated in the urban energy system, to balance energy production and demand, within a green-power grid. The energy demand, renewable energy distribution and energy imbalance were investigated for a simulated city incorporating plant factories on a large scale in three climate zones. Certain aspects were not included in this study. Firstly, the effects of a stochastic light distribution on crop growth were not fully understood and were therefore not incorporated in the crop growth model. The investigation, modelling and validation of these processes were considered to lie beyond the scope of this study. Secondly, an algorithm to optimise the duration and flexibility of operation in plant factories was not included. This algorithm could determine the correct balance between maximising food production and minimising energy system imbalance. Thirdly, an extensive thermodynamic analysis could provide more detailed insight into the energy and exergy efficiency of the energy system. Finally, other technologies that produce heat at a higher coefficient of performance should be incorporated. For example, central heat pumps can provide a flexible operation similar to that of plant factories with less electricity, but without a valuable industrial by-product: food.

The model described in Chapter 5 incorporated modules tailored for urban energy use, climate series, and regional energy systems as a first step toward identifying the energetic consequences of food-resilient cities. The presented strategies can reduce energy imbalance and provide a foundation for an integrated energy system design tailored to the local climate. In the future, the model can be applied to additional locations and incorporate the various suggested improvements listed above.

6.2.5 STACKED method

The main objective of this research was to quantify the resource use efficiency of plant factories and explore their potential as a method for urban food production. Existing studies typically focus on a single scale, situation or location, which

prevented drawing comparisons. The STACKED method analysed performance across multiple scales, from leaf to facility to city. The model can be applied to different climates, locations or situations to calculate the potential of plant factories. Unfortunately, the construction of a large-scale plant factory for extensive experimentation and validation was not feasible under the time and financial constraints of this project.

This research therefore focused on the development and combination of various models. Being inherently abstractions of reality, these models were based on numerous assumptions and simplifications. Established models that had been extensively validated were therefore used. New models were validated through experiments, in order to ensure reliable results. Extensive validation of the integrated model was not possible, because sufficient data on plant factories was not accessible. In the end, the STACKED model offered detailed insights into resource use efficiency, but also illuminated several new challenges (see Section 6.4).

6.3 Broader implications

Both the feasibility and effectiveness of plant factories depend on a variety of factors. This section discusses the implications of this study for the role that plant factories play in the security, quality, sustainability and socio-economic aspects of food production.

6.3.1 Food security

One of the great challenges of this century is to keep up with increasing nutritional demand in the context of limited natural resources, climate change, population growth and extensive urbanisation. Crop production and the food supply network are both subject to various disturbances, which may limit food availability, accessibility and stability.

Food production is put at risk by global resource constraints, structural climate change and extreme weather events. This study has shown that plant factories can effectively reduce pressure on the most limited resources: water and land

area. Furthermore, plant factories were shown to exercise greater control over the production climate, reducing the impact of climate variability and long-term climate change when compared to traditional agriculture. However, prioritising global food production in plant factories in light of climate change would be counterproductive. Unless only renewable or nuclear energy is used, the high electricity use of plant factories would likely only exacerbate CO₂ emissions and long-term climate change. The system should therefore primarily serve areas most at risk.

Food supply networks focus on just-in-time management, which puts them at risk in times of large disturbances. Urban centres were of particular interest in this research, as they are amongst the most vulnerable locations. This study did not investigate the role of plant factories in shortening supply chains, nor their capacity to scale up or respond effectively during times of crisis. Instead, it provided a quantified foundation for determining the environmental and economic impacts of localising food production. The system is technically capable of localising food production, but its effectiveness needs to be further investigated.

In short, plant factories can improve food security and resilience for a broad range of future climate conditions by exercising greater control over the production climate. However, the associated costs and electricity use efficiency are expected to limit their effectiveness.

6.3.2 Food quality and diet

Plant factories have been promoted to ensure a consistent production of nutritious, high-quality crops that could shift the diet of consumers. The nutritional content of crops, the effects of shorter supply chains on crop quality and the impacts of individual and global diet were beyond the scope of this study.

Steering the nutritional content and quality of crops requires extensive control over the production climate. This study has illustrated that limiting influences from the exterior climate allows plant factories to more precisely control the production climate than traditional agriculture and produce in any location or season. The effects of the microclimate on crop production need to be further investigated for this level of climate control to become effective.

6.3.3 Sustainable production of food

The global food system has one of the largest environmental impacts of any industry and places significant pressure on global natural resources. Modern agriculture is partly responsible for and directly vulnerable to climate change. The sustainability of the system could be improved by reducing the resources required for crop production and transport.

Transport contributes relatively little to the total emissions attributed to most agricultural products or diets. This study did not investigate the environmental impact of reducing transport distance, nor of completely shifting to local food production in plant factories. Instead, it provided a quantified basis for determining these impacts. A detailed life cycle assessment is necessary to determine the merit of producing locally.

Crop production and land use change make up the largest share of total food system emissions. The effectiveness of plant factories will therefore primarily depend on their resource use efficiency. In this study, higher climate control resulted in higher resource use efficiencies for water, CO₂ and land, but at the cost of lower electricity use efficiency. Moreover, this study highlighted the importance of the local situation with respect to climate, resource availability and energy system. As explained in Section 6.3.1, prioritising food production in plant factories would be counterproductive with respect to environmental impact when using non-renewable energy sources. Local resource availability will determine whether a plant factory will be beneficial or detrimental to the climate. A full life cycle assessment of plant factories is necessary, but that was beyond the scope of this study.

In short, the environmental impact of plant factories is closely related to the local availability of resources and energy mix. Whether or not to use them for local food production should therefore be carefully considered.

6.3.4 Economic impacts

This study addressed only the technical aspects of plant factories, whereas their viability also has financial determinants. The required price of a crop of lettuce and the perceived value to the consumer were not included in this study.

To forgo solar energy increased the energy use and consequently the operational expenses of plant factories, compared to other production systems, despite the

higher efficiency of usage for all other resources. Additional product value would need to offset this increase in operational costs. Plant factories could create this value through improved logistics (e.g. precisely timed supply), improved quality (e.g. crop freshness), increased nutritional content (e.g. steering the development of metabolites), risk reduction (e.g. minimal risk of pathogens or need for protective chemicals), transport reduction (e.g. lower transport costs) or other marketing advantages (e.g. novelty and customer appeal). This study provided detailed, quantitative input on key operational expenses to expedite the financial assessment of plant factories.

6.3.5 Social impacts

Plant factories are still in an early stage of development and remain largely unknown to the public. Neither public perception nor societal impact were covered in this study. The perception of sustainability, ethical aspects and general social acceptance will vary for each novel technology. In this regard, food production is a particularly contentious topic. Possible social barriers to the operation of plant factories are their unclear benefits, concerns about health risks, a lack of familiarity with the crops, ethical concerns regarding global versus local production, or even an outright rejection of food produced in high-tech systems. The overview presented in this study offered insight in the technological potential and benefits of food production in plant factories, but social barriers should be investigated and addressed accordingly.

6.4 Recommendations for future research

Realisation of plant factories in the future will depend on research in various domains. Recommendations for future research are listed below.

Scale of the crop

Crop selection

Lettuce or other leafy greens alone will not be able to satisfy global food demand. Additional research is necessary to determine the performance of plant factories

for the production of other foods. Staple crops and protein-rich crops are of particular interest.

Crop measurements

Detailed crop measurements during production are necessary to study the optimal production climate and unravel the relation between phenotype and genotype. Continuous, non-destructive measurements can provide new insight into crop growth that can benefit plant breeding, the production climate and systems design in agriculture. The development of new sensors or applications for hyperspectral imaging is of particular interest.

Production climate

The impact of production climate and cultivation strategy on crop development will determine the systems design of the future. Further research into the universal and specific biological responses of crops to air temperature, root-zone temperature, ventilation, humidity, nutrient supply, light intensity, light spectrum and light duration is paramount. Species-specific parameters have to be investigated.

Photosynthetic efficiency

Genetic engineering can improve the photosynthetic processes and the yield potential of crops. To this end, approaches and technologies will need to be studied, including new breeding techniques such as genome editing for the modification of endogenous genes and synthetic biology to produce designer promoters and proteins. The potential hazards for existing plant life need to be carefully examined.

Scale of the facility

Software integration

It is necessary to further integrate existing and new sub-models in a comprehensive simulation program for plant factories. These models could be used to describe, analyse and simulate crop processes through data-integration, artificial intelligence and machine learning. This integration would allow us to better understand, describe and analyse reality, as well as to simulate crop and system behaviour more accurately.

Lighting systems

Among the components of the climate system, the lighting system requires the most electrical energy, exceeding the HVAC, fans and pumps. The energy use efficiency of plant factories can therefore be improved by high efficiency lighting systems, crop spacing during growth cycles to maximise light interception, and crop varieties

optimised for plant factory production. Research into improving the photosynthetic efficacy ($\mu\text{mol}_{\text{PAR}} \text{J}^{-1}$) of different LEDs producing different wavelengths is imperative.

Climate control - transpiration

The explicit use of transpiration as a set-point, as opposed to temperature and relative humidity for climate control in plant factories, should be investigated. This approach encompasses multiple variables and should be able to increase the efficiency of climate control.

Climate control – spatial uniformity

Spatial variation in the production climate can significantly affect plant growth and development. Methods to guarantee adequate air supply, treatment and circulation should be investigated in greater depth. Computational Fluid Dynamics may prove instrumental in studying airflow patterns and climate homogeneity.

Scale of the region

Urban energy systems

Integration into the broader city is a key element in conceptualising urban food production. Additional research is needed on the practical exchange of (residual) energy between adjacent urban functions. The efficiencies of energy conversion, storage and transport in such integrated energy networks are of particular interest.

Circular systems

An investigation of the further integration of food production into the urban system is essential to determine the future of circular cities. The integration of food production with urban energy, water, material and nutrient flows could be an important strategy in closing several loops and reducing waste streams. The technical, biological and financial feasibility of such complex circular systems need to be investigated.

Financial assessment

Additional research is required on the economic viability of plant factories, including financial aspects concerning investment costs, operational costs and market characteristics. Comparisons with traditional production systems and supply chains can inform growers, investors and policy makers.

Scalability of plant factories

It remains uncertain whether local production systems and plant factories have the capacity to scale up or respond effectively during times of crisis to cover regional

food demand. The technical, logistical, structural and regulatory barriers and repercussion to upscaling should be further investigated.

Scale of the planet

Long-term climate change

Further research into the effects of climate change and extreme weather events on the global food production is recommended. Long-term climate change and short-term climate variability will likely exceed our historical experiences. The question is how much of a headwind climate change could present in the race to keep productivity growing as fast as demand at the global scale.

Life cycle assessment

A thorough inventory of the energy, resources and materials that are required across the industry value chain of plant factories is required to calculate the corresponding emissions to the environment. The aim should be to document and improve the overall environmental footprint of global food production. In the light of climate change, especially the carbon-equivalent footprint of food production is extremely relevant.

Social impact

The level of acceptance by the general public of plant factories remains unclear. The impact of accelerating external factors such as pandemics, extreme climate events or severe environmental degradation and the public awareness thereof should be investigated. Policy and legal frameworks are considered important conditions, laying the foundation for a successful dissemination of innovative food production.

Scale of the universe

Extraterrestrial food production

A critical component of manned space exploration and migration to other planets will be the continuous supply of food. Cultivating food in closed-loop systems will become integral to future missions outside of the EarthMoon system. Construction demands and the interfaces between the production system and the other modules of regenerative life support systems are of particular interest.

6.5 Outlook

Vertical farms or plant factories have often been heralded as a transformative technology that will shape our future. In recent years, they have drawn the interest of a large number of stakeholders, ranging from consumers, policy makers and investors, to scientists, engineers and even growers. Dense, metropolitan areas would no longer have to depend on the global food network and inhabitants could enjoy locally produced, fresh, high-quality crops. Structurally vacant buildings in the heart of the city could be transformed into plant factories. The technology would revolutionise the global agricultural system and minimise its spatial and environmental footprints. This study has illustrated the limitations of these strategies, as well as their potential. Over the past years, the plant factory has become one of the idols of a futuristic world. In that sense, it exists in the interplay between science fiction and reality.

Several actionable insights were identified to bring plant factories closer to the latter in the foreseeable future:

- 1 The development of crop models that link the crop blueprint (genome map) and expected plant responses to the actual plant status in real-time via sophisticated plant-based sensors.
This development will take advantage of the extensive climate control that plant factories offer and will enable an optimal growing strategy.
- 2 The development of lighting systems with increased effectiveness and photosynthetic efficacy.
 - a In the short term, designing lighting systems to optimise light interception and to enable an efficient collection of residual heat will improve the energy effectiveness of plant factories.
 - b In the long term, an improved photosynthetic efficacy of lighting systems for all wavelengths within photosynthetically active radiation will reduce the operational energy use of plant factories to a certain extent.⁸
- 3 The exploration and optimisation of the production of high-value-added crops.

⁸ This development will diminish the future value of plant factories in balancing the energy network.

The production of high-value crops, which can be optimised by plant factories, will increase revenue to offset the high operational expenses and investment costs.

- 4 The predominant use of renewable sources for energy production and storage
Renewable energy will reduce the environmental impact of the low energy use efficiency of plant factories.
- 5 The design of plant factories tailored to local climate and integrated into local (urban) energy systems.
A tailored design will reduce the resource requirement of plant factories.
Furthermore, a design integrated within the urban energy network will improve the energy effectiveness of the system as a whole.

The objective of growers should always be to select the production method best suited for their crop: one that can produce crops of maximum quality with a minimum input of resources. In this case, the objective to start with a plant factory is backward reasoning. Researchers, on the other hand, aim to devise strategies to improve the nature of our future food supply. The plant factory can offer unprecedented insights into crop behaviour, production climate and crop genetics. These insights can then be implemented in agriculture across the world, at various technological levels, and thus improve the sustainability and resilience of the global agricultural system.

The plant factory is not the answer to current global issues. In the current market, the demand for fine-tuned crops is insignificant. In the current supply network, the need for structural, hyperlocal crop production is minimal. In the current climate, excluding freely available solar energy increases energy use for most locations. The plant factory is the answer to the questions that have not been asked yet.

Summary

Expanding cities across the world rely increasingly on the global food network, but should they? A steady population growth, extensive urbanisation and quantifiable climate change place pressure on this network, bringing its resilience into question. Perspectives for a robust urban agricultural network may lie in the development of local food production systems. The dense metropolitan area, however, presents a challenging climate for crop production. The first modern greenhouses were built to protect crops from the exterior climate. Over the past centuries their design has been optimised with developing technologies to enhance control over the production climate. Plant factories or vertical farms are the most recent product of the search for absolute control over the production climate and consequently crop production. In plant factories, crops are produced in vertically stacked layers inside a closed environment with extensive climate control. LED systems are used for illumination and hydroponic systems are generally used for the delivery of water and nutrients to the crop. Plant factories have already been promoted to ensure global food security, improve food quality and increase the sustainability of food production and supply. The question remains whether the extensive climate control that plant factories offer is necessary, effective and/or efficient. The main objective of this research was to quantify the efficiency of plant factories and explore their potential as a method for urban food production. The STACKED method was developed with this objective in mind.

Chapter 1 is the introduction to this thesis. The numerous benefits of plant factories that had been mentioned in popular media were discussed, focusing on food security, quality and sustainability. Until now there was no format available to provide a detailed insight into the technical potential of plant factories, particularly for the urban context. The agricultural and building engineering disciplines are independently extensive, but there was no comprehensive research that covered the system design, design implications and performance assessment of a plant factory. Performance was assessed by analysing the resource requirements of plant factories for the production of fresh vegetables, also known as the resource use efficiency. In order to adequately determine the resource use efficiency this research had to connect multiple scales: from the crop, to the individual plant factory, to the city as a whole. These connections and the study design are explained.

Chapter 2 describes the crop energy balance. Insight into the explicit role of plant processes in the total energy balance of production systems is required to determine the potential of these systems. The crop directly impacts its environment by absorbing radiation, exchanging heat with the surrounding air and transpiring water vapour. The vapour flux and the relation between sensible and latent heat were key to calculating the energy requirement of plant factories. Using the Penman-Monteith equation, the three-dimensional crop canopy was reduced to a one-dimensional ‘big leaf’ where net radiation is absorbed, energy is exchanged and water vapour escapes. Methods for determining the aerodynamic resistance and the stomatal resistance were formulated to use the Penman-Monteith equation in a predictive setting. Subsequently, the model was validated for the effects of photosynthetic photon flux density, cultivation area cover and vapour concentration deficit. We conclude that the crop energy balance model was able to determine the relation between sensible and latent heat exchange from the crop canopy.

Chapter 3 investigates the resource use efficiency of lettuce production in plant factories and in greenhouses. To this end, the crop energy balance model was combined with existing models for crop growth and building energy to calculate resource use efficiency. The energy, electricity, water, CO₂ and land area use of plant factories was calculated and compared with those in greenhouses. Three different climates and latitudes were studied to illustrate the effect of external climate and to explore the limitations of the model. Plant factories demonstrated a higher resource use efficiency for water and CO₂ as a result of their closed nature, as well as for land area due to the high crop yield per production area and stackable production layers. The electricity use efficiency, however, was notably lower in plant factories across the three climates. This primarily results from the predominance of artificial illumination in the total energy balance and to a lesser extent from the high internal heat loads. We conclude that the potential of plant factories as a method for urban food production can be improved by increasing their electricity use efficiency.

Chapter 4 describes the systems design for improving energy and electricity use efficiencies of plant factories. The impact of the façade and cooling system design was analysed in greater detail. Submodels for calculating the coefficient of performance of the climate system were developed and integrated. The calculations provided insight into the effects of operation schedule, cooling system design, form factor and façade design on the energy and electricity use of plant factories. We analysed the effects of transparency, insulation, albedo, solar heat gain coefficient and wall-to-floor ratio on total energy use. This chapter illustrated the potential of passive measures to reduce energy use, such as the dissipation of internal heat through the façade and the use of solar radiation for photosynthesis. We conclude

that this passive approach reduces the energy use for climate systems and increases the energy use efficiency of the plant factory, albeit to a limited extent.

Chapter 5 describes the potential for recovery and reuse of heat from plant factories in the urban energy system. The integration of the essential networks (energy, food, water, supplies and data) will determine the resilience of cities in the future. In this study, the effects of local food production on the urban energy balance were calculated for various scenarios. Where in Chapter 4 excess heat from plant factories was dissipated to the ambient air, this chapter investigated how it could be integrated in the urban energy network. Alternative strategies were investigated where plant factories were used to balance an energy system that predominantly or exclusively relies on intermittent energy sources. In other words, could plant factories use excess renewable energy production to provide heat and food for the city? On the one hand, a flexible operation of plant factories can adequately match the fluctuations of such an energy system. On the other hand, for plant factories to be feasible they must operate above a minimum number of hours per year. We conclude that the technical manner in which urban and horticultural systems can be integrated will depend highly on the urban design, local climate, energy demand and energy production.

Chapter 6 synthesises and discusses the results obtained in this study. It gives the main conclusions and makes recommendations for future development and potential applications. To accomplish the main objective of this research, the STACKED method was developed. The corresponding model was able to analyse the performance of plant factories across multiple scales, from leaf to facility to city. Existing studies typically focused on a single scale, situation or location, which limited the type of comparisons that may be drawn. The method in this study was designed to be applicable to different climates, locations and situations. The required model assumptions and simplifications were discussed in this chapter. In the end, the STACKED model offered detailed insights into resource use efficiency of plant factories, but also illuminated several new challenges and opportunities. Several actionable insights were identified to improve the feasibility of plant factories in the foreseeable future. One key insight was that the optimal production system follows a gradual shift from a nearly natural to a fully controlled interior production climate, depending on location. The design of plant factories should therefore always be tailored to the local climate, context and market: one size does not fit all.

Samenvatting

Overall ter wereld is de bevolking van grote steden in toenemende mate afhankelijk van het internationale voedselnetwerk. Het is evenwel de vraag of dit niet voor verbetering vatbaar zou kunnen zijn. Het functioneren van dit netwerk komt steeds verder onder druk te staan onder invloed van bevolkingsgroei, voortschrijdende verstedelijking en klimaatverandering. Het aanpassingsvermogen en de veerkracht van deze manier van voedselvoorziening valt te betwijfelen. In stedelijke gebieden zou lokale voedselproductie een alternatief kunnen zijn. Echter, voor het verbouwen van gewassen is het klimaat van dichtbevolkte grootstedelijke gebieden nauwelijks geschikt. De eerste kassen werden gebouwd om gewassen tegen de heersende klimaatinvloeden te beschermen. In de afgelopen eeuwen werd het ontwerp van kassen steeds aangepast om het productieklimaat te verbeteren. Hierbij vormen plant factories of vertical farms het resultaat van de meest recente ontwikkelingen voor wat betreft geavanceerde klimaatbeheersing en controle over het teeltproces. In plant factories wordt het gewas in een gesloten systeem en in gestapelde teeltlagen geproduceerd, daarbij ondersteund door een zorgvuldige klimaatbeheersing. LED-belichting- en hydrocultuursystemen worden normaliter toegepast voor respectievelijk het bevorderen van de fotosynthese en de toediening van nutriënten. In de populaire media zijn plant factories reeds aanbevolen als oplossing voor problemen in de voedselveiligheid en de voedselvoorziening op internationale schaal. Daarnaast zouden hiermee de kwaliteit en de duurzaamheid van het voedsel verbeterd kunnen worden. De vraag is echter of de geavanceerde klimaatbeheersing van plant factories nu wel nodig of doeltreffend of efficiënt is. De hoofddoelstelling van het in dit proefschrift beschreven onderzoek was de doelmatigheid van plant factories te kwantificeren en daarmee een beeld te vormen van hun potentie voor stedelijke voedselproductie. Met dit doel voor ogen is de STACKED methode ontwikkeld.

In **Hoofdstuk 1**, de inleiding, worden de in populaire media vermelde, talrijke voordelen van plant factories uiteengezet en van commentaar voorzien. De discussie wordt daarbij gefocust op de veiligheid, de kwaliteit en de duurzaamheid van het voedsel. Tot op heden is er geen methode om de technische potentie van plant factories inzichtelijk te maken, met name niet in de stedenbouwkundige context. Er is veel kennis separaat binnen de landbouwtechnische en bouwtechnische disciplines. Echter, wat ontbreekt is een geïntegreerd kennis- en onderzoeksdomein, gericht op het systeemontwerp, de technische prestaties en de doelmatigheid

van plant factories. In het onderzoek van dit proefschrift werd de doelmatigheid onderzocht door de grondstofbehoefte voor de productie van verse groenten in plant factories in kaart te brengen. Deze parameter staat ook wel bekend als de 'grondstofverbruiksefficiëntie' (Engels: resource use efficiency). Voor het bepalen van deze grondstofverbruiksefficiëntie dienden verbindingen te worden gemaakt tussen diverse schaalniveaus, van het gewas tot de individuele plant factory en tot de gehele stad. Deze verbindingen en de onderzoeksopzet worden in dit hoofdstuk uiteengezet en toegelicht.

In **Hoofdstuk 2** wordt de energiebalans van het gewas beschreven. Om de potentie van het systeem te kunnen bepalen is inzicht in de rol van de energetische processen van het gewas binnen de totale energiebalans van het productiesysteem is noodzakelijk. Het gewas beïnvloedt zijn directe omgeving door straling te absorberen, warmte met de omgevingslucht uit te wisselen en water te verdampen. De waterdampflux en de relatie tussen voelbare en latente warmte zijn essentieel om de energiebehoefte van plant factories te kunnen berekenen. Met behulp van het Penman-Monteith model kon het driedimensionale gewas worden gereduceerd tot een eendimensionaal 'groot blad'. In dit 'grote blad' werd netto straling geabsorbeerd, energie omgezet en uitgewisseld en water verdampt. De aerodynamische en stomatale weerstand van het gewas werden vervolgens bepaald om het Penman-Monteith model toe te kunnen passen in simulaties. Het model werd gevalideerd voor de effecten van fotosynthetische foton flux dichtheid, bedekking van het teeltgebied en verschil in vochtconcentratie. Het aldus vastgestelde model voor de gewas-energiebalans was in staat de relatie tussen de uitwisseling van voelbare en latente warmte vanuit het gewas te berekenen.

In **Hoofdstuk 3** wordt de grondstofverbruiksefficiëntie van het verbouwen van sla in plant factories en kassen onderzocht. Het model voor de gewas-energiebalans werd gecombineerd met bestaande modellen voor gewasontwikkeling en gebouwenergie teneinde de grondstofverbruiksefficiëntie te kunnen berekenen. Het verbruik van energie, elektriciteit, water, CO₂ en grondoppervlak in plant factories werd berekend en vergeleken met dit verbruik in kassen. Drie locaties op verschillende breedtegraden en met uiteenlopende klimaten werden onderzocht met als doel inzicht te verwerven over de invloed van het buitenklimaat en de beperkingen van het model. Plant factories bestaan uit een gesloten constructie en hebben daardoor een hogere grondstofverbruiksefficiëntie voor water en CO₂. Daarnaast behalen plant factories een hogere grondstofverbruiksefficiëntie voor landoppervlak door een hogere productie per teeltoppervlak en door de uitbreiding van het teeltoppervlak in de vorm van meerdere gestapelde lagen. Echter, de grondstofverbruiksefficiëntie voor elektriciteit was significant lager in plant factories in alle drie klimaten. Deze lagere efficiëntie was het gevolg van het grotere aandeel van de kunstmatige

belichting en in zekere mate ook van de hogere interne warmtelasten in de totale energiebalans. De potentie en doelmatigheid van plant factories voor de stedelijke voedselproductie kan worden vergroot door de grondstofverbruiksefficiëntie voor elektriciteit te optimaliseren.

In **Hoofdstuk 4** wordt het systeemontwerp in plant factories onderzocht teneinde de grondstofverbruiksefficiëntie voor energie en elektriciteit te kunnen verhogen. De invloed van het façade- en koelsysteemontwerp werden nauwkeurig geanalyseerd. Submodellen voor de berekening van de prestatiecoëfficiënt (Engels: coefficient of performance) van het klimaatsysteem werden ontworpen en geïntegreerd. De berekeningen in dit hoofdstuk bieden inzicht in de invloed van de activiteit, het inzetplan, het koelsysteemontwerp, de vormfactor en het façadeontwerp op de behoefte aan energie en elektriciteit. De invloeden van transparante constructies, isolatiewaardes, albedowaardes, toetreding van zonnewarmte en vormfactor op het totale energieverbruik werden nauwkeurig geanalyseerd. In dit hoofdstuk wordt de doelmatigheid van verschillende passieve klimatiseringsmethodes onderzocht, waaronder de decentrale dissipatie van warmte door de gevel en het gebruik van zonnestraling voor fotosynthese. Dergelijke passieve methodes konden het energieverbruik en de grondstofverbruiksefficiëntie voor elektriciteit in plant factories wel verbeteren, maar dat slechts in beperkte mate.

In **Hoofdstuk 5** wordt het onderzoek beschreven naar het herwinnen en het gebruik van restwarmte uit plant factories binnen het stedelijke energienetwerk. In de toekomst zal in de steden het aanpassingsvermogen aan wisselende omstandigheden grotendeels bepaald worden door de integratie van essentiële netwerken zoals energie, voedsel, water, goederen en data. Lokale voedselproductie in de vorm van stedelijke land- en tuinbouw heeft een directe invloed op deze netwerken. In dit onderzoek werd het effect van dit soort land- en tuinbouw in plant factories op de stedelijke energiebalans geanalyseerd uitgaande van diverse scenario's. In de modellen beschreven in hoofdstuk 4 wordt de restwarmte uit plant factories direct naar de buitenlucht afgevoerd. In dit hoofdstuk wordt onderzocht of deze restwarmte kan worden geïntegreerd in het stedelijk energienetwerk. Alternatieve strategieën werden onderzocht waarbij plant factories aangewend worden om vraag en aanbod in balans te brengen, dit in energiesystemen die vooral gebruik maken van duurzame energiebronnen met een telkens wisselende opbrengst. Met andere woorden, zouden plant factories een overschot aan duurzame energieproductie kunnen aanwenden om warmte en voedsel te produceren in en voor de stad? Enerzijds is het flexibel gebruik van plant factories het meest geschikt om in te spelen op de fluctuaties van duurzame energieproductie. Anderzijds zullen plant factories daarbij een minimum aantal vollasturen moeten behalen om rendabel te kunnen zijn. De technische

integratie van stedelijke en landbouwtechnische systemen zal afhankelijk zijn van het stadsontwerp, het lokale klimaat, de energievraag en de energieproductie.

In **Hoofdstuk 6** worden de resultaten van dit proefschrift op een rij gezet en bediscussieerd. In dit hoofdstuk wordt een overzicht gegeven van de conclusies, de aanbevelingen voor toekomstig onderzoek en de potentiële toepassingen. De STACKED methode werd ontwikkeld voor de hoofddoelstelling van dit onderzoek. Het bijbehorende model was in staat de doelmatigheid van plant factories te analyseren op diverse schaalniveaus: van het blad tot de stad. De bestaande literatuur is voornamelijk gericht op één enkele schaal, context of locatie, waardoor uitwisseling en vergelijking van informatie beperkt is gebleven. De STACKED methode werd ontwikkeld om toegepast te kunnen worden in diverse klimaten, locaties en contexten. Dit hoofdstuk licht de benodigde aannames en vereenvoudigingen van het model toe. De STACKED methode voorziet in een gedetailleerd overzicht van de grondstofverbruiksefficiëntie van plant factories en brengt nieuwe uitdagingen en kansen aan het licht. Een en ander resulteerde in praktische inzichten waarmee de haalbaarheid van plant factories in de nabije toekomst verbeterd kan worden. Zo hoeft bijvoorbeeld de keuze niet te vallen tussen kas of plant factory; afhankelijk van het lokale klimaat vindt een geleidelijke transitie plaats van een natuurlijk naar een volledig beheerst productieklimaat. Het ontwerp van plant factories zou dus altijd moeten worden aangepast aan het lokale klimaat, de context en de markt: er bestaat geen universele aanpak.

Dankwoord

Ik ben dankbaar voor de vele personen die deel zijn van en hebben bijgedragen aan mijn leven, loopbaan en dit proefschrift. Enkelens wil ik graag in het bijzonder bedanken.

Prof.dr.ir. A.A.J.F. van den Dobbelsteen. Beste Andy, tijdens mijn periode bij de TU Delft en het promotietraject heb ik veel geleerd van je enthousiasme, onbevengden blik en niet te evenaren werkhoud. Je hebt me altijd uitgedaagd om naast de verdieping ook de verbreding te zoeken en vooral het grotere plaatje niet uit het oog te verliezen. Met dit proefschrift komt onze officiële samenwerking ten einde, maar ik hoop dat we elkaar in de toekomst nog vaak zullen spreken en nieuwe projecten zullen starten! Hartelijk dank voor je wetenschappelijke en filosofische begeleiding en voor de goede samenwerking!

Dr. C. Stanghellini. Beste Cecilia, je was de eerste deur die open ging in Wageningen. We doken samen in de formules en je leerde me biologie te vertalen naar natuurkunde; van processen tot formules. Het eerste overleg in Wageningen legde eigenlijk de basis voor dit proefschrift. Ik heb veel geleerd van je kwantitatieve benadering, ontoombare energie en razendsnelle denkt tempo tijdens onze besprekingen. Hartelijk dank voor de wetenschappelijke vonk en voor de prettige samenwerking!

Dr.ir. M.J. Tenpierik. Beste Martin, als ik echt de modellen in moest duiken, dook jij vaak mee. Door gezamenlijk door het model of de variabelen te lopen of door het model te herstructureren werd de oplossing vaak helder. Daarnaast werden de diverse manuscripten door jou binnen enkele dagen van duidelijke en gestructureerd commentaar voorzien. Deze structuur zorgde voor een vloeiender en doelgericht proces. Hartelijk dank voor je toewijding, technische inzicht en de plezierige samenwerking!

I would like to thank the international members of the committee, Prof. G. Keeffe and Dr. R. Choudhary, for their time and effort spent on evaluating this thesis. It is my privilege to defend this thesis before you.

Graag wil ik de leden van de beoordelingscommissie, te weten Prof.dr.ir. A. van Timmeren, Prof.dr.ir. L.F.M. Marcelis en Prof.dr.ir.arch. I.S. Sariyildiz, bedanken voor

de tijd en moeite die u in het beoordelen van dit proefschrift heeft gestoken. Het is een eer en genoegen om mijn proefschrift tegenover u te mogen verdedigen.

Graag wil ik tevens Westland Infra en Staij Food Group bedanken voor hun bijdrage aan dit onderzoek.

This study was partially funded by the EU European Regional Development Fund “Kansen voor West” with the programme “Fieldlab FreshTeq”. I am thankful for their support of this research.

Greenhouse Horticulture. To my colleagues who became friends, thank you for being there the past years, sharing the foods and drinks of your respective countries and for helping me establish my first roots in Wageningen. I would like to thank Estéban, Ilias and Frank in particular for their assistance throughout the project and for providing the social glue that kept the team together.

Dr.ir. J.C. Bakker & Dr. S. Hemming. Beste Sjaak en Silke, hartelijk dank dat jullie mij de kans en de ruimte hebben gegeven om dit onderzoeksproject zelf in te richten als een samenwerking tussen Wageningen University & Research en de Technische Universiteit Delft.

Dr. ir. J.A. Dieleman. Beste Anja, hartelijk dank voor de mogelijkheid en de ruimte om het proefschrift af te ronden. Ik kijk er naar uit om verder samen te werken en het onderzoek op het gebied van vertical farming verder vorm te geven.

Ing. E. Meinen. Beste Esther, met jou heb ik de eerste experimenten met planten gedaan in de klimaatcellen. Planten waren voor mij een volkomen nieuw onderwerp en mijn benadering was/is vaak enigszins onorthodox. Hartelijk dank voor je deskundige inzichten, ondersteuning en meedenken in alle experimenten.

Dr. N. Vilfan. Dear Nastassia, thank you for setting an example, for pushing the academic quality of this thesis and for reminding me to never settle. I appreciate our discussions on plants, biology and everything else.

C. Pont. Beste Chantal, eigenlijk had ik helemaal niet in Wageningen mogen zijn, maar jij hebt toch plek voor me weten te maken. Hartelijk dank voor al je goede advies en je hulp met bureaucratie de afgelopen jaren!

Architectural Engineering + Technology. It was initially somewhat daunting to go from being a student to becoming your colleague, but the enthusiasm you all shared made the transition smooth. Thank you for exchanging ideas on your fascinating,

original, technical, complex and sometimes crazy research with me throughout the years. You created an inspiring atmosphere at TU Delft.

B. Song. Beste Bo, mijn dagen in Delft begonnen altijd goed met jouw opgewekte groet vanuit het secretariaat. Hartelijk dank voor al je ondersteuning en aanmoediging de afgelopen jaren!

M.I. Dornhelm. Dear Mister Dornhelm, I appreciate all our discussions on cooling systems and the many books and resources you have sent me from Brooklyn. I look forward to delve into even more detail with you in the future.

ir. D.W. Hoogterp. Beste Dirk, hartelijk dank voor het delen van je kennis en informatie op het gebied van warmtewisselaars.

ir. E.B. Wissink. Beste meneer Wissink, hartelijk dank voor het advies op het gebied van koelsystemen en het vastleggen van enkele belangrijke variabelen.

Dr. T.K.J. Groenhof. Katrien, het was vanaf het moment dat ik begon met schrijven aan dit proefschrift een uitgemaakte zaak dat jij paranimf zou worden. Sinds de studie kan met helder Gronings verstand alles in perspectief geplaatst worden en dat waardeer ik zeer. We hebben van elkaar geleerd dat perfectie niet bestaat, maar dat het nastreven ervan toch ook heel mooi kan zijn. Ik heb altijd veel bewondering voor je motivatie en doorzettingsvermogen.

ir. S.R. Andary. Samy, al bijna 27 jaar lang moedigen we elkaar aan om nog *nét* iets verder te gaan, van die hogere tak in de klimboom, tot een hogere opleiding en tot de wereld verder ontdekken. Hoe kan het beter, sneller, mooier, vloeiender en vooral indrukwekkender? De wereld is altijd te klein om niet beter gemaakt te worden en jouw enthousiasme, creativiteit en flexibiliteit zijn altijd een inspiratie geweest.

Als paranimfen wil ik jullie beiden bedanken voor jullie steun en advies tijdens het hele proces en voor de verdediging. Het zal hoogstwaarschijnlijk een digitale verdediging zonder paranimfen moeten zijn en dat is een groot gemis.

Familie Andary. Nicole en Simon, jullie hebben als gezin een ongelooflijk grote rol gespeeld in mijn opvoeding en ontwikkeling en ik zie jullie dan ook als een tweede familie. Wissam en Hani, bedankt dat jullie waar het soms nodig was de rol van oudere broer op jullie namen.

G.J. Kühne. Papa, je vroeg je vaak af wanneer ik een keer uitgestudeerd zou zijn en met dit proefschrift is het dan mogelijk eindelijk zover. Net zoals vroeger gaf je me

het advies om het gewoon eerst te proberen en dan vanzelf te zien waar het schip strandt. Hartelijk dank voor het advies, het zetje en voor de hoognodige dosis droge humor.

K. Graamans. Papa, je hebt me als eerste geleerd hoe je op een wetenschappelijke manier een probleem analyseert en aanpakt. Ik ben altijd onder indruk geweest van hoe jij complexe materie op een begrijpelijke en gestructureerde manier kan toelichten. Je bent altijd mijn eerste mentor geweest en zonder jou had ik hier nooit gestaan.

D.P.M.J. Graamans-Winkel. Lieve mama, met trots draag ik dit proefschrift aan jou op. Je staat niet graag in het middelpunt van de aandacht en verdient het daarom juist. Jij zorgt er voor dat iedereen het onderste uit de kan te halen, door alle andere zaken voor ze weg te nemen. Je hebt me altijd gestimuleerd om net een stap extra te zetten: 'Als je het doet, doe het dan goed'.

Ik wil jullie allen graag bedanken voor alle kansen en het voorbeeld die jullie mij hebben gegeven.

E.R. Dornhelm. Lieve Esther, de laatste woorden zijn voor jou. Vanaf het begin van dit traject heb je over mijn schouder mee gekeken. Zonder jouw advies en overtuiging was ik niet aan dit traject begonnen. Ik heb ongelooflijk veel respect voor jou en voor jouw kijk op het leven. Bedankt voor je tomeloze interesse en humor, voor het helpen kiezen tussen optie A of B, het meedenken, het aanhoren en met name het motiveren! Nu is het tijd voor een nieuw avontuur samen.

Curriculum vitae

Luuk Graamans was born on the 3rd of May, 1990 in Utrecht, the Netherlands. In 2013 he began his MSc studies in Building Technology at the faculty of Architecture and the Built Environment at Delft University of Technology (DUT). During his studies, Luuk dedicated one year applying theory to practice by participating in multiple internships abroad. Interested in the challenges facing megacities and in a change of environment, he worked in the fields of architectural design in Shanghai, lighting and product design in Taipei and building engineering in Ho Chi Minh City. These environments sparked his interest in the food resilience of cities.

For his MSc thesis he explored the potential of re developing structurally vacant buildings into food production centres using controlled environment agriculture. In 2015, Luuk graduated cum laude with a perfect score on his thesis work *'VERTICAL - the re-development of vacant urban structures into viable food production centres utilising agricultural production techniques'*.

Following his MSc, Luuk began working as an engineering consultant with DUT within the Climate Design & Sustainability team. Here he worked on projects related to the sustainability and circularity of buildings and supply chains. The collaboration between DUT and Wageningen University & Research (WUR) was formed to research vertical farming in greater detail. Within this collaboration Luuk started his PhD position in 2018 on the interface of agricultural and building engineering to explore the potential integration of plant factories in cities. He aimed to combine the expertise of both universities to produce this thesis outlining the building design, systems engineering, and performance analysis of plant factories for urban food production. During his PhD work, Luuk presented his research at multiple (inter)national conferences, including GreenSys 2019 in Angers, Vertifarm 2019 in Wageningen and the 2019 Asian Leadership Conference in Seoul.

As of March 2020, Luuk started working as a researcher in the Crop Physiology group at WUR. He is currently focused on further developing vertical farming research for international markets and on several projects pertaining to food resilience.

List of publications

This study

Plant factories; crop transpiration and energy balance.

Graamans, L., van den Dobbelsteen, A., Meinen, E., Stanghellini, C.
Agricultural Systems. 2017; 153: 138-147.

Plant factories versus greenhouses: Comparison of resource use efficiency.

Graamans, L., Baeza, E., van den Dobbelsteen, A., Tsafaras, I., Stanghellini, C.
Agricultural Systems. 2018; 160: 31-43.

Plant factories: Reducing energy demand at high internal heat loads through façade design.

Graamans, L., Tenpierik, M., van den Dobbelsteen, A., Stanghellini, C.
Applied energy. 2020; 262: 114544.

Plant factories: Integrating food production to balance the renewable energy system in cities.

Graamans, L., Tenpierik, M., van den Dobbelsteen, A., Stanghellini, C.
Applied energy. 2020; under review.

Other

Plant factories are heating up: hunting for the best combination of light intensity, air temperature and root-zone temperature in lettuce production.

Carotti, L., **Graamans, L.**, Puksic, F., Butturini, M., Meinen, E., Heuvelink, E., Stanghellini, C.
Frontiers in Plant Science. 2020; 11.

Towards fossil free cities - A supermarket, greenhouse & dwelling integrated energy system as an alternative to district heating: Amsterdam case study.

ten Caat, N., **Graamans, L.**, Tenpierik, M., van den Dobbelsteen, A.
Energies. 2021; 14(2): 347.

STACKED

The building design, systems engineering and performance analysis of plant factories for urban food production

Luuk Graamans

Expanding cities across the world rely increasingly on the global food network, but should they? Population growth, urbanisation and climate change place pressure on this network, bringing its resilience into question. For decades urban agriculture has been discussed in popular media and academia as a potential solution to improve food security, quality and sustainability. The new idol in this discussion is the plant factory: A fully closed system for crop production. Arrays of LEDs provide light and hydroponics provide water and nutrients to vertically stacked layers of crops, hence the term vertical farming. The plant factory features more extensive climate control than high-tech greenhouses. The question remains whether this level of climate control is necessary, effective and/or efficient.

The scope of this research is therefore to investigate the potential and limitations of plant factories for urban food production. The STACKED method was developed to address the performance of plant factories across multiple scales, from leaf to facility to city. The role of plant processes in the total energy balance was outlined first. Performance was assessed by analysing the resource requirements, including energy, electricity, water, CO₂ and land area use, for the production of fresh vegetables. The impact of façade and cooling system design was analysed in detail. Lastly, the effects of local food production on the urban energy balance were assessed for various scenarios. The results of this dissertation can serve as a foundation for future studies on the application of plant factories in both theoretical and real world applications.

A+BE | Architecture and the Built Environment | TU Delft BK